Effect of Penta-arylated Cp Ligands on Synthesis and Reactivity of Transition Metal E_n (E = P, As) Ligand Complexes

DISSERTATION

ZUR ERLANGUNG DES

DOKTORGRADES DER NATURWISSENSCHAFTEN

(DR. RER. NAT.)

DER FAKULTÄT CHEMIE UND PHARMAZIE

DER UNIVERSITÄT REGENSBURG

vorgelegt von

Moritz Modl

aus München

im Jahr 2018

Diese Arbeit wurde angeleitet von Prof. Dr. Manfred Scheer.

Promotionsgesuch eingereicht am:	17. April 2018
Tag der mündlichen Prüfung:	18. Mai 2018

Vorsitzender:	Prof. Dr. Alkwin Slenczka
Prüfungsausschuss:	Prof. Dr. Manfred Scheer
	Prof. Dr. Henri Brunner
	Prof. Dr. Frank-Michael Matysik

Universität Regensburg

Eidesstattliche Erklärung

Ich erkläre hiermit an Eides statt, dass ich die vorliegende Arbeit ohne unzulässige Hilfe Dritter und ohne Benutzung anderer als der angegebenen Hilfsmittel angefertigt habe; die aus anderen Quellen direkt oder indirekt übernommenen Daten und Konzepte sind unter Angabe des Literaturzitats gekennzeichnet.

Moritz Modl

This thesis was elaborated within the period from January 2014 until April 2018 in the Institute of Inorganic Chemistry at the University of Regensburg, under the supervision of Prof. Dr. Manfred Scheer.

Results from collaborations, which are not mentioned within this work, have been published during the thesis:

U. Chakraborty, M. Modl, B. Mühldorf, M. Bodensteiner, S. Demeshko, N. J. C. van Velzen, M. Scheer, S. Harder, R. Wolf, *Inorg. Chem.* **2016**, *55*, 3065-3074.

dedicated to Claudia and my family

Preface

At the beginning of each chapter a list of authors is given and the individual contribution of each author is described. Also on the first page of each chapter, if some of the results have already been discussed in other theses, it is stated.

Each chapter includes an own short introduction. However, a general ‘Introduction’ and the ‘Research Objectives’ are given in the beginning of this thesis. In the end of this manuscript, a comprehensive ‘Conclusion’ of this work is presented. To ensure uniform design of this thesis, all chapters are subdivided into ‘Introduction’, ‘Results and Discussion’, ‘Conclusion’, ‘References’ and ‘Supporting Information’. Furthermore, all chapters have the same text settings and the numeration of compounds, schemes and figures begins anew.

Table of Contents

1 Introduction

1.1 Phosphorus and Arsenic

The german apothecary and alchemist Hennig Brand discovered the first modification of elemental phosphorus in 1669, while searching for the “philosopher’s stone”.[1] Nowadays various allotropes are known, which are divided into three main modifications: white, red and black phosphorus. They vary considerably in their thermodynamic stability as well as in their molecular structure (Scheme 1).[2]

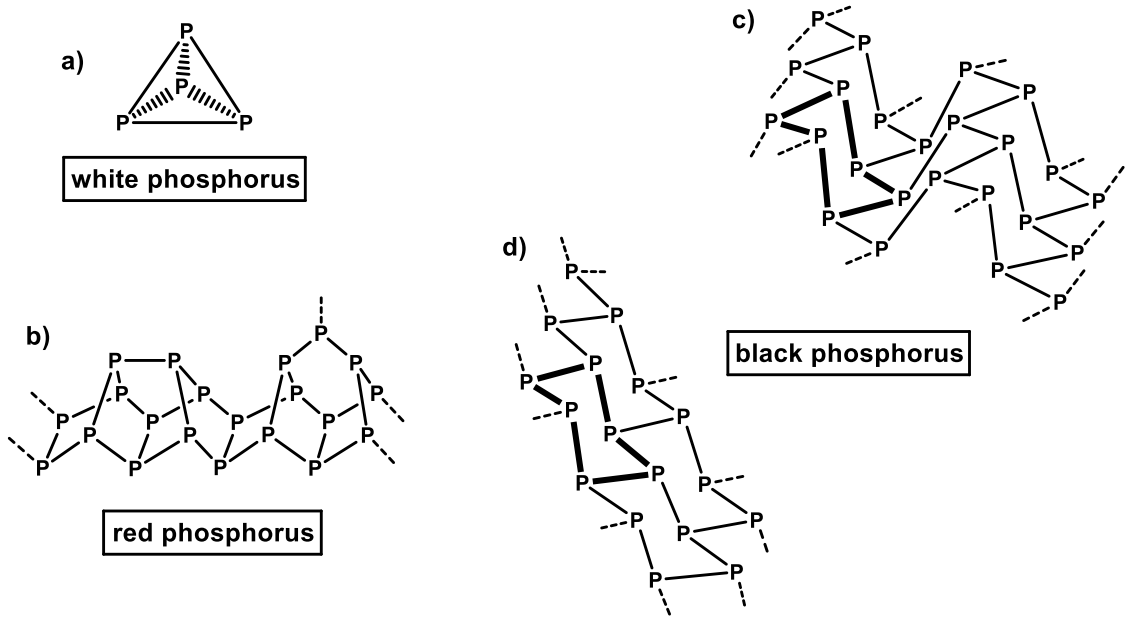

Scheme 1. Main modifications of phosphorus: a) tetrahedral P_4 molecule; b) P_{21} repeating unit found in fibrous and violet or Hittorf’s phosphorus; c) orthorhombic black phosphorus; d) rhombohedral high pressure modification of black phosphorus.

The thermodynamically stable black phosphorus consists of condensed P_6 rings, adopting a chair conformation (orthorhombic) and exhibiting semi-conducting properties.[3,4] It can be synthesized by heating white phosphorus to 200 °C under 12 kbar pressure.[5] At higher pressures, the conformation of the P_6 units in orthorhombic black phosphorus changes to give a flat layer of coherent P_6 moieties (rhombohedral), which are analogous arranged in comparison to grey arsenic.

Red phosphorus is classified into types I – V. While type I is an amorphous, commercially available solid composed of polymeric networks as reported by Roth *et al.* by performing a variety of analytical methods,[6] the nature of types II and III is still not elucidated. The type IV is known as fibrous red phosphorus, because of its property of splitting into fine fibers by applying mechanical stress. It consists of infinite tubes formed by P_2 units, linking P_8 and P_9

moieties in a [P_2-P_8-P_2-P_9] fashion.[7] These tubes are interconnected pairwise to form parallel double-tubes. Otherwise, a perpendicular linkage of similar tubes is found in the so-called violet or Hittorf's phosphorus, referred to as type V red phosphorus.[8] It was discovered in 1865 by Johann Willhelm Hittorf, a german physicist.[9] All types of red phosphorus can be obtained from white phosphorus under elevated temperatures and different reaction times.

As mentioned before, the first known molecular modification of phosphorus is white phosphorus. It consists of discrete P_4 tetrahedra. The corresponding P-P distances were revealed by single crystal diffraction (2.209(5) Å), Raman spectroscopy (2.2228(5) Å) and electron diffraction (2.1994(3) Å) on gaseous P_4.[10] It is the most reactive allotrope, being slightly light sensitive and highly flammable in air. Nonetheless, it is of exceptional importance for the preparation of phosphorus containing compounds in industrial as well as in academic application.

The discovery of arsenic, the heavier homologue of phosphorus, by Albertus Magnus is roughly traced back to the year 1250.[2] Similar to its lighter relative, different allotropes of arsenic are known, whom also differ significantly by their thermodynamic stability and molecular structure. The modifications are grouped into grey, black and yellow arsenic.

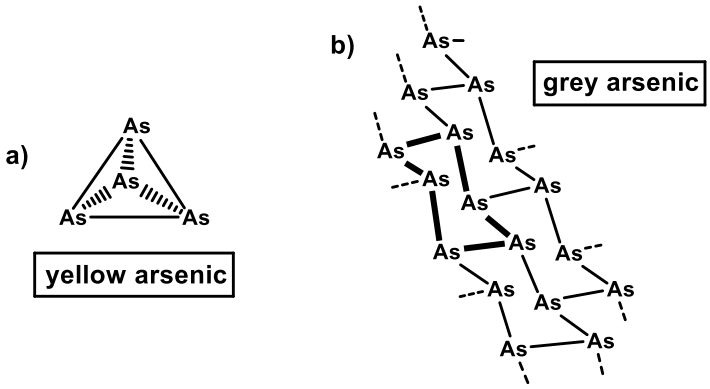

Scheme 2. Main modifications of arsenic: a) tetrahedral As_4 molecule; b) layer of rhombohedral grey arsenic.

The thermodynamically most stable modification is grey (metallic) arsenic. It is isostructural to the high-pressure modification of black phosphorus (rhombohedral) and is composed of connected As_6 rings to form dense layers.[2]

Black arsenic is supposed to resemble the amorphous structure of red phosphorus (type I), consisting of polymeric networks.[2] It is synthesized by arsenic vapor deposition onto heated surfaces, though it decomposes to grey arsenic at elevated temperatures.[11]

In analogy to white phosphorus, yellow arsenic consists of As_4 tetrahedra and is highly labile with respect to transformation into grey arsenic.[12] This process is strongly accelerated by light, thus practically yellow arsenic cannot be stored. According to Bettendorff, As_4 can be obtained

by sublimation of grey arsenic above 600 °C.[13] The arsenic-arsenic bond distances are about 2.435(4) Å within the tetrahedron, revealed by electron diffraction studies on As_4 vapor.[14]

1.2 Bulky Ligands - Penta-arylated Cp Ligands

A large number of different ligands like phosphines or nitrogen bases, among others, are applied in organometallic chemistry. However, cyclopentadienyl (Cp) ligands are probably the most widely used ligand system, since the discovery of the prominent molecule ferrocene [$(\eta^5\text{-}C_5H_5)_2Fe$].[15] This might be due to versatile coordination modes ranging from η^1 up to η^5, with pentahapto being the most common one, or the relatively low intrinsic reactivity that makes them to exceptional spectator ligands, e.g. for catalysis.[16]

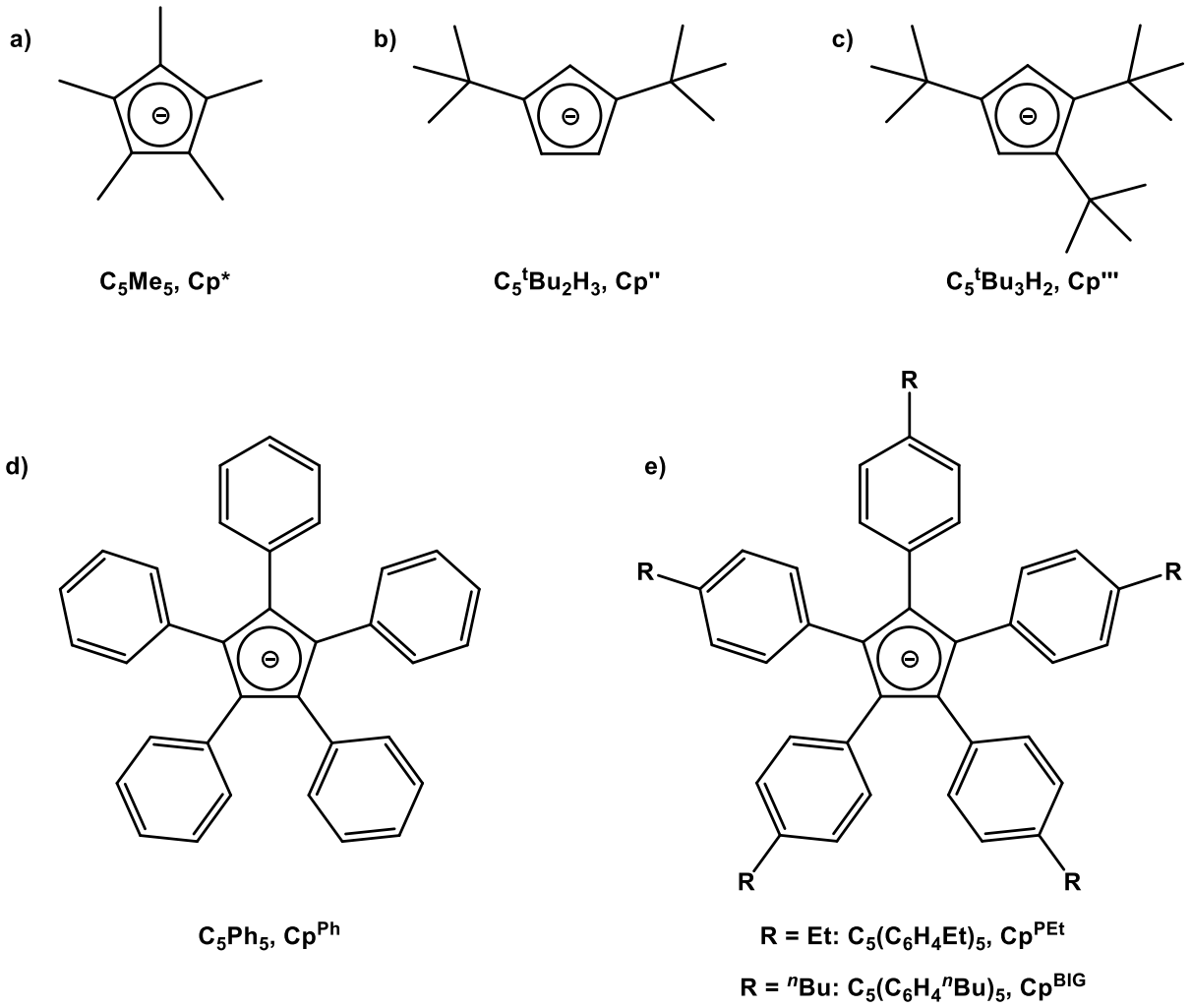

Scheme 3. Selected examples of substituted Cp^R ligands as negatively charged $6e^-$ donors.

Substitutions on the cyclopentadienyl ring gave rise to numerous Cp ligands with different kinds and numbers of substituents, respectively. Therefore, they can be readily modified to fit

certain needs in terms of electronic properties and steric demands. Walter *et al.* introduced the concept of cone angles for the Cp substituted complexes,[17] derived from the work of Tolman concerning phosphine ligands,[18] to develop a convenient way to judge the relative steric demand of Cp ligands. For this purpose they chose the reference system [(η^7-C_7H_7)Zr(η^5-Cp^R)] (**1**), as it can accommodate a variety of different ligands and it is well crystallizing. The determination of the cone angles is based on crystallographic and calculated data. Similarly to other studies, they measured the cone angle Θ, which they state, is a good descriptor for the steric bulk parallel to the Cp ring. Additionally, they introduced the angle Ω to consider the ligand size vertical to the ring plane to better indicate the shielding of the metal center. Comparison of the values gave an "order of bulk" with Cp'' < Cp* < Cp''' < Cp^{Ph} < Cp^{BIG-1} (see **a** - **e** in Scheme 3; Cp^{BIG-1} = $C_5Ph_4(C_6H_4{}^nBu)$).

Sterically demanding cyclopentadienyl ligands and their metal complexes are the subject of different review articles.[19] Schumann and Janiak established four main reasons for the introduction of such ligands: the kinetic stabilization of reactive species, the possibility to obtain novel molecular structures, investigation of rotation dynamics and the introduction of chirality.[19a]

A concrete example for the kinetic stabilization effect of sterically demanding ligands is given by transition metal carbonyl complexes with the general composition $[Cp^RM(CO)_n]_2$ (M = Cr, Mo, n = 3; M = Fe, n = 2; M = Ni, n = 1). These dimeric compounds consist of 17 VE, $\{Cp^RM(CO)_n\}$, fragments, which are not stable in the case of smaller Cp^R ligands. Therefore they dimerize to get the preferred 18 VE configuration.[20] However, if the penta-arylated Cp^{Ar} (Cp^{Ar} = Cp^{Ph} ($C_5(C_6H_5)_5$), Cp^{BIG} ($C_5(C_6H_4{}^nBu)_5$)) ligands are introduced, the dimerization process is completely prohibited or an equilibrium between a 17 VE monomer and a 18 VE dimeric species can be found in solution. For complexes $[Cp^{Ar}Fe(CO)_2]_2$ (Cp^{Ar} = Cp^{Ph} (**2**)[21], Cp^{BIG} (**3**)[22]) and $[Cp^{Ph}Mo(CO)_3]_2$ (**4**)[23] both species are present in solution. This could be verified by IR spectroscopy measurements in solution as well as in the solid state. Furthermore, compound **3** was reacted with small molecules, e.g. E_4 (E = P, As), where a selective E-E bond cleavage is observed.[24] This confirms the presence of metal centered $\{Cp^{BIG}Fe(CO)_2\}$ radicals. Complex $[Cp^{Ph}Cr(CO)_3]$ (**5**)[25] exists exclusively as a radical monomer in solution and in the solid state, as the molecular structure suggests, obtained by X-ray diffraction investigations. Another example for the kinetic stabilization are the half-sandwich complexes of the type $[Cp^RMX]_2$ (X = halide). They tend to decompose into the homoleptic species MX_2 and $Cp^R{}_2M$ (Schlenk equilibrium), but can be stabilized by bulky cyclopentadienyl ligands. We could demonstrate this manner in cooperation with Wolf *et al.*, by synthesis of the dimeric halide-bridged compounds $[Cp^{Ar}MBr]_2$ (Cp^{Ar} = Cp^{PEt} ($C_5(C_6H_4Et)_5$), M = Fe (**6**), Co (**7**), Ni (**8**); Cp^{Ar} = Cp^{BIG} ($C_5(C_6H_4{}^nBu)_5$), M = Ni (**9**)).[26] We were able to isolate these species by using the perarylated cyclopentadienyl ligands Cp^{PEt} and Cp^{BIG}, respectively. Similar behavior was

observed by Hanusa *et al.* and Sitzmann *et al.* for alkaline earth metal derivatives $[Cp^RMX]_n$ (Cp^R = Cp''', Cp^{4iPr}, $C_5(SiMe_3)_3H_2$; M = alkaline earth metal; X = halide), bearing other bulky Cp^R ligands.[27]

The formation of novel structural motifs represents a further important reason to implement bulky cyclopentadienyl ligands. The steric demand can hamper the formation of certain motifs and forces the arrangement of others.

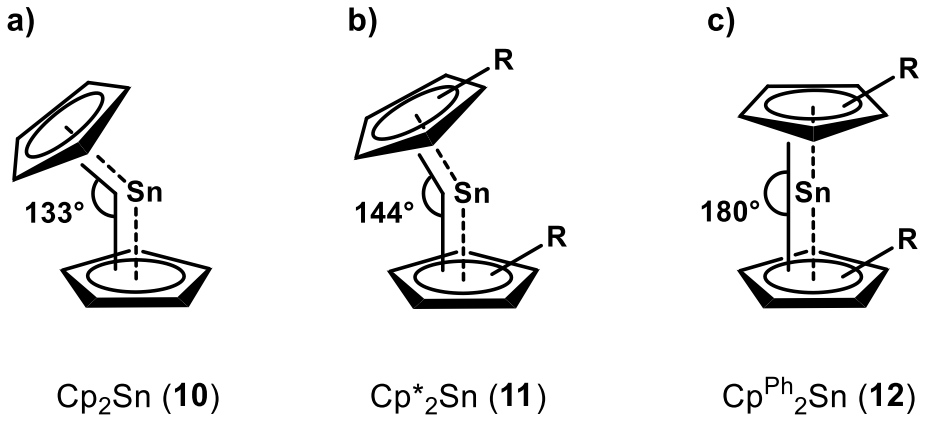

Scheme 4. Structures of stannocene derivatives **10**, **11** and **12** and the $Cp^R_{centroid}$-Sn-$Cp^R_{centroid}$ angles.

This is especially true in the case of metallocenes of Group 14 elements. Regarding the stannocene derivatives $[Cp_2Sn]$ (**10**)[28], $[Cp^*_2Sn]$ (**11**)[29] and $[Cp^{Ph}_2Sn]$ (**12**)[30] and comparing their molecular structure in the solid state, the great influence of the Cp^R ligands emerges. Thus the angle between the normals from Sn to the Cp^R ring planes is 133°/134° (**10**), 143.6°/144.6° (**11**) (two independent molecules in the unit cell) and 180° (**12**). The bent structures in **10** and **11**, respectively, arise from the stereochemical activity of the lone pair electrons (VSEPR: valence shell electron pair repulsion), whereas the lone pair electrons in compound **12** are stereochemically very inert, dominated by the bulky perarylated Cp^{Ph} ligands.

The aspect of ring and substituent rotation dynamics, as described by Schumann and Janiak, refers primarily to the rotation of the Cp ring around the metal-$Cp_{centroid}$ vector or the rotation around Cp-substituent bonds.[19a] This and the introduction of chirality via optically active substituents only possesses minor relevance for this thesis and is not further discussed.

With regard to the above-mentioned studies, it is apparent that bulky cyclopentadienyl ligands and penta-arylated derivatives in particular, provide interesting features and versatile applications. In the following chapters the focus is turned on the perarylated Cp^{PEt} ($C_5(C_6H_4Et)_5$) and Cp^{BIG} ($C_5(C_6H_4{}^nBu)_5$) ligands (see **e** in Scheme 3) and their transition metal complexes. By functionalization of the phenyl groups with ethyl and *n*-butyl groups, respectively, in *para* position, the solubility is highly improved compared to Cp^{Ph} ($C_5(C_6H_5)_5$), which enhances the investigations in solution.

1.3 Activation of E_4 (E = P, As) and other Cage Compounds

White phosphorus is the key starting material in the synthetic and industrial production of organophosphorus compounds.[31] The synthesis involves the chlorination of P_4 to generate PCl_3, before reacting with organic molecules.[32] Thereby very toxic chlorine gas is used and stoichiometric amounts of waste are produced as a side product during the reaction with the organic substrates. With regard to the great annual demand, the sought-after routine is more sustainable and environmentally friendly, but not found yet.

Considering that, a method for the direct and selective functionalization of white phosphorus is required. In 1971, Lindsell and Ginsberg opened up a potential way to solve this task by reacting P_4 with a transition metal complex.[33] The synthesized compound $[(PPh_3)_2RhCl(\eta^2\text{-}P_4)]$ (**13**) represents the first reported P_n ligand complex. So-called P_n ligand complexes comprise a substituent-free phosphorus ligand, where the P atoms are only bound to a metal or other P atom. The possibility of coordinating P_4 to transition metal complexes marks the starting point of intense research including the metal-mediated activation and transformation of white phosphorus. The above-mentioned synthesis of complex **13** by reacting P_4 with $[(PPh_3)_3RhCl]$ (**14**) under elimination of PPh_3 depicts one effective approach for the formation of P_n ligand complexes, involving the use of transition metal compounds, which contain labile leaving groups like CO or C_2H_4. These labile ligands can be split off under thermal, photolytic or even ambient conditions leaving a reactive metal fragment that readily converts P_4. The same procedure applies to the heavier homologue As_4 to synthesize As_n ligand complexes.

Up to now numerous E_n ligand complexes have been reported, composed of different E_n ligands as well as different ligand systems. A summary of this topic is given in several review articles including early and late transition metals or main group elements.[34] Therein a variety of E_n ligands is described. Besides P_4 ligands, there are P_1, P_2 and P_3 units, derived from gradual E_4 degradation by E-E bond cleavage. Additionally extended polypnictogenide moieties with E_n (n > 4) are observed, which arise from aggregation processes. The record holder, in this context, for the largest P_n ligand is the P_{24} unit in the complex $[(Cp'''Co)_5P_{24}\{Cr(CO)_4\}_3]$ (**14**), reported by our group in 2010.[35]

The first penta-arylated Cp^R ligand to be deployed in the synthesis of E_n ligand complexes, is the Cp^{Ph} ligand. In the recent years, also its alkylated derivatives Cp^{PEt} and Cp^{BIG} found their entry into P_4 activation chemistry. The benefits of bulky cyclopentadienyl ligands, like kinetic stabilization and new structural motifs, as described in the previous chapter, have been applied for E_n ligand complexes. An overview of all substituent-free E_n ligand complexes of transition metals in the literature until January 2018 obtained by E_4 activation, containing perarylated cyclopentadienyl ligands, is depicted in Scheme 5.

COBALT R' = C_6H_5; [Cr] = $Cr(CO)_5$

Photolysis

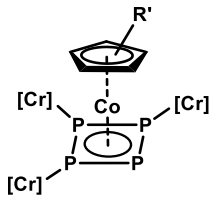

15

MANGANESE R = C_6H_4-4-^{n}Bu

Thermolysis

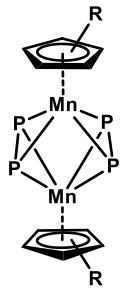

16

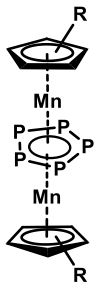

17

Photolysis

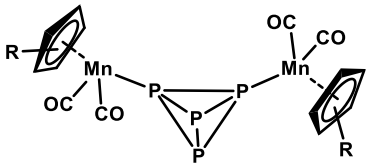

18

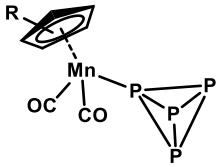

19

IRON R = C_6H_4-4-^{n}Bu

Thermolysis

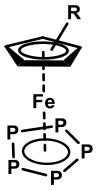

20

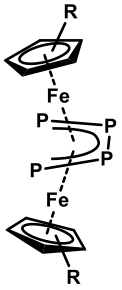

21

Ambient Conditions

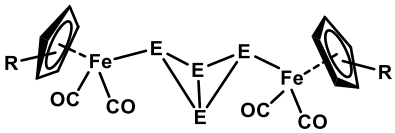

E = P (**22**)
E = As (**23**)

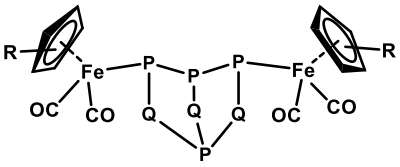

Q = S (**24**)
Q = Se (**25**)

Scheme 5. Overview of all reported E_n (E = P, As) and P_4Q_3 (Q = S, Se) ligand complexes with perarylated Cp^R ligands. They are grouped depending on the contained transition metal and are further distinguished by the reaction conditions.

The first representative was reported by Scheer *et al.*, when reacting P_4 with [$Cp^{Ph}Co(CO)_2$] (**26**) under photolytic conditions in the presence of [$Cr(CO)_5(THF)$] (**27**).[36] They obtained the mononuclear complex **15**, bearing a *cyclo*-P_4 moiety, which is stabilized by {$Cr(CO)_5$} fragments. In 2013, our group investigated the reaction of photolytically induced [$Cp^{BIG}Mn(CO)_2(THF)$] (**28**) with white phosphorus at ambient conditions.[37] It led to the formation of the neutral dinuclear compound **18** and the mononuclear compound **19**, the first manganese complexes with intact P_4 tetrahedra as bridging or terminal ligands. The co-thermolysis of [$Cp^{BIG}Mn(cht)$] (cht = cycloheptatriene, **29**) with P_4 resulted in the isolatable triple-decker complexes **16** and **17**.[38] They exhibit bridging P_2 (**16**) and *cyclo*-P_5 (**17**) ligands, respectively. In 2014, the reaction of [$(Cp^{BIG}Fe)_2(CO)_2]_2$ (**3**) with an excess of P_4 in boiling decalin was reported, leading to the mononuclear product **20** and the dinuclear complex **21**, bearing a *cisoid*-P_4 moiety.[39] In comparison, the activation of E_4 (E = P, As) at ambient conditions, reported by Scheer *et al.*, formed the complexes **22** and **23**, respectively, by selective E-E bond cleavage.[40] In the same way, the molecular cage compounds P_4Q_3 (Q = S, Se) can be activated by [$Cp^{BIG}Fe(CO)_2$] radicals whereby one P-P bond is selectively cleaved, yielding products **24** and **25**, respectively.[40]

Along with the preparation of these compounds, their reactivity aroused increasing interest. The reaction of **18** towards [$(Cp'''Co)_2(C_7H_8)$] (**30**), existing in solution as 14 valence electron [Cp'''Co] fragments, under reductive P-P bond cleavage was investigated.[41] The resulting trinuclear complex [$(Cp'''Co)P_4\{Cp^{BIG}Mn(CO)_2\}_2$] (**31**) displays a square planar *cyclo*-P_4 moiety. The majority of reactivity studies of the pentaphosphaferrocene derivative **20** is dedicated to the coordination chemistry towards Lewis acidic metals of Group 11, copper and silver, respectively. By using CuBr, a spherical cluster with fullerene topology is observed.[42] On the other hand, applying CuX_2 (X = Cl, Br) yields macromolecules with lens-shaped scaffolds.[41] The analogue reaction with [$\{Ag(CH_2Cl_2)\}Al\{OC(CF_3)_3\}_4$] results in the formation of a one-dimensional polymer.[43] The reaction behavior of the butterfly complexes **22** and **23**, respectively, have been studied under thermal as well as photolytic conditions.[41] In the case of the phosphorus derivative, the reaction resulted in the formation of compounds **20**, **21** and the new complex [$(Cp^{BIG}Fe)\{Cp^{BIG}Fe(CO)_2\}P_4$] (**32**), exhibiting a *cyclo*-P_4 moiety. In terms of the arsenic analogue **23**, irradiation gave [$(Cp^{BIG}Fe)_2As_4$] (**33**) with a rare *cylco*-As_4 unit, whereas co-thermolysis with yellow arsenic in toluene, led to the formation of the compounds [$Cp^{BIG}FeAs_5$] (**34**), similar to **20**, and [$(Cp^{BIG}Fe)_3As_6$] (**35**), bearing an As_6 prism, besides complex **33**.

As it is pointed out in this overview, only a few P_n ligand complexes of iron and manganese are known so far and just one example for a cobalt compound is reported for penta-arylated cyclopentadienyl ligand systems. In matters of As_4 activation, the examples are even rarer.

The reactivity of these compounds has been studied in some cases under thermal or photolytic conditions and towards a reactive cobalt(I) species, but more investigations are desired.

1.4 References

[1] F. Krafft, *Angew. Chem. Int. Ed. Engl.* **1969**, *8*, 660-671.

[2] A. F. Holleman, E. Wiberg, N. Wiberg, *Lehrbuch der Anorganischen Chemie*, *102. Auflage*, de Gruyter, Berlin, **2007**; ISBN 978-3-11-017770-1.

[3] R. Hultgren, N. S. Gingrich, B. E. Warren, *J. Chem. Phys.* **1935**, *3*, 351-355.

[4] R. W. Keyes, *Phys. Rev.* **1953**, *92*, 580-584.

[5] P. W. Bridgman, *J. Am. Chem. Soc.* **1914**, *36*, 1344-1363.

[6] W. L. Roth, T. W. DeWitt, A. J. Smith, *J. Am. Chem. Soc.* **1947**, *69*, 2881-2885.

[7] M. Ruck, D. Hoppe, B. Wahl, P. Simon, Y. Wang, G. Seifert, *Angew. Chem. Int. Ed.* **2005**, *44*, 7616-7619.

[8] H. Thurn, H. Krebs, *Acta Cryst. Section B* **1969**, *25*, 125-135.

[9] W. Hittorf, *Ann.Phys.* **1865**, *202*, 193-228.

[10] a) A. Simon, H. Borrmann, H. Craubner, *Phosphorus Sulfur Silicon Relat. Elem.* **1987,** *30*, 507; b) A. Simon, H. Borrmann, J. Horakh, *Chem. Ber.* **1997**, *130*, 1235-1240; c) H. Okudera, R. E. Dinnebier, A. Simon, *Z. Kristallogr*. **2005**, *220*, 259-264; d) N. J. Brassington, H. G. M. Edwards, D. A. Long, *J. Raman Spectrosc.* **1981**, *11*, 346-348; e) B. M. Cossairt, C. C. Cummins, A. R. Head, D. L. Lichtenberger, R. J. F. Berger, S. A. Hayes, N. W. Mitzel, G. Wu, *J. Am. Chem. Soc.* **2010**, *132*, 8459-8465.

[11] H. Stöhr, *Z. Anorg. Allg. Chem.* **1939**, *242*, 138-144.

[12] J. Eiduss, R. Kalendarev, A. Rodionov, A. Sazonov, G. Chikvaidze, *Phys. Status Solidi B* **1996**, *193*, 3-23.

[13] A. Bettendorff, *Justus Liebigs Ann. Chem.* **1867**, *144*, 110-114.

[14] a) Y. Morino, T. Ukaji, T. Ito, *Bull. Chem. Soc. Jpn.* **1966**, *39*, 64-71; b) L. R. Maxwell, S. B. Hendricks, V. M. Mosley, *J. Chem. Phys.* **1935**, *3*, 699-709.

[15] a) T. J. Kealy, P. L. Pauson, Nature **1951**, 168, 1039-1040; b) S. A. Miller, J. A. Tebboth, J. F. Tremaine, J. Chem. Soc. **1952**, 632-635.

[16] J. A. Gladysz, *Chem. Rev. (Washington, DC, U. S.)* **2000**, *100*, 1167-1168.

[17] a) A. Glockner, H. Bauer, M. Maekawa, T. Bannenberg, C. G. Daniliuc, P. G. Jones, Y. Sun, H. Sitzmann, M. Tamm, M. D. Walter, *Dalton Trans.* **2012**, *41*, 6614-6624; b) H. Bauer, A. Glockner, A. C. Tagne Kuate, S. Schafer, Y. Sun, M. Freytag, M. Tamm, M. D. Walter, H. Sitzmann, *Dalton Trans.* **2014**, *43*, 15818-15828.

[18] a) C. A. Tolman, *Chem. Rev.* **1977**, *77*, 313-348; b) K. A. Bunten, L. Chen, A. L. Fernandez, A. L. Poe, **Coord. Chem. Rev.** *2002*, *233–234*, 41-51.

[19] a) C. Janiak and H. Schumann, *Adv. Organomet. Chem.* **1991**, *33*, 291–393; b) J. Okuda, *Transition Metall Coordination Chemistry* (Ed.: W. A. Herrmann), Springer Berlin Heidelberg, Berlin, Heidelberg, **1992**, *160*, 97-145.

[20] C. Elschenbroich, *Organometallchemie, Vol. 6*, Teubner, Wiesbaden **2008**.

[21] I. Kuksis, M. C. Baird, *Organometallics* **1994**, *13*, 1551-1553.

[22] S. Heinl, G. Balázs, M. Scheer, *Phosphorus, Sulfur, and Silicon and the Related Elements* **2014**, *189*, 924-932.

[23] M. Fei, S. K. Sur, D. R. Tyler, *Organometallics* **1991**, *10*, 419-423.

[24] S. Heinl, M. Scheer, *Chem. Sci.* **2014**, *5*, 3221-3225.

[25] R. J. Hoobler, M. A. Hutton, M. M. Dillard, M. P. Castellani, A. L. Rheingold, A. L. Rieger, P. H. Rieger, T. C. Richards, W. E. Geiger, *Organometallics* **1993**, *12*, 116.

[26] U. Chakraborty, M. Modl, B. Mühldorf, M. Bodensteiner, S. Demeshko, N. J. C. van Velzen, M. Scheer, S. Harder, R. Wolf, *Inorg. Chem.* **2016**, *55*, 3065-3074.

[27] a) D. J. Burkey, E. K. Alexander, T. P. Hanusa, *Organometallics* **1994**, *13*, 2773-2786; b) M. J. Harvey, T. P. Hanusa, *Organometallics* **2000**, *19*, 1556-1566; c) H. Sitzmann, F. Weber, M. D. Walter, G. Wolmershaeuser, *Organometallics* **2003**, *22*, 1931-1936.

[28] J. L. Atwood, W. E. Hunter, A. H. Cowley, R. A. Jones, C. A. Stewart, *J. Chem. Soc., Chem. Commun.* **1981**, 925-927.

[29] P. Jutzi, F. Kohl, P. Hofmann, C. Krüger, Y.-H. Tsay, *Chem. Ber.* **1980**, *113*, 757-769.

[30] C. Janiak, H. Schumann, C. Stader, B. Wrackmeyer, J. J. Zuckerman, *Chem. Ber.* **1988**, *121*, 1745-1751.

[31] H. Diskowski, T. Hofmann, *Ullmann's Encyclopedia of Industrial Chemistry*, Wiley-VCH, Weinheim, **2000**.

[32] a) D. Corbridge, *Phosphorus: An Outline of its Chemistry, Biochemistry and Technology*, 5th ed.; Elsevier: New York, **1994**; b) R. Engel, *Synthesis of Carbon Phosphorus Bonds*, 2nd ed.; CRC Press: Boca Raton, **2004**.

[33] A. P. Ginsberg, W. E. Lindsell, *J. Am. Chem. Soc.* **1971**, *93*, 2082-2084.

[34] a) M. Caporali, L. Gonsalvi, A. Rossin, M. Peruzzini, *Chem. Rev.* **2010**, *110*, 4178-4235; b) B. M. Cossairt, N. A. Piro, C. C. Cummins, *Chem. Rev.* **2010**, *110*, 4164-4177; c) M. Scheer, G. Balázs, A. Seitz, *Chem. Rev.* **2010**, *110*, 4236-4256; d) N. A. Giffin, J. D. Masuda, *Coord. Chem. Rev.* **2011**, *255*, 1342-1359; e) S. Khan, S. S. Sen, H. W. Roesky, *Chem. Commun.*, **2012**, *48*, 2169-2179; f) O. J. Scherer, *Angew. Chem. Int. Ed. Engl.* **1985**, *24*, 924-943; g) O. J. Scherer, *Angew. Chem.* **1990**, *102*, 1137-1155; h) B. Rink, O. J. Scherer, G. Heckmann, G. Wolmershauser, *Chem. Ber.* **1992**, *125*, 1011-1016; i) O. J. Scherer, *Acc. Chem. Res.* **1999**, *32*, 751-762.

[35] F. Dielmann, M. Sierka, A. V. Virovets, M. Scheer, *Angew. Chem., Int. Ed.* **2010**, *49*, 6860-6864.

[36] M. Scheer, U. Becker, *J. Organomet. Chem.* **1997**, *545-546*, 451-460.

[37] S. Heinl, E. V. Peresypkina, A. Y. Timoshkin, P. Mastrorilli, V. Gallo, M. Scheer, *Angew. Chem., Int. Ed.* **2013**, *52*, 10887-10891.

[38] S. Heinl, G. Balazs, M. Bodensteiner, M. Scheer, *Dalton Trans.* **2016**, *45*, 1962-1966.

[39] S. Heinl, G. Balázs, M. Scheer, *Phosphorus, Sulfur, and Silicon and the Related Elements* **2014**, *189*, 924-932.

[40] S. Heinl, M. Scheer, *Chem. Sci.* **2014**, *5*, 3221-3225.

[41] S. Heinl, PhD thesis, *University of Regensburg*, **2014**.

[42] S. Heinl, E. Peresypkina, J. Sutter, M. Scheer, *Angew. Chem., Int. Ed.* **2015**, *54*, 13431-13435.

[43] C. Heindl, S. Heinl, D. Lüdeker, G. Brunklaus, W. Kremer, M. Scheer, *Inorg. Chim. Acta* **2014**, *422*, 218-223.

2 Research Objectives

Until now, numerous E_n ligand complexes of transition metals are reported, containing different ligand systems. However, examples with sterically highly demanding Cp^R ligands and perarylated cyclopentadienyl ligands in particular, are rather rare. They are restricted to compounds of manganese, iron and cobalt due to the lack of appropriate precursors for the preparation. The penta-arylated ligands Cp^{PEt} ($C_5(C_6H_4Et)_5$) and Cp^{BIG} ($C_5(C_6H_4{}^nBu)_5$) have been chosen for this task, since they provide the high steric demand and show good solubility in all established organic solvents. Furthermore, only few E_n ligand complexes, bearing perarylated Cp^R ligands, have been investigated concerning their reaction behavior.

Therefore, the research objectives for this work are:

- Preparation of transition metal complexes, containing the bulky Cp^{PEt} or Cp^{BIG} ligands
- Synthesis of E_n (E = P, As) ligand complexes by activation of E_4 or from other suitable pnictogenide sources
- Investigation of the reactivity of the compounds under thermal conditions or towards reactive metal(I) complexes
- Characterization and comparison of the obtained E_n ligand complexes

3 Splitting of Coordinated E_4 (E = P, As) Ligands into Separated cyclo-E_3 and E_1 Units

Moritz Modl, Gabor Balazs, Alexandru Lupan, Amr A. A. Attia, Manfred Scheer

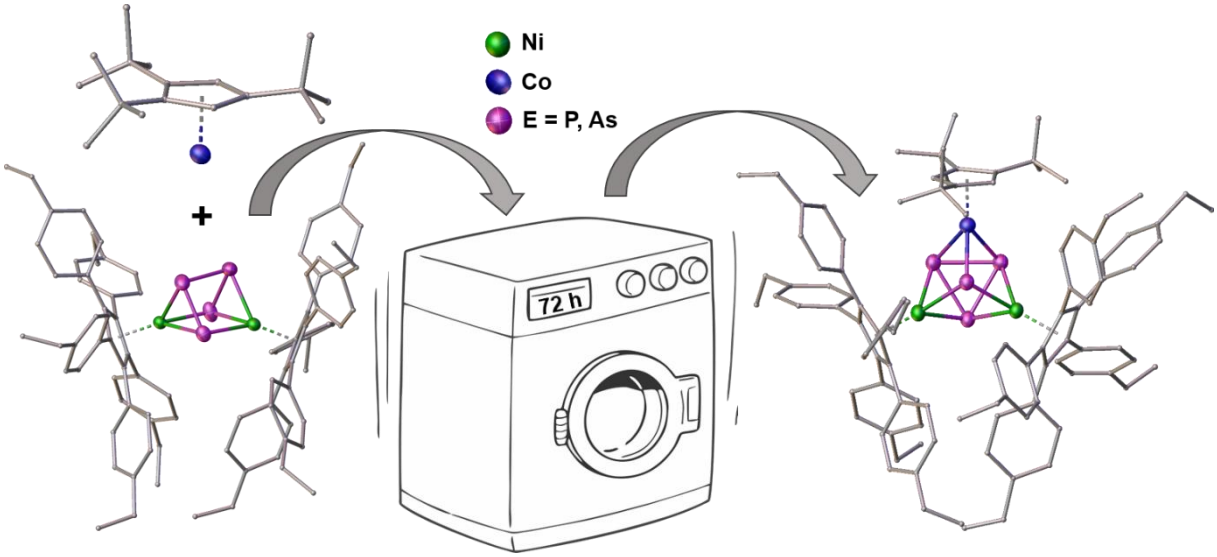

- **All syntheses and characterizations were performed by Moritz Modl, unless subsequently noted otherwise**
- **Manuscript was written by Moritz Modl except part for DFT calculations (Gabor Balázs)**
- **Figures were made by Moritz Modl except pictures corresponding to DFT calculations**
- **DFT calculations were performed by Alexandru Lupan and Amr Attia**
- **X-Ray structure analyses and refinement were performed by Moritz Modl**

3.1 Introduction

White phosphorus, P_4, represents the key compound in the synthetic and industrial production of organophosphorus derivatives.[1] The synthesis is based on the chlorination of P_4 with Cl_2 gas to generate PCl_3, which in turn is reacted with an organic substrate.[2] This procedure involves the use of very toxic chlorine gas and the generation of large amounts of waste as a side product in the reaction with organic molecules. It thus is neither sustainable nor environmentally friendly, regarding the great annual demand.[3] In this context, the coordination and activation of white phosphorus under mild conditions came into the focus of research interest to gain access to the direct functionalization of P_4. Therefore, during the last decades, the metal-mediated activation has drawn considerable attention and, starting from P_4, P_n ligand complexes of almost all transition metals have been synthesized.[4]

Along with the preparation of P_n ligand complexes, their versatile reaction pathways aroused increasing interest. Thermolytic and photolytic conversions represent a possible approach, which can lead to the transformation of the P_n moiety. In this regard, Scherer *et al.* reported on the thermolytically or photolytically induced decarbonylation and subsequent P-P bond cleavage of the so-called butterfly complex $[\{Cp^RFe(CO)_2\}_2(\mu,\eta^{1:1}\text{-}P_4)]$ (Cp^R = $\eta^5\text{-}C_5H_3{}^tBu_2$ (Cp''), $\eta^5\text{-}C_5H_2{}^tBu_3$ (Cp''')), yielding different P_4 ligand complexes and the pentaphosphaferrocene derivative ($[Cp^RFe(\eta^5\text{-}P_5)]$).[5] Similar behavior was observed for other P_n ligands and metals.[6] A functionalization of the P_n ligand can be achieved by its reactivity towards main-group nucleophiles. This was shown by Scheer *et al.* based on the complexes $[Cp^*Fe(\eta^5\text{-}P_5)]$ (Cp^* = $\eta^5\text{-}C_5H_5$) and $[Cp'''Ni(\eta^3\text{-}P_3)]$,[7] respectively. The redox behavior of $[Cp^*Fe(\eta^5\text{-}P_5)]$ has also been investigated. Winter *et al.* initially found one irreversible reduction and oxidation, followed by an equilibration to dimeric products.[8] The formed diionic species $[(Cp^*Fe)_2(\mu,\eta^{4:4}\text{-}P_{10})]^{2-/2+}$ could be isolated and characterized by Scheer *et al.*.[9] Based on these results, a manifold redox chemistry, using different P_n ligand complexes and a variety of reducing and oxidizing agents, has been developed.[10] Another area of interest is the utilization of the Lewis acidity of P_n ligand complexes in coordination chemistry. Besides the coordination to transition metal species like $[M(CO)_5]$ (M = Cr, Mo, W)[11], $[Fe(CH_3CN)_6][PF_6]$[12] or $[Cu(CH_3CN)_4][BF_4]$,[13] the formation of 1D and 2D polymers or even fullerene-like spherical aggregates is observed for certain P_n ligands, coordinating to coinage metal(I) halides.[14]

The analogue As_n ligand complexes react under similar conditions. However, this chemistry is much less established owing to the limited access to suitable sources of arsenic and their high sensitivity towards temperature and light, compared to phosphorus.[13,15]

The triple-decker sandwich complex $[(Cp'''Co)_2(\mu\text{-toluene})]$ (**2**),[16] forming 14 valence electron [Cp'''Co] fragments in non-coordinating solvent, turned out to be able of activating P_4 under mild conditions to form $[Cp'''Co(\eta^4\text{-}P_4)]$, $[(Cp'''Co)_2(\mu,\eta^{2:2}\text{-}P_2)_2]$ and different poly-

phosphorus aggregates, depending on the reaction conditions.[17] Referring to this, we got interested, in the reactivity of **2** towards P_n moieties, which are already coordinating to other transition metal fragments. For this purpose, the prismatic complex $[(Cp^RNi)_2P_4]$ (Cp^R = η^5-C_5Me_5 (Cp*), η^5-$C_5H^iPr_4$ (Cp^4)) seemed to be suitable (Scheme 1),[18] since it shows dynamic behavior in solution, as indicated by ^{31}P NMR spectroscopic studies.[18a] Furthermore, two of the P atoms of the P_4 core are accessible for coordination, as it was shown in the reaction with $[M(CO)_5(THF)]$ (M = Cr, W), leading to the coordination compounds $[(Cp^RNi)_2P_4\{(M(CO)_5\}_2]$ (Scheme 1).[18]

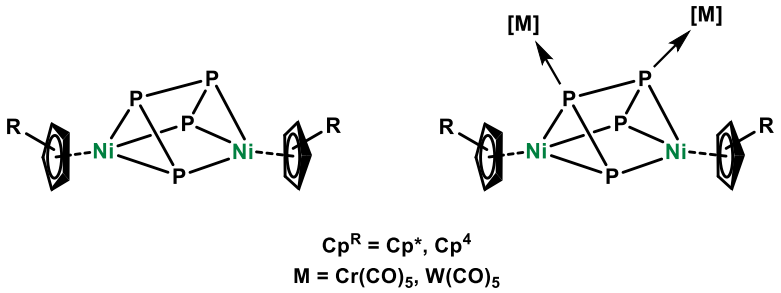

Scheme 1. $[(Cp^RNi)_2P_4]$ (left), $[(Cp^RNi)_2P_4\{(M(CO)_5\}_2]$ (right) (Cp^R = Cp*, Cp^4).

To get deeper insight into the dynamic behavior of such Ni_2P_4 prismanes in solution, we chose to synthesize the above-mentioned complex $[(Cp^RNi)_2P_4]$ using the sterically highly demanding Cp^{PEt} (Cp^{PEt} = $C_5(C_6H_4Et)_5$) ligand to presumably slow down the process. Herein we report on the synthesis of $[(Cp^{PEt}Ni)_2(\mu,\eta^{3:3}\text{-}E_4)]$ (E = P (**1a**), As (**1b**)), bearing a flexible E_4^{2-} ligand in solution and its reaction towards **2** to give a complete structural rearrangement of the E_4 moiety in the coordination sphere of Co(I). This has resulted in the first trinuclear complexes $[(Cp^{PEt}Ni)_2(Cp'''Co)(\mu_3,\eta^{1:1:1}\text{-}E)(\mu_3,\eta^{2:2:2}\text{-}E_3)]$ (E = P (**3a**), As (**3b**)), bearing an E_1 and a *cyclo*-E_3 ligand.

3.2 Results and Discussion

The reduction of $[Cp^{PEt}Ni(\mu\text{-}Br)]_2$ with two equivalents of potassium graphite in toluene leads to the formation of a "$Cp^{PEt}Ni(I)$" synthon, proposed by Wolf *et al.*.[19] The reaction of this "$Cp^{PEt}Ni(I)$" source with P_4 and As_4, respectively, at -10 °C gave the complexes $[(Cp^{PEt}Ni)_2(\mu,\eta^{3:3}\text{-}E_4)]$ (E = P (**1a**), As (**1b**)) (Scheme 2). After chromatographic workup, **1a** and **1b** can be isolated in moderate yields of 54% and 32%, respectively.

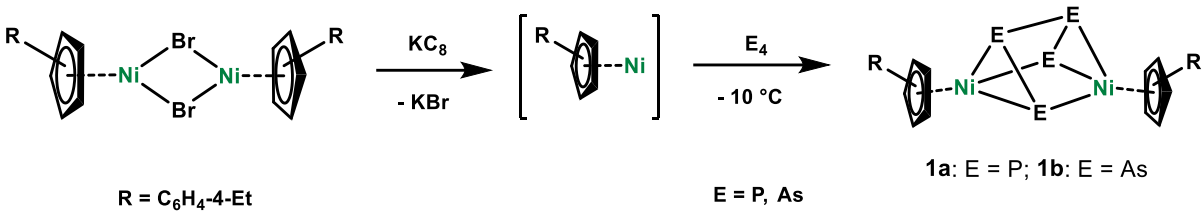

Scheme 2. Synthesis of complexes **1a** and **1b**.

Dark blackish single-crystals of **1a** and **1b**, respectively, were grown from CH_2Cl_2 solutions, layered with CH_3CN after complete diffusion. X-ray diffraction studies display the formation of prismatic Ni_2E_4 complexes in the solid state. In both cases, the two Ni atoms are bridged by an E_4^{2-} ligand with a $\eta^{3:3}$-coordination mode. The average P-P (**1a**: 2.1736(1) Å) and As-As (**1b**: 2.4132(1) Å) distances, respectively, lie in the range of E-E single bonds.[20] Comparable bond lengths were observed for the related Cp''' and Cp^4 derivatives.[18a,21]

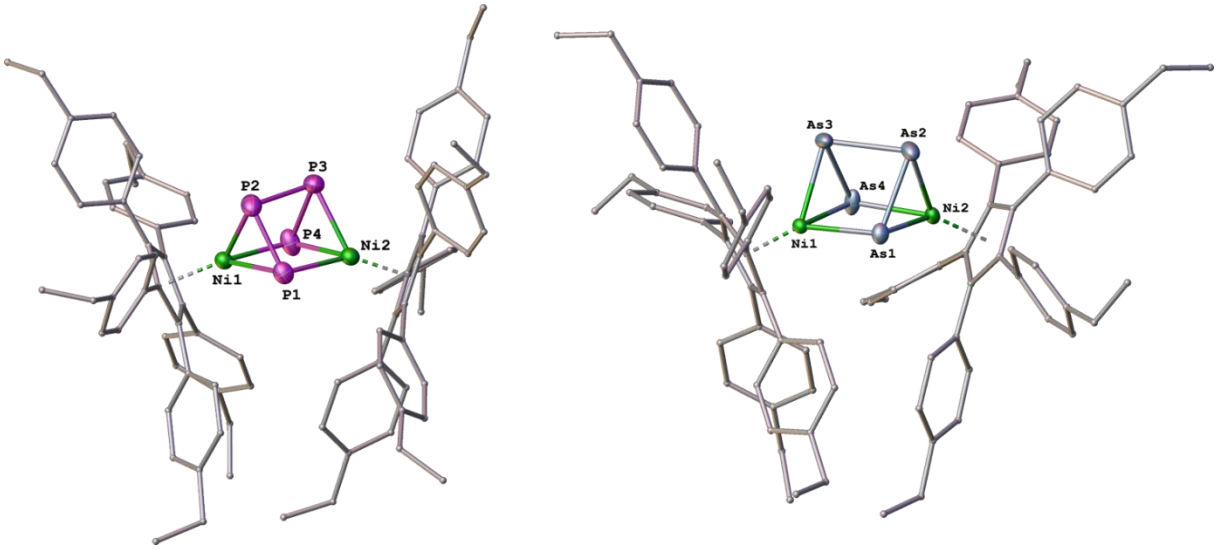

Figure 1. Solid-state molecular structures of **1a** (left) and **1b** (right). Thermal ellipsoids are set at 50% probability. In case of disorder, only the main part is shown. For clarity reasons solvent molecules and H atoms are omitted and Cp^{PEt} ligands are drawn in 'wire-or-stick' model. Selected bond lengths [Å] and angles [°] in **1a**: Ni1-P1 2.22927(7), Ni1-P2 2.28157(7), Ni1-P3 3.31211(11), Ni1-P4 2.21356(7), Ni2-P1 2.22303(7), Ni2-P2 3.31776(11), Ni2-P3 2.26007(6), Ni2-P4 2.21501(7), P1-P2 2.08330(6), P2-P3 2.22470(7), P3-P4 2.21268(6), P4-P1 2.67452(7), Ni1-Ni2 3.54417(13), Ni1-$Cp_{centroid}$ 1.772(1), Ni2-$Cp_{centroid}$ 1.766(1), P1-P2-P3 83.775(2), P2-P3-P4 84.692(3), $(Ni1\text{-}P2\text{-}P3\text{-}P4)_{plane}$-$(Ni2\text{-}P1\text{-}P2\text{-}P3)_{plane}$ 59.208(2). Selected bond lengths [Å] and angles [°] in **1b**: Ni1-As1 2.32824(7), Ni1-As2 3.60885(11), Ni1-As3 2.35683(7), Ni1-As4 2.33882(10), Ni2-As1 2.3355(1), Ni2-As2 2.40905(10), Ni2-As3 3.59124(12), Ni2-As4 2.32565(7), As1-As2 2.34873(7), As2-As3 2.43926(7), As3-As4 2.45152(11), As4-As1 2.90626(11), Ni1-Ni2 3.64458(13), Ni1-$Cp_{centroid}$ 1.761(1), Ni2-$Cp_{centroid}$ 1.778(1), As1-As2-As3 79.468(2), As2-As3-As4 81.710(3), $(Ni1\text{-}As1\text{-}As2\text{-}As3)_{plane}$-$(Ni2\text{-}As2\text{-}As3\text{-}As4)_{plane}$ 56.979(2).

The ^1H and $^{13}C\{^1H\}$ NMR spectra of **1a** and **1b**, respectively, show that the Cp^{PEt} ligands are magnetically equivalent. For **1a**, a triplet and a quartet, corresponding to the ethyl groups, arise at 1.03 ppm and 2.36 ppm, while the aromatic protons appear as two doublets at 6.69 ppm and 7.22 ppm. The analogous set of resonances is observed for **1b** at 0.99 ppm (t), 2.34 ppm

(q), 6.71 ppm (d) and 7.32 ppm (d), respectively. Complex **1a** was further investigated by $^{31}P\{^1H\}$ NMR spectroscopy, which revealed a broadened singlet at 104.6 ppm ($\omega_{1/2}$ = 265 Hz) at 300 K, suggesting a dynamic behavior in solution. Detailed investigations were made by variable-temperature $^{31}P\{^1H\}$ NMR spectroscopy. Cooling down a toluene-d_8 solution to 243 K leads to breakdown of coalescence of the signal and at lower temperatures, a successive signal splitting is observed. At 193 K two doublets can be identified at 123.9 ppm and 85.3 ppm with a coupling constant of $^1J_{PP} \approx 246$ Hz and relative intensities of 1:1 (see Figure 2).

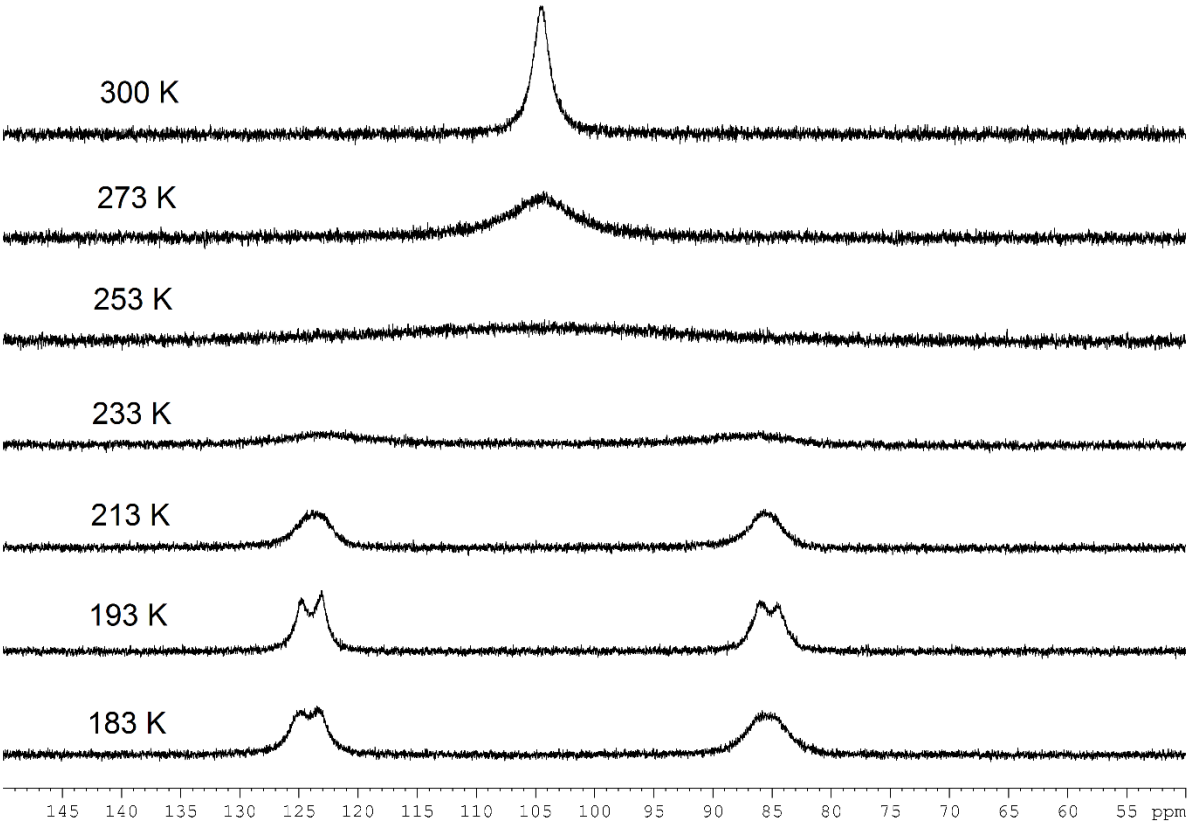

Figure 2. VT $^{31}P\{^1H\}$ NMR spectrum of **1a** in toluene-d_8.

This behavior is characteristic of a dynamic process involving the P_4 ligand. The structural change via a *cyclo*-P_4 ligand (Scheme 3) at room temperature on NMR timescale can be discussed, resulting from a proposed rotation of the P atoms and the formation of two new Ni-P bonds. The rapid occurrence of this process on the NMR time scale leads to the observed spectrum of **1a** with a single P resonance at room temperature. A similar rearrangement was proposed by Scherer *et al.* for the Cp^4 derivative in solution.[18a] Compared to the Cp''' and Cp^4 derivatives, that exhibit a sharp singlet at room temperature and a broadened singlet at 173 K,[18a,21] it can be reasoned that the very bulky Cp^{PEt} ligand is also involved in the dynamics and slows down the motion, being trackable on the NMR time scale.

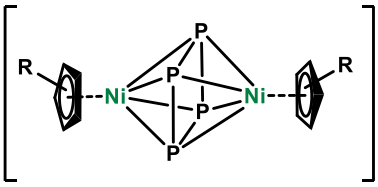

Scheme 3. Suggested time-averaged octahedral structure with a *cyclo*-P_4 unit in solution, based on spectroscopic investigations on **1a**.

Complexes **1a** and **1b** react with the complex [(Cp'''Co)$_2$(μ-toluene)] (**2**) at room temperature. In both cases, a complete transformation of **1a** and **1b**, respectively, to a single product is observed, as shown by the ^{1}H and ^{31}P NMR spectra of the crude reaction mixture. The resulting trinuclear compounds [(Cp^{PEt}Ni)$_2$(Cp'''Co)(μ$_3$,η$^{1:1:1}$-E)(μ$_3$,η$^{2:2:2}$-E$_3$)] (E = P (**3a**), As (**3b**)), exhibit an E_1 and a *cyclo*-E_3 ligand, bridging the metal atoms (Scheme 4) and can be isolated in 28% and 26% crystalline yield, respectively.[22]

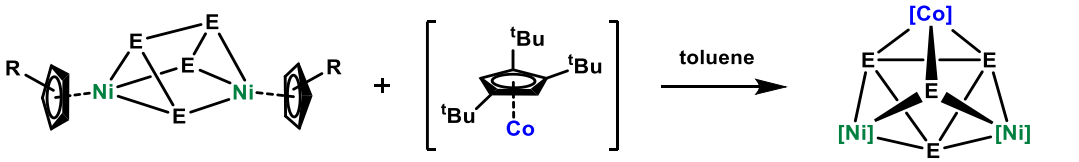

1a: E = P; **1b**: E = As

2

3a: E = P; **3b**: E = As
[Ni] = Cp^{PEt}Ni; [Co] = Cp'''Co

Scheme 4. Synthesis of complexes **3a** and **3b**.

Single crystals of **3a** and **3b** were grown from CH_2Cl_2 solutions, layered with CH_3CN, after complete diffusion. X-ray diffraction measurements revealed the formation of an unusual Ni_2CoE_4 core, composed of a tetrahedral E_4 with three metal-capped faces. The observed distances between the E_1 ligand and the metal atoms of 2.26045(3), 2.28831(3) (Ni-P) and 2.24447(5) Å (Co-P) in **3a** and 2.39967(3), 2.36826(3) (Ni-As) and 2.36158(6) Å (Co-As) in **3b**, respectively, are comparable to those of related compounds.[23] An E_1 moiety, bridging three metal centers has been reported for phosphorus and arsenic, respectively.[23] Furthermore, it has been found in different clusters of iron, cobalt, nickel and mixed ones.[23] Regarding the *cyclo*-E_3 ligand, the E-E bond lengths (**3a**: 2.35274(5), 2.32849(5), 2.38493(3) Å; **3b**: 2.57541(6), 2.60338(6), 2.61359(5) Å) are quite similar and lie in the range of strongly elongated E-E single bonds.[20] The *cyclo*-As_3 ligand of **3b** is similar to those found in [(Cp*Fe)$_2$(Cp*Co)(μ$_3$,η$^{2:2:2}$-As$_3$)$_2$],[15f] which is also threefold coordinated by metal fragments. However, the E-E bonds are considerably longer than those observed for other cyclopentadienyl transition metal complexes, containing a *cyclo*-E_3 moiety.[24] The distance between the E_1 and E_3 ligand is in average 2.6493 Å (**3a**: P-P distances) and 2.8508 Å (**3b**: As-As distances), respectively, which is considered to be nonbonding.

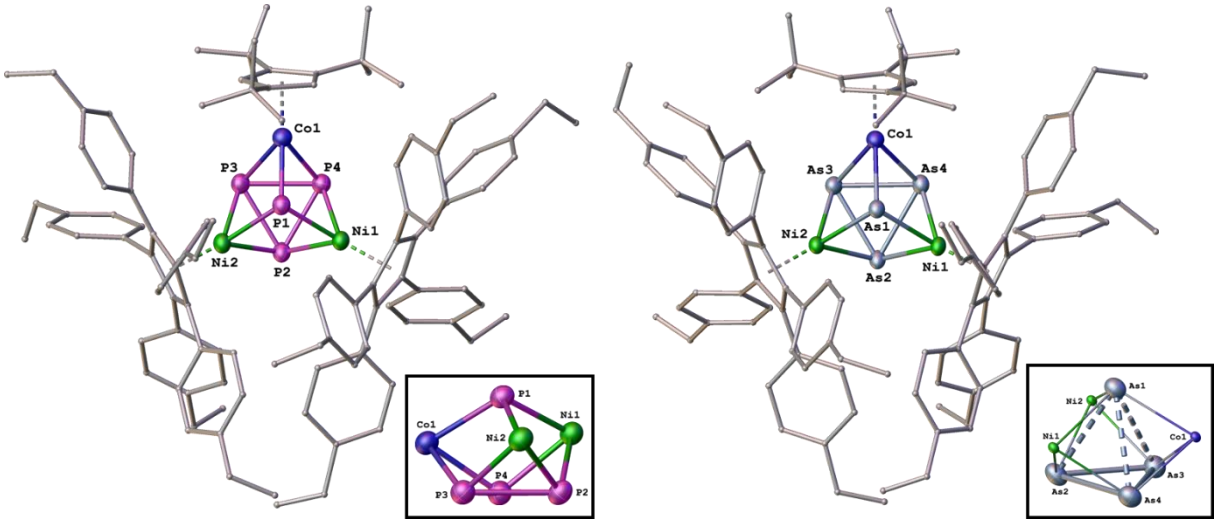

Figure 3. Solid-state molecular structures of **3a** (left) and **3b** (right). Thermal ellipsoids are set at 50% probability. In case of disorder, only the main part is shown. For clarity reasons solvent molecules and H atoms are omitted and Cp^{PEt} ligands are drawn in 'wire-or-stick' model. Selected bond lengths [Å] and angles [°] in **3a**: Ni1-P1 2.26045(3), Ni1-P2 2.21865(2), Ni1-P4 2.21963(5), Ni2-P1 2.28831(3), Ni2-P2 2.22437(2), Ni2-P3 2.21049(5), Co1-P1 2.24447(5), Co1-P3 2.16507(3), Co2-P4 2.18801(4), P1-P2 2.69066(5), P1-P3 2.58419(4), P1-P4 2.67300(4), P2-P3 2.35274(5), P2-P4 2.32849(5), P3-P4 2.38493(3), Ni1-Ni2 3.49664(5), Co1-Ni1 3.48913(8), Co1-Ni2 3.57948(7), P2-P3-P4 58.8717(7), P3-P4-P2 59.8743(8), P4-P2-P3 61.2539(15). Selected bond lengths [Å] and angles [°] in **3b**: Ni1-As1 2.39967(3), Ni1-As2 2.32932(3), Ni1-As4 2.32629(6), Ni2-As1 2.36826(3), Ni2-As2 2.32793(3), Ni2-As3 2.33144(6), Co1-As1 2.36158(6), Co1-As3 2.30605(4), Co1-As4 2.28344(4), As1-As2 2.87061(6), As1-As3 2.88128(5), As1-As4 2.80055(5), As2-As3 2.57541(6), As2-As4 2.60338(6), As3-As4 2.61359(5), Ni1-Ni2 3.66201(6), Co1-Ni1 3.71431(8), Co1-Ni2 3.62463(8), As2-As3-As4 60.2213(9), As3-As4-As2 59.1625(8), As4-As2-As3 60.6162(17). A representation of the Ni_2CoE_4 cores of **3a** (Cp^R ligands are omitted for clarity) and **3b** (stippled bonds between the As_1 and As_3 ligand to show the tetrahedral geometry; Cp^R ligands are omitted and metal atoms are sized down for clarity) are shown in the insets.

In order to clarify the bonding situation DFT calculations have been performed for **3a** at the M11-L/6-31g(d) level. The optimized geometry reproduces well the experimental one, although the P···P distances between the P_1 and P_3 unit are slightly longer than the experimental ones. The P-P bond lengths within the *cyclo*-P_3 ligand are well reproduced by the calculations. The Wiberg Bond indices (WBI) of the P-P bonds within the *cyclo*-P_3 unit correspond to elongated single bonds (0.51, 0.55 and 0.61), while the WBI of the P···P interactions between the P_1 and *cyclo*-P_3 ligand are considerably lower indicating only a weak interaction (WBI 0.13, 0.14 and 0.22). These results are in agreement with the structural parameters as well as the results of the ^{31}P NMR spectroscopic investigations.

The ^{1}H and $^{13}C\{^{1}H\}$ NMR spectra of **3a** and **3b** in C_6D_6, respectively, display the expected number of resonances and multiplicities for a Cp''' and two chemically equivalent Cp^{PEt} ligands (see the Supporting Information). The $^{31}P\{^{1}H\}$ NMR spectrum of **3a** reveals three groups of signals with an integral ratio of 2:1:1. A singlet at 193.9 ppm corresponds to the P_1 ligand, while

the *cyclo*-P_3 ligand appears as a doublet at 204.1 ppm (P_x) and a triplet at 274.8 ppm (P_A) with a coupling constant of $^1J_{PP}$ = 133.9 Hz (Figure 4). The relatively small P_A-P_X coupling reflects the long distances between the atoms of the *cyclo*-P_3 moiety, as observed in the X-ray structure. The sharpness of the signals indicates the rigidity of the structure. Furthermore, the absence of a coupling between the P_1 and the P_3 ligand confirms their separation.

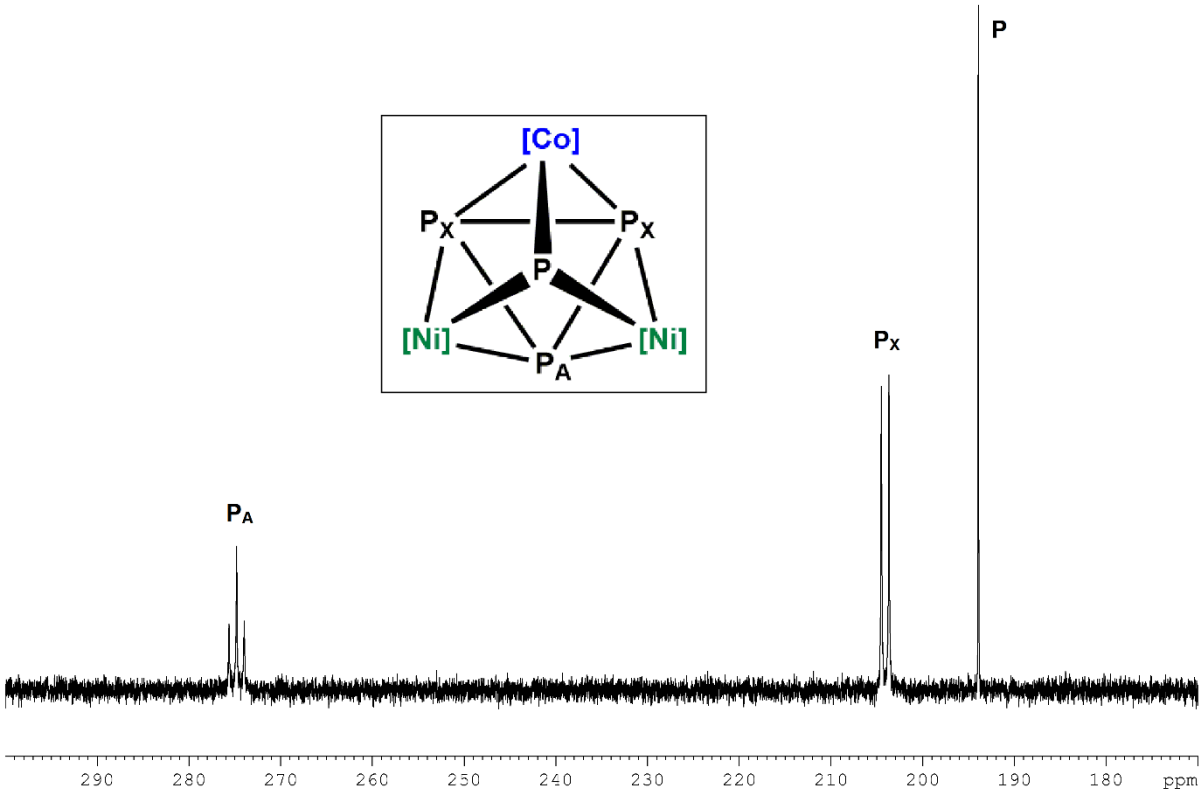

Figure 4. $^{31}P\{^1H\}$ NMR spectrum of **3a** in C_6D_6 at 298 K.

3.3 Conclusion

In summary, we have synthesized the novel complexes $[(Cp^{PEt}Ni)_2(\mu,\eta^{3:3}\text{-}E_4)]$ (E = P (**1a**), As (**1b**)) with a prismatic structural motif. The E_4 ligand of **1a** and **1b**, respectively, shows dynamic behavior in solution, as investigated for **1a** by $^{31}P\{^1H\}$ NMR spectroscopy. The steric bulk of the Cp^{PEt} ligands slows this dynamic behavior as indicated by the breakdown of the coalescence at lower temperatures, leading to a successive signal splitting into two doublets. Furthermore, we have shown that the 14 valence electron fragment [Cp'''Co] (**2**) reacts with the newly synthesized complexes **1a** and **1b**, respectively, by splitting the coordinated E_4 ligand into a *cyclo*-E_3 and an E_1 unit, leading to the unique trinuclear complexes $[(Cp^{PEt}Ni)_2(Cp'''Co)(\mu_3,\eta^{1:1:1}\text{-}E)(\mu_3,\eta^{2:2:2}\text{-}E_3)]$ (E = P (**3a**), As (**3b**)).

3.4 References

[1] H. Diskowski, T. Hofmann, *Ullmann's Encyclopedia of Industrial Chemistry*, Wiley-VCH, Weinheim, **2000**.

[2] a) D. Corbridge, *Phosphorus: An Outline of its Chemistry, Biochemistry and Technology*, 5th ed.; Elsevier: New York, **1994**; b) R. Engel, *Synthesis of Carbon Phosphorus Bonds*, 2nd ed.; CRC Press: Boca Raton, **2004**.

[3] D. Cordell, S. White, *Annual Review of Environment and Resources* **2014**, *39*, 161-188.

[4] a) B. M. Cossairt, N. A. Piro, C. C. Cummins, *Chem. Rev.* **2010**, *110*, 4164-4177; b) M.Caporali, L.Gonsalvi, A. Rossin, M. Peruzzini, *Chem. Rev.* **2010**, *110*, 4178–4235.

[5] **Thermolysis:** a) O. J. Scherer, T. Hilt, G. Wolmershäuser, *Organometallics* **1998**, *17*,4110– 4112; **Photolysis:** b) O. J. Scherer, G. Schwarz, G. Wolmershäuser, *Z. Anorg.Allg. Chem.* **1996**, *622*, 951-957.

[6] **Fe:** a) C. Eichhorn, O. J. Scherer, T. Sögding, G. Wolmershäuser, *Angew. Chem., Int. Ed.* **2001**, *40*, 2859-2861; **Co:** b) S. Dürr, D. Ertler, U. Radius, *Inorg. Chem.* **2012**, *51*, 3904-3909; c) F. Dielmann, A. Timoshkin, M. Piesch, G. Balázs, M. Scheer, *Angew. Chem., Int. Ed.* **2017**, *56*, 1671-1675; **Ni:** d) M. Scheer, U. Becker, *Chem. Ber.* **1996**, *129*, 1307-1310.

[7] a) E. Mädl, M. V. Butovskii, G. Balázs, E. V. Peresypkina, A. V. Virovets, M. Seidl, M. Scheer, *Angew. Chem., Int. Ed.* **2014**, *53*, 7643-7646. b) E. Mädl, G. Balázs, E. V. Peresypkina, M. Scheer, *Angew. Chem., Int. Ed.* **2016**, *55*, 7702-7707.

[8] R. F. Winter, W. E. Geiger, *Organometallics* **1999**, *18*, 1827-1833.

[9] M. V. Butovskiy, G. Balázs, M. Bodensteiner, E. V. Peresypkina, A. V. Virovets, J. Sutter, M. Scheer, *Angew. Chem., Int. Ed.* **2013**, *52*, 2972–2976.

[10] a) E. Mädl, G. Balázs, E. V. Peresypkina, M. Scheer, *Angew. Chem., Int. Ed.* **2016**, *55*, 7702-7707; b) T. Li, N. Arleth, M. T. Gamer, R. Köppe, T. Augenstein, F. Dielmann, M. Scheer, S. N. Konchenko, P. W. Roesky, *Inorg. Chem.* **2013**, *52*, 14231-14236; c) O. J. Scherer, S. Weigel, G. Wolmershäuser, *Heteroat. Chem.* **1999**, *10*, 622-626; d) T. Li, J. Wiecko, N. A. Pushkarevsky, M. T. Gamer, R. Köppe, S. N. Konchenko, M. Scheer, P. W. Roesky, *Angew. Chem. Int. Ed.* **2011**, *50*, 9491-9495.

[11] a) O. J. Scherer, J. Braun, P. Walther, G. Wolmershäuser, *Chem. Ber.* **1992**, *125*, 2661-2665; b) M. Scheer, U. Becker, J. C. Huffman, M. H. Chisholm, *J. Organomet. Chem.* **1993**, *461*, C1-C3; c) O. J. Scherer, G. Berg, G. Wolmershäuser, *Chem. Ber.* **1995**, *128*, 635-639; d) M. Scheer, U. Becker, M. H. Chisholm, J. C. Huffman, F. Lemoigno, O. Eisenstein, *Inorg. Chem.* **1995**, *34*, 3117-3119; e) M. Scheer, U. Becker, *Chem. Ber.* **1996**, *129*, 1307-1310; f) M. Scheer, U. Becker, *J. Organomet. Chem.* **1997**, *545–546*, 451-460.

[12] J. Müller, S. Heinl, C. Schwarzmaier, G. Balázs, M. Keilwerth, K. Meyer, M. Scheer, *Angew. Chem., Int. Ed.* **2017**, *56*, 7312-7317.

[13] C. Schwarzmaier, S. Heinl, G. Balázs, M. Scheer, *Angew. Chem., Int. Ed.* **2015**, *54*, 13116-13121.

[14] a) J. Bai, A. V. Virovets, M. Scheer, *Angew. Chem., Int. Ed.* **2002**, *41*, 1737-1740; b) J. Bai, A. V. Virovets, M. Scheer, *Science* **2003**, *300*, 781-783; c) S. Heindl, D. Luedeker, G. Brunklaus, W.

Kremer, M. Scheer, *Inorganica Chimica Acta* **2014**, 218-223; d) F. Dielmann, M. Fleischmann, C. Heindl, E. V. Peresypkina, A. V. Virovets, R. M. Gschwind, M. Scheer, *Chem. Eur. J.* **2015**, *21*, 6208-6214; e) F. Dielmann, C. Heindl, F. Hastreiter, E. V. Peresypkina, A. V. Virovets, R. M. Gschwind, M. Scheer, *Angew. Chem., Int. Ed.* **2014**, *53*, 13605-13608; f) F. Dielmann, E. V. Peresypkina, B. Krämer, F. Hastreiter, B. P. Johnson, M. Zabel, C. Heindl, M. Scheer, *Angew. Chem., Int. Ed.* **2016**, *55*, 14833-14837; g) F. Dielmann, A. Schindler, S. Scheuermayer, J. Bai, R. Merkle, M. Zabel, A. V. Virovets, E. V. Peresypkina, G. Brunklaus, H. Eckert, M. Scheer, *Chem. Eur. J.* **2012**, *18*, 1168-1179; h) M. Fleischmann, L. Dütsch, M. Elsayed Moussa, G. Balázs, W. Kremer, C. Lescop, M. Scheer, *Inorg. Chem.* **2016**, *55*, 2840-2854; i) M. Fleischmann, S. Welsch, E. V. Peresypkina, A. V. Virovets, M. Scheer, *Chem. Eur. J.* **2015**, *21*, 14332-14336; j) C. Heindl, E. Peresypkina, A. V. Virovets, I. S. Bushmarinov, M. G. Medvedev, B. Krämer, B. Dittrich, M. Scheer, *Angew. Chem., Int. Ed.* **2017**, *56*, 13237-13243; k) C. Heindl, E. V. Peresypkina, D. Lüdeker, G. Brunklaus, A. V. Virovets, M. Scheer, *Chem. Eur. J.* **2016**, *22*, 2599-2604; l) C. Heindl, E. V. Peresypkina, A. V. Virovets, W. Kremer, M. Scheer, *J. Am. Chem. Soc.* **2015**, *137*, 10938-10941; m) M. Scheer, A. Schindler, J. Bai, B. P. Johnson, R. Merkle, R. Winter, A. V. Virovets, E. V. Peresypkina, V. A. Blatov, M. Sierka, H. Eckert, *Chem. Eur. J.* **2010**, *16*, 2092-2107; n) A. Schindler, C. Heindl, G. Balázs, C. Gröger, A. V. Virovets, E. V. Peresypkina, M. Scheer, *Chem. Eur. J.* **2012**, *18*, 829-835.

[15] a) M. Schmidt, D. Konieczny, E. V. Peresypkina, A. V. Virovets, G. Balázs, M. Bodensteiner, F. Riedlberger, H. Krauss, M. Scheer, *Angew. Chem., Int. Ed.* **2017**, *56*, 7307-7311; b) C. Schwarzmaier, M. Bodensteiner, A. Y. Timoshkin, M. Scheer, *Angew. Chem., Int. Ed.* **2014**, *53*, 290-293; c) C. Schwarzmaier, A. Y. Timoshkin, G. Balázs, M. Scheer, *Angew. Chem., Int. Ed.* **2014**, *53*, 9077-9081; d) C. Schwarzmaier, A. Y. Timoshkin, M. Scheer, *Angew. Chem., Int. Ed.* **2013**, *52*, 7600-7603; e) O. J. Scherer, C. Blath, G. Wolmershäuser, *J. Organomet. Chem.* **1990**, *387*, C21-C24; f) G. Friedrich, O. J. Scherer, G. Wolmershäuser, *Z. Anorg. Allg. Chem.* **1996**, *622*, 1478-1486; g) B. Rink, O. J. Scherer, G. Heckmann, G. Wolmershäuser, *Chem. Ber.* **1992**, *125*, 1011-1016; h) B. Rink, O. J. Scherer, G. Wolmershäuser, *Chem. Ber.* **1995**, *128*, 71-73; i) M. Detzel, G. Friedrich, O. J. Scherer, G. Wolmershäuser, *Angew. Chem. Int. Ed. Engl.* **1995**, *34*, 1321-1323; j) H. Krauss, G. Balázs, M. Bodensteiner, M. Scheer, *Chem. Sci.* **2010**, *1*, 337-342; k) H. Krauss, G. Balázs, M. Bodensteiner, M. Scheer, *Chem. Sci.* **2010**, *1*, 337-342; l) M. Fleischmann, S. Welsch, H. Krauss, M. Schmidt, M. Bodensteiner, E. V. Peresypkina, M. Sierka, C. Gröger, M. Scheer, *Chem. Eur. J.* **2014**, *20*, 3759-3768; m) M. Fleischmann, J. S. Jones, F. P. Gabbai, M. Scheer, *Chem. Sci.* **2015**, *6*, 132-139; n) T. Li, M. T. Gamer, M. Scheer, S. N. Konchenko, P. W. Roesky, *Chem. Commun.* **2013**, *49*, 2183-2185; o) M. Fleischmann, L. Dütsch, M. E. Moussa, A. Schindler, G. Balazs, C. Lescop, M. Scheer, *Chem. Commun.* **2015**, *51*, 2893-2895; p) L. J. Gregoriades, H. Krauss, J. Wachter, A. V. Virovets, M. Sierka, M. Scheer, *Angew. Chem. Int. Ed.* **2006**, *45*, 4189-4192; q) N. Arleth, M. T. Gamer, R. Köppe, S. N. Konchenko, M. Fleischmann, M. Scheer, P. W. Roesky, *Angew. Chem. Int. Ed.* **2016**, *55*, 1557-1560.

[16] J. J. Schneider, D. Wolf, C. Janiak, O. Heinemann, J. Rust, C. Krüger, *Chem. Eur. J.* **1998**, *4*, 1982-1991.

[17] a) F. Dielmann, M. Sierka, A. V. Virovets, M. Scheer, *Angew. Chem. Int. Ed.* **2010**, *49*, 6860-6864; b) F. Dielmann, A. Timoshkin, M. Piesch, G. Balázs, M. Scheer, *Angew. Chem., Int. Ed.* **2017**, *56*, 1671-1675.

[18] a) O. J. Scherer, J. Braun, P. Walther, G. Wolmershäuser, *Chem. Ber.* **1992**, *125*, 2661-2665; b) M. Scheer, U. Becker, *Chem. Ber.* **1996**, *129*, 1307-1310.

[19] a) U. Chakraborty, B. Mühldorf, N. J. C. van Velzen, B. de Bruin, S. Harder, R. Wolf, *Inorg. Chem.* **2016**, *55*, 3075-3078; b) U. Chakraborty, F. Urban, B. Mühldorf, C. Rebreyend, B. de Bruin, N. van Velzen, S. Harder, R. Wolf, *Organometallics* **2016**, *35*, 1624-1631.

[20] P. Pyykkö, M. Atsumi, *Chem. Eur. J.* **2009**, *15*, 186-197.

[21] M. D. Eberl, *Ph.D. thesis*, Universität Regensburg, **2011**.

[22] The ^{1}H and ^{31}P{^{1}H} NMR measurements suggest the full conversion of **1a** and **1b** and the exclusive formation of **3a** and **3b**, respectively. Analytically pure samples of **3a** and **3b** can be obtained by crystallization, which leads to lower isolated yields due to the high solubility of the Cp^{PEt} ligands.

[23] a) O. J. Scherer, J. Braun, G. Wolmershäuser, *Chem. Ber.* **1990**, *123*, 471-475; b) M. Scheer, U. Becker, M. H. Chisholm, J. C. Huffman, F. Lemoigno, O. Eisenstein, *Inorg. Chem.* **1995**, *34*, 3117-3119; c) O. J. Scherer, G. Kemény, G. Wolmershäuser, *Chem. Ber.* **1995**, *128*, 1145-1148; d) O. J. Scherer, S. Weigel, G. Wolmershäuser, *Chem. Eur. J.* **1998**, *4*, 1910-1916.

[24] **Phosphorus:** a) O. J. Scherer, J. Braun, G. Wolmershäuser, *Chem. Ber.* **1990**, *123*, 471-475; b) L. Y. Goh, C. K. Chu, R. C. S. Wong, T. W. Hambley, *J. Chem. Soc., Dalton Trans.* **1989**, 1951-1956; c) S. Umbarkar, P. Sekar, M. Scheer, *J. Chem. Soc., Dalton Trans.* **2000**, 1135-1137; d) J. Scherer, H. Sitzmann, G. Wolmershauser, *Acta Cryst.* **1985**, C*41*, 1761-1763; e) L. J. Gregoriades, B. K. Wegley, M. Sierka, E. Brunner, C. Gröger, E. V. Peresypkina, A. V. Virovets, M. Zabel, M. Scheer, *Chem. Asian J.* **2009**, *4*, 1578-1587; **Arsenic:** f) O. J. Scherer, W. Wiedemann, G. Wolmershäuser, *Chem. Ber.* **1990**, *123*, 3-6; g) W. Chen, R. C. S. Wong, L. Y. Goh, *Acta Cryst.* **1994**, C*50*, 998-1000. h) I. Bernal, H. Brunner, W. Meier, H. Pfisterer, J. Wachter, M. L. Ziegler, *Angew. Chem., Int. Ed.* **1984**, *23*, 438-439; i) O. J. Scherer, J. Braun, P. Walther, G. Wolmershäuser, *Chem. Ber.* **1992**, *125*, 2661-2665.

3.5 Supporting Information

General Remarks

All experiments were performed with dry argon or nitrogen using glove box and Schlenk techniques. Solvents were dried using a MB SPS-800 device of company MBRAUN. KC_8 and P_4 were available and solutions of As_4,[1] $[Cp^{PEt}NiBr]_2$[2] and $[(Cp'''Co)_2(\mu\text{-toluene})]$[3] were prepared according to literature procedures. ^1H, ^{13}C and ^{31}P NMR spectra were measured on a Bruker Avance 400 (^1H: 400.130 MHz, ^{13}C: 100.613 MHz, ^{31}P: 161.976 MHz). The chemical shifts are reported in ppm relative to external TMS (^1H, ^{13}C) and H_3PO_4 (^{31}P). Mass spectra were performed on a Finnigan MAT95 LIFDI-MS spectrometer. Elemental analysis (CHN) was determined using a Vario micro cube and Vario EL III instrument.

Synthesis of $[(Cp^{PEt}Ni)_2(\mu,\eta^{3:3}\text{-}E_4)]$ (E = P (1a), E = As (1b))

To a mixture of $[Cp^{PEt}Ni(\mu\text{-Br})]_2$ (E = P: 1.00 g, 0.69 mmol; E = As: 300 mg, 0.20 mmol) and KC_8 (E = P: 0.23 g, 1.38 mmol; E = As: 65 mg, 0.40 mmol) 30 mL toluene was added at room temperature and stirred for 18 h. The resulting green solution was filtered over celite and added dropwise to a solution of E_4 (E = P: 0.08 g, 0.69 mmol in 25 mL toluene; E = As: freshly prepared solution of As_4 in 200 mL toluene) at -10 °C. A color change to dark brown occurred and the reaction mixture was stirred for 1 h. After removal of the solvent, the crude product was purified by column chromatography (silica, hexane/toluene 4:1). Evaporation of the solvent gives pure **1a**/**1b**.

1a: Yield 0.51 g (54 %).

^1H NMR (298 K, Tol-d_8): δ [ppm] = 1.03 (30H, t, $^3J_{HH}$ = 7.6 Hz, CH_3), 2.36 (20H, q, $^3J_{HH}$ = 7.6 Hz, CH_2), 6.69 (20H, d, $^3J_{HH}$ = 7.9 Hz, C*H*), 7.22 (20H, d, $^3J_{HH}$ = 7.9 Hz, C*H*).

$^{13}C\{^1H\}$ NMR (298 K, Tol-d_8): δ [ppm] = 15.1 (Et), 28.7 (Et), 109.9 (C_5), 127.5 (Ph), 130.7 (Ph), 132.9 (Ph), 142.3 (Ph).

$^{31}P\{^1H\}$ NMR (298 K, Tol-d_8): δ [ppm] = 104.6 (4P, s br).

Elemental analysis ($C_{90}H_{90}Ni_2P_4$): calculated: C 76.50, H 6.42; found: C 76.50, H 6.57.

Mass spectrometry (LIFDI, toluene): m/z 1412.57 (57%) $[M]^+$, 1381.58 (100%) $[M\text{-}P]^+$, 1350.61 (32%) $[M\text{-}P_2]^+$, 736.24 (4%) $[Cp^{PEt}NiP_3]^+$, 586.38 (1%) $[Cp^{PEt}]^+$.

1b: Yield 0.10 g (32 %).

^1H NMR (298 K, C_6D_6): δ [ppm] = 0.99 (30H, t, $^3J_{HH}$ = 7.6 Hz, CH_3), 2.34 (20H, q, $^3J_{HH}$ = 7.6 Hz, CH_2), 6.71 (20H, d, $^3J_{HH}$ = 8.2 Hz, C*H*), 7.32 (20H, d, $^3J_{HH}$ = 8.2 Hz, C*H*).

$^{13}C\{^1H\}$ NMR (298 K, Tol-d_8): δ [ppm] = 15.1 (Et), 28.7 (Et), 109.1 (C_5), 127.5 (Ph), 131.0 (Ph), 132.9 (Ph), 142.3 (Ph).

Elemental analysis ($C_{90}H_{90}Ni_2As_4$ * 2 CH_2Cl_2): calculated: C 62.83, H 5.39; found: C 62.84, H 5.62.

Mass spectrometry (LIFDI, toluene): m/z 1588.29 (100%) $[M]^+$, 1513.37 (15%) $[M\text{-}As]^+$, 868.06 (8%) $[Cp^{PEt}NiAs_3]^+$, 586.38 (3%) $[Cp^{PEt}]^+$.

Synthesis of $[(Cp^{PEt}Ni)_2(Cp'''Co)(\mu_3,\eta^{1:1:1}\text{-}E)(\mu_3,\eta^{2:2:2}\text{-}E_3)]$ (E = P (3a), As (3b))

A mixture of $[(Cp'''Co)_2(toluene)]$ (**1a**: 50 mg, 0.07 mmol; **1b**: 15 mg, 0.015 mmol) and $[(Cp^{PEt}Ni)_2(\mu,\eta^{3:3}\text{-}E_4)]$ (**1a**: 200 mg, 0.14 mmol; **1b:** 45 mg, 0.03 mmol) was dissolved in 10 mL toluene and stirred for 72 h. The solvent was removed in vacuum and the residue was washed once with 3 mL CH_3CN and pentane. The remaining solid was dissolved in 5 mL CH_2Cl_2 and layered with 10 mL CH_3CN. After complete diffusion, greenish brown crystals of **3** were obtained (**3a**: 65 mg; **3b**: 15 mg).

3a: Yield 65 mg (28%).

^1H NMR (298 K, C_6D_6): δ [ppm] = 1.03 (30H, t, $^3J_{HH}$ = 7.6 Hz, Cp^{PEt}/C*H*3), 1.16 (9H, s, Cp'''/CH_3), 1.38 (18H, s, Cp'''/CH_3), 2.37 (20H, q, $^3J_{HH}$ = 7.6 Hz, Cp^{PEt}/CH_2), 5.54 (2H, s, Cp'''/C*H*), 6.73 (20H, d, $^3J_{HH}$ = 8.0 Hz, Cp^{PEt}/C*H*), 6.94 (1H, s, Cp'''/C*H*), 7.32 (20H, d, $^3J_{HH}$ = 8.0 Hz, Cp^{PEt}/C*H*).

$^{13}C\{^1H\}$ NMR (298 K, C_6D_6): δ [ppm] = 15.2 (Cp^{PEt}/Et), 28.8 (Cp^{PEt}/Et), 31.4 (Cp'''/tBu), 31.8 (Cp'''/tBu), 33.6 (Cp'''/tBu), 33.8 (Cp'''/tBu), 85.4 (Cp'''/C_5), 111.3 (Cp^{PEt}/C_5), 115.5 (Cp'''/C_5), 118.4 (Cp'''/C_5) 127.4 (Ph), 131.7 (Ph), 133.1 (Ph), 141.8 (Ph).

$^{31}P\{^1H\}$ NMR (298 K, C_6D_6): δ [ppm] = 193.9 (1P, s), 204.1 (2P, d, $^1J_{PP}$ = 133.9 Hz), 274.8 (1P, t, $^1J_{PP}$ = 133.9 Hz).

Elemental analysis ($C_{107}H_{119}Ni_2CoP_4$ * 2 CH_2Cl_2): calculated: C 69.82, H 6.61; found: C 69.60, H 6.33.

Mass spectrometry (LIFDI, toluene): m/z 1704.56 (100%) $[M]^+$.

3b: Yield 15 mg (26%).

^1H NMR (C_6D_6): δ [ppm] = 1.04 (30H, t, $^3J_{HH}$ = 7.6 Hz, Cp^{PEt}/C*H*3), 1.20 (9H, s, Cp'''/CH_3), 1.38 (18H, s, Cp'''/CH_3), 2.38 (20H, q, $^3J_{HH}$ = 7.6 Hz, Cp^{PEt}/CH_2), 5.43 (2H, s, Cp'''/C*H*), 6.73 (20H, d, $^3J_{HH}$ = 7.9 Hz, Cp^{PEt}/C*H*), 6.95 (1H, s, Cp'''/C*H*), 7.33 (20H, d, $^3J_{HH}$ = 7.9 Hz, Cp^{PEt}/C*H*).

$^{13}C\{^1H\}$ NMR (Tol-d_8): δ [ppm] = 15.2 (Cp^{PEt}/Et), 28.8 (Cp^{PEt}/Et), 31.4 (Cp‘‘‘/tBu), 32.0 (Cp‘‘‘/tBu), 33.5 (Cp‘‘‘/tBu), 34.2 (Cp‘‘‘/tBu), 82.1 (Cp‘‘‘/C_5), 110.2 (Cp^{PEt}/C_5), 113.6 (Cp‘‘‘/C_5), 116.9 (Cp‘‘‘/C_5) 127.4 (Ph), 131.9 (Ph), 133.2 (Ph), 141.8 (Ph).

Elemental analysis ($C_{107}H_{119}Ni_2CoAs_4$ * CH_2Cl_2): calculated: C 65.98, H 6.20; found: C 65.95, H 6.15.

Mass spectrometry (LIFDI, toluene): m/z 1880.49 (100%) $[M]^+$, 586.36 (5%) $[Cp^{PEt}]^+$.

NMR Investigations

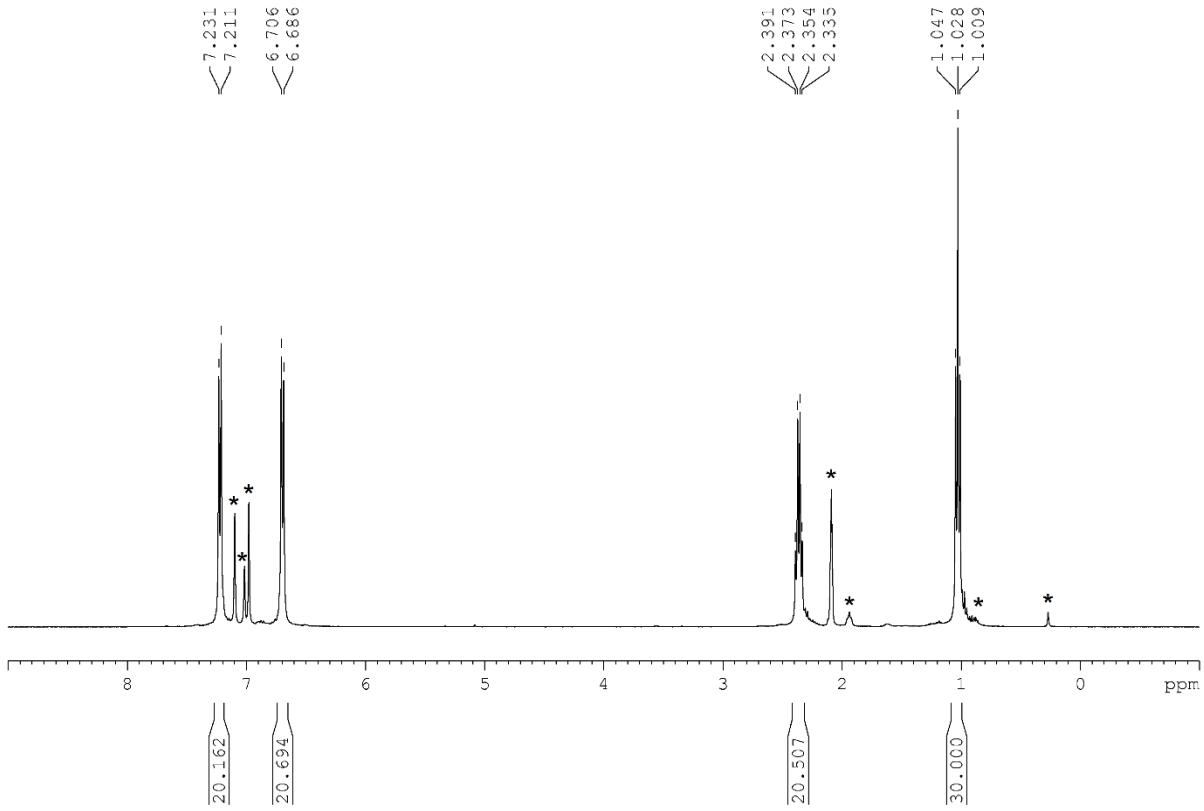

Figure S1. ^1H NMR spectrum of **1a** in Tol-d_8. * = impurities (toluene, $Cp^{PEt}H$, silicon grease).

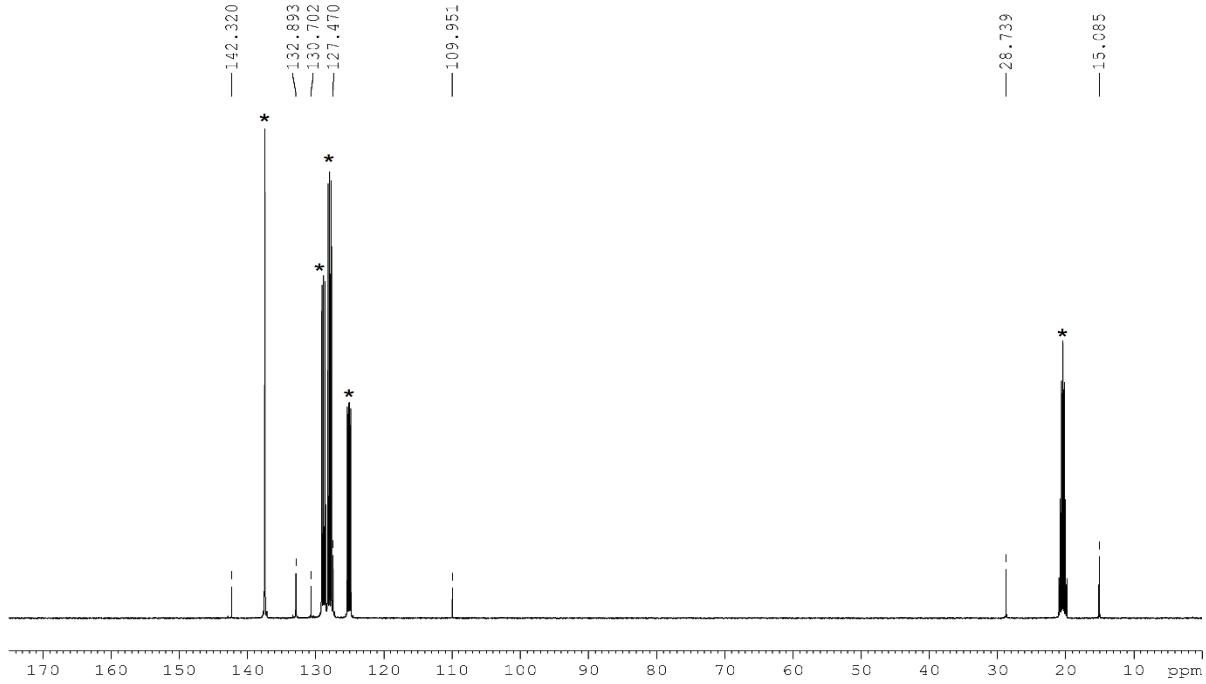

Figure S2. $^{13}C\{^1H\}$ NMR spectrum of **1a** in Tol-d_8. * = solvent (toluene).

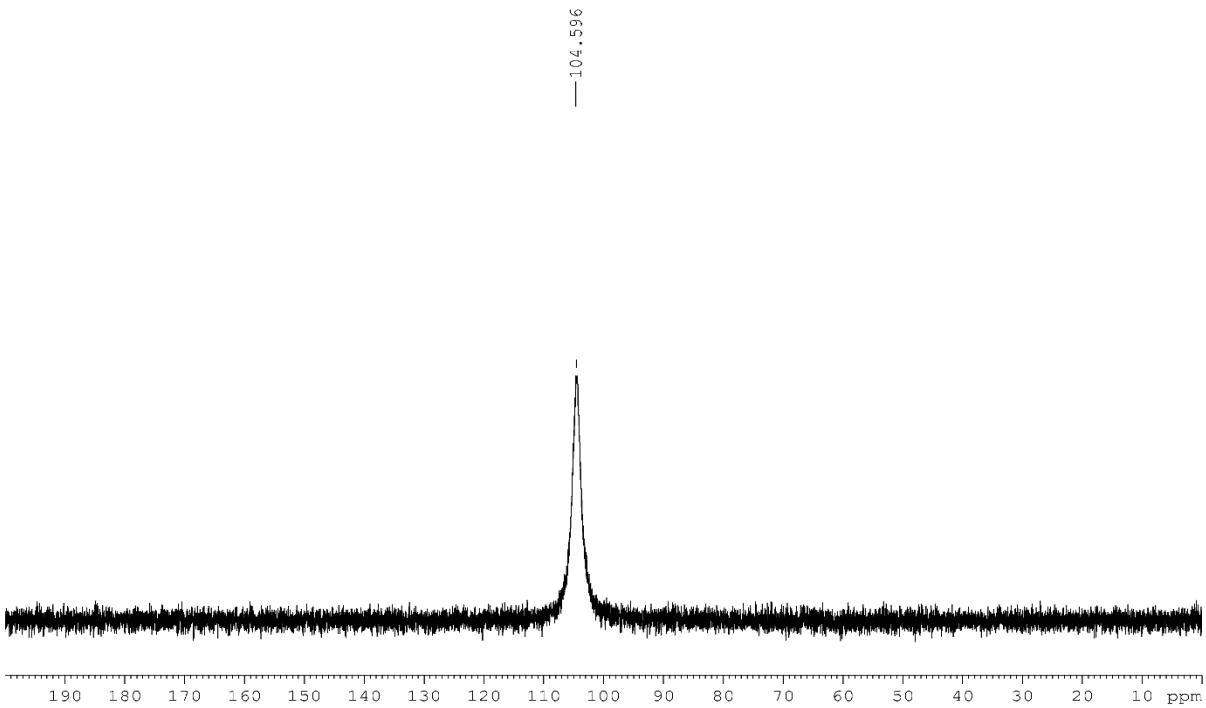

Figure S3. $^{31}P\{^1H\}$ NMR spectrum of **1a** in Tol-d_8.

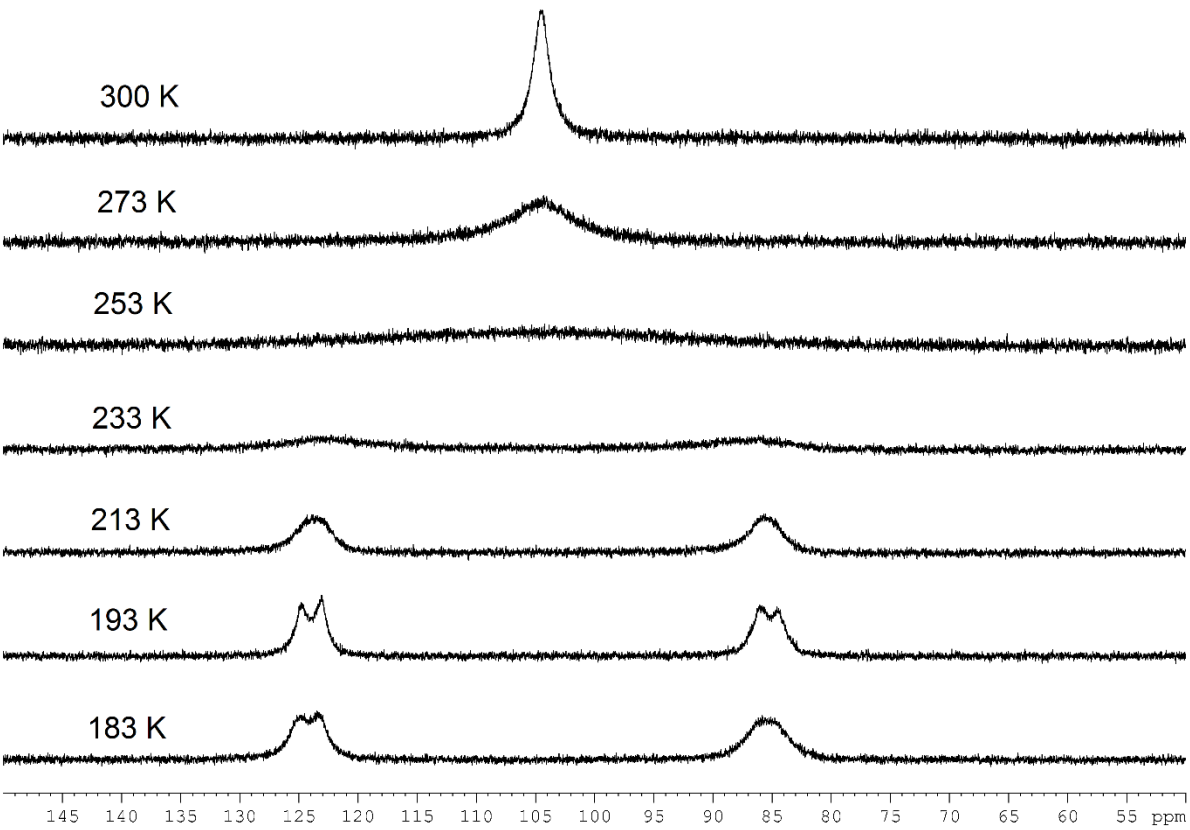

Figure S4. VT $^{31}P\{^1H\}$ NMR spectra of **1a** in Tol-d_8.

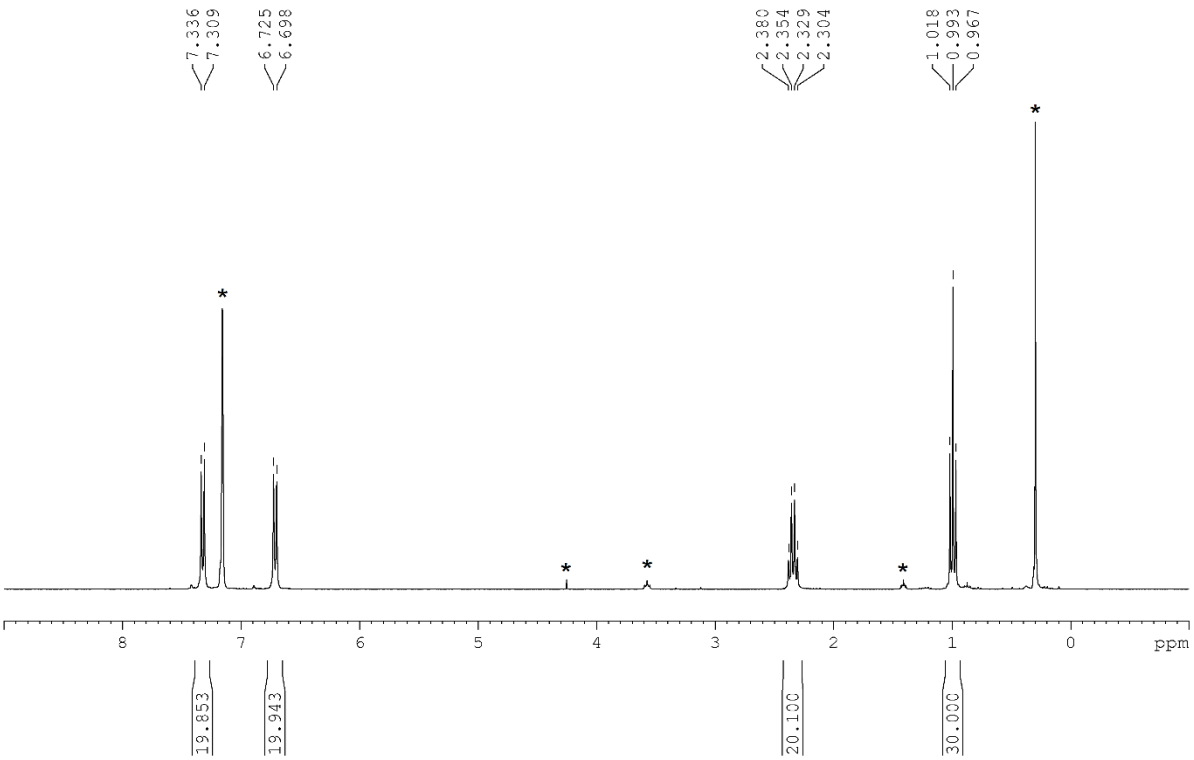

Figure S5. ^1H NMR spectrum of **1b** in C_6D_6. * = impurities (solvent, THF, CH_2Cl_2, silicon grease).

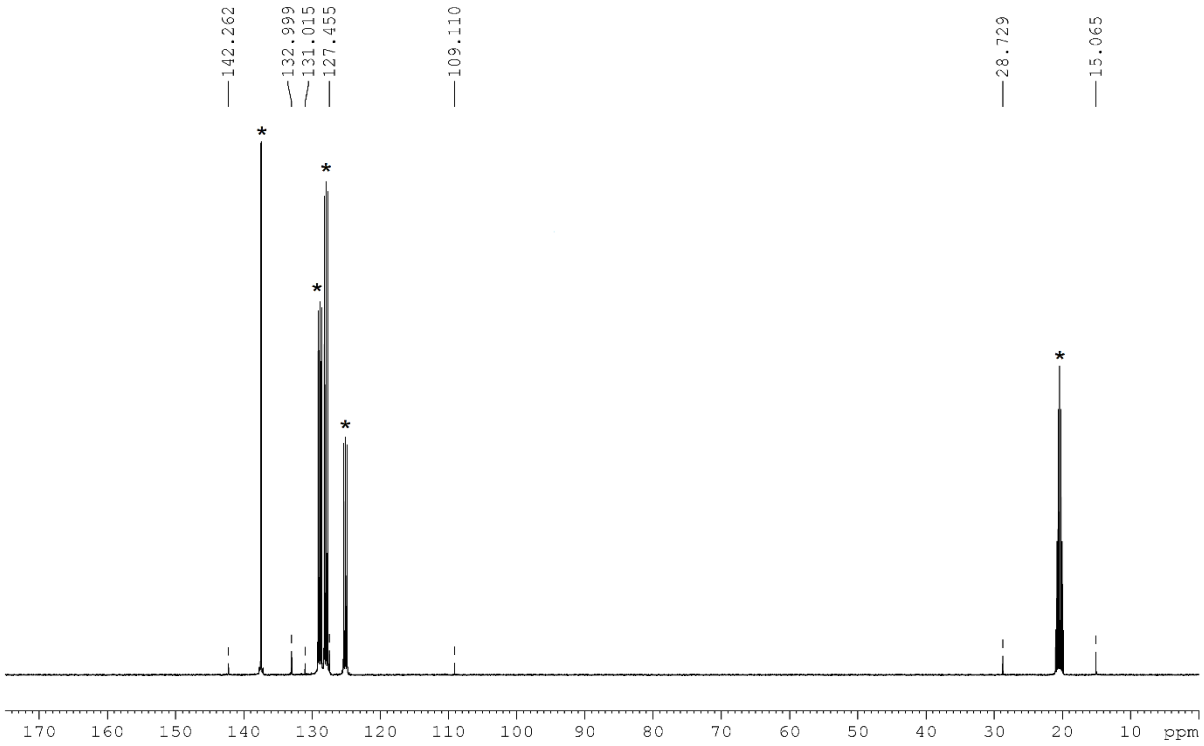

Figure S6. $^{13}C\{^1H\}$ NMR spectrum of **1b** in Tol-d_8. * = solvent (toluene).

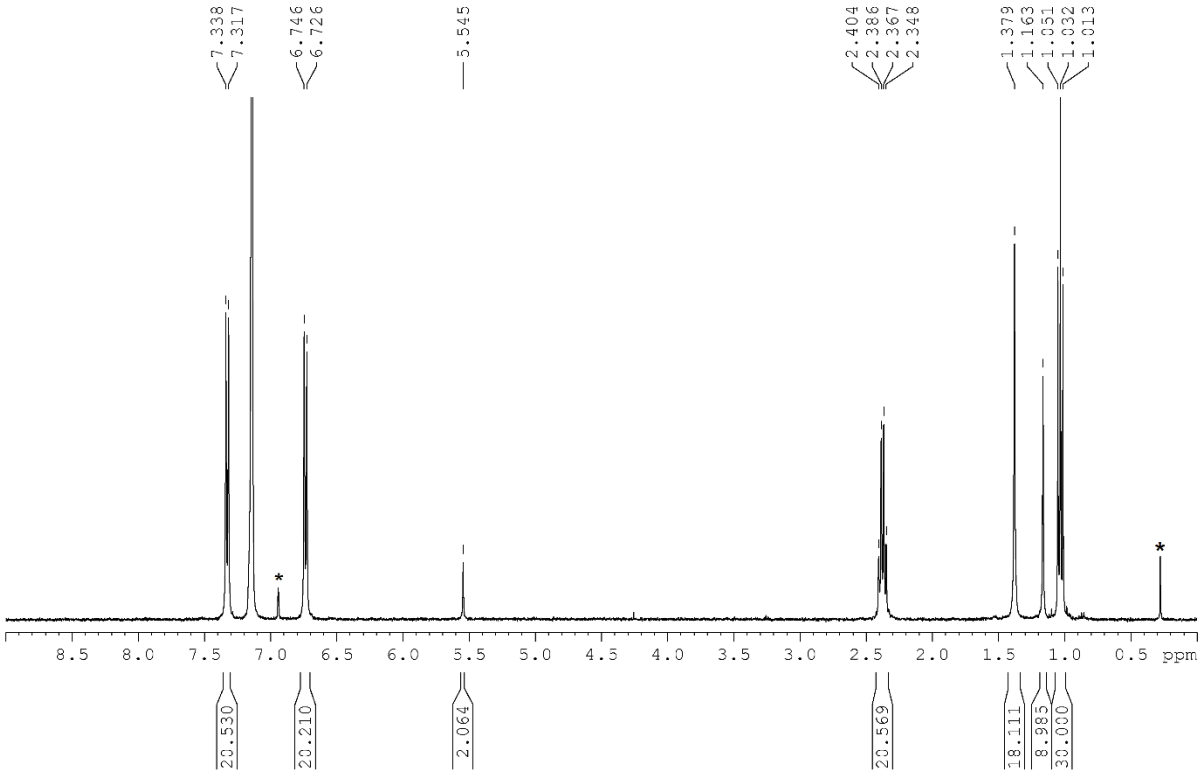

Figure S7. ^1H NMR spectrum of **3a** in C_6D_6. * = impurities (silicon grease).

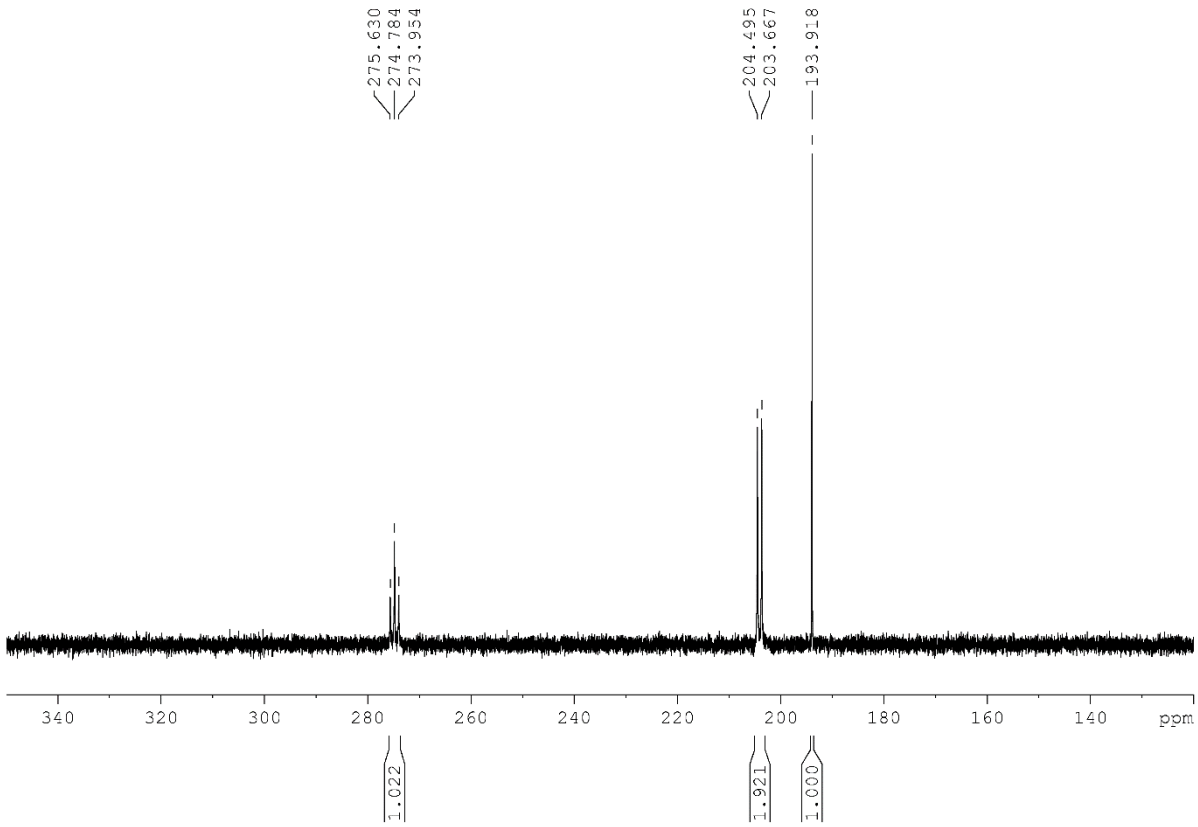

Figure S8. $^{31}P\{^1H\}$ NMR spectrum of **3a** in C_6D_6.

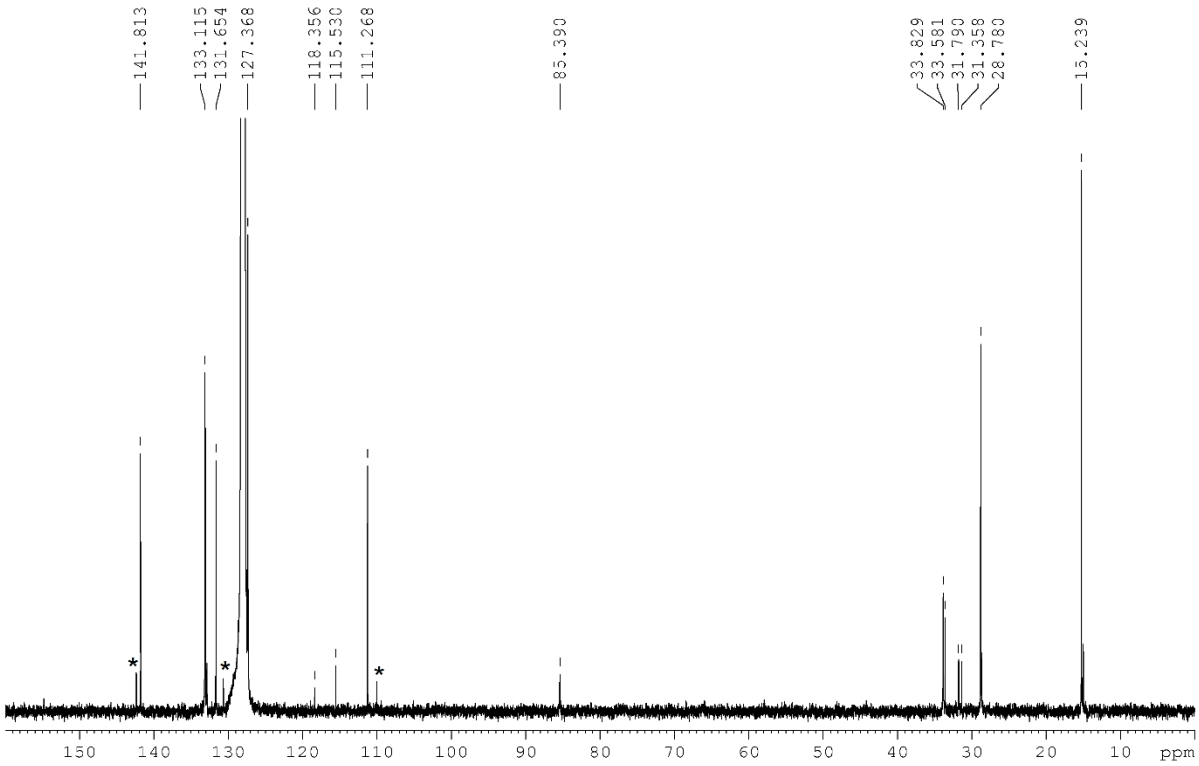

Figure S9. $^{13}C\{^1H\}$ NMR spectrum of **3a** in C_6D_6. * = impurities ($Cp^{PEt}H$).

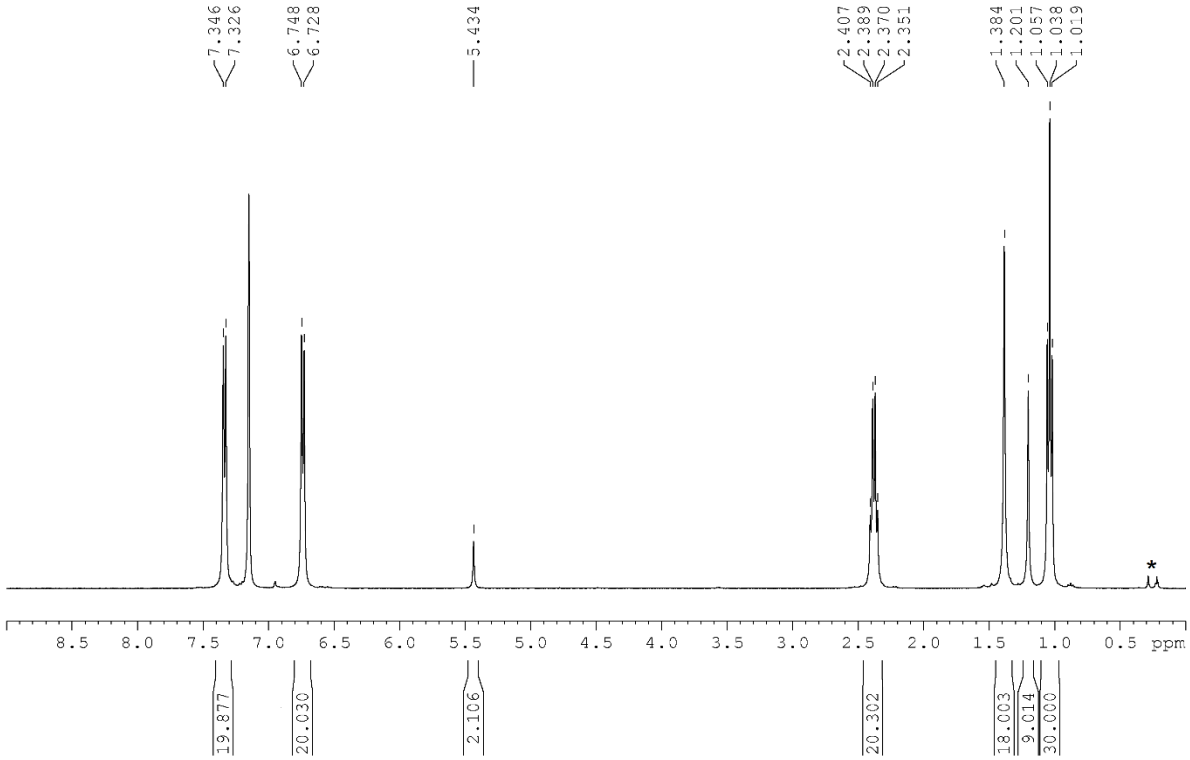

Figure S10. ^{1}H NMR spectrum of **3b** in C_6D_6. * = impurities (silicon grease).

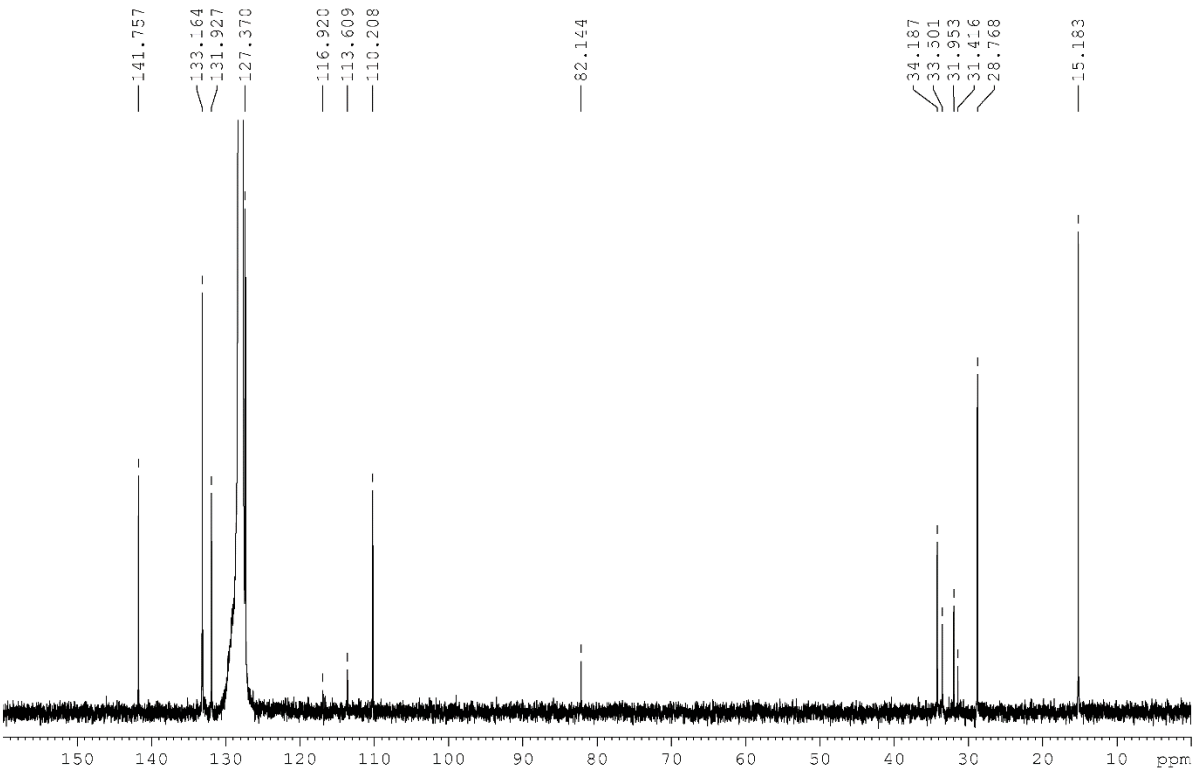

Figure S11. $^{13}C\{^{1}H\}$ NMR spectrum of **3b** in C_6D_6.

Crystallographic Details

Single crystal structure analyses were performed on a Rigaku Technologies diffractometer (GV50, Titan^{S2}). Data reduction was performed using the CrysAlisPro[4] software package. The structure solution was carried out using the program ShelXT[5] (Sheldrick, 2015) using the Olex2[6] software. Least squares refinements on F_0^2 were employed using SHELXL-2014.[7]

Compound **1a** co-crystallized with CH_2Cl_2, which could not be refined accordingly. Hence, the structure was treated with the SQUEEZE function of PLATON software[8] resulting in a void of about 196 Å^3 containing 59 electrons. This agrees well with one CH_2Cl_2 molecule per formula unit.

Table S1. Crystallographic data and details of diffraction experiments for **1a** · CH_2Cl_2, **1b** · CH_2Cl_2, **3a** and **3b**.

Compound	**1a** · CH_2Cl_2	**1b** · CH_2Cl_2	**3a**	**3b**
Formula	$C_{90}H_{90}Ni_2P_4$	$C_{90}H_{90}Ni_2As_4$	$C_{107}H_{119}CoNi_2P_4$	$C_{107}H_{119}CoNi_2As_4$
$\rho_{calc.}$/ g cm^{-3}	1.218	1.444	1.261	1.378
μ/mm^{-1}	1.723	3.501	2.945	3.872
Formula Weight	1412.91	1673.64	1705.24	1881.04
Colour	black	brown	greenish brown	greenish brown
Shape	irregular	plate	block	plank
Size/mm^3	0.25×0.17×0.09	0.27×0.13×0.04	0.20×0.20×0.11	0.36×0.10×0.05
T/K	123.00(17)	123.00(10)	122.97(14)	122.97(18)
Crystal System	triclinic	triclinic	monoclinic	monoclinic
Space Group	P-1	P-1	$C2/c$	$C2/c$
a/Å	14.0627(4)	13.8232(4)	28.3637(5)	28.3424(6)
b/Å	15.2160(4)	14.1534(4)	22.8577(3)	23.0523(4)
c/Å	18.7152(5)	23.0600(7)	29.2992(6)	29.3300(7)
α/°	97.826(2)	73.212(3)	90	90
β/°	100.195(2)	78.743(2)	108.938(2)	108.841(2)
γ/°	97.746(2)	63.388(3)	90	90
V/Å^3	3852.5(2)	3850.3(2)	17967.3(6)	18136.2(7)
Z	2	2	8	8
Z'	1	1	1	1
Wavelength/Å	1.54184	1.54184	1.54184	1.54184
Radiation type	CuK_α	CuK_α	CuK_α	CuK_α
Θ_{min}/°	2.432	3.587	2.540	2.527
θ_{max}/°	74.280	67.079	67.078	67.076
Measured Refl.	27287	22558	45230	41984
Independent Refl.	14892	13573	15908	16143
Reflections Used	12644	11696	14056	14445
R_{int}	0.0250	0.0290	0.0239	0.0277
Parameters	941	911	1107	1110
Restraints	35	11	65	89
Largest Peak	0.767	2.166	1.281	0.950
Deepest Hole	-0.573	-1.523	-0.513	-0.499
GooF	1.046	1.034	1.048	1.035
wR_2 (all data)	0.1599	0.1651	0.1340	0.1103
wR_2	0.1516	0.1562	0.1296	0.1065
R_1 (all data)	0.0605	0.0649	0.0533	0.0433
R_1	0.0527	0.0570	0.0478	0.0389

Computational Details

The model structures have been optimized at the M11L/6-311G(d,p) level of theory.[9] Frequency analysis has been performed to ensure that the stationary points found are genuine minima. Wiberg bond indices (WBIs) determined using NBO analysis were used since they are well-established as means for evaluating M-M interactions.[10] In addition, M-M Mayer bond order values (MBOs) were also calculated.[11]

Optimization starting from the experimental $Cp^R{}_3CoNi_2P_4$ cluster leads to an optimized geometry having P-P distances of 2.693 Å, 2.803 Å and 2.837 Å.

Table S2. Experimental and optimized bond distance of compound **3a** and the corresponding Wiberg bond indices and Mayer bond orders.

	Experimental distance [Å]	Optimized distance [Å]	Wiberg bond index	Mayer bond order
P1-P3	2.584	2.693	0.22	0.29
P1-P4	2.673	2.837	0.14	0.19
P1-P2	2.691	2.803	0.13	0.22
P3-P4	2.385	2.332	0.51	0.49
P2-P3	2.353	2.311	0.55	0.51
P2-P4	2.329	2.260	0.61	0.57
Ni1-P1	2.260	2.228	0.97	0.80
Ni1-P2	2.219	2.191	0.88	0.76
Ni1-P4	2.220	2.197	0.90	0.76
Ni2-P1	2.288	2.251	0.92	0.76
Ni2-P2	2.224	2.197	0.87	0.77
Ni2-P3	2.210	2.166	0.91	0.78
Co-P1		2.264	0.79	0.81
Co-P3		2.180	0.78	0.84
Co-P4		2.215	0.77	0.80

Table S3. Interatomic distances for the optimized $Cp_2Ni_2P_4$ and $Cp_3CoNi_2P_4$ structures.

the core of the $Cp_2Ni_2P_4$ trigonal prism	The core of the $Cp_3CoNi_2P_4$ cluster (exp distance matrix)
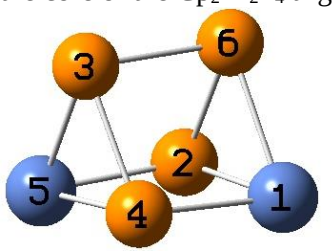 1 2 3 4 5 1 Ni 0.000000	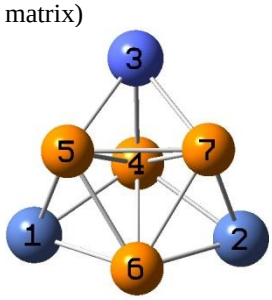

2 P 2.227809 0.000000 3 P 3.217382 2.981056 0.000000 4 P 2.200713 2.933922 2.136397 0.000000 5 Ni 3.318558 2.198788 2.219451 2.237716 0.000000 6 P 2.220205 2.141249 2.222112 2.985653 3.223263	1 2 3 4 5 1 Ni 0.000000 2 Ni 3.496648 0.000000 3 Co 3.489121 3.579483 0.000000 4 P 2.260454 2.288306 2.244464 0.000000 5 P 2.219630 3.666329 2.188008 2.672998 0.000000 6 P 2.218655 2.224368 3.599899 2.690661 2.328496 7 P 3.609443 2.210491 2.165073 2.584190 2.384935 6 7 6 P 0.000000 7 P 2.352747 0.000000

References

[1] O. J. Scherer, H. Sitzmann, G. Wolmershäuser, *J. Organomet. Chem.* **1986**, *309*, 77-86.

[2] U. Chakraborty, M. Modl, B. Mühldorf, M. Bodensteiner, S. Demeshko, N. J. C. van Velzen, M. Scheer, S. Harder, R. Wolf, *Inorg. Chem.* **2016**, *55*, 3065-3074.

[3] J. J. Schneider, D. Wolf, C. Janiak, O. Heinemann, J. Rust, C. Krüger, *Chem. Eur. J.* **1998**, *4*, 1982-1991.

[4] CrysAlisPro Software System, Agilent Technologies UK Ltd, Yarnton, Oxford, UK (2014).

[5] Sheldrick, G.M., ShelXT, *Acta Cryst.*, **2014**, *A71*, 3-8.

[6] O.V. Dolomanov and L.J. Bourhis and R.J. Gildea and J.A.K. Howard and H. Puschmann, Olex2: A complete structure solution, refinement and analysis program, *J. Appl. Cryst.*, **2009**, *42*, 339-341.

[7] Sheldrick, G.M., A short history of ShelX, *Acta Cryst.*, **2008**, *A64*, 339-341.

[8] P. van der Sluis & A.L.Spek (1990).Acta Cryst., A46, 194-201.

[9] R. Peverati, D. G. Truhlar, *J. Phys. Chem. Lett.*, **2011**, *2*, 2810–2817.

[10] F. Weinhold, C. R. Landis, Valency and Bonding: A Natural Bond Order Donor-Acceptor Perspective, Cambridge University Press, Cambridge, England, U.K., **2005**, 32-36.

[11] I. Mayer, *J. Comput. Chem.*, **2007**, *28*, 204.

4 Na(PCO) as a P Source – Synthesis of Nickel Complexes Containing μ,η$^{3:3}$-P_3 and μ,η$^{2:2}$-P_2 Ligands

Moritz Modl, Michael Bodensteiner, Gabor Balazs, Alexandru Lupan, Amr A. A. Attia, Manfred Scheer

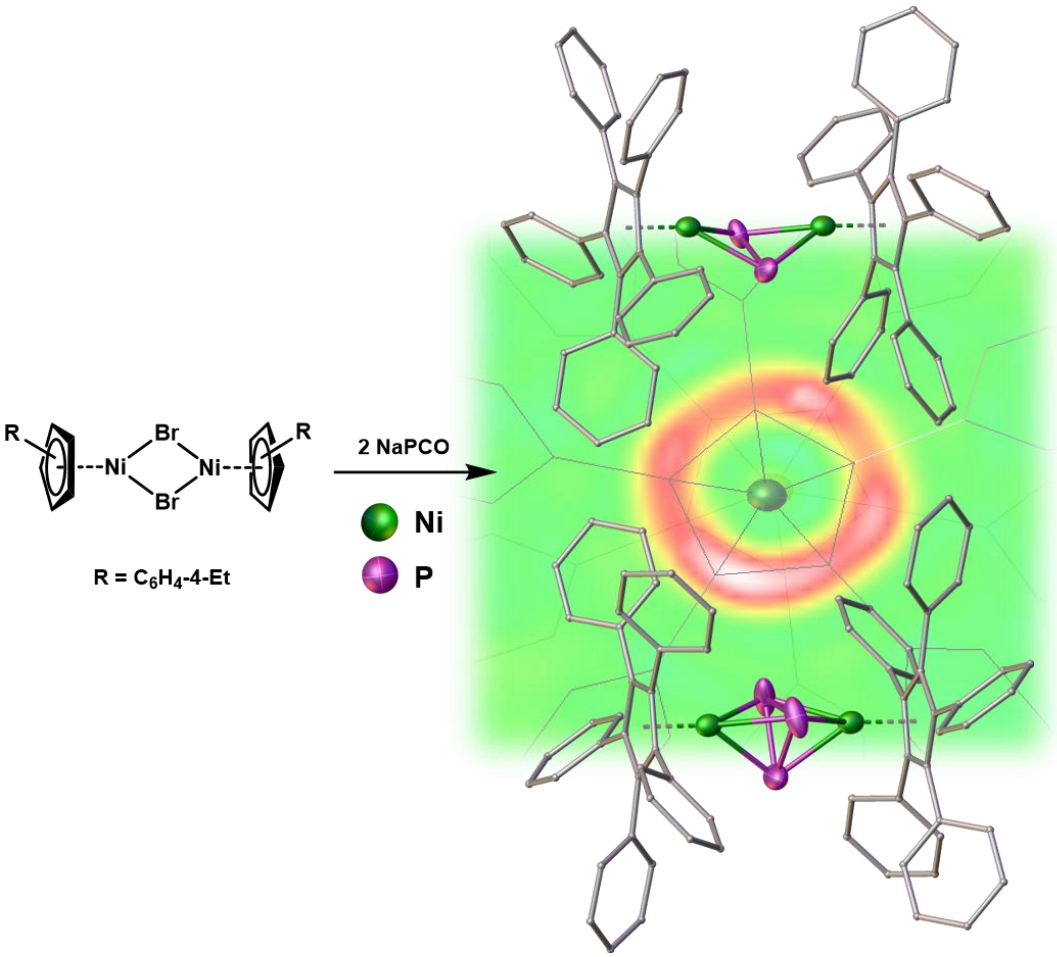

- **All syntheses and characterizations were performed by Moritz Modl, unless subsequently noted otherwise**
- **Manuscript was written by Moritz Modl except part for DFT calculations (Gabor Balázs)**
- **Figures were made by Moritz Modl except pictures corresponding to DFT calculations**
- **DFT calculations were performed by Alexandru Lupan and Amr Attia**
- **X-Ray structure analyses and refinement were jointly performed by Moritz Modl and Michael Bodensteiner**

4.1 Introduction

A common way to access P_n ligand complexes of main group elements and transition metals is the activation of white phosphorus.[1] The general approach includes the generation of reactive complex fragments under thermal or photolytic conditions and the subsequent reaction with P_4. The activation chemistry of P_4 with cyclopentadienyl ligand complexes of nickel, derived from $[Cp^RNi(CO)]_2$, ranges from the degradation of the P_4 tetrahedron into P_1 (**II**), P_2 (**IV**), P_3 (**I**) and P_4 (**II**, **III**) units (see Scheme 1),[2] but aggregation to larger poly-phosphorus compounds has not yet been observed. This is in contrast to the reaction of $[(Cp'''Co)_2(\mu\text{-toluene})]$ with P_4, where complexes containing large P_n ligands, i.e. $[(Cp'''Co)_5P_{24}]$, are formed.[3]

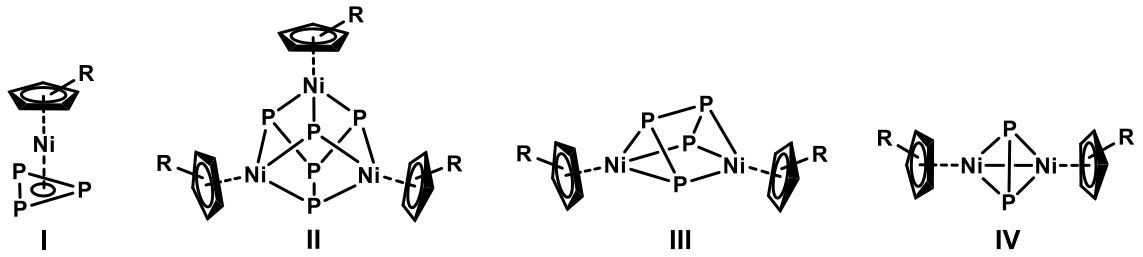

Scheme 1. Selected examples of nickel P_n ligand complexes with P_1 (**II**), P_2 (**IV**), P_3 (**I**) and P_4 (**II**, **III**) unit, obtained by P_4 activation under thermal or photolytic conditions.

In the recent years, the 2-phosphaethynolate anion, PCO^-, has emerged as a versatile reagent for the preparation of various phosphorus containing compounds. The lithium salt was isolated for the first time by Becker *et al.* as $[Li(DME)_2][PCO]$ in 1992.[4] Much more recently more convenient and safer syntheses of the better manageable sodium and potassium salts have been reported, so that these reagents are readily available in reasonable quantities.[5] The 2-phosphaethynolate anion has been utilized for the synthesis of new phosphines and organophosphorus compounds.[6,7] Moreover, the introduction into the coordination sphere of main group, transition metal and actinide species as a pseudo-halide was achieved usually via salt metathesis reaction with the corresponding halide. A subsequent decarbonylation process that can also be induced by thermal or photolytic conditions, if the moiety is attached via the phosphorus atom (M-P=C=O), reveals it as a formal "P^-" source.[8,9,10] Thus, CO elimination can afford P_n ligand complexes with a M_2P_2 core (**A**, **B** and **C** in Scheme 2).[9a,9b,9f] These M_2P_2 species can be described as diphosphene-bridged moieties or diphosphacyclobutadiene analogues. Beside the P_2 units only a P_1 ligand has been derived so far from the reaction of transition metal precursors with the 2-phosphaethynolate anion via CO release (**D** in Scheme 2).[9a]

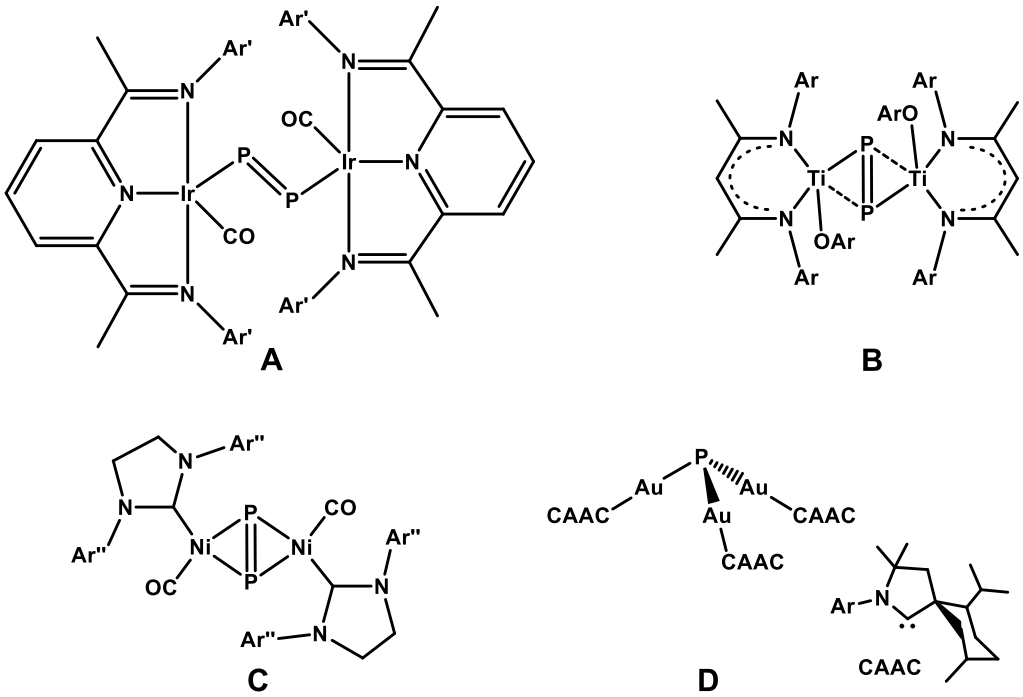

Scheme 2. Selected CO-release products **A** - **D** from transition metals (Ar = 2,6-diisopropylphenyl; Ar' = 2,6-dimethylphenyl; Ar'' = 2,4,6-trimethylphenyl, 2,6-diisopropylphenyl; R = H, Me).

We were intrigued by the reactivity of [Na(dioxane)$_x$][PCO] (x = 2 - 3) with the cyclopentadienyl metal halide [Cp^{PEt}Ni(μ-Br)]$_2$ (Cp^{PEt} = C$_5$(C$_6$H$_4$-4-Et)$_5$), to evaluate if this salt metathesis reaction can provide P$_n$ ligand complexes with larger P$_n$ ligands (n > 2) than the reported P$_2$ and P$_1$ units. Furthermore, comparison of the obtained products by such reactions with the products formed by P$_4$ activation processes was of interest. Herein we report on the reaction of [Na(dioxane)$_x$][PCO] with the bromo-bridged dimer [Cp^{PEt}Ni(μ-Br)]$_2$, leading to the rare type of complexes [(Cp^{PEt}Ni)$_2$(μ,η$^{3:3}$-P$_3$)] (**1**), bearing a *cyclo*-P$_3$ moiety, and the unprecedented butterfly-like compound [(Cp^{PEt}Ni)$_2$(μ,η$^{2:2}$-P$_2$)] (**2**), along with the carbonyl-bridged dimer [Cp^{PEt}Ni(μ-CO)]$_2$ (**3**).

4.2 Results and Discussion

Reaction of [Cp^{PEt}Ni(μ-Br)]$_2$ with two equivalents of [Na(dioxane)$_{2.4}$][PCO] in THF at ambient temperatures afforded the compounds [(Cp^{PEt}Ni)$_2$(μ,η$^{3:3}$-P$_3$)] (**1**), [(Cp^{PEt}Ni)$_2$(μ,η$^{2:2}$-P$_2$)] (**2**) and [Cp^{PEt}Ni(μ-CO)]$_2$ (**3**), together with NaBr as a precipitate (Scheme 3).

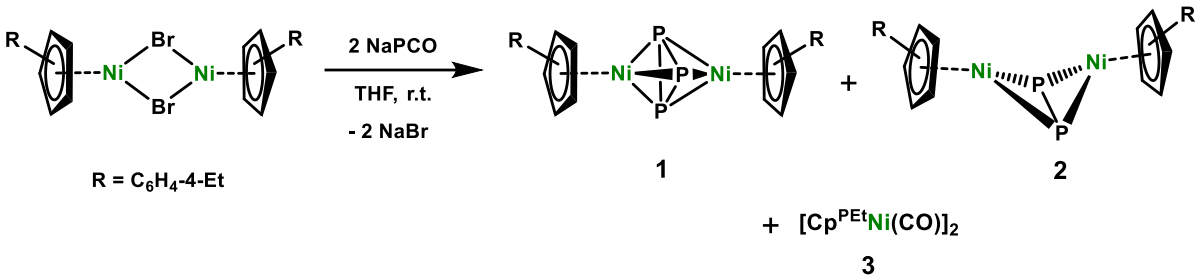

Scheme 3. Synthesis of **1**, **2** and **3**.

The ^{1}H NMR spectroscopic investigations of the crude reaction mixture in C_6D_6 show a complete conversion of the educt $[Cp^{PEt}Ni(\mu\text{-}Br)]_2$ (see the Supporting Information). After purification, a dark violet solid, consisting of a mixture of the complexes **1**, **2** and **3**, respectively, could be isolated in about 68 % yield. Despite many intensive attempts have been made by column and thin-layer chromatography the separation of this mixture was unsuccessful due to a similar solubility caused by the bulky Cp^{PEt} ligands.

Greenish red single-crystals could be grown from CH_2Cl_2 solutions, layered with CH_3CN after complete diffusion. X-ray diffraction studies display the complexes **1**, **2** and **3**, respectively, co-crystallizing on the same position owing to their similar structure and the dominating effect of the sterically highly demanding Cp^{PEt} ligands. According to the occupancies of the *cyclo*-P_3 and the P_2 atom positions, a 3:1 mixture of **1** and **2** is found in the crystal (for further details see Supporting Information). Compound **3** could not be refined properly because of the low occupancy.

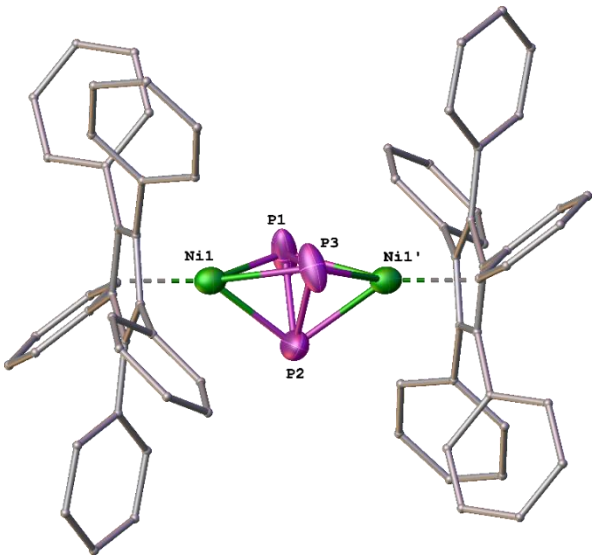

Figure 1. Solid-state molecular structure of **1**. Thermal ellipsoids are set at 50% probability. In case of disorder, only the main part is shown. For clarity reasons H atoms and ethyl groups are omitted and Cp^{PEt} ligands are drawn in 'wire-or-stick' model. Selected bond lengths [Å] and angles [°] in **1**: Ni1-P1 2.2547(1), Ni1-P2 2.3053(1), Ni1-P3 2.2893(1), P1-P2 2.1622(1), P1-P3 2.3772(1), P2-P3 2.1194(1), Ni1-Ni1' 3.7817(2), P1-P2-P3 67.441(5), P2-P3-P1 57.138(5), P3-P1-P2 55.421(4). Symmetry operation: −x, 1−y, 1−z.

The molecular structure of **1** reveals a triple-decker sandwich complex with a three-membered P_3 ring as the middle deck. The P_3 ring shows an allylic distortion with two shortened P-P bonds (P1-P2: 2.1622(1) Å; P2-P3: 2.1194(1) Å) and one elongated bond (P1-P3: 2.3772(1) Å). The Ni-P distances vary from 2.2547(1) to 2.3053(1) Å, hence resulting in a shift of the P_3 ring out of the center of the complex. This structural motif is confirmed by DFT calculations and is similar to that observed in the Cp''' derivative, reported by Scheer *et al.*.[2d] However, it differs in the arrangement of the Cp^R ligands, whereas the Cp''' ligands in $[(Cp'''Ni)_2(\mu,\eta^{3:3}\text{-}P_3)]$ ($Cp''' = C_5H_2{}^tBu_3$) are not parallel, a result from the nonlinear conformation (Ni1-$P_{3center}$-Ni2: 160.67(1)°), the Cp^{PEt} ligands in **1** are almost parallel to each other (Ni1-$P_{3center}$-Ni1': 172.432(1)°).

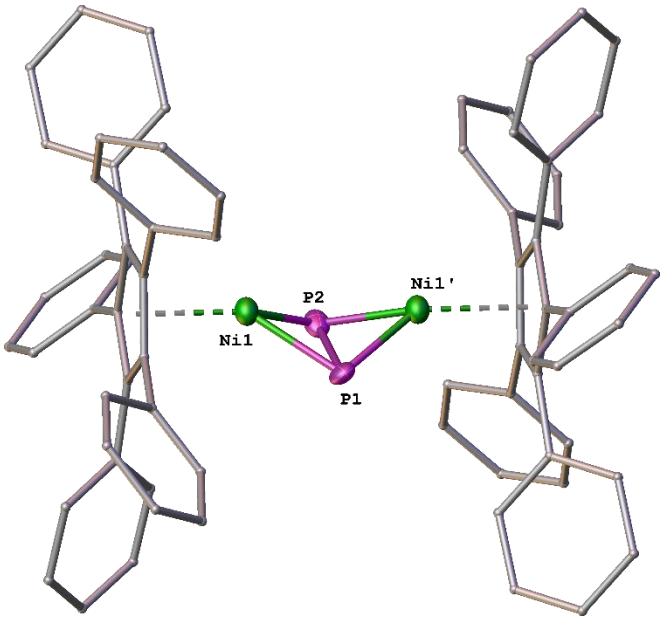

Figure 2. Solid-state molecular structure of **2**. Thermal ellipsoids are set at 50% probability. In case of disorder, only the main part is shown. For clarity reasons H atoms and ethyl groups are omitted and Cp^{PEt} ligands are drawn in 'wire-or-stick' model. Selected bond lengths [Å] and angles [°] in **2**: Ni1-P1 2.0623(1), Ni1-P2 1.9844(1), P1-P2 2.1152(1), Ni1-Ni1' 3.1364(1), Ni1-P1-Ni1' 100.407(4), N1-P2-Ni1' 103.947(4), P1-Ni1-P2 62.992(4), P1-Ni1'-P2 63.544(4). Symmetry operation: −x, 1−y, 1−z.

The single-crystal X-ray structure of **2** reveals a butterfly like Ni_2P_2 core. This is a novel structural motif, concerning the ligand and metal combination and the threefold coordination of nickel. It is known for Group 10 compounds with different phosphine ligands and coordination modes.[11] The P-P bond length of 2.1152(1) Å lies in the range of an elongated P=P double bond (2.04 Å).[12] It is close to the value reported for $(\mu,\eta^{2:2}\text{-}P_2)\{Ni(NHC)(CO)\}_2$ ($Cp = C_5H_5$; NHC = 1,3-bis(2,4,6-trimethylphenyl)imidazol-2-ylidene, 1,3-bis(2,6-diisopropylphenyl)imidazol-2-ylidene) with 2.076(2) Å and 2.072(3)/2.069(3) Å (two independent molecules in the asymmetric unit), respectively.[9f] The Ni-Ni distance in **2** with 3.1364(1) Å is considered non-bonding, whereas other reported cyclopentadienyl derivatives, exhibiting a Ni_2P_2 moiety, show

a diphospha-dinickela-tetrahedrane like structure with a Ni-Ni bond (Ni-Ni: 2.571(1) Å ([(Cp^{4}Ni)$_2$(μ,η$^{2:2}$-P$_2$)] (Cp^4 = C$_5$H^{i}Pr$_4$)); 2.526(2) Å ([(Cp*Ni)$_2$(μ,η$^{2:2}$-P$_2$)(Cr(CO)$_5$)$_2$] (Cp* = C$_5$Me$_5$)).[2c,13]

The ^{1}H NMR spectrum in C$_6$D$_6$ of the dissolved crystals, containing compounds **1**, **2** and **3**, respectively, displays different sets of signals between 0 and 11 ppm. A set of broadened and paramagnetically shifted signals with a singlet at 0.59 ppm, a triplet at 0.91 ppm, a pseudo-doublet at 7.74 ppm and another singlet at 10.52 ppm is observed with an integral ratio of approximately 20:30:20:20. This is in line with a paramagnetic complex, which can be assigned to the 33 valence electron compound **1**, given that the reported Cp''' analogue [(Cp'''Ni)$_2$(μ,η$^{3:3}$-P$_3$)] also shows paramagnetic behavior, possessing 33 valence electrons.[2d] The X-band EPR spectrum of the mixture, measured in toluene at 77 K, also confirms the presence of a paramagnetic compound by revealing a weak, broad signal with $g_{iso} \approx 2.056$.

The remaining signals in the ^{1}H NMR spectrum, a triplet at 0.96 ppm and a quartet at 2.32 ppm arise from the ethyl groups (ratio 30:20), while the aromatic protons appear in the range of 6.5 to 7.5 ppm as several doublets due to a hindered rotation of the Cp^{PEt} ligands. The diamagnetic signals cannot doubtlessly be assigned to product **2** or **3**, but considering the occupancies found in the crystals, they should mainly arise from **2**. In the ^{31}P{^{1}H} NMR spectrum of the mixture, only one singlet is observed at -133.63 ppm. It can be assigned to compound **2**, since **1** is paramagnetic in analogy to the Cp''' derivative.[2d] Interestingly, DFT calculations predict a tetrahedrane like ground state geometry for **2** in the gas phase. A geometry similar to that found experimentally for **2** has also been detected by DFT calculation as being a local minimum, which is with 16.3 kcal/mol higher in energy. In this structure, the Ni-Ni distance amounts to 3.453 Å while the P-P distance is 2.148 Å, which are in agreement with the corresponding distances determined by X-ray diffraction (see Table S2, Supporting Information). This results show that the bulky Cp^{PEt} ligands have a decisive role on the obtained structure, leading to the kinetic product **2** with a butterfly-like structural motif in the solid state and not the thermodynamic tetrahedral product (see Table S2, Supporting Information).

A FD mass spectrum of crystals dissolved in toluene exhibits two strong peaks at m/z = 1350.6 (100%) and m/z = 1381.6 (86%), corresponding to **2** and **1**, respectively. Cp^{PEt}H and **3** are observed with relative intensities of 19% and 2%, respectively. The IR spectroscopic measurements reveal two CO absorption bands at 1876 (w) and 1840 (s) cm^{-1}, corresponding to complex **3**. This is in line with analogous compounds, bearing different cyclopentadienyl ligands.[14]

4.3 Conclusion

In conclusion, we prepared the compounds $[(Cp^{PEt}Ni)_2(\mu,\eta^{3:3}\text{-}P_3)]$ (**1**) and $[(Cp^{PEt}Ni)_2(\mu,\eta^{2:2}\text{-}P_2)]$ (**2**), besides small amounts of $[Cp^{PEt}Ni(\mu\text{-}CO)]_2$ (**3**) by the salt metathesis reaction of $[Cp^{PEt}Ni(\mu\text{-}Br)]_2$ with $[Na(dioxane)_{2.4}][PCO]$. During the reaction the 2-phosphaethynolate anion readily decarbonylates without the need of thermal or photolytic activation as usually required for such products. Complex **1** is only the second neutral nickel-nickel sandwich compound, exhibiting a $\eta^{3:3}\text{-}P_3$ middle deck with cyclopentadienyl ligands and the first example of a P-rich P_n ligand complex with n > 2, synthesized from PCO^-. Compound **2** reveals a $\mu,\eta^{2:2}\text{-}P_2$ unit and represents, to the best of our knowledge, the first example of a butterfly-like Ni_2P_2 complex of Cp^RNi complex ligands, in contrast to reported diphospha-dinickela-tetrahedrane like structures.[2c,13] This difference might arise from the employment of $[PCO]^-$ as a formal "P^-" source, through decarbonylation reactions, and/or the sterically highly demanding Cp^{PEt} ligands, prohibiting the formation of the favored tetrahedrane like structural motif. Hence, the 2-phosphaethynolate anion is shown to be a suitable phosphorus source for the formation of polyphosphorus compounds and leads to other products than those obtained by using P_4.

4.4 References

[1] a) M. Scheer, G. Balázs, A. Seitz, *Chem. Rev. (Washington, DC, U. S.)* **2010**, *110*, 4236-4256; b) B. M. Cossairt, N. A. Piro, C. C. Cummins, *Chem. Rev. (Washington, DC, U. S.)* **2010**, *110*, 4164-4177; c) M. Caporali, L. Gonsalvi, A. Rossin, M. Peruzzini, *Chem. Rev. (Washington, DC, U. S.)* **2010**, *110*, 4178-4235.

[2] a) O. J. Scherer, J. Braun, G. Wolmershäuser, *Chem. Ber.* **1990**, *123*, 471-475; b) O. J. Scherer, J. Braun, P. Walther, G. Wolmershäuser, *Chem. Ber.* **1992**, *125*, 2661-2665; c) O. J. Scherer, J. Braun, P. Walther, C. Heckmann, G. Wolmershäuser, *Angew. Chem., Int. Ed.* **1991**, *30*, 852-854; d) E. Mädl, G. Balázs, E. V. Peresypkina, M. Scheer, *Angew. Chem., Int. Ed.* **2016**, *55*, 7702-7707; e) M. Scheer, U. Becker, *Chem. Ber.* **1996**, *129*, 1307-1310.

[3] F. Dielmann, M. Sierka, A. V. Virovets, M. Scheer, *Angew. Chem., Int. Ed.* **2010**, *49*, 6860-6864.

[4] G. Becker, W. Schwarz, N. Seidler, M. Westerhausen, *Z. Anorg. Allg. Chem.* **1992**, *612*, 72-82.

[5] a) D. Heift, Z. Benko, H. Grutzmacher, *Dalton Trans.* **2014**, *43*, 831-840; b) F. F. Puschmann, D. Stein, D. Heift, C. Hendriksen, Z. A. Gal, H.-F. Grützmacher, H. Grützmacher, *Angew. Chem., Int. Ed.* **2011**, *50*, 8420-8423; c) I. Krummenacher, C. C. Cummins, *Polyhedron* **2012**, *32*, 10-13; d) A. R. Jupp, J. M. Goicoechea, *Angew. Chem., Int. Ed.* **2013**, *52*, 10064-10067.

[6] a) A. R. Jupp, J. M. Goicoechea, *J. Am. Chem. Soc.* **2013**, *135*, 19131-19134; b) M. B. Geeson, A. R. Jupp, J. E. McGrady, J. M. Goicoechea, *Chem. Commun.* **2014**, *50*, 12281-12284; c) A. R. Jupp, G. Trott, É. Payen de la Garanderie, J. D. G. Holl, D. Carmichael, J. M. Goicoechea, *Chem. Eur. J.*

2015, *21*, 8015-8018; d) E. N. Faria, A. R. Jupp, J. M. Goicoechea, *Chem. Commun.* **2017**, *53*, 7092-7095.

[7] a) X. Chen, S. Alidori, F. F. Puschmann, G. Santiso-Quinones, Z. Benkő, Z. Li, G. Becker, H.-F. Grützmacher, H. Grützmacher, *Angew. Chem., Int. Ed.* **2014**, *53*, 1641-1645; b) D. Heift, Z. Benkő, H. Grützmacher, *Angew. Chem., Int. Ed.* **2014**, *53*, 6757-6761; c) D. Heift, Z. Benkő, H. Grützmacher, *Chem. Eur. J.* **2014**, *20*, 11326-11330; d) T. P. Robinson, J. M. Goicoechea, *Chem. Eur. J.* **2015**, *21*, 5727-5731; e) Z. Li, X. Chen, M. Bergeler, M. Reiher, C.-Y. Su, H. Grutzmacher, *Dalton Trans.* **2015**, *44*, 6431-6438; f) R. Suter, Z. Benkő, H. Grützmacher, *Chem. Eur. J.* **2016**, *22*, 14979-14987; g) Z. Li, X. Chen, Z. Benkő, L. Liu, D. A. Ruiz, J. L. Peltier, G. Bertrand, C.-Y. Su, H. Grützmacher, *Angew. Chem., Int. Ed.* **2016**, *55*, 6018-6022; h) R. Suter, Y. Mei, M. Baker, Z. Benkő, Z. Li, H. Grützmacher, *Angew. Chem., Int. Ed.* **2017**, *56*, 1356-1360; i) Z. Li, X. Chen, D. M. Andrada, G. Frenking, Z. Benkö, Y. Li, J. R. Harmer, C.-Y. Su, H. Grützmacher, *Angew. Chem., Int. Ed.* **2017**, *56*, 5744-5749.

[8] Main Group: a) S. Yao, Y. Xiong, T. Szilvási, H. Grützmacher, M. Driess, *Angew. Chem., Int. Ed.* **2016**, *55*, 4781-4785; b) Y. Wu, L. Liu, J. Su, J. Zhu, Z. Ji, Y. Zhao, *Organometallics* **2016**, *35*, 1593-1596; c) N. Del Rio, A. Baceiredo, N. Saffon-Merceron, D. Hashizume, D. Lutters, T. Müller, T. Kato, *Angew. Chem., Int. Ed.* **2016**, *55*, 4753-4758; d) Y. Xiong, S. Yao, T. Szilvási, E. Ballestero-Martínez, H. Grützmacher, M. Driess, *Angew. Chem., Int. Ed.* **2017**, *56*, 4333-4336; e) D. Heift, Z. Benko, H. Grutzmacher, A. R. Jupp, J. M. Goicoechea, *Chem. Sci.* **2015**, *6*, 4017-4024; f) A. M. Tondreau, Z. Benko, J. R. Harmer, H. Grutzmacher, *Chem. Sci.* **2014**, *5*, 1545-1554; g) T. P. Robinson, M. J. Cowley, D. Scheschkewitz, J. M. Goicoechea, *Angew. Chem., Int. Ed.* **2015**, *54*, 683-686.

[9] Transition Metal: a) L. Liu, D. A. Ruiz, F. Dahcheh, G. Bertrand, R. Suter, A. M. Tondreau, H. Grutzmacher, *Chem. Sci.* **2016**, *7*, 2335-2341; b) L. N. Grant, B. Pinter, B. C. Manor, R. Suter, H. Grützmacher, D. J. Mindiola, *Chem. Eur. J.* **2017**, *23*, 6272-627; c) S. Alidori, D. Heift, G. Santiso-Quinones, Z. Benkő, H. Grützmacher, M. Caporali, L. Gonsalvi, A. Rossin, M. Peruzzini, *Chem. Eur. J.* **2012**, *18*, 14805-14811; d) A. R. Jupp, M. B. Geeson, J. E. McGrady, J. M. Goicoechea, *Eur. J. Inorg. Chem.* **2016**, *2016*, 639-648; e) L. Weber, B. Torwiehe, G. Bassmann, H.-G. Stammler, B. Neumann, *Organometallics* **1996**, *15*, 128-132; f) G. Hierlmeier, A. Hinz, R. Wolf, J. M. Goicoechea, *Angew. Chem., Int. Ed.* **2018**, *57*, 431-436.

[10] Actinide: C. Camp, N. Settineri, J. Lefevre, A. R. Jupp, J. M. Goicoechea, L. Maron, J. Arnold, *Chem. Sci.* **2015**, *6*, 6379-6384.

[11] a) H. Schäfer, D. Binder, D. Fenske, *Angew. Chem. Int. Ed. Engl.* **1985**, *24*, 522-524; b) H. Schäfer, D. Binder, *Z. Anorg. Allg. Chem.* **1988**, *560*, 65-79; c) W. Dománska-Babul, J. Chojnacki, E. Matern, J. Pikies, *J. Organomet. Chem.* **2007**, *692*, 3640-3648; d) W. Dománska-Babul, J. Chojnacki, E. Matern, J. Pikies, *Dalton Trans.* **2009**, 146-151; e) M. Demange, X.-F. LeGoff, P. LeFloch, N. Mézailles, *Chem. Eur. J.* **2010**, *16*, 12064-12068; f) B. Zarzycki, T. Zell, D. Schmidt, U. Radius, *Eur. J. Inorg. Chem.* **2013**, 2051-2058; g) H. Schäufer, D. Binder, *Z. Anorg. Allg. Chem.* **1987**, *546*, 55-78.

[12] P. Pyykkö, M. Atsumi, *Chem. Eur. J.* **2009**, *15*, 12770-12779.

[13] M. Scheer, K. Schuster, A. Krug, H. Hartung, *Chem. Ber.* **1996**, *129*, 973-979.

[14] a) H. Sitzmann, G. Wolmershäuser, *Z. Naturforsch., B: Chem. Sci.* **1995**, *50*, 750; b) L. R. Byers, L. F. Dahl, *Inorg. Chem.* **1980**, *19*, 680-692; c) C. Evans, L. J. Farrugia, *Acta Crystallographica Section E* **2003**, *59*, 510-511.

4.5 Supporting Information

General Remarks

All experiments were performed with dry argon or nitrogen using glove box and Schlenk techniques. Solvents were dried using a MB SPS-800 device of company MBRAUN. $[Cp^{PEt}NiBr]_2$[1] and $[Na(dioxane)_x][PCO]$[2] were prepared according to literature procedures. ^1H, ^{13}C and ^{31}P NMR spectra were measured on a Bruker Avance 400 (^1H: 400.130 MHz, ^{13}C: 100.613 MHz, ^{31}P: 161.976 MHz). The chemical shifts are reported in ppm relative to external TMS (^1H, ^{13}C) and H_3PO_4 (^{31}P). Mass spectra were performed on a Finnigan MAT95 LIFDI-MS spectrometer. Elemental analysis (CHN) was determined using a Vario micro cube and Vario EL III instrument. The IR spectra were measured on a VARIAN FTS-800 FT-IR spectrometer or a Thermo Scientific Nicolet iS5 spectrometer. The X-band EPR measurements were carried out with a MiniScope MS400 device equipped with a Magnettech GmbH rectangular TE102 resonator at a frequency of 9.5 GHz.

Synthesis of $[(Cp^{PEt}Ni)_2(\mu,\eta^{3:3}\text{-}P_3)]$ (1), $[(Cp^{PEt}Ni)_2(\mu,\eta^{2:2}\text{-}P_2)]$ (2) and $[Cp^{PEt}Ni(\mu\text{-}CO)]_2$ (3)

To a mixture of $[Cp^{PEt}NiBr]_2$ (150 mg, 0.10 mmol) and $[Na(dioxane)_{2.4}][PCO]$ (61 mg, 0.20 mmol) 10 mL THF was added and the resulting burgundy red solution was stirred at ambient temperature for 18 h. After removal of all volatiles in vacuum, the dark residue was extracted with 10 mL toluene. The filtrate was dried and subsequently washed with *n*-hexane, which afforded a dark violet solid of a mixture of **1**, **2** and **3** (97 mg). Single crystals suitable for X-ray analysis were grown from CH_2Cl_2 (5 mL) solutions, layered with double the amount of CH_3CN.

Mixture of **1**, **2** and **3**:

^1H NMR (C_6D_6): δ [ppm] = 0.59 (20H, br s), 0.91 (30H, br t, $^3J_{HH}$ = 7.4 Hz, CH_3), 0.96 (10H, t, $^3J_{HH}$ = 7.4 Hz, CH_3), 2.32 (7H, q, $^3J_{HH}$ = 7.4 Hz, CH_2), 6.6 - 7.5 (20H, m, Ph), 7.74 (20H, br d, , $^3J_{HH}$ = 7.4 Hz, CH_3), 10.52 (20H, br s).

IR (toluene): ν_{CO} [cm^{-1}] = 1876 (w), 1840 (s); corresponding to **3**.

Mass spectrometry (LIFDI, toluene): m/z 1350.60 (100%) [**2**]$^+$, 1381.58 (86%) [**1**]$^+$, 586.39 (19%) $[Cp^{PEt}]^+$, 1344.60 (2%) [**3**]$^+$.

NMR and EPR Investigations

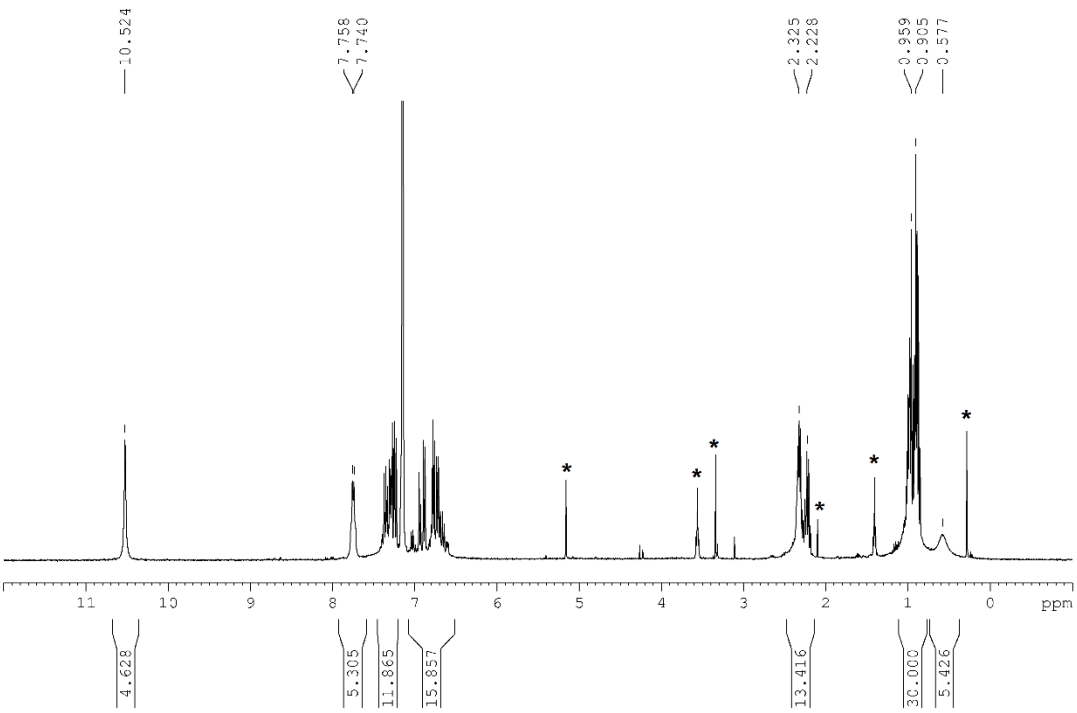

Figure S1. ^{1}H NMR spectrum of the crude reaction mixture in C_6D_6. * = impurities (THF, toluene, 1,4-dioxane, silicon grease).

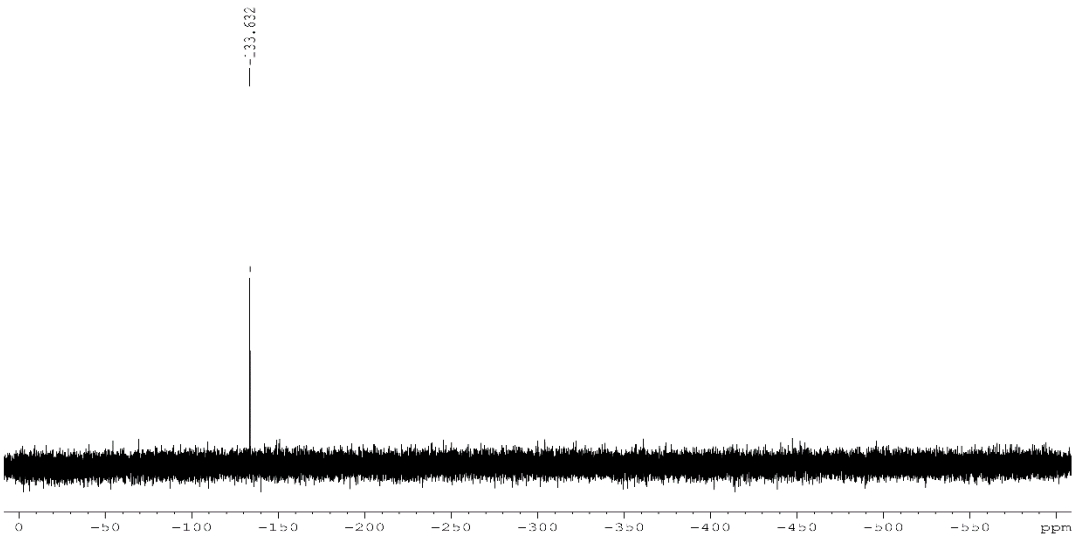

Figure S2. ^{31}P{^{1}H} NMR spectrum of the crude reaction mixture in C_6D_6. Depicted range: 0 to -600 ppm.

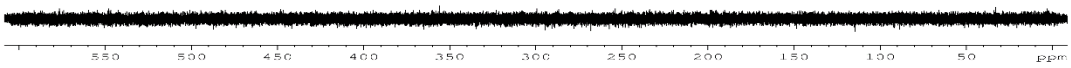

Figure S3. $^{31}P\{^{1}H\}$ NMR spectrum of the crude reaction mixture in C_6D_6. Depicted range: 600 to 0 ppm.

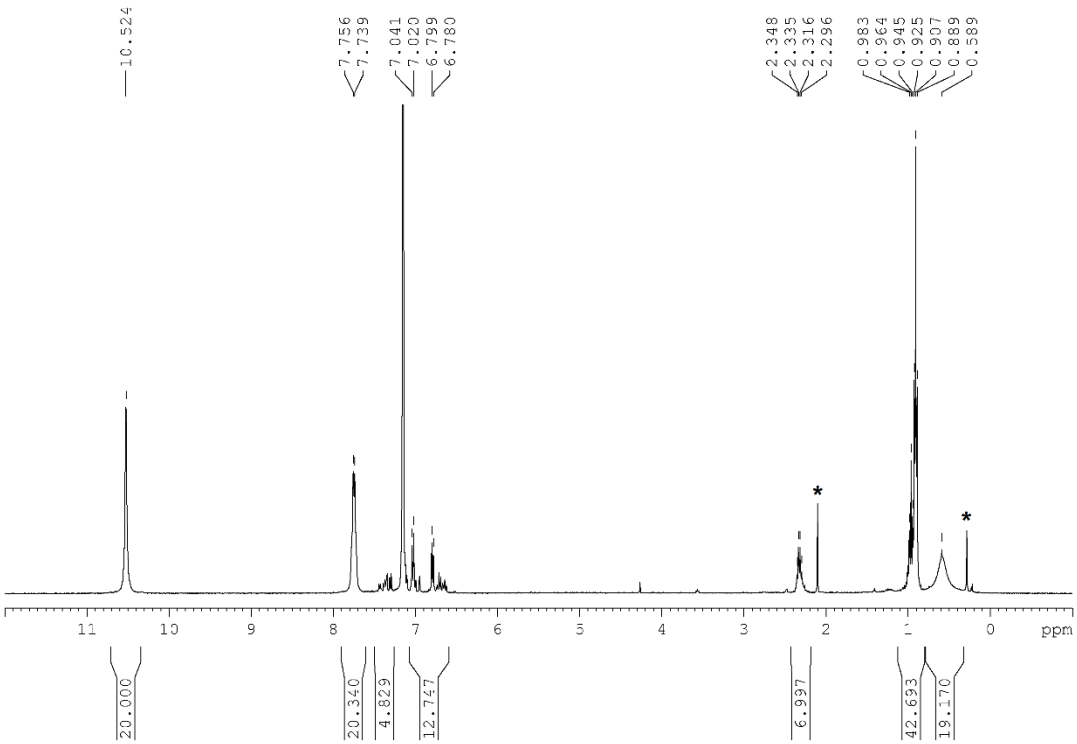

Figure S4. ^{1}H NMR spectrum of a mixture of **1**, **2** and **3** (crystals) in C_6D_6. Depicted range: 12 to -1 ppm. * = impurities (toluene, silicon grease).

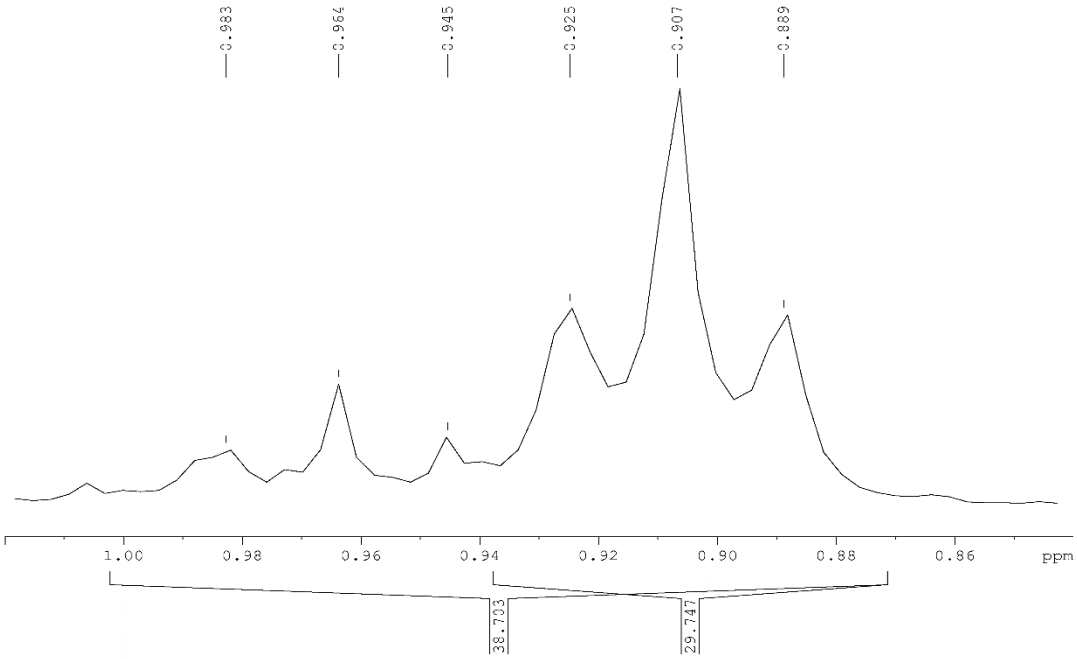

Figure S5. ^{1}H NMR spectrum of a mixture of **1**, **2** and **3** (crystals) in C_6D_6. Depicted range: 1.2 to 0.84 ppm.

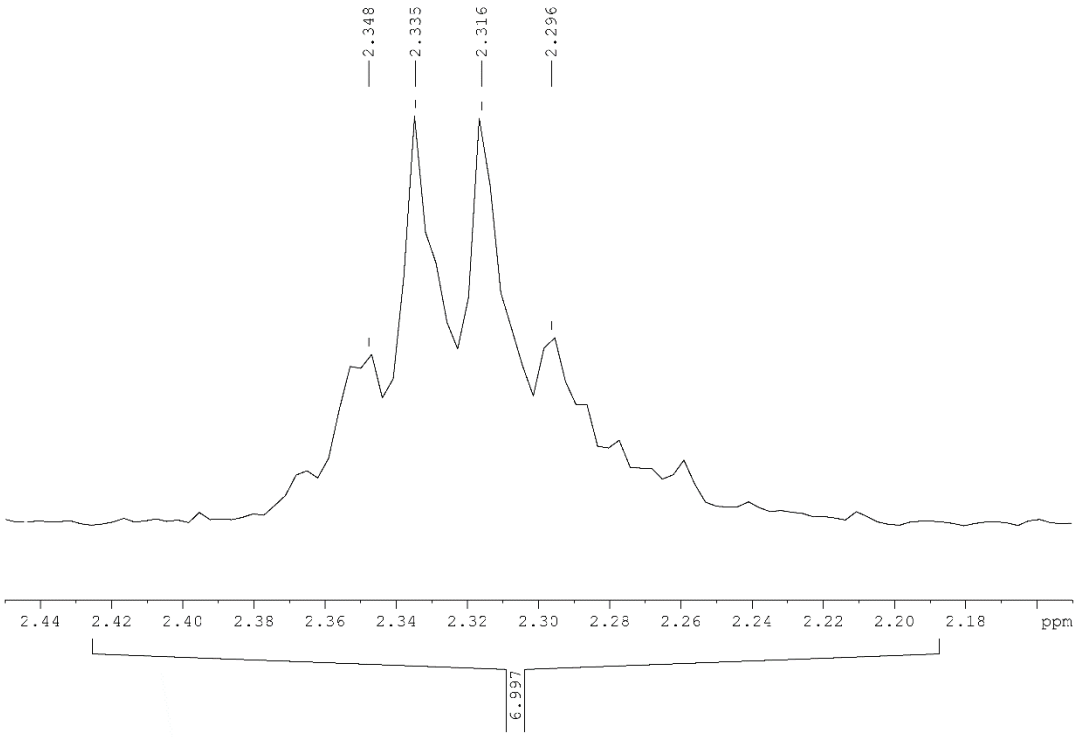

Figure S6. ^{1}H NMR spectrum of a mixture of **1**, **2** and **3** (crystals) in C_6D_6. Depicted range: 2.45 to 2.15 ppm.

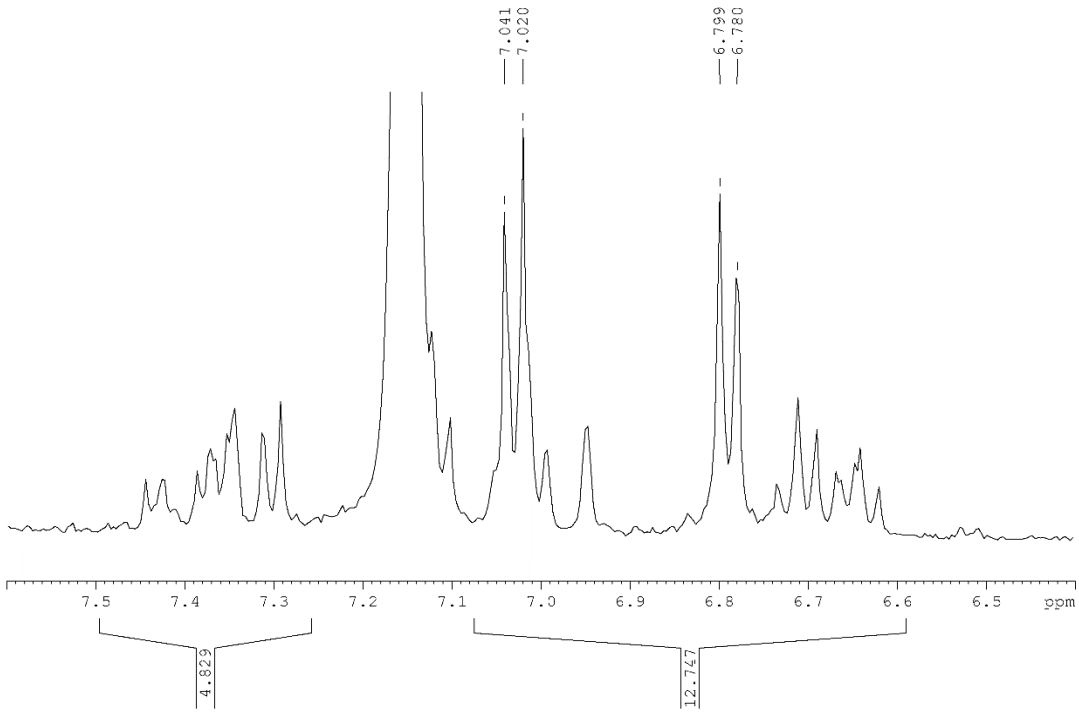

Figure S7. ^{1}H NMR spectrum of a mixture of **1**, **2** and **3** (crystals) in C_6D_6. Depicted range: 7.6 to 6.4 ppm.

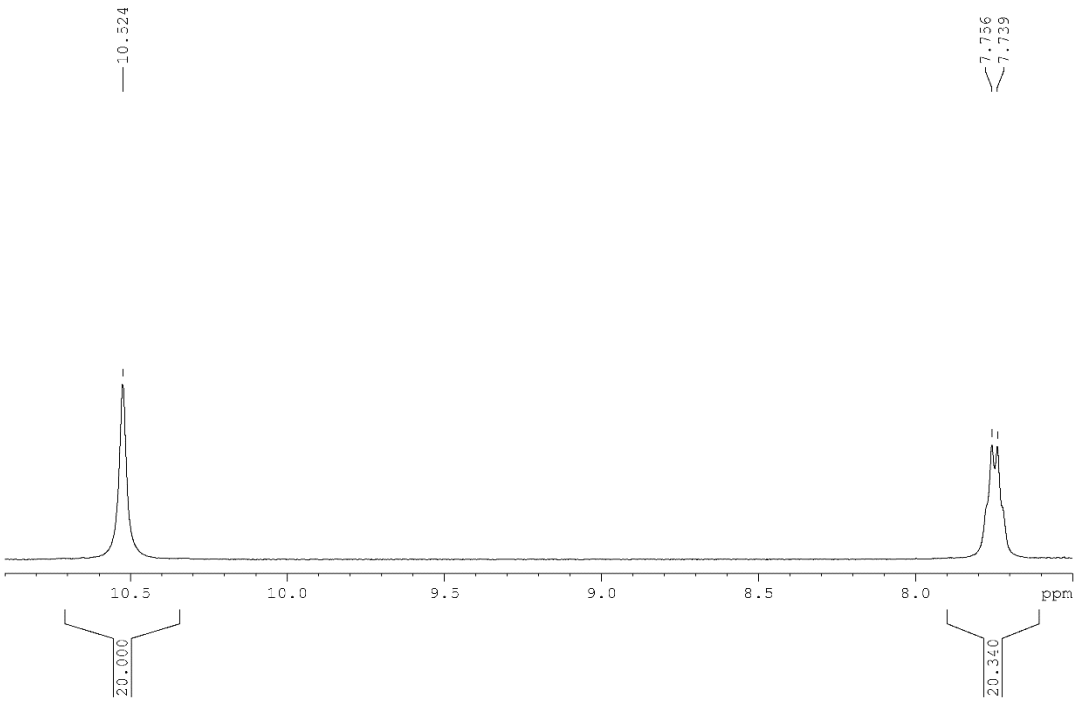

Figure S8. ^{1}H NMR spectrum of a mixture of **1**, **2** and **3** (crystals) in C_6D_6. Depicted range: 10.9 to 7.5 ppm.

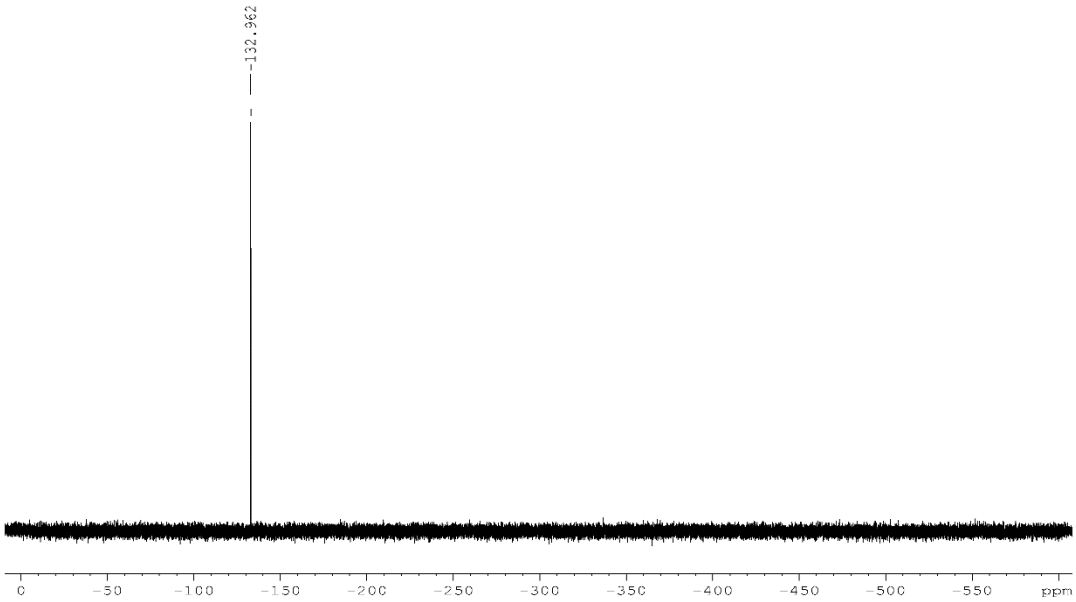

Figure S9. $^{31}P\{^{1}H\}$ NMR spectrum of a mixture of **1**, **2** and **3** (crystals) in C_6D_6. Depicted range: 0 to -600 ppm.

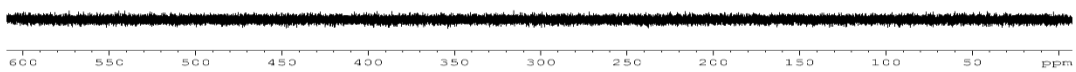

Figure S10. $^{31}P\{^{1}H\}$ NMR spectrum of a mixture of **1**, **2** and **3** (crystals) in C_6D_6. Depicted range: 600 to 0 ppm.

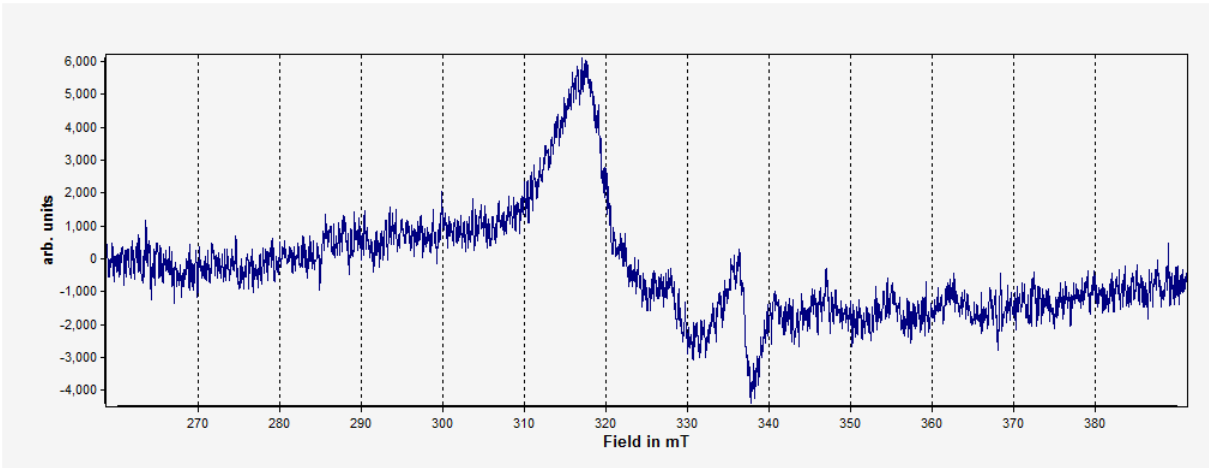

Figure S11. X-Band EPR spectrum of a mixture of **1**, **2** and **3** in toluene at 77 K with $g_{iso} \approx 2.056$.

Crystallographic Details

Single crystal structure analyses were performed on a Rigaku Technologies diffractometer (GV50, Titan^{S2}). Data reduction was performed using the CrysAlisPro[3] software package. The structure solution was carried out using the program ShelXT[4] (Sheldrick, 2015) using the Olex2[5] software. Least squares refinements on F_0^2 were employed using SHELXL-2014.[6]

Table S1. Crystallographic data and details of diffraction experiments for **1**, **2** (mixture).

Compound	**1, 2**
Formula	$C_{90}H_{90}Ni_2P_{2.74}$
$\rho_{calc.}$/ g cm^{-3}	1.193
μ/mm^{-1}	1.481
Formula Weight	1372.99
Colour	greenish red
Shape	block
Size/mm^3	0.13×0.12×0.10
T/K	123.00(10)
Crystal System	triclinic
Space Group	P-1
a/Å	12.4757(6)
b/Å	13.9916(6)
c/Å	14.0722(6)
α/°	64.724(4)
β/°	64.393(4)
γ/°	64.645(4)
V/Å^3	1911.51(18)
Z	1
Z'	0.5
Wavelength/Å	1.54184
Radiation type	CuK_a
θ_{min}/°	3.647
Θ_{max}/°	67.076
Measured Refl.	14510
Independent Refl.	6712
Reflections Used	5752
R_{int}	0.0196
Parameters	488
Restraints	79
Largest Peak	1.048
Deepest Hole	-0.477
GooF	1.085
wR_2 (all data)	0.1450
wR_2	0.1384
R_1 (all data)	0.0545
R_1	0.0482

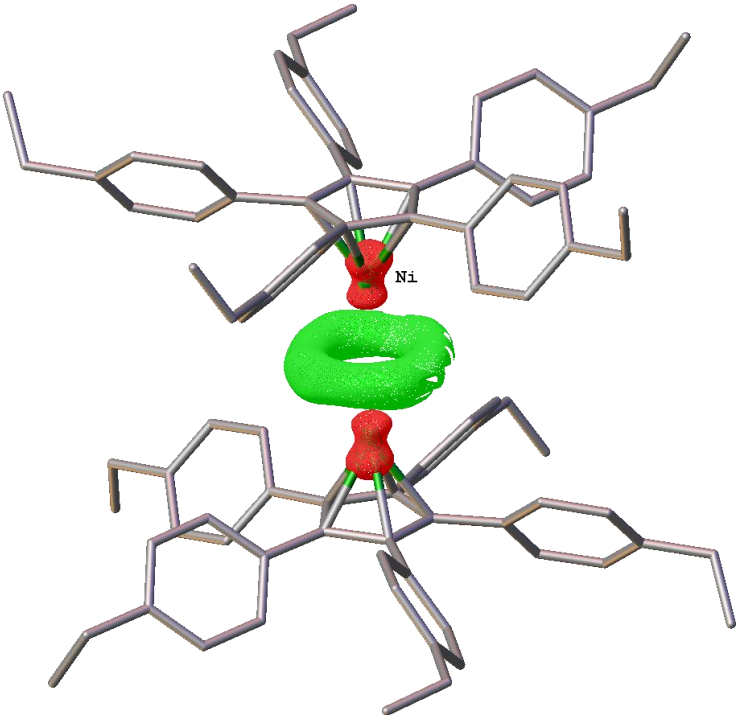

Figure S12. Electron density map in the crystal of a mixture of compounds **1**, **2** and **3**. Hydrogen atoms are omitted and Cp^{PEt} ligands are drawn in 'wire-or-stick' model for clarity.

Computational Details

All the structures have been optimized using the M11-L hybrid meta-GGA DFT functional[7] coupled with the 6-31G(d,p) basis set. The recently developed M11-L DFT functional was shown to provide excellent performance for main-group energies, proton and electron affinities, barrier heights, bond dissociation and non-covalent interaction energies. All the optimizations were followed by frequency analysis to ensure that the structures are real minima, without imaginary frequencies.

Table S2. Interatomic distances for the optimized $Cp_2Ni_2P_2$ structures.

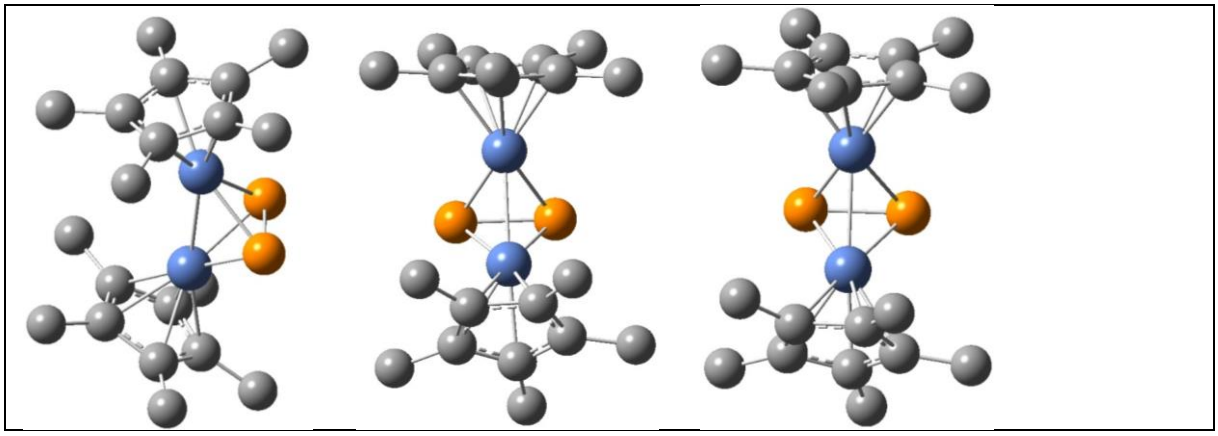

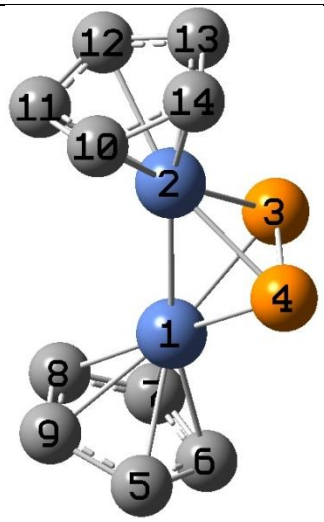

1. -7180.994821 a.u. Cs
0.0 kcal/mol (global minimum)

	1	2	3	4	5
1 Ni	0.000000				
2 Ni	2.421190	0.000000			
3 P	2.162276	2.162070	0.000000		
4 P	2.160420	2.168070	2.082738	0.000000	
5 C	2.076246	4.271752	4.096644	3.462937	0.000000
6 C	2.051943	4.444520	3.553485	3.487315	1.429962
7 C	2.084122	4.308470	3.363089	4.011164	2.317598
8 C	2.072023	3.978166	3.768484	4.230570	2.314730
9 C	2.105295	3.999170	4.233362	3.957268	1.419933
10 C	4.126196	2.090255	4.225448	3.617600	5.520109
11 C	4.051636	2.134130	4.138197	4.184233	5.610158
12 C	4.199006	2.086033	3.573790	4.195035	6.079562
13 C	4.408925	2.054148	3.346562	3.686562	6.320051
14 C	4.391124	2.082637	3.811617	3.315637	6.018269

	6	7	8	9	10
6 C	0.000000				
7 C	1.431744	0.000000			
8 C	2.306222	1.421014	0.000000		
9 C	2.306996	2.317407	1.444647	0.000000	
10 C	6.100699	6.072535	5.415760	5.078312	0.000000
11 C	6.069703	5.709136	4.906660	4.876913	1.432577
12 C	6.215520	5.716469	5.168596	5.462960	2.315191
13 C	6.387507	6.136574	5.842009	6.007761	2.305736
14 C	6.343837	6.367436	5.999144	5.816314	1.424398

	11	12	13	14
11 C	0.000000			
12 C	1.429095	0.000000		
13 C	2.308439	1.431307	0.000000	
14 C	2.313726	2.319789	1.429962	0.000000

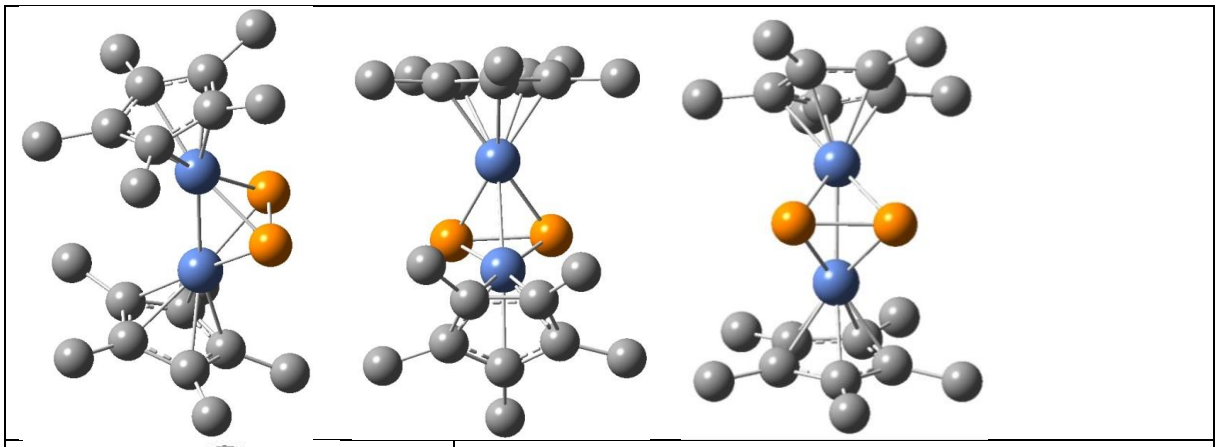

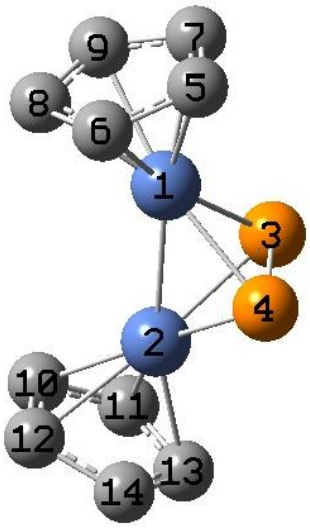

2. -7180.986593 a.u.
+5.2 kcal/mol Cs

		1	2	3	4	5
1	Ni	0.000000				
2	Ni	2.407134	0.000000			
3	P	2.165753	2.160848	0.000000		
4	P	2.164729	2.163873	2.083587	0.000000	
5	C	2.072377	4.396796	3.745848	3.334108	0.000000
6	C	2.074528	4.122714	4.191531	3.535729	1.427084
7	C	2.067274	4.391853	3.359953	3.783930	1.429111
8	C	2.129432	4.007614	4.183080	4.125633	2.313356
9	C	2.085629	4.133992	3.642349	4.221822	2.315521
10	C	3.959003	2.076244	3.852378	4.227437	5.980507
11	C	4.269363	2.089036	3.395537	4.069625	6.333047
12	C	4.007517	2.097172	4.245526	3.879192	5.862980
13	C	4.423683	2.048282	3.476348	3.520517	6.363901
14	C	4.295771	2.078977	4.036858	3.417080	6.106710

		6	7	8	9	10
6	C	0.000000				
7	C	2.308995	0.000000			
8	C	1.429441	2.312511	0.000000		
9	C	2.314445	1.428821	1.434301	0.000000	
10	C	5.401529	5.777160	4.830977	5.048911	0.000000
11	C	6.046335	6.046648	5.619432	5.570882	1.420594
12	C	5.126151	6.008216	4.859598	5.409068	1.443013
13	C	6.122765	6.350575	6.023740	6.119741	2.305036

	14 C 5.604929 6.353144 5.621106 6.050401 2.312731 11 12 13 14 11 C 0.000000 12 C 2.318050 0.000000 13 C 1.431196 2.308786 0.000000 14 C 2.317497 1.420253 1.431637 0.000000
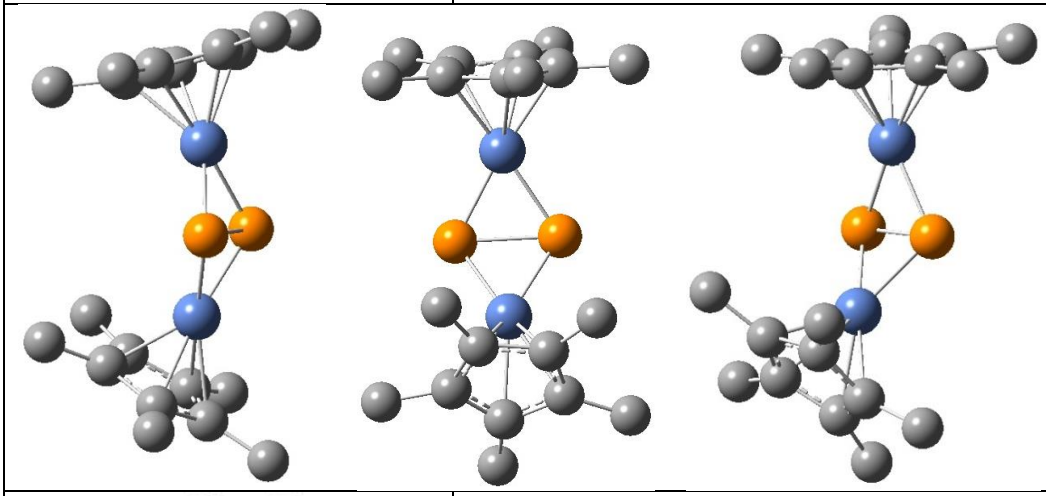	
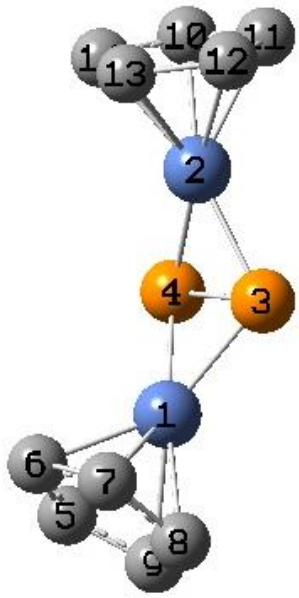 3. -7180.968852 a.u. +16.3 kcal/mol C_{2v}	1 2 3 4 5 1 Ni 0.000000 2 Ni 3.452887 0.000000 3 P 2.124975 2.119016 0.000000 4 P 2.123561 2.128495 2.147830 0.000000 5 C 2.067675 5.197098 4.187962 3.519428 0.000000 6 C 2.018146 4.719531 3.871381 3.561677 1.433298 7 C 2.041370 4.823810 3.500187 4.004111 2.319236 8 C 2.083377 5.324949 3.599073 4.195199 2.313403 9 C 2.110476 5.549757 4.040412 3.931684 1.421849 10 C 5.380771 2.070239 4.102920 3.601505 6.921113 11 C 5.456839 2.084393 3.727829 3.999737 7.266758 12 C 5.185916 2.066333 3.489938 4.188424 7.002598 13 C 4.942748 2.052875 3.764203 3.948912 6.478551 14 C 5.074147 2.059427 4.132618 3.574248 6.428264 6 7 8 9 10 6 C 0.000000 7 C 1.437176 0.000000 8 C 2.314452 1.425502 0.000000 9 C 2.307752 2.308525 1.428915 0.000000

	10 C 6.512247 6.811125 7.346051 7.422034 0.000000 11 C 6.786286 6.782068 7.235585 7.533765 1.431507 12 C 6.273280 6.123380 6.761279 7.279879 2.310742 13 C 5.628374 5.722850 6.587730 7.015017 2.309749 14 C 5.800025 6.191674 6.969370 7.110256 1.422341 11 12 13 14 11 C 0.000000 12 C 1.420418 0.000000 13 C 2.308118 1.433995 0.000000 14 C 2.311995 2.320788 1.437128 0.000000
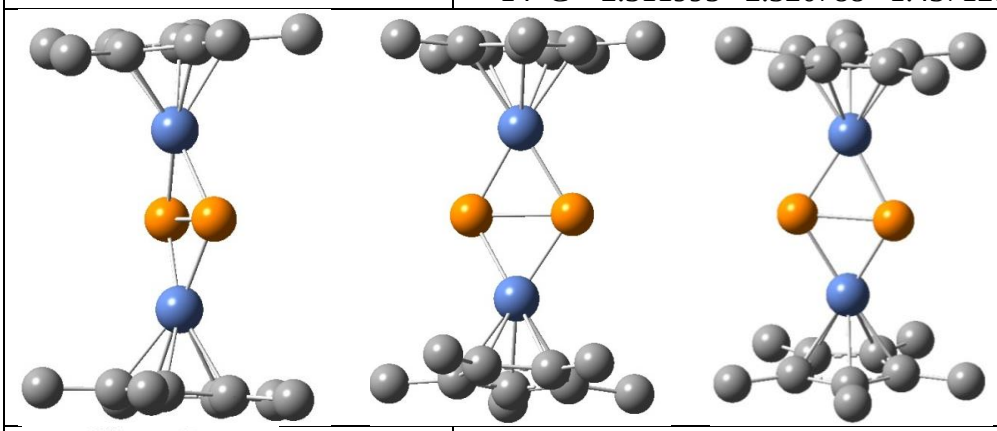	
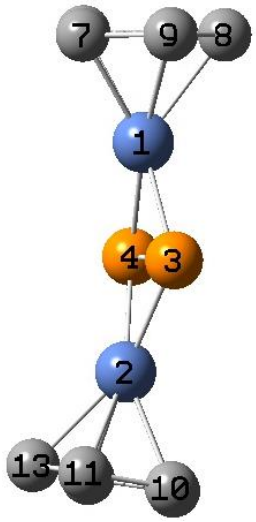 4. -7180.944221 a.u. +31.8 kcal/mol C_{2v}	1 2 3 4 5 1 Ni 0.000000 2 Ni 3.564932 0.000000 3 P 2.100954 2.108743 0.000000 4 P 2.108294 2.101591 2.159461 0.000000 5 C 2.070391 5.347445 4.140350 3.578738 0.000000 6 C 2.073881 5.397629 4.066657 3.505039 1.421526 7 C 2.036709 5.306911 3.766369 3.966267 1.435867 8 C 2.085282 5.437075 3.682734 3.903270 2.311474 9 C 2.081065 5.398939 3.499662 4.181767 2.321803 10 C 5.420482 2.085226 3.525896 4.098059 7.337872 11 C 5.323612 2.061919 3.575307 4.120717 7.077728 12 C 5.454798 2.084357 3.906495 3.711532 7.236669 13 C 5.281767 2.034586 3.964392 3.737243 6.787557 14 C 5.391648 2.076717 4.177461 3.491806 6.918645

	6 7 8 9 10 6 C 0.000000 7 C 2.307368 0.000000 8 C 1.436342 2.301594 0.000000 9 C 2.316595 1.429647 1.420961 0.000000 10 C 7.281073 7.140576 7.095411 7.024113 0.000000 11 C 7.298084 6.787595 7.202790 6.905400 1.421357 12 C 7.089245 7.322809 7.135037 7.295422 1.434658 13 C 7.101175 6.740762 7.290971 7.093171 2.310566 14 C 6.996596 7.106007 7.275819 7.356707 2.320088 11 12 13 14 11 C 0.000000 12 C 2.307331 0.000000 13 C 1.435523 2.301924 0.000000 14 C 2.321670 1.422946 1.431212 0.000000

Table S3. Interatomic distances for the optimized $Cp_2Ni_2P_3$ structures.

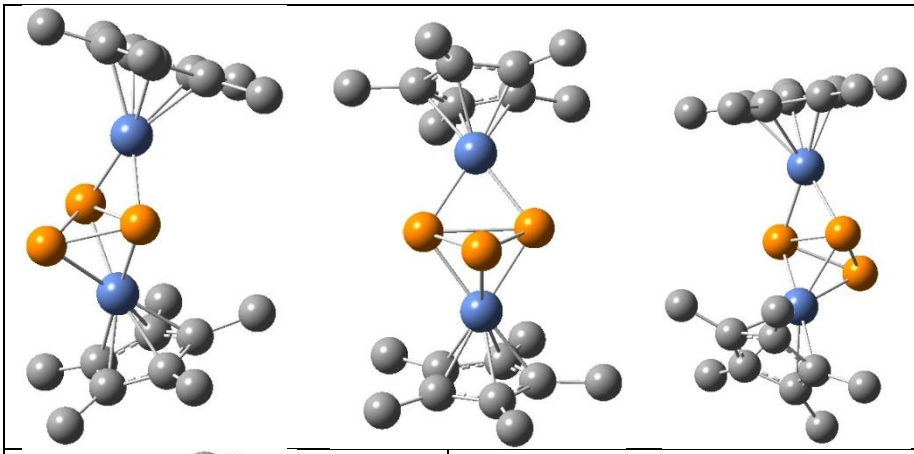

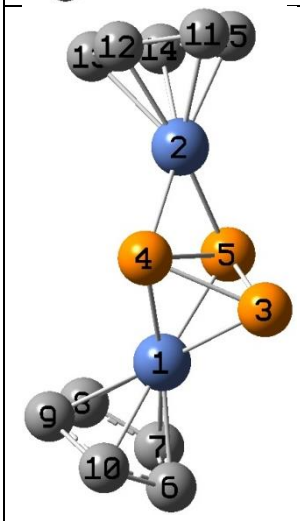

1. -7522.325047 a.u.
0.0 kcal/mol Cs

Spin density Ni2: 0.92

	1	2	3	4	5
1 Ni	0.000000				
2 Ni	3.563866	0.000000			
3 P	2.215889	3.135263	0.000000		
4 P	2.194229	2.184906	2.154915	0.000000	
5 P	2.196341	2.183434	2.158897	2.471697	0.000000
6 C	2.076075	5.622225	3.590664	4.121387	3.959100
7 C	2.061497	5.262943	3.899242	4.228878	3.450689
8 C	2.049075	4.818906	4.233330	3.803611	3.475597
9 C	2.059046	4.944409	4.158772	3.389885	4.000776
10 C	2.064223	5.430317	3.751725	3.597455	4.258193
11 C	5.552839	2.066125	4.643097	3.818958	4.077591
12 C	5.362044	2.111325	4.953607	3.514180	4.284247
13 C	5.160993	2.139188	5.222947	3.766949	3.979677
14 C	5.262917	2.140328	5.124057	4.214405	3.573659
15 C	5.484724	2.076530	4.745602	4.225857	3.620395

	6	7	8	9	10
6 C	0.000000				
7 C	1.423694	0.000000			
8 C	2.313941	1.434817	0.000000		
9 C	2.314234	2.315318	1.430797	0.000000	
10 C	1.432135	2.313468	2.316804	1.431647	0.000000
11 C	7.596151	7.314503	6.870328	6.900344	7.341491
12 C	7.430704	7.126540	6.425926	6.321631	6.956093

13 C	7.196537	6.637045	5.823442	5.959349	6.812810
14 C	7.248977	6.554250	5.963933	6.381639	7.145893
15 C	7.477376	6.967201	6.600316	6.926688	7.444395

	11	12	13	14	15
11 C	0.000000				
12 C	1.424140	0.000000			
13 C	2.303857	1.429532	0.000000		
14 C	2.310938	2.315664	1.426582	0.000000	
15 C	1.430038	2.311816	2.304444	1.426171	0.000000

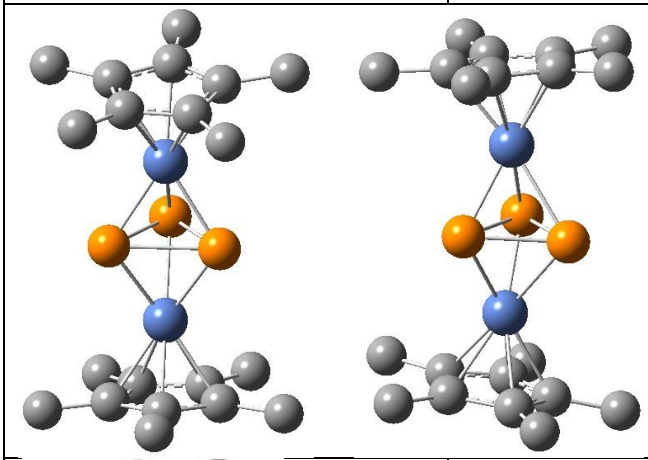

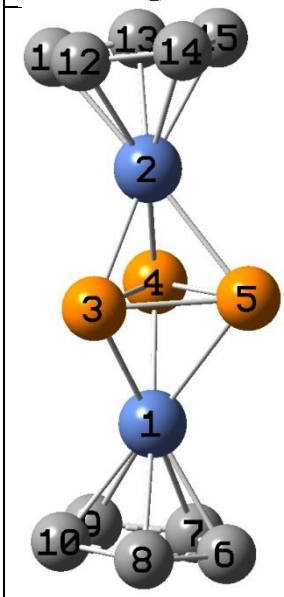

2. -7522.312329 a.u.
+8.0 kcal/mol CS

Spin densities
Ni1 0.44 and Ni2 0.34

	1	2	3	4	5
1 Ni	0.000000				
2 Ni	3.594420	0.000000			
3 P	2.176956	2.178469	0.000000		
4 P	2.173318	2.181074	2.337018	0.000000	
5 P	2.342574	2.292277	2.185293	2.182926	0.000000
6 C	2.081511	5.496134	4.061103	4.019794	3.656855
7 C	2.087610	5.446097	4.258039	3.553583	3.966378
8 C	2.080086	5.438610	3.573707	4.252433	3.908420
9 C	2.059960	5.328252	3.898523	3.487159	4.346552
10 C	2.078701	5.349704	3.474887	3.964212	4.336853
11 C	5.287082	2.046092	3.651277	3.646397	4.337026
12 C	5.409701	2.082518	3.471814	4.164386	4.127209
13 C	5.373176	2.088864	4.154399	3.419622	4.122783
14 C	5.493770	2.077979	3.824424	4.207863	3.684154

	15 C 5.459519 2.070582 4.214491 3.757621 3.668540 6 7 8 9 10 6 C 0.000000 7 C 1.427432 0.000000 8 C 1.429285 2.317988 0.000000 9 C 2.305351 1.430084 2.311882 0.000000 10 C 2.308448 2.318076 1.427611 1.431438 0.000000 11 C 7.317848 7.088800 7.112775 6.697936 6.739524 12 C 7.335935 7.385524 7.026795 7.082410 6.879618 13 C 7.281259 6.966078 7.356419 6.816930 7.090917 14 C 7.236616 7.377535 7.146489 7.349621 7.233238 15 C 7.190099 7.108300 7.337329 7.181008 7.347277 11 12 13 14 15 11 C 0.000000 12 C 1.433002 0.000000 13 C 1.433572 2.323378 0.000000 14 C 2.305177 1.420174 2.317933 0.000000 15 C 2.303623 2.313751 1.421909 1.439232 0.000000
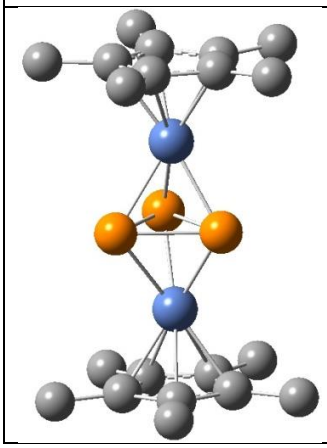 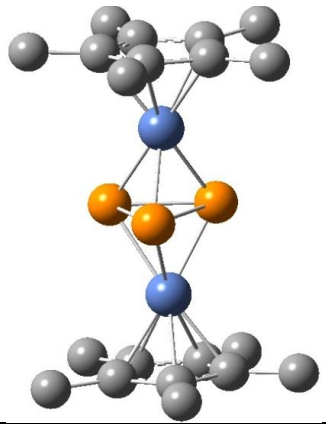	

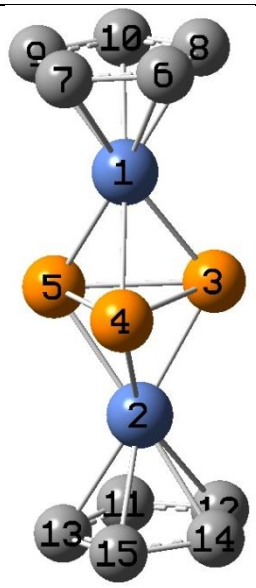

3. -7522.309936 a.u.
+9.5 kcal/mol

Spin densities
Ni1: 0.43 Ni2

		1	2	3	4	5
1	Ni	0.000000				
2	Ni	3.613544	0.000000			
3	P	2.184102	2.186816	0.000000		
4	P	2.269278	2.288425	2.202943	0.000000	
5	P	2.203851	2.198770	2.295171	2.180687	0.000000
6	C	2.076742	5.447445	3.797089	3.614307	4.237828
7	C	2.070483	5.439487	4.202994	3.574042	3.821095
8	C	2.086779	5.441309	3.492818	4.107633	4.190383
9	C	2.088460	5.440997	4.187828	4.060386	3.497832
10	C	2.048656	5.389186	3.710650	4.317136	3.697289
11	C	5.403392	2.051951	3.840572	4.315781	3.602407
12	C	5.427911	2.084992	3.492007	4.226390	4.093204
13	C	5.457429	2.087285	4.250460	3.954593	3.552498
14	C	5.428946	2.076927	3.663640	3.728669	4.270160
15	C	5.446500	2.075594	4.128226	3.539228	3.957840

		6	7	8	9	10
6	C	0.000000				
7	C	1.439798	0.000000			
8	C	1.422321	2.315661	0.000000		
9	C	2.317220	1.419941	2.324169	0.000000	
10	C	2.304285	2.302116	1.432216	1.433326	0.000000
11	C	7.359038	7.281029	7.155392	7.038594	6.904655
12	C	7.190671	7.382315	6.978890	7.307256	7.004978
13	C	7.345409	7.099239	7.407781	7.022328	7.164606
14	C	7.001868	7.200349	7.061903	7.388665	7.254823
15	C	7.100483	7.022024	7.326561	7.215153	7.349695

		11	12	13	14	15
11	C	0.000000				
12	C	1.432148	0.000000			
13	C	1.433130	2.323600	0.000000		
14	C	2.307519	1.424541	2.319334	0.000000	
15	C	2.303568	2.313312	1.423574	1.436318	0.000000

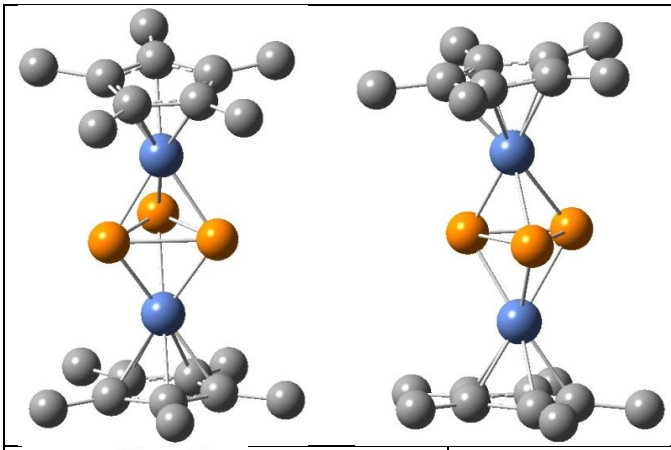

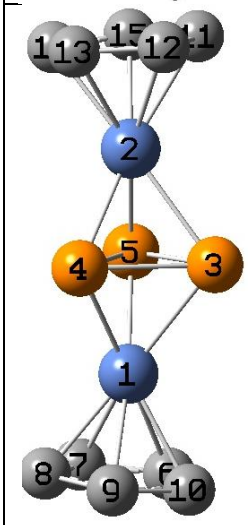

4. -7522.309178 a.u.
+10.0 kcal/mol Cs

Spin densities
Ni1: 0.41 Ni2: 0.34

	1	2	3	4	5
1 Ni	0.000000				
2 Ni	3.598355	0.000000			
3 P	2.322284	2.291989	0.000000		
4 P	2.174973	2.186182	2.186086	0.000000	
5 P	2.181711	2.179048	2.187536	2.324633	0.000000
6 C	2.078544	5.437697	3.890738	4.251712	3.575862
7 C	2.073694	5.355891	4.316508	3.950629	3.481552
8 C	2.060352	5.342488	4.321876	3.484141	3.912132
9 C	2.087495	5.449079	3.932650	3.563638	4.263798
10 C	2.082330	5.493270	3.630440	4.032310	4.062969
11 C	5.474768	2.078462	3.656379	4.213849	3.813385
12 C	5.460247	2.073808	3.659749	3.780223	4.214560
13 C	5.402701	2.089900	4.127799	3.458180	4.161525
14 C	5.317433	2.045381	4.336837	3.675293	3.655884
15 C	5.409635	2.081417	4.108811	4.174626	3.463340

	6	7	8	9	10
6 C	0.000000				
7 C	1.427320	0.000000			
8 C	2.311840	1.431780	0.000000		
9 C	2.318327	2.318183	1.429441	0.000000	
10 C	1.429016	2.307177	2.303569	1.426552	0.000000
11 C	7.112824	7.223028	7.349599	7.352106	7.193849
12 C	7.327941	7.352170	7.195797	7.105530	7.175857

	13 C 7.377386 7.125607 6.870199 7.006815 7.305558 14 C 7.133190 6.781273 6.761449 7.133935 7.340795 15 C 7.012687 6.891983 7.111488 7.390104 7.318127 11 12 13 14 15 11 C 0.000000 12 C 1.438948 0.000000 13 C 2.316971 1.420234 0.000000 14 C 2.305627 2.302262 1.432283 0.000000 15 C 1.421387 2.313374 2.322116 1.432840 0.000000

References

[1] U. Chakraborty, M. Modl, B. Mühldorf, M. Bodensteiner, S. Demeshko, N. J. C. van Velzen, M. Scheer, S. Harder, R. Wolf, *Inorg. Chem.* **2016**, *55*, 3065-3074.

[2] F. F. Puschmann, D. Stein, D. Heift, C. Hendriksen, Z. A. Gal, H.-F. Grützmacher, H. Grützmacher, *Angew. Chem., Int. Ed.* **2011**, *50*, 8420-8423.

[3] CrysAlisPro Software System, Agilent Technologies UK Ltd, Yarnton, Oxford, UK (2014).

[4] Sheldrick, G.M., ShelXT, *Acta Cryst.*, **2014**, *A71*, 3-8.

[5] O.V. Dolomanov and L.J. Bourhis and R.J. Gildea and J.A.K. Howard and H. Puschmann, Olex2: A complete structure solution, refinement and analysis program, *J. Appl. Cryst.*, **2009**, *42*, 339-341.

[6] Sheldrick, G.M., A short history of ShelX, *Acta Cryst.*, **2008**, *A64*, 339-341.

[7] R. Peverati, D. G. Truhlar, *J. Phys. Chem. Lett.*, **2011**, *2*, 2810–2817.

5 Metal-assisted Opening of Intact P_4 Tetrahedra

Moritz Modl, Sebastian Heinl, Fuencisla Delgado Calvo, Maria Caporali, Gabriele Manca, Martin Keilwerth, Karsten Meyer, Maurizio Peruzzini, Manfred Scheer

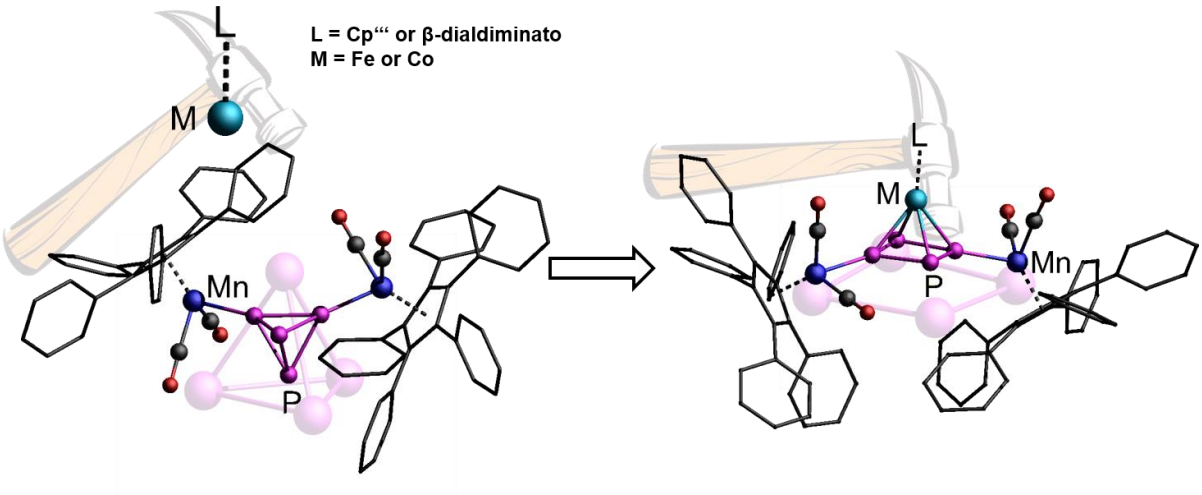

- **All syntheses and characterizations of compound 5 and 6 were performed by Sebastian Heinl with the aid of Dr. Maria Caporali, Fuencisla Delgado Calvo and Dr. Maurizio Peruzzini in the course of a short term scientific mission (STSM; COST Action CM0802), unless subsequently noted otherwise. These results are also subject of the PhD thesis of Sebastian Heinl**
- **All syntheses and characterizations of compound 7a and 7b were performed by Moritz Modl, unless subsequently noted otherwise**
- **Manuscript in this version was written by Moritz Modl**
- **Discussion of compound 5 and 6 was written by Sebastian Heinl. Discussion of compound 7a and 7b was written by Moritz Modl**
- **Figures of crystal structures and NMR pictures of compound 5 and 6 were made by Sebastian Heinl, compound 7a and 7b by Moritz Modl**
- **$^{31}P\{^1H\}$ NMR and simulation of compound 6 were performed by Moritz Modl**
- **DFT calculations were performed and interpreted by Fuencisla Delgado Calvo**
- **Mössbauer measurements were performed and interpreted by Martin Keilwerth and Karsten Meyer**
- **X-Ray structure analyses and refinement of compound 5 and 6 were performed by Sebastian Heinl, compound 7a and 7b by Moritz Modl**

5.1 Introduction

In the quest for a selective activation and functionalization of white phosphorus, a protocol for the straightforward preparation of organophosphorus compounds from elemental phosphorus needs to be established. Therefore, the reactivity of P_4 towards a large number of transition metal fragments, including almost all transition metals,[1] and a large number of main group elements[2] has been examined. Among these studies, the P_4 ligand containing transition metal complexes can be classified into complexes bearing intact, tetrahedral P_4 ligands and complexes with transformed P_4 ligands, e.g. *cyclo*-P_4 moieties. Moreover, they can be grouped corresponding to coordination mode of the P_4 ligand as well as the number of metal centers. After the seminal work of Sacconi, who reported on the first complex bearing an intact P_4 tetrahedron η^1-coordinated to nickel (type **A** in Scheme **1**),[3] a large number of cationic type **A** complexes were synthesized by Peruzzini *et al.* under mild reaction conditions.[4] Also some dicationic bi-nuclear complexes were obtained (type **B**).[4a-d] Recently, neutral manganese complexes of the type **A** and **B** were reported by the Scheer group.[4e]

These end-on coordinated P_4 complexes of type **A** and **B** stand in contrast to their side-on coordinated relatives, which also exist as complexes containing edge cleaved P_4^{2-} moieties[5] and compounds revealing an intact P_4 tetrahedron as ligand.[6] Recently Scheer *et al.* reported on the first neutral mono- and binuclear complexes bearing intact white phosphorus as ligands (type **C**).[6a] Having all these complexes with an intact P_4 tetrahedron as ligands in mind, the question arose, how intact is the ligand and show these complexes a similar or a different reactivity as free white phosphorus did? Besides the detailed DFT calculations showing the intact status of the ligand, the experimental removal of free P_4 could be achieved.[6a] Moreover, the cationic derivatives of type **A** show an interesting reactivity towards water, in which unexpectedly, the formation of PH_3, P_2H_4 and other phosphorus containing products PO_nH_m was observed, revealing a changed reaction behavior in comparison to free P_4.[4b,4h,7]

Furthermore, the reductive degradation of the P_4 tetrahedron leads to a stepwise P_4 transformation, revealing as the next step either the P_4^{2-} species mono- or di-coordinated by transition metal fragments[5] or the square planar *cyclo*-P_4^{2-} species as an end-deck (type **D**),[8] a middle deck in a triple-decker sandwich complex (type **F**)[9] or as recently reported by Scheer *et al.*, as end decks in homoleptic iron sandwich complexes (type **G**).[10]

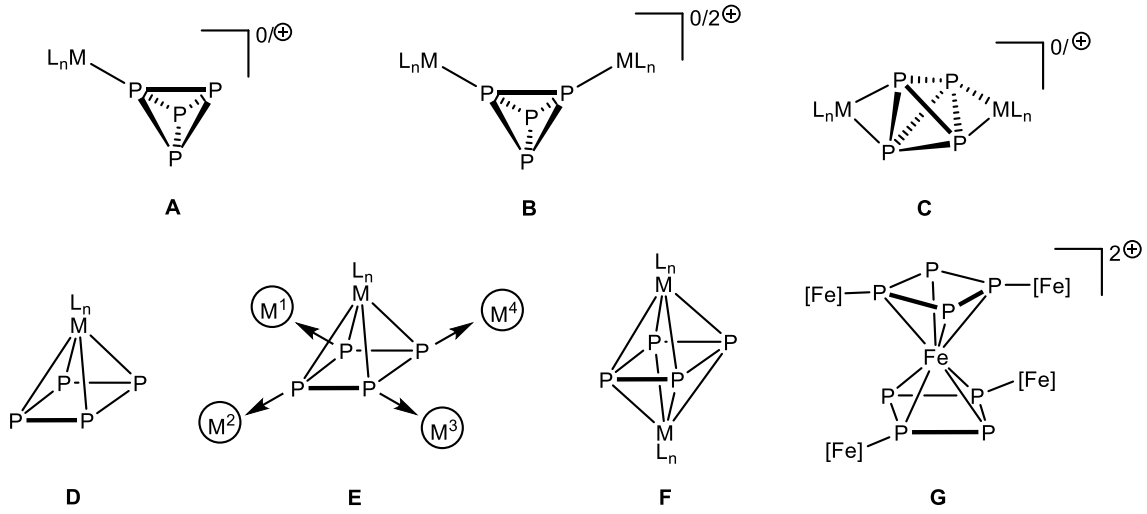

Scheme 1. Selected complexes bearing intact white phosphorus (**A**-**C**), and *cyclo*-P_4 (**D**-**G**) as ligand.

As a representative approach the triple-decker complex [(Cp'''Co)$_2$(μ-toluene)] (**1**) (Cp''' = $C_5H_2{}^tBu_3$-1,2,4),[11] existing in solution as 14 valence electron [Cp'''Co] fragment enables the reaction with P_4 under very mild conditions. Tuning the stoichiometry and conditions of the two component reaction of **1** with free white phosphorus, different P_n polyphosphorus aggregates (n ≤ 29) and the binuclear derivative [(Cp'''Co)$_2$(μ,η$^{2:2}$-P$_2$)$_2$] were obtained.[12] The missing building block [Cp'''Co(η^4-P$_4$)] was recently accessible as one of the rare representatives of complexes containing a *cyclo*-P_4 endo-deck (type **D**).[8a] The latter sandwich complex is part of the derivative family consisting from versatile combinations of Group 6 (Cr, Mo, W) and 9 metal centers (Co, Rh, Ir) coordinated up to four [M(CO)$_5$] fragments (M = Cr, W; see type **E** in Scheme 1).[13] In the 1990s these compounds were generated via three component reactions of [Cp^{R}M(CO)$_2$]$_2$ (M = Co, Rh, Ir) with P_4 in the presence of Lewis acidic [M(CO)$_5$] fragments.[13b-e]

Besides the above mentioned complex **1**, recent reports by Driess *et al.* and Scheer *et al.* presented the transformation of P_4 under mild conditions by low-valent β-diiminato (L^R) Fe^I and Co^I complexes [L^{R}M(μ-toluene)] (M = Fe (**2a**), Co (**2b**)).[9e,9f,14a,14b] Depending on the different aromatic flanking groups and α-backbone substituents of the β-diiminato ligand, different P_n ligand complexes could be obtained. The products are dominated by binuclear derivatives with the general composition [(L^{R}M)$_2$(μ,η$^{4:4}$-P$_4$)] (type **F**).

We were intrigued by the study of the reactivity of complexes containing formally intact white phosphorus as ligands (type **A** and **B**), towards the above mentioned triple-decker complexes **1, 2a** and **2b**, respectively, to highlight any differences in the reactivity in comparison with free P_4, as mentioned above. Herein we report on the reactions of the P_4 ligand complexes, bearing a formally intact P_4 tetrahedron as ligand, [CpRu(PPh$_3$)$_2$(η^1-P$_4$)][CF$_3$SO$_3$] (**3**; cationic type **A**) and [{Cp^{BIG}Mn(CO)$_2$}$_2$(μ,η$^{1:1}$-P$_4$)] (**4**; neutral type **B**), (Cp^{BIG} = C$_5$(C$_6$H$_5{}^n$Bu)$_5$) with the

unsaturated complexes **1**, **2a** and **2b**, respectively. This leads to the selective synthesis of the new *cyclo*-P_4 ligand complexes $[\{CpRu(PPh_3)_2\}\{CoCp'''\}(\mu,\eta^{1:4}\text{-}P_4)][CF_3SO_3]$ (**5**), $[\{Cp^{BIG}Mn(CO)_2\}_2\{CoCp'''\}(\mu,\eta^{1:1:4}\text{-}P_4)]$ (**6**) and $[\{Cp^{BIG}Mn(CO)_2\}_2\{ML^0\}(\mu,\eta^{1:1:4}\text{-}P_4)]$ (M = Fe (**7a**), Co (**7b**); $L^0 = CH[CHN(2,6\text{-}Me_2C_6H_3)]_2$), respectively.

5.2 Results and Discussion

The reaction of **3** with 0.5 equivalents of **1** is conducted in THF, starting at -50 °C and stirring for 16 h while warming up to room temperature. After purification complex **5** can be isolated as a red solid in 82 % yield. Complex **5** can be dissolved in polar solvents like THF or CH_2Cl_2. Complex **6** is synthesized by adding a solution of 0.5 equivalents of **1** in toluene to a toluene solution of **4** and stirring for 16 h. Compound **6** is obtained from a CH_2Cl_2 solution stored at -35 °C in 25% crystalline yield.[15] A stoichiometric mixture of **4** and **2a** or **2b**, respectively, is dissolved in toluene and stirred for 18 h at room temperature. Complex **7a** and **7b**, can be isolated from a saturated *n*-hexane solution, stored at 4 °C in 31% (**7a**) and 26% (**7b**) crystalline yield, respectively.[15] In all cases, a complete and selective transformation of the P_4 tetrahedron to a planar *cyclo*-P_4 unit is observed as one single reaction product is detected by the ^{31}P NMR spectra of the crude reaction mixture. The rather moderate isolatable yields are caused by the excellent solubility of the complexes **6**, **7a** and **7b**, respectively, in all common organic solvents like THF, CH_2Cl_2, toluene or *n*-pentane, due to the large Cp^{BIG} ligands.[15] No further degradation or aggregation, as seen for the reaction with free white phosphorus, takes place even if an excess of **1**, **2a** or **2b** is used. The isolated binuclear and trinuclear compounds $[\{CpRu(PPh_3)_2\}\{CoCp'''\}(\mu,\eta^{1:4}\text{-}P_4)][CF_3SO_3]$ (**5**), $[\{Cp^{BIG}Mn(CO)_2\}_2\{CoCp'''\}(\mu,\eta^{1:1:4}\text{-}P_4)]$ (**6**) and $[\{Cp^{BIG}Mn(CO)_2\}_2\{ML^0\}(\mu,\eta^{1:1:4}\text{-}P_4)]$ (M = Fe (**7a**), Co (**7b**); $L^0 = CH[CHN(2,6\text{-}Me_2C_6H_3)]_2$), respectively, show *cyclo*-P_4 units bridging the metal atoms (Scheme 2). They can be described as $[LM(\eta^4\text{-}P_4)]$ (M = Fe, Co) complexes, additionally coordinating to the 16 VE complex fragments $\{CpRu(PPh_3)_2\}$ and $\{Cp^{BIG}Mn(CO)_2\}$, respectively.

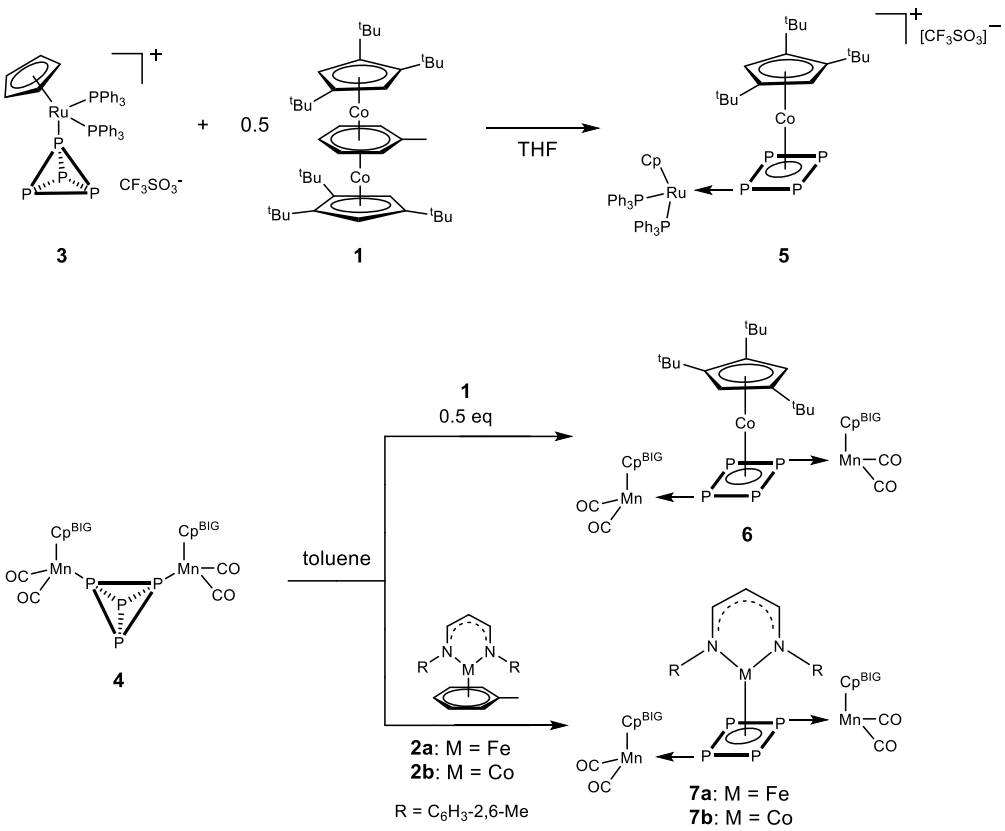

Scheme 2. Synthesis of complexes **5**, **6, 7a** and **7b**.

The formed products show that the P_4 tetrahedron in the starting complexes behave like free P_4 in the reaction with formal 14 VE complex fragments. However, the by the P lone pairs initially coordinated Lewis acids are still coordinated in the final products **5** – **7**. Therefore, for the first time this rather strong Lewis acid coordination in **4** leads to the first end-on coordinated *cyclo*-P_4 complexes in the reaction with 'NacNac' metal fragments, avoiding the formation of triple-decker complexes in the case of **7a** and **7b**. Moreover, for the bidentate complexed compound **6** no further aggregation occurs, what is usually found during the synthesis of the type **D** complex [Cp'''Co(η^4-P_4)] due to its instability in solution.

From the products **5** and **6**, crystals suitable for single crystal X-ray diffraction could be obtained by cooling concentrated CH_2Cl_2 solutions to -30 °C (**5**: Figure 1, **6**: Figure 2). Single crystals of **7a** and **7b** suitable for X-ray diffraction were grown from saturated *n*-hexane solutions at 4 °C (**7a**, **7b**: Figure 3). The average P–P bond length in the *cyclo*-P_4 ligand in **5**, **6**, **7a** and **7b** is 2.151(1) Å and lies in between a P–P single bond (2.21 Å)[16] and a P=P double bond (2.05 Å).[17] This indicates almost perfectly planar, aromatic P_4 cycles.

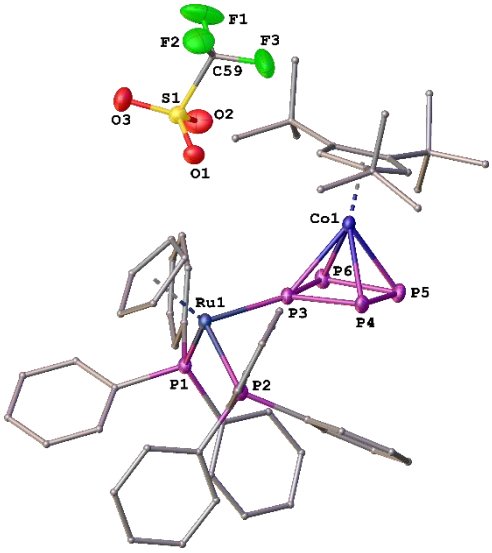

Figure 1. Molecular structure of **5** in the crystal. Thermal ellipsoids are set at 50% probability. For clarity solvent molecules are omitted and C atoms are depicted in 'wire-or-stick' model. Selected bond lengths [Å] and angles [°]: Ru1-P1 2.3548(8), Ru1-P2 2.3681(7), Ru1-P3 2.2945(6), P3-P4 2.1243(9), P4-P5 2.1549(8), P5-P6 2.1722(9), P3-P6 2.1481(8), Co1-P3 2.3927(10), Co1-P4 2.3412(9), Co1-P5 2.2825(9), Co1-P6 2.3247(10), Cp'''_{cent}-Co1-$P_{4,cent}$ 172.61(3), Ru1-P3-P4 129.23(4), Ru1-P3-P6 135.05(3), P4-P3-P6 93.58(4), P3-P4-P5 87.57(4), P4-P5-P6 92.05(4), P3-P6-P5 86.53(4).

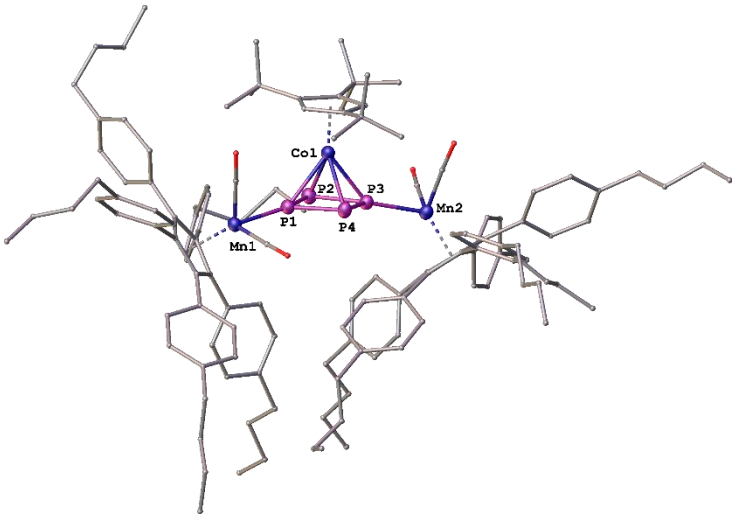

Figure 2. Molecular structure of **6** in the crystal. Thermal ellipsoids are set at 50% probability. For clarity solvent molecules are omitted, in case of disorder only the main part is shown and C atoms are depicted in 'wire-or-stick' model. Selected bond lengths [Å] and angles [°]: Mn1-P1 2.222(1), Mn2-P3 2.203(1), P1-P2 2.161(2), P2-P3 2.168(1), P3-P4 2.131(2), P1-P4 2.143(1), Co1-P1 2.338(1), 2.339(1), 2.297(1), 2.359(1), Cp'''_{cent}-Co1-$P_{4,cent}$ 175.21(5), P1-P2-P3 85.19(6), P2-P3-P4 94.16(6), P1-P4-P3 86.58(6), P2-P1-P4 93.97(6).

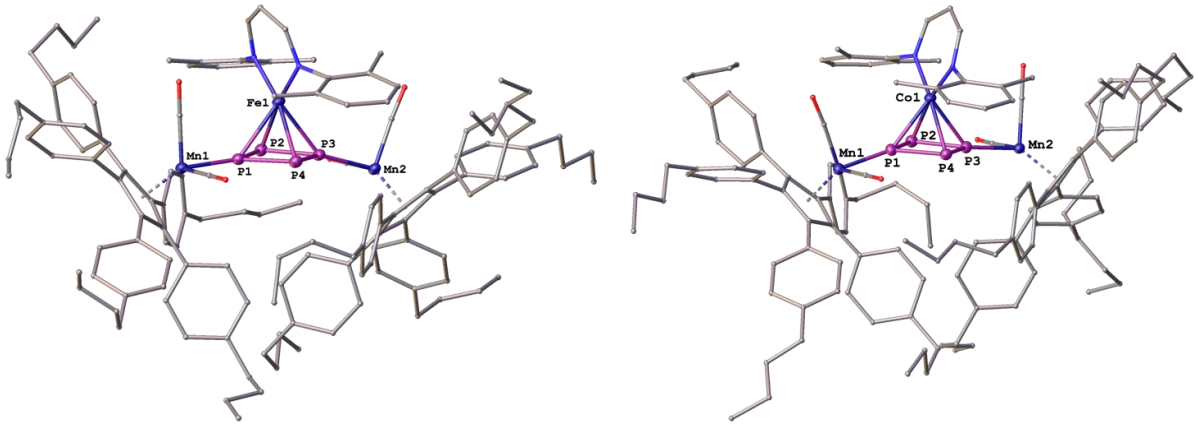

Figure 3. Molecular structure of **7a** (left) and **7b** (right) in the crystal. Thermal ellipsoids are set at 50% probability. For clarity solvent molecules and hydrogen atoms are omitted, in case of disorder only the main part is shown and C atoms are depicted in 'wire-or-stick' model. Only one of the two unique molecules in the asymmetric unit is shown. Selected bond lengths [Å] and angles [°] for **7a**: Mn1-P1 2.204(1), Mn2-P3 2.216(1), P1-P2 2.154(1), P2-P3 2.165(1), P3-P4 2.157(1), P1-P4 2.149(1), Fe1-P 2.377(1), 2.410(1), 2.363(1), 2.430(1), Fe1-N 1.959(1), 1.948(1), P1-P2-P3 85.01(3), P2-P3-P4 94.51(3), P1-P4-P3 85.33(3), P2-P1-P4 95.07(3). Selected bond lengths [Å] and angles [°] for **7b**: Mn1-P1 2.211(1), Mn2-P3 2.200(1), P1-P2 2.145(1), P2-P3 2.146(1), P3-P4 2.147(1), P1-P4 2.158(1), Co1-P 2.334(1), 2.406(1), 2.332(1), 2.388(1), Co1-N 1.914(1), 1.924(1), P1-P2-P3 85.16(2), P2-P3-P4 95.15(2), P1-P4-P3 84.81(2), P2-P1-P4 94.83(2).

The ^{t}Bu groups of the Cp''' ligand and the phenyl groups of the L^0 ligand, respectively, are orientated along the non-coordinating P atoms to minimize the steric repulsion. A distortion of the co-planar orientation of the Cp''' rings and the *cyclo*-P_4 ligands by 11.05(8)° in **5** and 4.7(1)° in **6** is observed. Nevertheless, the structural parameters of **5**, **6**, **7a** and **7b**, respectively, do not show significant differences in comparison to the complexes obtained from free P_4 (**D** - **E**, Scheme 1), bearing square planar *cyclo*-P_4 ligands.[9,13,14b]

Since the P-P distances of **5**, **6**, **7a** and **7b**, respectively, are in between single and double bonds and the structures are planar, suggesting a π-delocalized system, the *cyclo*-P_4 ligand can be described as an aromatic dianion $[P_4]^{2-}$ unit, which is also in agreement with DFT calculations and in analogy to $[Cs_2(\eta^4\text{-}P_4)]\cdot 2NH_3$ reported by Korber *et al.*[9a]

The $^{31}P\{^1H\}$ NMR spectrum of **5** shows an AM_2XY_2 spin system, where at room temperature, three of the four signals are strongly broadened. NMR investigations at variable temperatures were carried out (Figure 4) and it was observed that while cooling, the signals A and X steadily get sharper, signal M first gets sharper until it reaches a maximum at 233 K and then progressively broadens again. At 233 K, a spectrum of first order is obtained, where the coupling constants can be determined. It can be expected that further cooling would result in a splitting of signal M into two sets of signals. However, this was not possible due to limitation of the used solvent. At the lowest temperature achieved (193 K), signal M is nearby at the coalescence point.

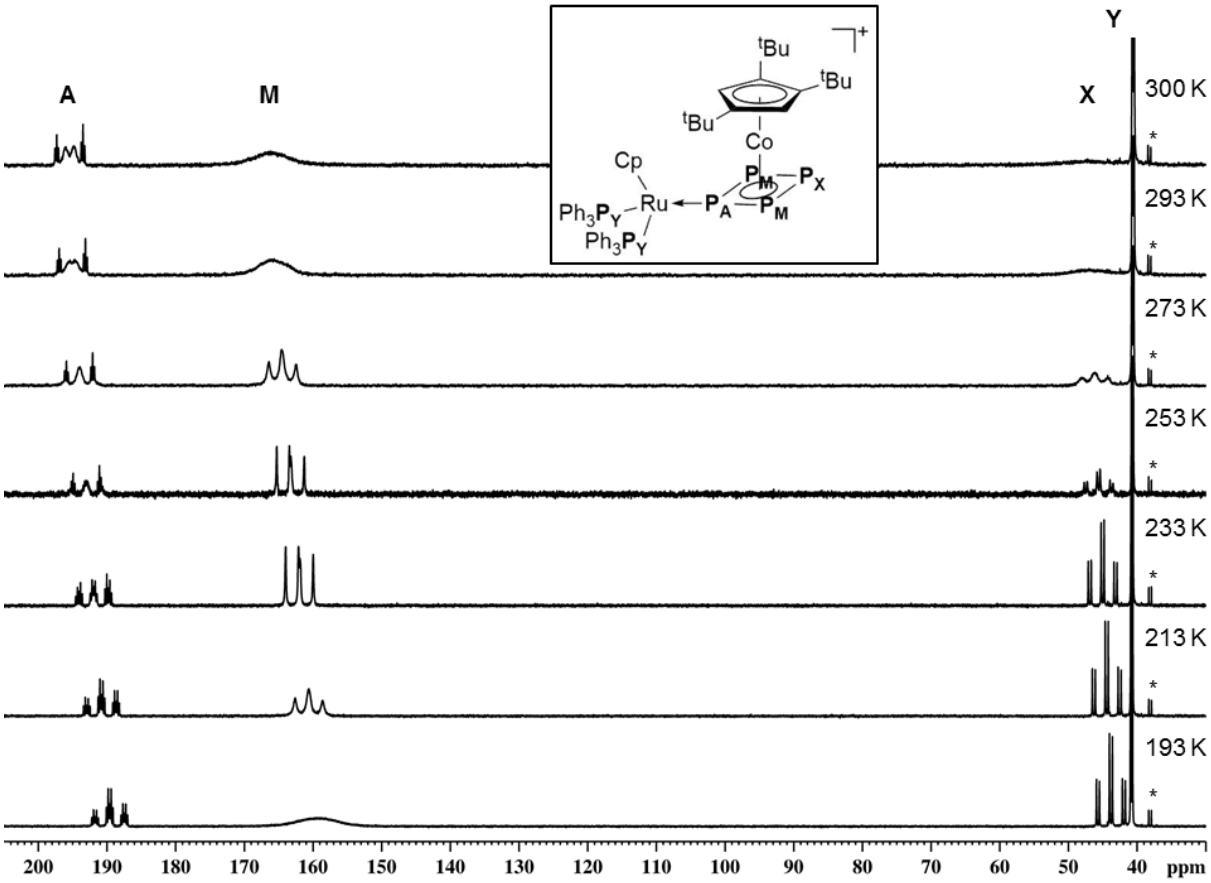

Figure 4. $^{31}P\{^1H\}$ NMR spectra of **5** in CD_2Cl_2 at various temperatures. $^{31}P\{^1H\}$ (233 K, CD_2Cl_2) δ [ppm] = 191.9 (tdt, $^1J_{PP}$ = 345 Hz, $^2J_{PP}$ = 71 Hz, $^2J_{PP}$ = 42 Hz, $1P_A$), 162.0 (dd, $^1J_{PP}$ = 345 Hz, $^1J_{PP}$ = 303 Hz, $1P_M$), 45.0 (td, $^1J_{PP}$ = 303 Hz, $^2J_{PP}$ = 71 Hz, $1P_X$), 40.7 (d, $^2J_{PP}$ = 42 Hz, $2P_Y$). Signal marked with an asterisk are due to small impurities.

Furthermore, in the ^1H NMR at various temperatures the signals for the phenyl protons steadily get broader. Finally, at 213 K the signals split into several new resonances combined with a broadening of the signals of the Cp''' ligand. Further cooling again results in a sharpening of the phenyl signals in contrast to that of the Cp''' moiety (Figure S2, Supporting Information). These observations in the ^1H and $^{31}P\{^1H\}$ NMR spectra might be explained by a hindered rotation of the Cp''' ligand at room temperature. In addition to this, starting from 213 K the rotation of the $\{CpRu(PPh_3)_2\}$ fragment around the Ru-P_A bond could also be hampered. The positive ion ESI mass spectrum exhibits the basic peak at *m/z* = 1107.4 corresponding to $[\{CpRu(PPh_3)_2\}\{CoCp'''\}(\mu,\eta^{1:4}\text{-}P_4)]^+$.

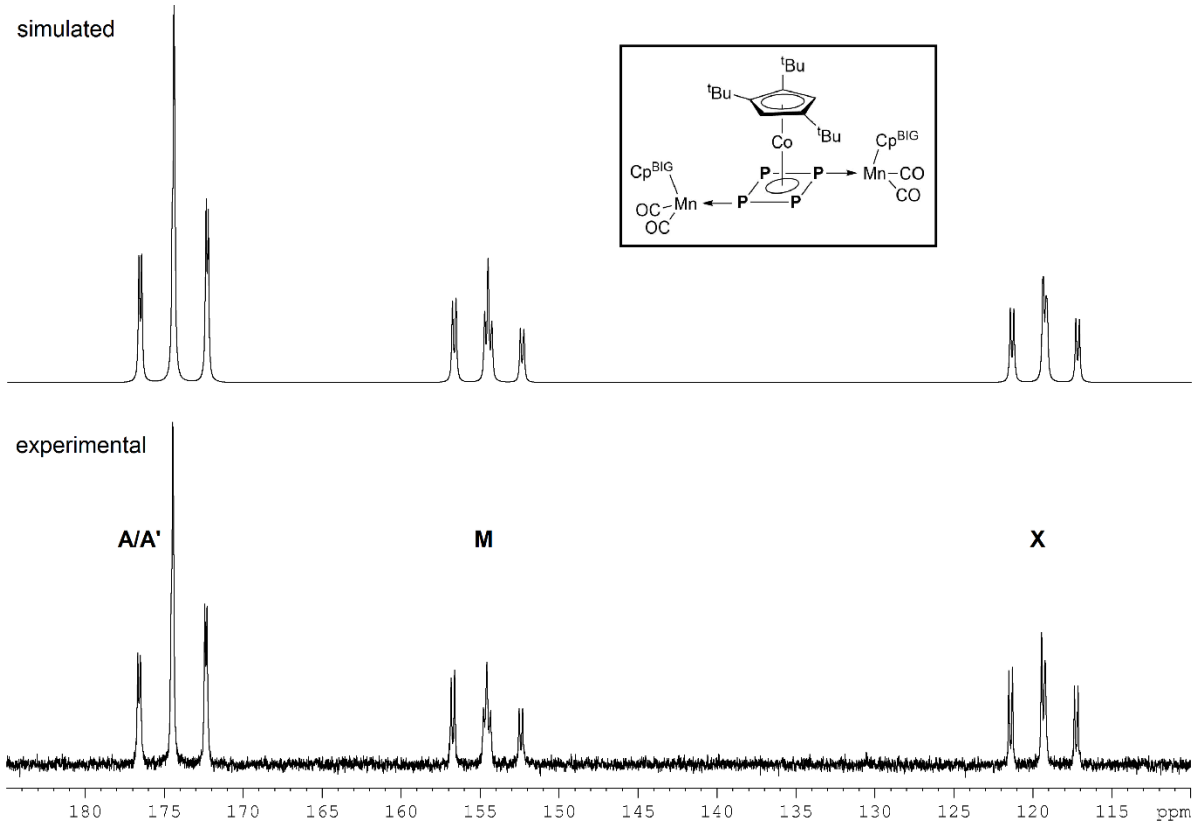

Figure 5. $^{31}P\{^1H\}$ NMR spectrum of **6** in C_6D_6 (bottom) at 298 K and simulated spectrum (top). Parameters from simulated $^{31}P\{^1H\}$ NMR spectrum: δ [ppm] = 174.34 (P_A), 174.31 ($P_{A'}$), 154.68 (P_M), 119.35 (P_X); $^2J(P_AP_{A'})$ = -25.2 Hz, $^1J(P_AP_M)$ = 347.6 Hz, $^1J(P_AP_X)$ = 336.0 Hz, $^1J(P_{A'}P_M)$ = 351.2 Hz, $^1J(P_{A'}P_X)$ = 339.7 Hz, $^2J(P_MP_X)$ = 33.3 Hz.

In the $^{31}P\{^1H\}$ NMR spectrum of **6**, instead of the expected two sets of signals, three are observed in an integral ratio of 2:1:1. The spectrum is of higher order and was simulated to determine the coupling constants. The fit was successful with an AA'MX spin system (see Figure 5). This indicates magnetically non-equivalent P atoms in **6** due to the fixed orientation of the *t*Bu groups of the Cp''' ligand (see Figure 2), making the uncoordinated P atoms magnetically non-equivalent. The ^1H NMR spectrum shows the expected number of resonances and multiplicities for the Cp^{BIG} and Cp''' ligands. Because of the expected C_S-symmetry and the close chemical shifts, it was not possible to definitely assign the signals to the related P atoms in the P_4 ring. One could tentatively propose that P atoms coordinated to manganese are the ones more deshielded (A/A', δ = 174.3 ppm), as expected also by comparison with **5**, where P_A (which is coordinated to Ru) resonates at lowest field, (δ = 190 ppm), while the naked P atoms, P_M and P_X are more shielded, δ = 154.7 and δ = 119.3 ppm, respectively. The corresponding FD mass spectrum shows the molecular ion peak of 6 with an intensity of 100 % and an additional peak with relative intensity of 6 %, where one $\{Cp^{BIG}Mn(CO)_2\}$ fragment is split off.

No signals were detected in the $^{31}P\{^1H\}$ NMR spectrum of **7a**. However, the ^1H NMR spectrum of **7a** shows four broad signals in the range from 3 ppm to 0 ppm with the intensity ratio 20:20:20:30 as expected for the ^nBu groups of the Cp^{BIG} ligand. In addition two very broad signals at 7.96 ppm and 6.86 ppm, respectively, were detected, which can be assigned to the phenyl protons of the Cp^{BIG} ligand. In the measured range from 900 ppm to -425 ppm only one broad singlet at 5.05 ppm can be allocated to the L^0 ligand, but no further signals are observed. Furthermore, the effective magnetic moment of **7a** at room temperature in C_6D_6 was determined by the Evans NMR method to be 2.06 μ_B. The X-band EPR spectrum, measured in toluene at 77 K, shows only a broad signal without resolved hyperfine interactions. The value of g_{iso} = 2.0354 and the effective magnetic moment (Evans method) suggest the presence of one unpaired electron. The zero-field ^{57}Fe Mössbauer spectrum of **7a** at 77 K features a doublet with an isomer shift δ of 0.49 $mm \cdot s^{-1}$ and a quadrupole splitting ΔE_Q of 1.74 $mm \cdot s^{-1}$. These values suggest a low–spin iron(III) center bearing one unpaired electron, confirming the paramagnetic spin state.

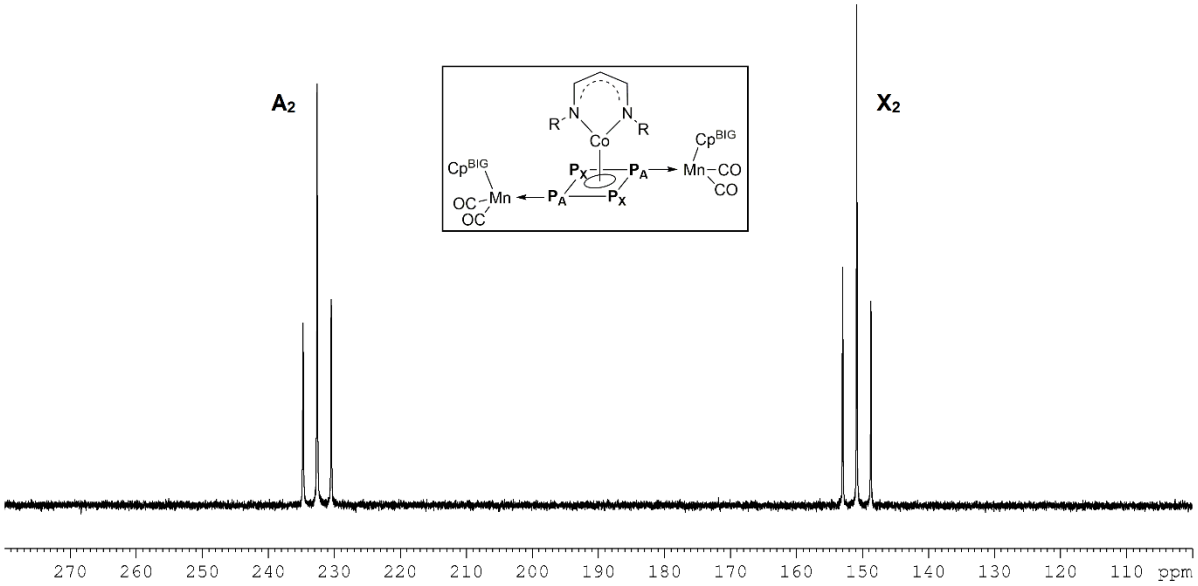

Figure 6. $^{31}P\{^1H\}$ NMR spectrum of **7b** in C_6D_6 at 298 K: δ [ppm] = 232.61 (t, $^1J_{PP}$ = 346.4 Hz, $2P_A$), 150.86 (t, $^1J_{PP}$ = 346.4 Hz, $2P_X$).[18]

Compared to the paramagnetic **7a**, the complex **7b** shows diamagnetic behavior. The $^{31}P\{^1H\}$ NMR spectrum of **7b** shows the expected two sets of signals in an integral ratio of 1:1, corresponding to an A_2X_2 spin system (Figure 6), which indicates the suggested molecular structure. Regarding the ^1H NMR spectrum, one set of sharp signals is observed. This is in line with freely rotating Cp^{BIG} and L^0 ligands in solution.

In the FD mass spectra the molecular ion peaks can be observed for the complexes **7a** and **7b**, together with $Cp^{BIG}H$ and minor fragmentation products.

To the best of our knowledge, **7a** and **7b**, respectively, represent the first end-on complexes with β-diiminato ligands. Until now, all reported compounds possess an inverted-sandwich structural motif (Scheme 1, type **F**) in the solid state. This might be caused by the permanent coordinated $\{Cp^{BIG}Mn(CO)_2\}$ fragments during the reaction, which prevents the formation of the above-mentioned bimetallic complexes.

DFT calculations were carried out to understand how the unsaturated cobalt fragment [Cp'''Co], formed *in situ* from the triple decker **1**, could interact with the P_4 moiety coordinated to ruthenium. A simplified model complex was used in the calculations hereafter indicated with **m,** with the substitution of phenyl rings of the PPh_3 ligands by methyl groups, while the *tert*-butyl groups on the cyclopentadienyl ring coordinated to cobalt were maintained and indicated as Cp'''. Once the triple-decker **1** dissolves in solution, the first putative change may be the formation of two mono-nuclear complexes of formula $[(Cp''')Co(THF)_2]$ (optimized structure is shown in Figure S11 in the Supporting Information). All efforts to optimize a structure with three coordinated THF molecules failed possibly due to a high steric hindrance. Once $[(Cp''')Co(THF)_2]$ is formed, the two solvent molecules may be displaced by the coordination of the cobalt center to the free face of the P_4 tetrahedron belonging to $[CpRu(PPh_3)_2(\eta^1\text{-}P_4)]^+$. In this regards, we found a minimum in the energy profile which corresponds to the formation of the plausible bimetallic intermediate, namely **5m'** shown in Figure 7. The formation of the putative intermediate **5m'** from the reagents $[CpRu(PR_3)_2(\eta^1\text{-}P_4)]^+$ and $[(Cp''')Co(THF)_2]$ was estimated to be highly exergonic (free energy gain of -73.2 kcal mol^{-1}).

In **5m'**, the initial P_4 moiety has undergone a P-P bond cleavage, resulting in a *quasi*-butterfly type ligand, behaving as a trihapto ligand towards cobalt while maintaining an intact η^1-coordination to ruthenium. In fact, there are really few examples in literature of a naked tetraphosphorus moiety η^3-coordinated to a metal center, like the bimetallic complex $[LNi(\eta^3\text{-}P_4)NiL]$ (L: L^{Et} = $CH[CMeN(2,6\text{-}Et_2C_6H_3)]_2$, L^{iPr} = $CH[CMeN(2,6\text{-}iPr_2C_6H_3)]_2$) featuring a doubly trihapto coordinated P_4.[19] The optimized structure of the intermediate shows an asymmetric coordination of the new tetraphosphorus moiety to the cobalt center with two shorter (2.20 Å) and one longer 2.27 Å Co-P distances. Such a feature has been observed recently in the iridium complex $[Ir(\kappa^2\text{-dppm})(\kappa^1\text{-dppm})(\eta^3\text{-}P_3\{P(O)H\})]$ prepared by Peruzzini *et al.*,[20] where a naked P_3 unit (coming from P_4 as well) behaves as a stable triphosphaallyl group and posesses an asymmetric structure.

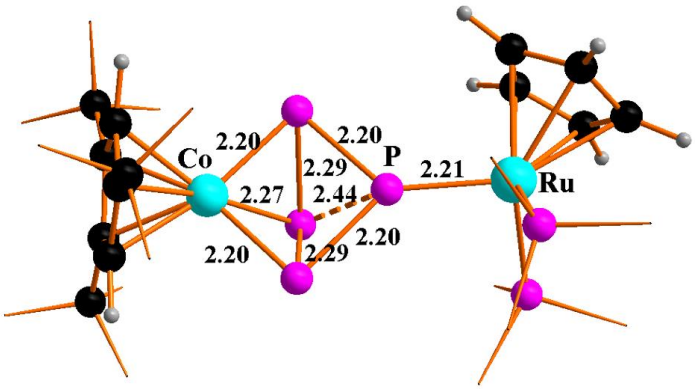

Figure 7. Optimized structure of the intermediate **5m'** from the reaction between $[CpRu(PR_3)_2(\eta^1\text{-}P_4)]^+$ and the solvate species $[(Cp''')Co(THF)_2]$.

Then, the tetraphosphorus moiety in the intermediate **5m'** will reassemble towards the final η^4-coordination to the cobalt in **5m**, as shown in Figure 8, with a further free energy gain of -12.6 kcal mol^{-1}. The optimized structure satisfactorily reproduces the X-ray one, as confirmed for example by four Co-P distances between 2.30 and 2.36 Å. The P-P distances are somewhat overestimated with 2.17- 2.20 Å *vs*. 2.12-2.17 Å in the X-ray structure.

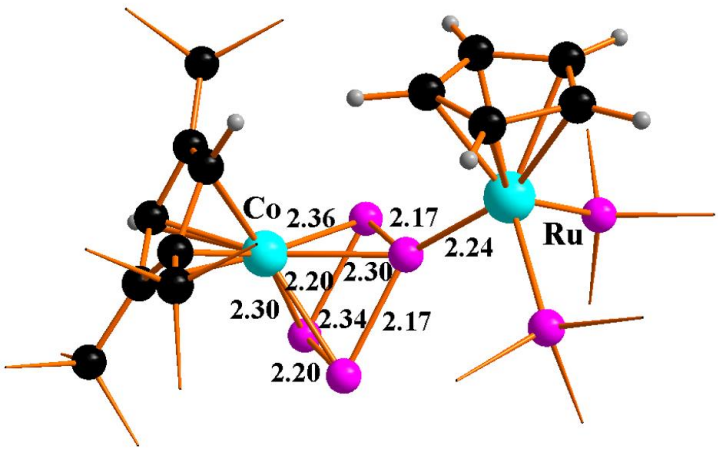

Figure 8. Computed optimized structure of the final bimetallic product, **5m**.

5.3 Conclusion

In summary, we proved the existence of intact P_4 ligands in the starting materials by subsequent reactions with 14 VE complex fragments. It really behaves like free P_4 in the reaction with the difference that during the P_4 conversion the coordination of the Lewis acidic fragments stays intact, so that different structured products are formed. Furthermore, we developed a new route to assemble the square planar *cyclo*-P_4 ligand starting from metal-coordinated intact, white phosphorus and the low valent [Cp'''Co] and $[L^0M]$ (M = Fe, Co)

fragments, respectively, while previously reported *cyclo*-P_4 complexes have been prepared by straightforward reaction with free P_4. The reactions are highly favored even at low temperature and are highly selective based on NMR spectroscopy. Starting from complexes **3** and **4**, which represent mono- and bimetallic compounds, respectively, bearing white phosphorus as intact tetrahedron, selectively two P-P bond cleavages take place causing the opening of the tetrahedron and lead to the unexpected square planar *cyclo*-P_4 moiety. The latter represents a very labile ligand, which in the present case benefits from the stabilization deriving by the coordination to two and three metal fragments, respectively, in **5**, **6**, **7a** and **7b**. Above all no further degradation or aggregation takes place, in contrast to the reaction starting from uncoordinated, free P_4. An exemplified DFT study showed as a putative intermediate in the reaction of **1** with **3**, a bimetallic complex where the P_4 moiety captures a *quasi*-butterfly geometry, with a trihapticity towards cobalt, forming in this way a rare example of a triphosphallyl ligand.

5.4 References

[1] a) B. M. Cossairt, N. A. Piro, C. C. Cummins, *Chem. Rev.* **2010**, *110*, 4164-4177; b) M. Caporali, L. Gonsalvi, A. Rossin, M. Peruzzini, *Chem. Rev.* **2010**, *110*, 4178-4235.

[2] a) M. Scheer, G. Balazs, A. Seitz, *Chem. Rev.* **2010**, *110*, 4236-4256; b) N. A. Giffin, J. D. Masuda, Coord. *Chem. Rev.* **2011**, *255*, 1342-1359; c) S. Khan, S. S. Sen, H. W. Roesky, *Chem. Commun.* **2012**, *48*, 2169-2179.

[3] a) P. Dapporto, S. Midollini, L. Sacconi, *Angew. Chem. Int. Ed.* **1979**, *18*, 469-469; b) P. Dapporto, L. Sacconi, P. Stoppioni, F. Zanobini, *Inorg. Chem.* **1981**, *20*, 3834-3839; for corresponding Mo and W derivatives $[M(CO)_3(PR_3)_2(\eta^1\text{-}P_4)]$ (M = Mo, W; R = Cy, iPr) cf.: T. Gröer, G. Baum, M. Scheer, *Organometallics* **1998**, *17*, 5916–5919.

[4] **for mono- and binuclear compounds:** a) M. Peruzzini, L. Marvelli, A. Romerosa, R. Rossi, F. Vizza, F. Zanobini, *Eur. J. Inorg. Chem.* **1999**, 931-933; b) M. Di Vaira, P. Frediani, S. Seniori Costantini, M. Peruzzini, P. Stoppioni, *Dalton Trans.* **2005**, 2234-2236; c) M. Di Vaira, M. Peruzzini, S. Seniori Costantini, P. Stoppioni, *J. Organomet. Chem.* **2010**, *695*, 816-820; d) M. Caporali, M. Di Vaira, M. Peruzzini, S. Seniori. Costantini, P. Stoppioni, F. Zanobini, *Eur. J. Inorg. Chem.* **2010**, 152-158; e) S. Heinl, E. V. Peresypkina, A. Y. Timoshkin, P. Mastrorilli, V. Gallo, M. Scheer, *Angew. Chem. Int. Ed.* **2013**, *52*, 10887-10891; **for mono-nuclear compounds:** f) T. Gröer, G. Baum, M. Scheer, *Organometallics* **1998**, *17*, 5916-5919; g) I. de los Rios, J.-R. Hamon, P. Hamon, C. Lapinte, L. Toupet, A. Romerosa, M. Peruzzini, *Angew. Chem., Int. Ed.* **2001**, *40*, 3910-3912; h) M. Di Vaira, M. Peruzzini, S. Seniori Costantini, P. Stoppioni, *J. Organomet. Chem.* **2006**, *691*, 3931-3937; i) V. Mirabello, M. Caporali, V. Gallo, L. Gonsalvi, A. Ienco, M. Latronico, P. Mastrorilli, M. Peruzzini, *Dalton Trans.* **2011**, *40*, 9668-9671; j) V. Mirabello, M. Caporali, V. Gallo, L. Gonsalvi,

D. Gudat, W. Frey, A. Ienco, M. Latronico, P. Mastrorilli, M. Peruzzini, *Chem. Eur. J.* **2012**, *18*, 11238-11250.

[5] **e.g. for bi- (and mono)-nuclear compounds:** a) O. J. Scherer, M. Swarowsky, G. Wolmershaeuser, *Organometallics* **1989**, *8*, 841-842; b) Y. Peng, H. Fan, H. Zhu, H. W. Roesky, J. Magull, C. E. Hughes, *Angew. Chem.* **2004**, *116*, 3525-3527; c) Y. Xiong, S. Yao, M. Brym, M. Driess, *Angew. Chem. Int. Ed.* **2007**, *46*, 4511-4513; d) S. Dürr, D. Ertler, U. Radius, *Inorg. Chem.* **2012**, *51*, 3904-3909; e) C. C. Mokhtarzadeh, A. L. Rheingold, J. S. Figueroa, *Dalton Trans.* **2016**, *45*, 14561-14569; **e.g. for mono-nuclear compounds:** f) A. P. Ginsberg, W. E. Lindsell, *J. Am. Chem. Soc.* **1971**, *93*, 2082-2084; g) A. P. Ginsberg, W. E. Lindsell, K. J. McCullough, C. R. Sprinkle, A. J. Welch, *J. Am. Chem. Soc.* **1986**, *108*, 403-416; h) G. Prabusankar, A. Doddi, C. Gemel, M. Winter, R. A. Fischer, *Inorg. Chem.* **2010**, *49*, 7976-7980, i) J. W. Dube, C. M. E. Graham, C. L. B. Macdonald, Z. D. Brown, P. P. Power, P. J. Ragogna, *Chem. Eur. J.* **2014**, *20*, 6739-6744.

[6] a) F. Spitzer, M. Sierka, M. Latronico, P. Mastrorilli, A. V. Virovets, M. Scheer, *Angew. Chem. Int. Ed.* **2015**, *54*, 4392-4396; b) L. C. Forfar, T. J. Clark, M. Green, S. M. Mansell, C. A. Russell, R. A. Sanguramath, J. M. Slattery, *Chem. Commun.* **2012**, *48*, 1970-1972; c) G. Santiso-Quinones, A. Reisinger, J. Slattery, I. Krossing, *Chem. Commun.* **2007**, 5046-5048; d) I. Krossing, L. van Wüllen, *Chem. Eur. J.* **2002**, *8*, 700-711.

[7] a) P. Barbaro, M. Di Vaira, M. Peruzzini, S. Seniori Costantini, P. Stoppioni, *Angew. Chem., Int. Ed.* **2008**, *47*, 4425-4427; b) P. Barbaro, M. Di Vaira, M. Peruzzini, S. Seniori Costantini, P. Stoppioni, *Inorg. Chem.* **2009**, *48*, 1091-1096; c) M. Di Vaira, M. Peruzzini, P. Stoppioni, *C. R. Chim.* **2010**, *13*, 935-942.

[8] a) F. Dielmann, A. Timoshkin, M. Piesch, G. Balázs, M. Scheer, *Angew. Chem., Int. Ed.* **2017**, *56*, 1671-1675; b) for $[Cp^*Nb(CO)_2(\eta^4\text{-}P_4)]$ ($Cp^*= C_5Me_5$): O. J. Scherer, J. Vondung, G. Wolmershäuser, *Angew. Chem. Int. Ed.* 1989, *28,* 1355-1357; c) for $[Cp''Ta(CO)_2(\eta^4\text{-}P_4)]$ ($Cp''= C_5H_3{}^tBu_2$-1,3): O. J. Scherer, R. Winter, G. Wolmershäuser, *Z. Anorg. Allg. Chem.* **1993**, *619*, 827-835.

[9] a) for $[Cs_2(\eta^4\text{-}P_4)]\cdot 2NH_3$: F. Kraus, J. C. Aschenbrenner, N. Korber, *Angew. Chem. Int. Ed.* **2003**, *42,* 4030-4033; b) for $[(P_2N_2)Zr(\mu_2,\eta^{4:4}\text{-}P_4)]_2$: W. W. Seidel, O. T. Summerscales, B. O. Patrick, M. D. Fryzuk, *Angew. Chem. Int. Ed*. **2009**, *48*, 115-117; c) for $[\{(DippO)_3Nb\}_2(\mu_2,\eta^{4:4}\text{-}P_4)]$: A. Velian, C. C. Cummins, *Chem. Sci*. **2012**, *3*, 1003-1006; d) C. Camp, L. Maron, R. G. Bergman, J. Arnold, *J. Am. Chem. Soc.* **2014**, *136*, 17652-17661; e) $[(nacnacCo)_2(\mu_2,\eta^{4:4}\text{-}P_4)]$: S. Yao, N. Lindenmaier, Y. Xiong, S. Inoue, T. Szilvasi, M. Adelhardt, J. Sutter, K. Meyer, M. Driess, *Angew. Chem. Int. Ed.* **2015**, *54,* 1250-1254; f) $[(nacnacFe)_2(\mu_2,\eta^{4:4}\text{-}P_4)]$: F. Spitzer, C. Graßl, G. Balázs, E. M. Zolnhofer, K. Meyer, M. Scheer, *Angew. Chem. Int. Ed.* **2016**, *55*, 4340-4344; g) for $[(BIANCo)_2(\mu_2,\eta^{4:4}\text{-}P_4)]$: S. Pelties, T. Maier, D. Herrmann, B. de Bruin, C. Rebreyend, S. Gärtner, I. G. Shenderovich, R. Wolf, *Chem. Eur. J.* **2017**, *23*, 6094-6102.

[10] J. Müller, S. Heinl, C. Schwarzmaier, G. Balázs, M. Keilwerth, K. Meyer, M. Scheer, *Angew. Chem., Int. Ed.* **2017**, *56*, 7312-7317.

[11] J. J. Schneider, D. Wolf, C. Janiak, O. Heinemann, J. Rust, C. Krüger, *Chem. Eur. J.* **1998**, *4*, 1982-1991.

[12] F. Dielmann, M. Sierka, A. V. Virovets, M. Scheer, *Angew. Chem. Int. Ed.* **2010**, *49*, 6860-6864.

[13] a) group 4: M. Scheer, E. Herrmann, J. Sieler, M. Oehme, *Angew. Chem. Int. Ed. Engl.* **1991**, *30*, 969-971; b) Rh compounds: M. Scheer, C. Troitzsch, P. G. Jones, *Angew. Chem. Int. Ed. Engl.* **1992**, *31*, 1377-1379; c) Co compounds: M. Scheer, U. Becker, J. C. Huffman, M. H. Chisholm, *J. Organomet. Chem*. **1993**, *461,* C1 – C3; d) Ir compounds: M. Scheer, U. Becker, E. Matern, *Chem. Ber.* **1996**, *129*, 721-724; e) Co compounds: M. Scheer, U. Becker, *J. Organomet. Chem.* **1997**, *545-546*, 451-460.

[14] **Fe:** a) S. Yao, T. Szilvasi, N. Lindenmaier, Y. Xiong, S. Inoue, M. Adelhardt, J. Sutter, K. Meyer, M. Driess, *Chem. Commun.* **2015**, *51*, 6153-6156; **Co:** b) F. Spitzer, C. Graßl, G. Balázs, E. Mädl, M. Keilwerth, E. M. Zolnhofer, K. Meyer, M. Scheer, *Chem. Eur. J.* **2017**, *23*, 2716-2721.

[15] Due to the high solubility of the products **6**, **7a** and **7b**, the isolated yields are lower in comparison of a complete conversion of the educts detected by ^{31}P NMR spectroscopy.

[16] P. Pyykkö, M. Atsumi, *Chem. Eur. J.* **2009**, *15*, 186-197.

[17] P. Pyykkö, M. Atsumi, *Chem. Eur. J.* **2009**, *15*, 12770-12779.

[18] The spin system observed in the $^{31}P\{^1H\}$ NMR spectrum of compound **7b** can be best described as A_2XX', since the signal at 150.86 ppm shows a minor $^2J(P_XP_{X'})$ coupling of = 1.8 Hz. For further information see SI.

[19] S. Yao, Y. Xiong, C. Milsmann, E. Bill, S. Pfirrmann, C. Limberg, M. Driess, *Chem. Eur. J.* **2010**, *16*, 436-439.

[20] V. Mirabello, M. Caporali, L. Gonsalvi, G. Manca, A. Ienco, M. Peruzzini, *Chem. Asian. J.* **2013**, *8*, 3177-3184.

5.5 Supporting Information

General Remarks

All experiments were carried out under an atmosphere of dry argon or nitrogen using glovebox and Schlenk techniques. Solvents were dried using a MB SPS-800 device of company MBRAUN and degassed prior to use. [(Cp'''Co)$_2$(μ-toluene)] (**1**),[1] [(L^{0}Fe)(μ-toluene)] (**2a**),[2] [(L^{0}Co)(μ-toluene)] (**2b**),[3] [CpRu(PPh$_3$)$_2$(η^1-P$_4$)][CF$_3$SO$_3$] (**3**)[4] and [{Cp^{BIG}Mn(CO)$_2$}$_2$(μ,η$^{1:1}$-P$_4$)] (**4**)[5] were prepared according to literature procedures. The NMR spectra were measured on a Bruker Avance 300, 400 or 600 spectrometer. ESI-MS spectra were measured on a ThermoQuest Finnigan TSG 7000 mass spectrometer and FD-MS spectra on a Finnigan MAT 95 mass spectrometer. The elemental analyses were determined on a Vario EL III apparatus. The IR spectra were measured on a VARIAN FTS-800 FT-IR spectrometer or a Thermo Scientific Nicolet iS5 spectrometer. The X-band EPR measurements were carried out with a MiniScope MS400 device equipped with a Magnettech GmbH rectangular TE102 resonator at a frequency of 9.5 GHz.

Synthesis of [{CpRu(PPh$_3$)$_2$}{CoCp'''}(μ,η$^{1:4}$-P$_4$)][CF$_3$SO$_3$] (5)

An orange solution of [CpRu(PPh$_3$)$_2$(η^1-P$_4$)][CF$_3$SO$_3$] (285 mg, 0.3 mmol) in 10 mL THF is cooled to -50 °C and a solution of [(Cp'''Co)$_2$toluene] (100 mg, 0.15 mmol) in 10 mL THF is added drop wise. The solution is stirred for 16 h while warming up to room temperature. A red precipitate of **5** is formed, which is filtered, washed with cold THF and dried in vacuum to give pure **5** (305 mg, 82%). Crystals can be obtained from CH_2Cl_2 solutions at -35 °C as solvate.

5: [$C_{59}H_{64}F_3CoO_3P_6RuS$] * 2 CH_2Cl_2 (solvent molecules were found in the crystal structure) calc: C, 51.38; H, 4.81; S, 2.25. found: C, 51.82; H, 4.93; S, 2.25. ESI-MS (CH_2Cl_2, cation): *m/z* (%) = 1107.4 (100%, [{CpRu(PPh$_3$)$_2$}{CoCp'''}(μ,η$^{1:4}$-P$_4$)]$^+$). ^{1}H NMR (CD_2Cl_2): δ [ppm] = 1.43 (9H, s, Cp'''/C*H*$_3$), 1.54 (18H, s, Cp'''/C*H*$_3$), 4.58 (5H, s, Cp/C*H*), 5.86 (2H, s, Cp'''/C*H*), 7.00 (12H, m, PPh$_3$/C*H*), 7.31 (12H, t, $^3J_{HH}$ = 7.1 Hz, PPh$_3$/C*H*), 7.46 (6H, t, $^3J_{HH}$ = 7.3 Hz, PPh$_3$/C*H*). ^{31}P{^{1}H} (233 K, CD_2Cl_2) δ [ppm] = 40.7 (2P$_Y$, d, $^2J_{PP}$ = 42 Hz), 45.0 (1P$_X$, td, $^1J_{PP}$ = 303 Hz, $^2J_{PP}$ = 71 Hz), 162.0 (1P$_M$, dd, $^1J_{PP}$ = 345 Hz, $^1J_{PP}$ = 303 Hz), 191.9 (1P$_A$, tdt, $^1J_{PP}$ = 345 Hz, $^2J_{PP}$ = 71 Hz, $^2J_{PP}$ = 42 Hz).^{31}P{^{1}H} (298 K, CD_2Cl_2) δ [ppm] = 40.5 (2P, d, $^2J_{PP}$ = 40 Hz), 42 - 55 (1P, br, too broad to assign ω$_{1/2}$), 166 (2P, s-br, ω$_{1/2}$ = 1060 Hz), 195.4 (1P, m). For more details on ^{31}P{^{1}H} NMR investigations see text. ^{19}F NMR (CD_2Cl_2) δ [ppm] = -78.8. ^{13}C{^{1}H} NMR (CD_2Cl_2): δ [ppm] = 31.7 (Cp''', ^{t}Bu), 32.0 (Cp''', ^{t}Bu), 33.8 (Cp''', ^{t}Bu), 34.3 (Cp''', ^{t}Bu), 80.5 (Cp''', C$_5$), 86.7 (Cp, C$_5$), 116.5 (Cp''', C$_5$), 118.4 (Cp''', C$_5$), 128.9 (PPh$_3$, Ph), 131.0 (PPh$_3$, Ph), 134.5 (PPh$_3$, Ph), 135.7 (PPh$_3$, Ph).

Synthesis of [{$Cp^{BIG}Mn(CO)_2$}$_2${CoCp'''}(μ,$η^{1:1:4}$-P_4)] (6)

To a brown solution of [{$Cp^{BIG}Mn(CO)_2$}$_2$($η^{1:1}$-P_4)] (100 mg, 56 µmol) in 5 mL toluene a solution of [(Cp'''Co)$_2$(toluene)] (19 mg, 28 µmol) in 5 mL toluene is added. The solution is stirred for 16 h and the solvent is removed in vacuum. The residue is dissolved in 5 mL CH_2Cl_2 and cooled to -35 °C. Product **6** is obtained as solvate with CH_2Cl_2 as brown plank-shaped crystals (30 mg, 25%).

5: [$C_{131}H_{159}CoMn_2O_4P_4$] * 4 CH_2Cl_2 (solvent molecules were found in the crystal structure) calc: C, 66.72; H, 6.93. found: C, 66.47; H, 7.15. FD-MS (toluene): *m/z* (%) = 2089.7 (100%, $[M]^+$), 1253.5 (6%, [M - {$Cp^{BIG}Mn(CO)_2$}]$^+$). IR (toluene): $ν_{CO}$ [cm^{-1}] = 1937 (s), 1887 (s). ^{1}H NMR (C_6D_6): δ [ppm] = 0.83 (30H, t, $^3J_{HH}$ = 7.3 Hz, Cp^{BIG}/C*H*$_3$), 1.21 (20H, m, Cp^{BIG}/C*H*$_2$), 1.45 (29H, m, Cp^{BIG}/C*H*$_2$ and Cp'''/C*H*$_3$), 1.66 (18H, s, Cp'''/C*H*$_3$), 2.39 (20H, t, $^3J_{HH}$ = 7.7 Hz, Cp^{BIG}/C*H*$_2$), 6.66 (2H, s, Cp'''/C*H*), 6.83 (20H, d, $^3J_{HH}$ = 8.1 Hz, Cp^{BIG}/C*H*), 7.36 (20H, d, $^3J_{HH}$ = 8.1 Hz, Cp^{BIG}/C*H*). ^{31}P{^{1}H} NMR (C_6D_6): δ [ppm] = 174.43 (2P), 154.56 (1P), 119.32 (1P). For details on ^{31}P{^{1}H} NMR investigations see text and supporting information. ^{13}C{^{1}H} NMR (C_6D_6): δ [ppm] = 14.1 (Cp^{BIG}, ^{n}Bu), 22.6 (Cp^{BIG}, ^{n}Bu), 31.7 (Cp''', ^{t}Bu), 33.4 (Cp^{BIG}, ^{n}Bu), 33.6 (Cp''', ^{t}Bu), 35.5 (Cp^{BIG}, ^{n}Bu), 102.3 (Cp^{BIG}, C_5), 119.6 (Cp''', C_5), 130.6 (Cp^{BIG}, Ph), 133.4 (Cp^{BIG}, Ph), 141.7(Cp^{BIG}, Ph), 231.6 (CO, low certainty); some quaternary C atoms are either obscured by other signals or not observed.

Synthesis of [{$Cp^{BIG}Mn(CO)_2$}$_2${L^0M}(μ,$η^{1:1:4}$-P_4)] (M = Fe (7a), Co (7b))

A mixture of [{$Cp^{BIG}Mn(CO)_2$}$_2P_4$] (210 mg, 0.12 mmol) and [L^0M(toluene)] (M = Fe: 51 mg, 0.12 mmol; M = Co: 51 mg, 0.12 mmol) is dissolved in 8 mL toluene and stirred for 18 h. The solvent is removed in vacuum and the remaining residue is dissolved in 15 mL *n*-hexane. The brown solution is filtered via a cannula. After concentration of the solution, it is stored at 4 °C over night to yield dark crystalline plates. The mother liquor is further concentrated and stored at 4 °C for 48 h to yield a second crop of crystals (**7a**: 76 mg, 31%; **7b**: 65 mg, 26%).

7a: [$C_{133}H_{151}Mn_2FeP_4O_4N_2$] calc: C, 74.95; H, 7.14; N, 1.31. found: C, 74.77; H, 6.96; N, 1.24. FD-MS (toluene): *m/z* = 2130.88 (45%, $[M]^+$), 1797.68 (2%, [{$Cp^{BIG}Mn(CO)_2$}$_2P_4$]$^+$), 1735.75 (2%, [{$Cp^{BIG}Mn(CO)_2$}$_2P_2$]$^+$), 864.35 (3%, [$Cp^{BIG}Mn(CO)_3$]$^+$), 726.43 (100%, [Cp^{BIG}]$^+$). IR (toluene): $ν_{CO}$ [cm^{-1}] = 1948 (w), 1939 (s), 1900 (s). ^{1}H NMR (C_6D_6): δ [ppm] = 0.80 (30H, br, Cp^{BIG}/C*H*$_3$), 1.21 (20H, br, Cp^{BIG}/C*H*$_2$), 1.48 (20H, br, Cp^{BIG}/C*H*$_2$), 2.46 (20H, br, Cp^{BIG}/C*H*$_2$), 5.05 (2H, br), 6.87 (18H, br), 7.96 (16H, br); Measured range: 900 ppm to -425 ppm. ^{31}P{^{1}H} NMR (C_6D_6): no signal (300 ppm to -300 ppm). Evans-NMR (C_6D_6): $μ_{eff}$ = 2.06 $μ_B$ (300 K).

7b: [$C_{133}H_{151}Mn_2CoP_4O_4N_2$] calc: C, 74.84; H, 7.13; N, 1.31. found: C, 74.92; H, 7.15; N, 1.05. FD-MS (toluene): *m/z* (%) = 2133.86 (100%, $[M]^+$), 1959.82 (4%, [M-$P_2(CO)_4$]$^+$), 1506.93 (6%, [$Cp^{BIG}{}_2Mn$]$^+$), 1057.57 (5%, [Cp^{BIG}MnNacnac(CO)]$^+$). IR (toluene): $ν_{CO}$ [cm^{-1}] = 1951 (w), 1941 (s),

1904 (s). ^{1}H NMR (C_6D_6): δ [ppm] = 0.86 (30H, t, $^3J_{HH}$ = 7.3 Hz, Cp^{BIG}/C*H*$_3$), 1.22 (20H, m, $^3J_{HH}$ = 7.3 Hz, Cp^{BIG}/C*H*$_2$), 1.44 (20H, m, $^3J_{HH}$ = 7.3 Hz, Cp^{BIG}/C*H*$_2$), 2.38 (20H, t, $^3J_{HH}$ = 7.3 Hz, Cp^{BIG}/C*H*$_2$), 2.82 (12H, s, L^0/C*H*$_3$), 5.16 (1H, t, $^3J_{HH}$ = 6.7 Hz, L^0/C*H*) 6.76 (20H, d, $^3J_{HH}$ = 7.9 Hz, Cp^{BIG}/C*H*), 7.11 (6H, m, L^0), 7.20 (20H, d, $^3J_{HH}$ = 7.9 Hz, Cp^{BIG}/C*H*); signals of L^0 in the region of 7.05 ppm to 7.25 ppm are obscured by signals of Cp^{BIG} and solvent. ^{31}P{^{1}H} NMR (C_6D_6): δ [ppm] = 150.86 (2P, t, $^1J_{PP}$ = 346.4 Hz), 232.61 (2P, t, $^1J_{PP}$ = 346.4 Hz). For more details on ^{31}P{^{1}H} NMR investigations see text and Figure S9. ^{13}C{^{1}H} NMR (C_6D_6): δ [ppm] = 14.1 (Cp^{BIG}, ^{n}Bu), 21.6 (L^0, Me), 22.6 (Cp^{BIG}, ^{n}Bu), 33.4 (Cp^{BIG}, ^{n}Bu), 35.5 (Cp^{BIG}, ^{n}Bu), 93.6 (L^0, HC*C*HCH), 103.1 (Cp^{BIG}, C_5), 125.1 (L^0, Ph), 130.3 (Cp^{BIG}, Ph), 131.4 (L^0, Ph), 133.2 (Cp^{BIG}, Ph), 141.8 (Cp^{BIG}, Ph), 154.6 (L^0, Ph), 166.9 (L^0, H*C*CH*C*H), 230.4 (CO), 230.6 (CO); some quaternary C atoms are either obscured by other signals or not observed.

NMR Investigations

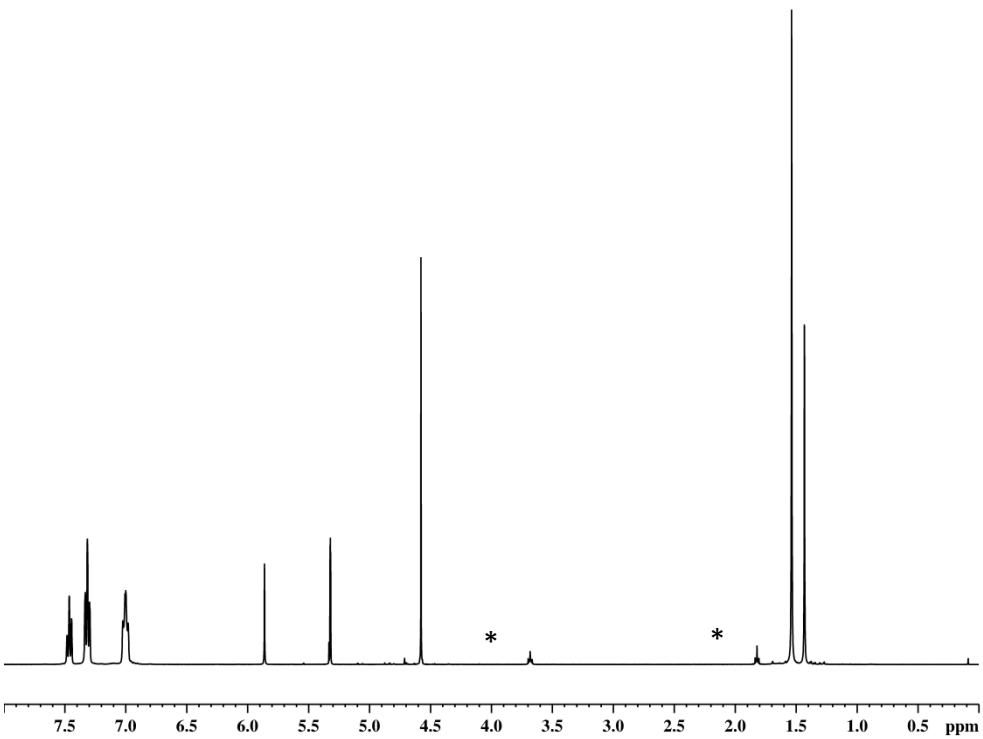

Figure S1. ^{1}H NMR spectrum of **5** in CD_2Cl_2 at 298 K. Signals marked with asterisks are due to THF.

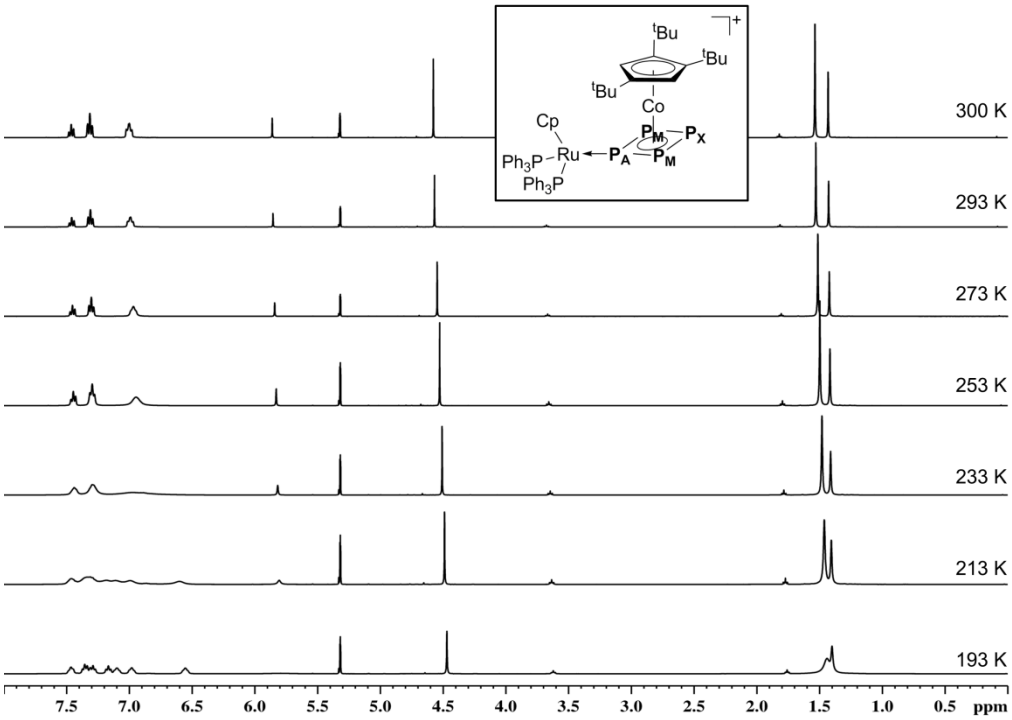

Figure S2. ^{1}H NMR spectra of **5** in CD_2Cl_2 at various temperatures.

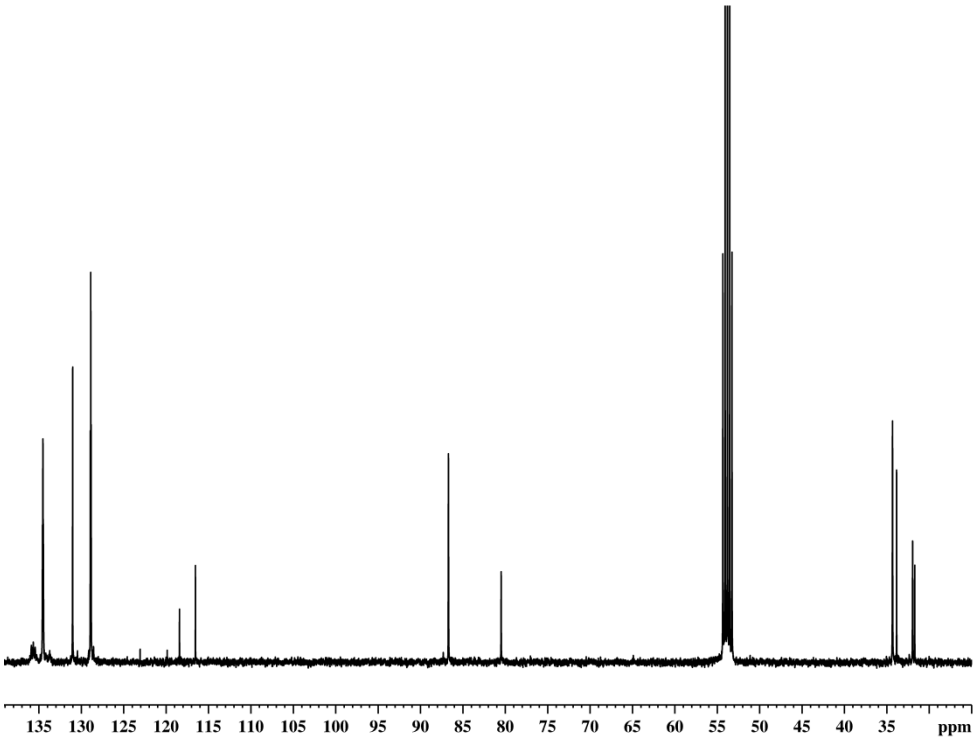

Figure S3. $^{13}C\{^1H\}$ NMR spectrum of **5** in CD_2Cl_2 at 298 K.

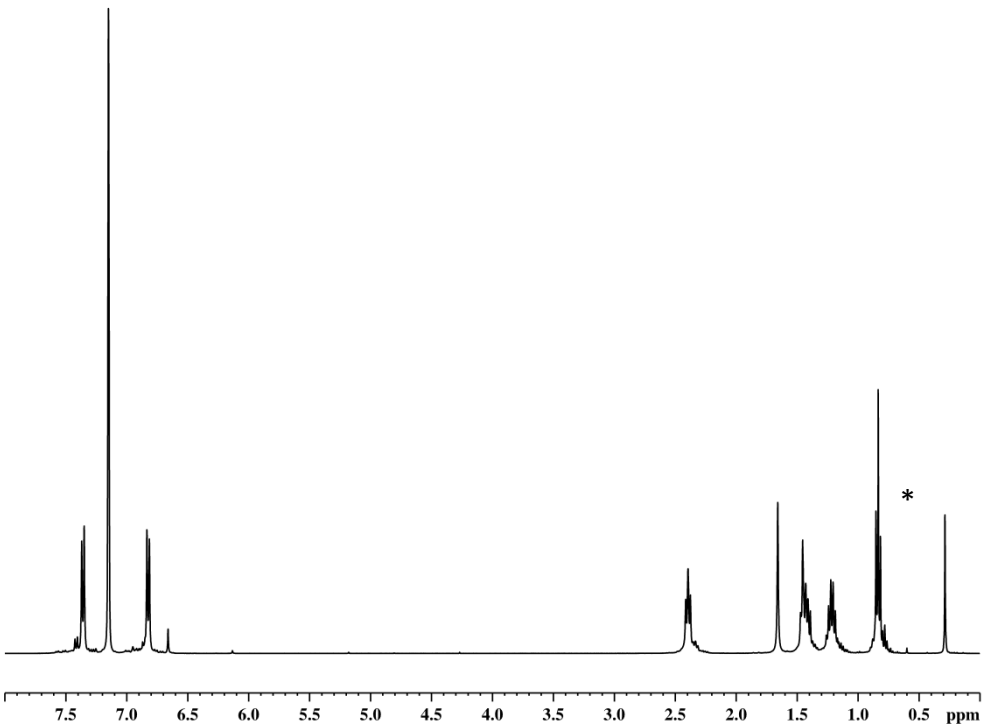

Figure S4. ^{1}H NMR spectrum of **6** in C_6D_6 at 298 K. Signal marked with an asterisk is due to silicon grease.

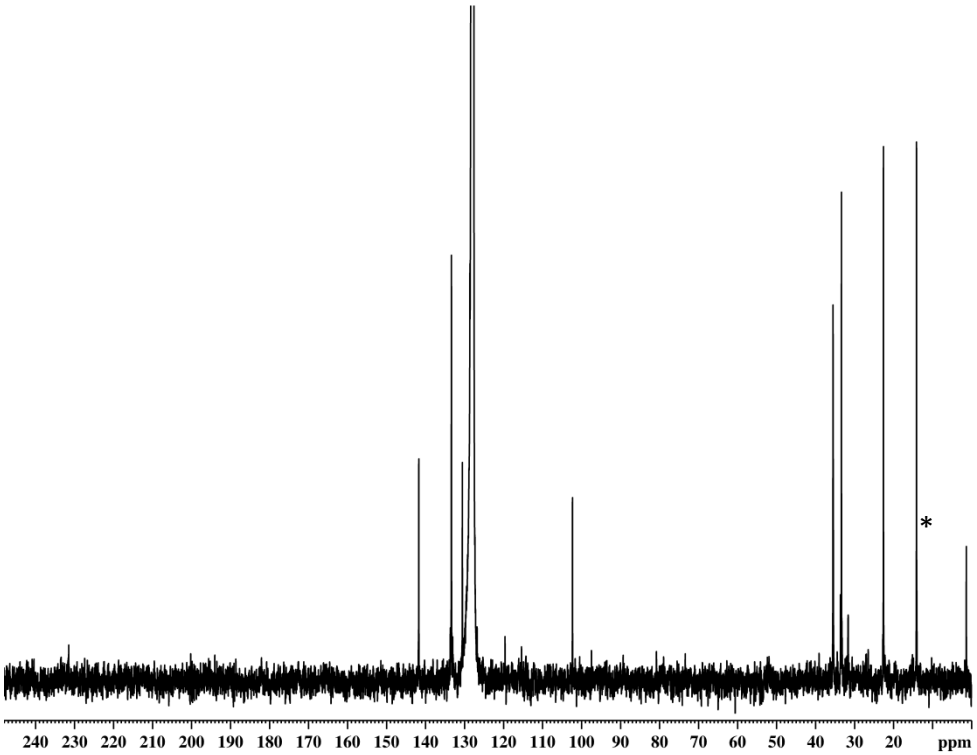

Figure S5. $^{13}C\{^{1}H\}$ NMR spectrum of **6** in C_6D_6 at 298 K. Signal marked with an asterisk is due to silicon grease.

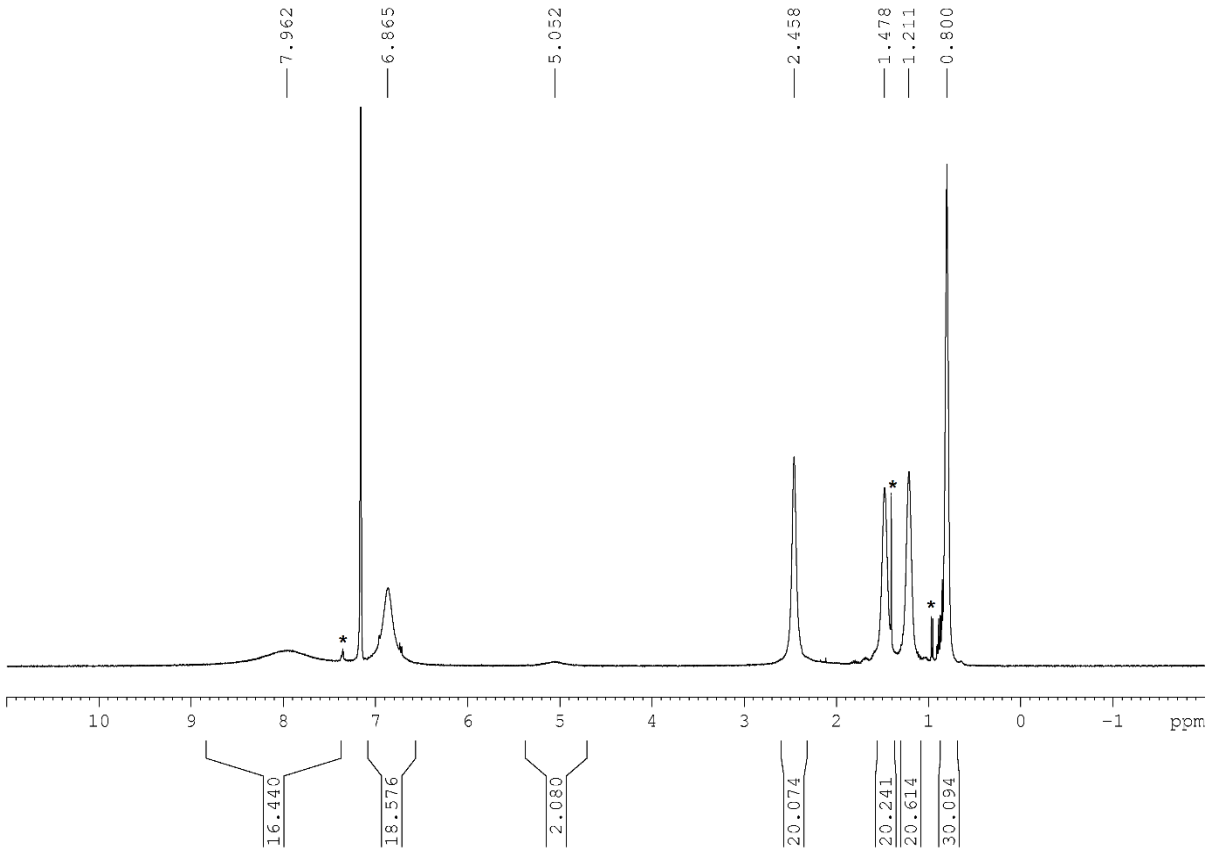

Figure S6. ^{1}H NMR spectrum of **7a** in C_6D_6 at 298 K. Signals marked with an asterisk are due to impurities.

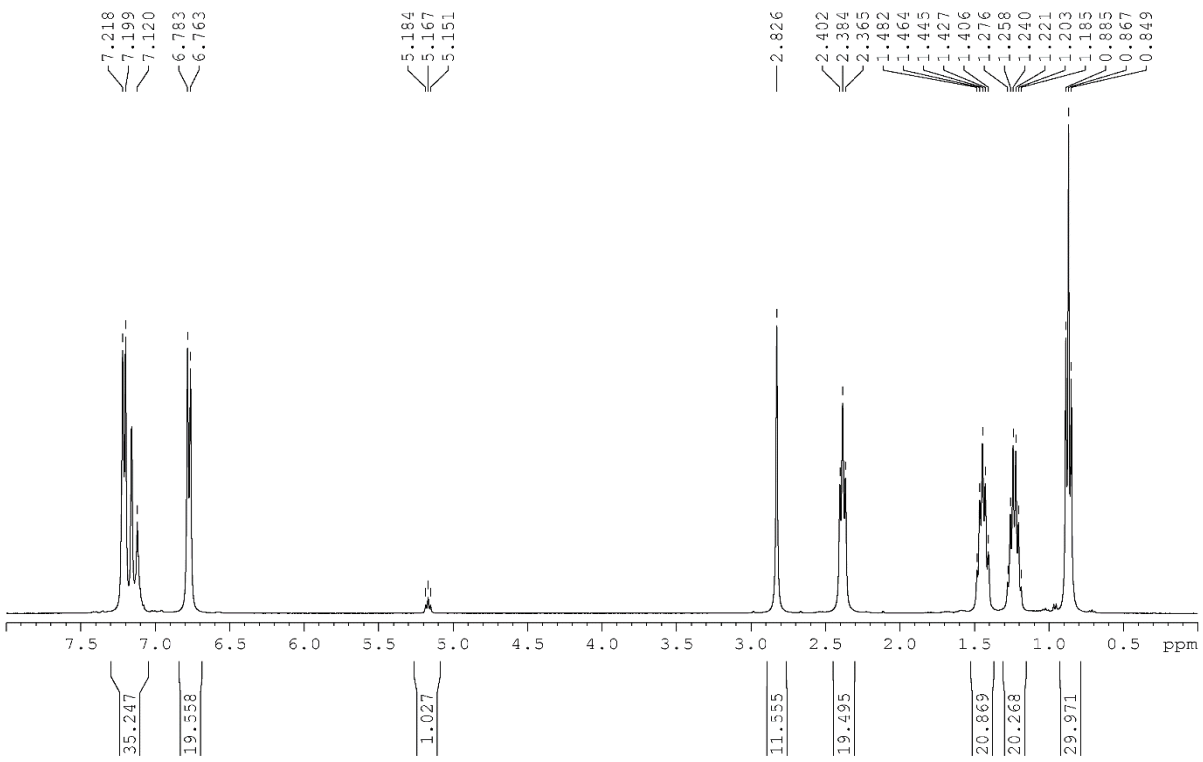

Figure S7. ^{1}H NMR spectrum of **7b** in C_6D_6 at 298 K. Depicted ranges: 8 to 0 ppm.

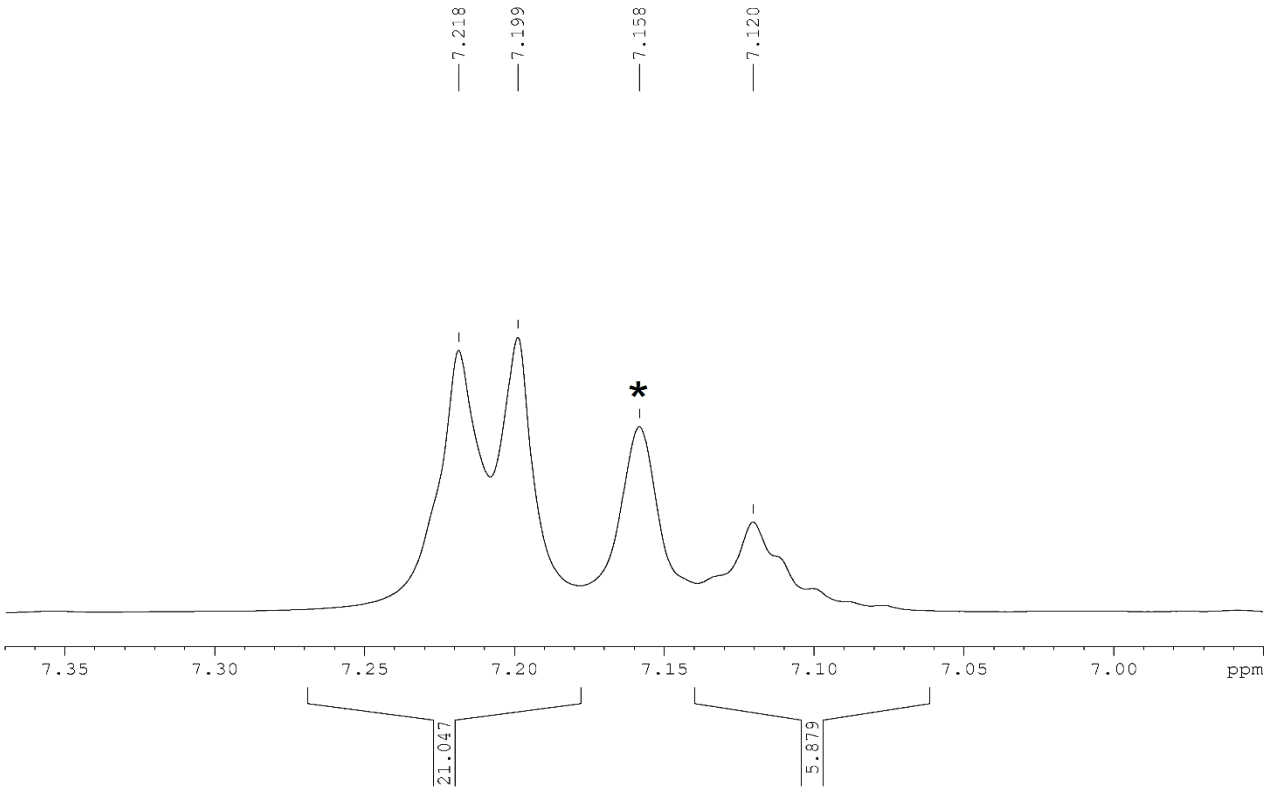

Figure S8. ^{1}H NMR spectrum of **7b** in C_6D_6 at 298 K. Depicted range: 7.37 to 6.95 ppm. Signal marked with an asterisk is due to solvent.

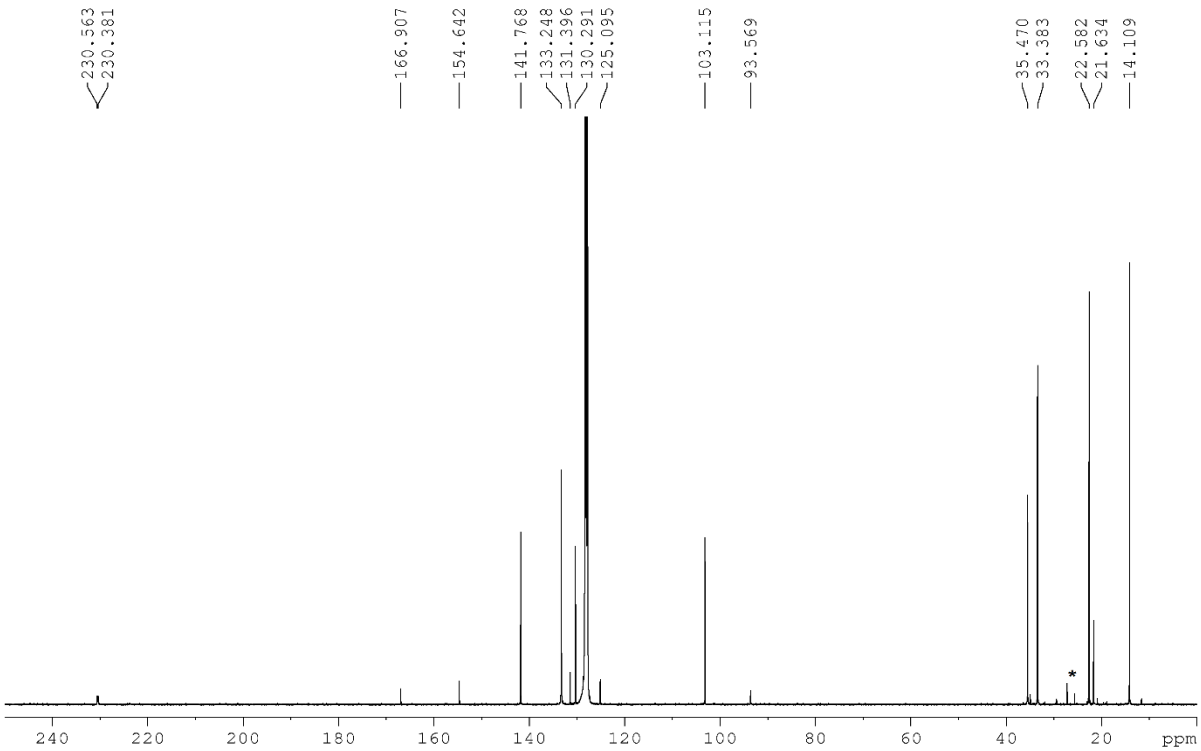

Figure S9. ^{13}C{^{1}H} NMR spectrum of **7b** in C_6D_6 at 298 K. Signals marked with an asterisk are due to impurities.

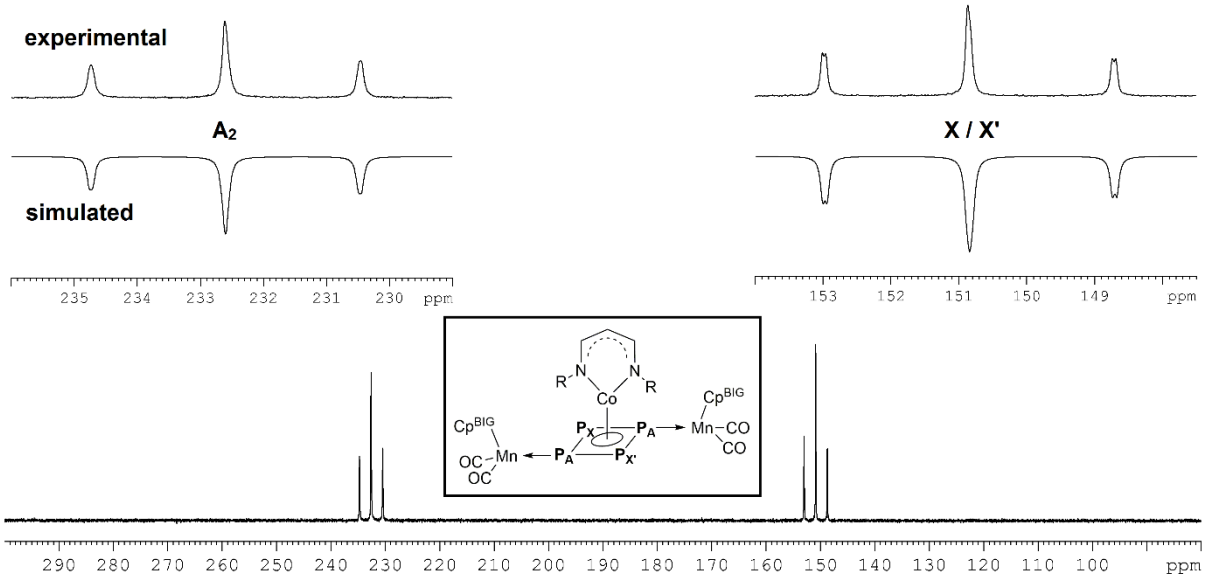

Figure S10. $^{31}P\{^1H\}$ NMR spectrum of **7b** in C_6D_6 (top) at 298 K and simulated spectrum (bottom). Parameters from simulated $^{31}P\{^1H\}$ NMR spectrum: δ [ppm] = 232.58 (P_A), 150.90 (P_X), 150.86 ($P_{X'}$); $^1J(P_AP_X)$ = 345.7 Hz, $^1J(P_AP_{X'})$ = 345.2 Hz, $^2J(P_XP_{X'})$ = 1.8 Hz.

Magnetic Measurements in Solution (Evans Method)

The magnetic susceptibility χ_M and the effective magnetic moment μ_{eff} of **7a** in C_6D_6 was determined by ^1H NMR spectroscopy using the Evans method with pure C_6D_6 as internal reference.[6] The diamagnetic contributions were neglected according to equations (1) and (2).[7] The ^1H spectrum was measured on a Bruker Avance 400 (^1H: 400.130 MHz). The chemical shift is reported in ppm relative to external TMS.

Equations:

$$\chi_M = \frac{3 \cdot \Delta f}{1000 \cdot f \cdot c} \tag{1}$$

$$\mu_{eff} = 798 \cdot \sqrt{T \cdot \chi_M} \tag{2}$$

χ_M: molar susceptibility of the sample in $m^3 \cdot mol^{-1}$

Δf: chemical shift difference between solvent in presence of paramagnetic solute and pure solvent in Hz

f: operating frequency of NMR spectrometer in Hz

c: concentration of paramagnetic sample in mol · L^{-1}

T: absolute temperature in K, and

μ_{eff}: effective magnetic moment in μ_B

EPR Spectroscopy

The simulation and fit of the EPR spectrum was done, using EasySpin,[8] a MATLAB toolbox. The calculated g-tensors of **7a** ($g_x = g_y = 2.0185$, $g_z = 2.0695$) are in line with an axial spectrum.

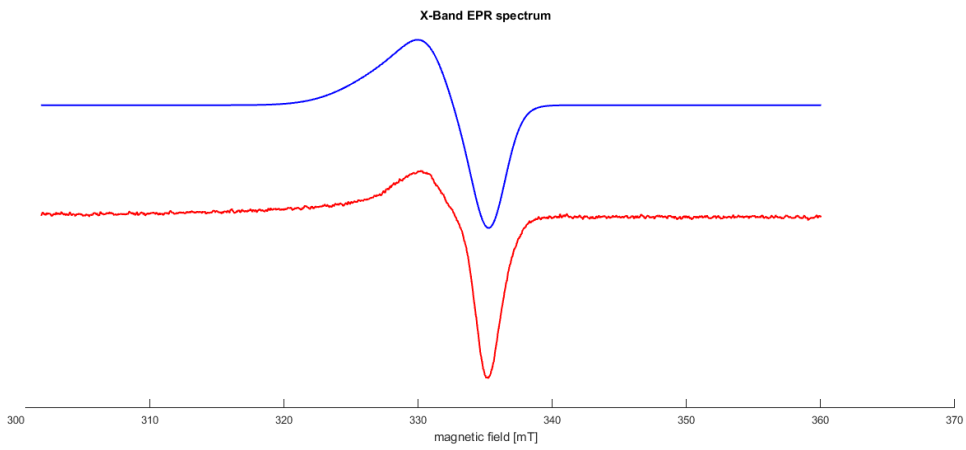

Figure S11. EPR spectrum of **7a** (bottom) in toluene (approx. 0.005 M) at 77 K; simulation (top); $g_{iso} = 2.0354$.

Mössbauer Spectrum

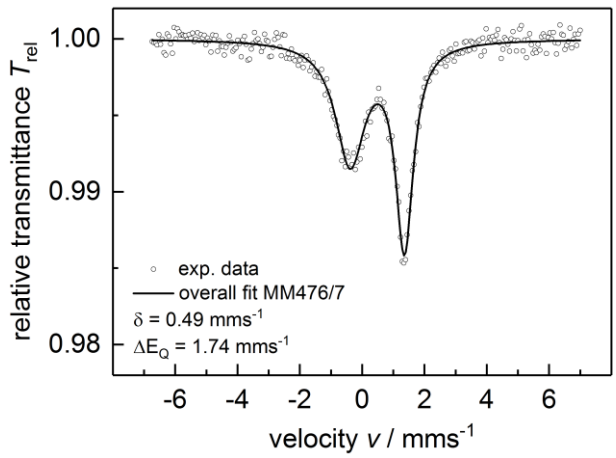

Figure S12. Zero-field ^{57}Fe Mössbauer spectrum of compound **7a**.

Crystallographic Details

The crystal structure analyses were performed either on a Rigaku Oxford Diffraction Gemini R Ultra CCD diffractometer (**5** · 2 CH_2Cl_2**)**, a Rigaku Oxford Diffraction SuperNova diffractometer (**6** · 4.8 CH_2Cl_2) or a Rigaku Technologies diffractometer GV50, Titan^{S2} (**7a** · 2 C_6H_{14} and **7b** · 2 C_6H_{14}). Data reduction was performed using the CrysAlisPro[9] software package. The structure solution was carried out using the programs SIR-92[10] (**5** and **6**) ShelXT[11] (**7a** and **7b**; Sheldrick, 2015) using the Olex2[12] software. Least squares refinements on F_0^2 were employed using SHELXL-97[13] (**5** · 2 CH_2Cl_2 and **6** · 4.8 CH_2Cl_2) and SHELXL-2014[14] (**7a** · 2 C_6H_{14} and **7b** · 2 C_6H_{14}**)** with anisotropic displacements for non-H atoms. All non-hydrogen atoms were refined anisotropically. Hydrogen atom positions were calculated geometrically and refined using the riding model.

Compound **7a** and **7b** were refined as a 2-component twin. Furthermore, **7a** and **7b** co-crystallized with *n*-hexane, which could not be refined accordingly. Hence, the structure was treated with the SQUEEZE function of PLATON software[15] resulting in a void of about 972 Å^3 containing 196 electrons (**7a**) and a void of about 947 Å^3 containing 191 electrons (**7b**). This agrees well with four *n*-hexane molecules in the asymmetric unit (two per formula unit).

Table S1. Crystallographic data and details of diffraction experiments for **5** · 2 CH_2Cl_2, **6** · 4.8 CH_2Cl_2, **7a**· 2 C_6H_{14} and **7b** · 2 C_6H_{14}.

Compound	**5** · 2 CH_2Cl_2	**6** · 4.8 CH_2Cl_2	**7a** · 2 C_6H_{14}	**7b** · 2 C_6H_{14}
Formula	$C_{59}H_{65}CoF_3O_3P_6RuS$	$C_{131}H_{159}CoMn_2O_4P_4$	$C_{133}H_{151}FeMn_2N_2O_4P_4$	$C_{133}H_{151}CoMn_2N_2O_4P_4$
$\rho_{calc.}$/ g cm^{-3}	1.508	1.244	1.162	1.175
μ/mm^{-1}	7.771	5.086	3.490	3.639
Formula Weight	1425.85	9989.69	2131.16	2134.24
Colour	red	brown	brown	red
Shape	block	planck	rhombohedral	rhombohedral
Size/mm^3	0.16×0.14×0.07	0.30×0.14×0.11	0.46×0.19×0.10	0.42×0.25×0.08
T/K	123.0(3)	123.0(1)	123.01(10)	89.9(4)
Crystal System	Triclinic	Triclinic	triclinic	triclinic
Space Group	P-1	$P2_1/n$	P-1	P-1
a/Å	13.8494(5)	18.5451(4)	18.1082(7)	18.0257(4)
b/Å	15.8930(6)	24.9628(5)	25.4978(9)	25.4699(4)
c/Å	16.3566(6)	28.8243(6)	27.6724(7)	27.5008(5)
α/°	69.257(3)	90	82.829(2)	83.1070(10)
β/°	75.544(3)	92.132(2)	77.258(3)	77.280(2)
γ/°	70.679(3)	90	78.987(3)	79.370(2)
V/Å^3	3141.2(2)	13334.6(5)	12187.0(7)	12063.2(4)
Z	2	1	4	4
Z'	1	0.25	2	2
Wavelength/Å	1.54178	1.54178	1.54184	1.54184
Radiation type	CuK$_\alpha$	CuK$_\alpha$	CuK$_\alpha$	CuK$_\alpha$
Θ_{min}/°	2.92	3.07	3.333	3.543
Θ_{max}/°	66.61	73.8710	67.336	74.243
Measured Refl.	35981	68456	63428	69409
Independent Refl.	11025	25963	63428	69409
Reflections Used	10513	18582	45945	53168
R_{int}	0.0323	0.0526	-	-
Parameters	757	1504	2724	2705
Restraints	45	119	124	14
Largest Peak	1.639	1.407	1.061	1.358
Deepest Hole	-0.928	-1.297	-0.635	-0.856
GooF	1.032	1.055	0.983	1.099
wR_2 (all data)	0.0865	0.2506	0.1713	0.2132
wR_2	0.0851	0.2401	0.1623	0.1986
R_1 (all data)	0.0333	0.0957	0.0778	0.0850
R_1	0.0318	0.0764	0.0618	0.0702

For compound **7a** and **7b** two crystallographically unique molecules are present in the asymmetric unit.

Table S2. Selected bond distances (Å) and angles (°) for the two crystallographically independent molecules of **7a** and **7b** present in the asymmetric unit.

	7a (molecule 1)	**7a** (molecule 2)	**7b** (molecule 1)	**7b** (molecule 2)
Mn - P	2.204(1), 2.204(1)	2.202(1), 2.213(1)	2.211(1), 2.200(1)	2.196(1), 2.209(1)
P - P	2.154(1), 2.165(1), 2.157(1), 2.149(1)	2.147(1), 2.155(1), 2.161(1), 2.155(1)	2.145(1), 2.146(1), 2.147(1), 2.158(1)	2.148(1), 2.146(1), 2.163(1), 2.148(1)
Fe/Co - P	2.377(1), 2.410(1), 2.363(1), 2.430(1)	2.380(1), 2.426(1), 2.356(1), 2.417(1)	2.334(1), 2.406(1), 2.332(1), 2.388(1)	2.332(1), 2.409(1), 2.343(1), 2.384(1)
Fe/Co - N	1.959(1), 1.948(1)	1.956(3), 1.961(4)	1.914(1), 1.924(1)	1.930(4), 1.914(4)
P - P - P	85.01(3), 94.51(3), 85.33(3), 95.07(3)	85.25(6), 94.70(6), 84.90(6), 95.09(6)	85.16(2), 95.15(2), 84.81(2), 94.83(2)	85.35(6), 94.65(6), 84.94(6), 95.01(6)

Computational Details

All the calculations were carried out within the Gaussian 09 package[16] at B97D-DFT[17] level of theory. All the optimized structures were validated as minima by calculations of vibrational frequencies. All the calculations were based on the CPCM[18] model for the THF solvent, the same used in the experiments. The effective Stuttgart/Dresden *pseudo*-potential (SDD)[19] was adopted for the ruthenium and cobalt centers, while for all the other atomic species the basis set was 6-31G, with the addition of the polarization functions (d,p).

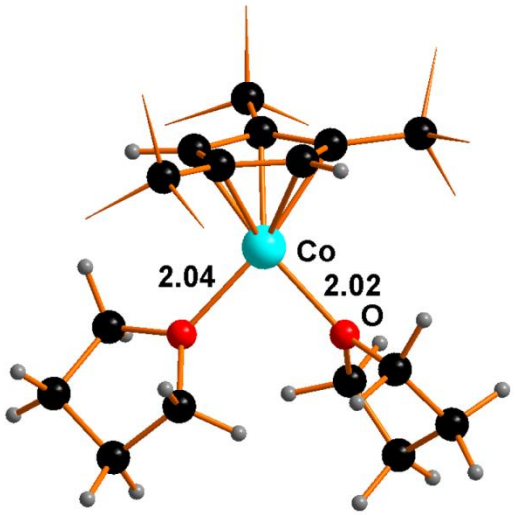

Figure S13. Optimized structure of [(Cp''')Co(THF)$_2$]. The methyl substituents of *tert*-butyl groups are hidden for clarity.

COODINATES AND ENERGY PARAMETERS OF ALL THE OPTIMIZED STRUCTURES at B97D-DFT level of theory.

Compound [(Cp''')Co(THF)$_2$].

Cartesian Coordinates

Co -0.198303 0.101327 -0.059397
C 1.648876 -0.664624 -0.506546
C 1.310866 -1.035838 0.871833
C 0.639990 -1.256486 -1.402549
C 0.040940 -1.714342 0.750218
H 0.644929 -1.174692 -2.484133
C -0.361030 -1.892596 -0.635945
H -0.552575 -2.068866 1.588003
C -1.559449 -2.687720 -1.126277
C 2.056896 -1.003295 2.217294
C 2.892719 0.039322 -1.093547
O -1.951625 0.675292 0.805387
C -3.052750 1.240704 0.035156
C -2.402920 0.307379 2.142922
C -4.111589 1.615093 1.076127
H -2.650471 2.090901 -0.527041
H -3.419358 0.474479 -0.668931
C -3.925648 0.501737 2.130362
H -2.091891 -0.726479 2.331042
H -1.898840 0.978468 2.857938
H -5.122589 1.635639 0.647000
H -3.889123 2.600729 1.512497
H -4.424145 -0.421235 1.797830
H -4.314211 0.775534 3.120475
O -0.112201 2.003223 -0.733142
C -0.299496 2.435132 -2.108941
C -0.080002 3.153725 0.166748
C 0.051357 3.926263 -2.100694
H 0.355410 1.816320 -2.733227
H -1.350832 2.258808 -2.396058
C -0.451473 4.361351 -0.706390
H -0.787269 2.953044 0.981683
H 0.942560 3.226475 0.568922
H -0.430673 4.472240 -2.923048

H 1.141281 4.060738 -2.173265
H -1.542537 4.504081 -0.723783
H 0.018211 5.287549 -0.347981
C 2.867184 0.015343 -2.646314
H 3.758385 0.537637 -3.028458
H 2.876993 -1.015700 -3.031403
H 1.976822 0.523125 -3.042987
C 3.010581 1.532676 -0.687547
H 2.835560 1.691021 0.379340
H 4.015180 1.908715 -0.945272
H 2.269185 2.128205 -1.233719
C 4.182846 -0.727452 -0.692928
H 4.091583 -1.792536 -0.958188
H 5.045210 -0.306683 -1.236536
H 4.398903 -0.660419 0.377702
C 2.867119 0.286394 2.485335
H 3.693267 0.429280 1.781903
H 2.206896 1.166120 2.426606
H 3.298675 0.239054 3.498944
C 1.042303 -1.107148 3.389975
H 0.526190 -2.078058 3.396971
H 1.576578 -1.005632 4.348066
H 0.288068 -0.309048 3.314515
C 2.997927 -2.238118 2.324489
H 3.525248 -2.238218 3.294496
H 2.406039 -3.164390 2.252008
H 3.746710 -2.248722 1.522279
C -2.720344 -2.605779 -0.108276
H -3.596827 -3.153747 -0.490354
H -2.432785 -3.050132 0.856696
H -2.998911 -1.558467 0.065767
C -2.054142 -2.154801 -2.489501
H -1.258342 -2.217672 -3.247697
H -2.913579 -2.749344 -2.840970
H -2.359149 -1.100854 -2.397979
C -1.145861 -4.175855 -1.288903
H -2.006038 -4.784643 -1.617384
H -0.342153 -4.271832 -2.035861
H -0.779661 -4.578696 -0.331030

Energy parameters

HF=-1275.6705256

Zero-point vibrational energy 1681852.3 (Joules/Mol)

Zero-point correction= 0.640584 (Hartree/Particle)

Thermal correction to Energy= 0.673932

Thermal correction to Enthalpy= 0.674876

Thermal correction to Gibbs Free Energy= 0.578981

Sum of electronic and zero-point Energies= -1275.029942

Sum of electronic and thermal Energies= -1274.996593

Sum of electronic and thermal Enthalpies= -1274.995649

Sum of electronic and thermal Free Energies= -1275.091544

Compound $[RuCp\{P(CH_3)_3\}_2(\eta^1\text{-}P_4)]^+$.

Cartesian Coordinates

Ru 1.142428 7.675954 5.656344
P 2.833698 8.588697 4.378004
P 0.223549 9.675877 6.341797
P -0.280198 7.483805 3.923379
P -2.265979 8.007134 3.170344
P -0.545042 7.688769 1.761645
C 2.566820 6.041657 6.320358
C 1.321381 5.427990 6.005965
C 0.316461 5.954237 6.910452
C 0.960593 6.889117 7.773614
C 2.351692 6.977545 7.403018
C 3.419481 7.389390 3.091271
C 2.617251 10.130773 3.373042
C 4.368661 8.960402 5.344946
C -0.232484 10.999521 5.127667
C 1.222657 10.587150 7.604857
C -1.407763 9.403243 7.181121
H 3.512516 5.846282 5.826096
H 1.149274 4.700384 5.219035
H -0.733150 5.679509 6.928948
H 0.485423 7.449476 8.571848
H 3.107751 7.584457 7.889201
H 0.662869 11.469959 4.708482
H -0.825532 10.563768 4.312126
H -0.832665 11.764408 5.642296
H -1.288002 8.729963 8.038872
H -1.823848 10.362835 7.523075
H -2.097929 8.939538 6.462611
H 2.165513 10.923915 7.152438
H 0.665095 11.459332 7.978414
H 1.454047 9.914011 8.441062
H 5.155439 9.341271 4.676486
H 4.144060 9.713515 6.112497
H 4.726092 8.047878 5.839641
H 4.289054 7.796794 2.553544
H 3.691147 6.438955 3.568294
H 2.603112 7.204920 2.379392
H 3.455032 10.212497 2.664709
H 1.672321 10.092742 2.815406
H 2.623947 11.011964 4.027278
P -1.412573 5.948366 2.884422

Energy parameters

HF=-2575.9089068

Zero-point vibrational energy 829988.3 (Joules/Mol)

Zero-point correction= 0.316126 (Hartree/Particle)

Thermal correction to Energy= 0.342387

Thermal correction to Enthalpy= 0.343331

Thermal correction to Gibbs Free Energy= 0.260275

Sum of electronic and zero-point Energies= -2575.592781

Sum of electronic and thermal Energies= -2575.566520

Sum of electronic and thermal Enthalpies= -2575.565576

Sum of electronic and thermal Free Energies= -2575.648631

Compound 5m'.

Cartesian Coordinates

Ru 3.177325 -0.231576 -0.523727
P 3.727708 1.746400 0.518352
P 3.420027 -1.596453 1.319475
P 1.010721 0.116230 -0.236461
P -0.452291 0.370865 1.392232
P -0.669704 -0.191559 -1.619546
C 4.289906 0.439814 -2.399743
C 3.055015 -0.151905 -2.809130
C 3.070171 -1.538408 -2.406864
C 4.325640 -1.787922 -1.765749
C 5.086938 -0.571680 -1.747830
C 2.976599 3.206822 -0.343969
C 3.291895 2.096010 2.284681
C 5.540875 2.121270 0.478720
C 2.651408 -1.222993 2.962256
C 5.187730 -1.918935 1.772455
C 2.754741 -3.298308 1.001030
H 4.582687 1.471477 -2.566882
H 2.242590 0.354918 -3.320368
H 2.276711 -2.260912 -2.567725
H 4.648481 -2.739808 -1.356353
H 6.083807 -0.444252 -1.339948
H 3.133629 -0.356668 3.427471
H 1.580233 -1.012670 2.839477
H 2.777408 -2.099291 3.615603
H 3.212310 -3.721066 0.098267
H 2.965782 -3.952042 1.861022
H 1.668779 -3.232556 0.848034
H 5.648846 -0.995019 2.147504
H 5.242264 -2.693993 2.552054
H 5.739743 -2.254040 0.884589
H 5.738257 3.086485 0.969047
H 6.089102 1.324886 0.999075
H 5.885052 2.164988 -0.562408
H 3.378429 4.146007 0.065547
H 3.188787 3.150171 -1.419733
H 1.887287 3.181813 -0.199700
H 3.420412 3.171259 2.479511
H 2.250669 1.809476 2.484423
H 3.960765 1.535706 2.950400
P -0.695285 -1.567043 0.206097
Co -2.127102 0.184768 -0.020868
C -4.067731 -0.260685 -0.745195
C -4.030960 -0.333852 0.728226
C -3.644287 1.071389 -1.090223
C -3.628762 0.966451 1.191475
H -3.525919 1.443372 -2.100080
C -3.348419 1.835545 0.088007
H -3.474914 1.236746 2.228005
C -2.941548 3.295884 0.129487
C -4.429904 -1.407266 1.754410
C -4.532611 -1.254203 -1.824379
C -4.176637 -2.867935 1.325370
H -4.460600 -3.530334 2.157149
H -4.760323 -3.170446 0.451960
H -3.109770 -3.026558 1.109959
C -5.939047 -1.210128 2.077441
H -6.248181 -1.938574 2.843604

H -6.113747 -0.196068 2.467845
H -6.567087 -1.351168 1.188386
C -3.636215 -1.210444 3.076601
H -2.553155 -1.222395 2.884598
H -3.895759 -0.270590 3.582736
H -3.882183 -2.032254 3.765058
C -3.584786 -2.471658 -1.984215
H -3.359033 -2.970659 -1.039984
H -4.044176 -3.201465 -2.669862
H -2.632191 -2.143017 -2.424151
C -5.987668 -1.708126 -1.532212
H -6.347566 -2.329656 -2.366743
H -6.076604 -2.294959 -0.613142
H -6.647364 -0.831241 -1.442933
C -4.568772 -0.560570 -3.213625
H -5.247766 0.305374 -3.214700
H -3.566579 -0.226534 -3.520275
H -4.927751 -1.284456 -3.959886
C -4.207904 4.142902 -0.178857
H -3.953409 5.213985 -0.153142
H -4.603742 3.899665 -1.176478
H -4.994310 3.950858 0.567196
C -1.861127 3.584746 -0.938414
H -1.597283 4.653616 -0.918912
H -0.963472 2.982827 -0.737200
H -2.223059 3.336330 -1.947067
C -2.399038 3.684688 1.520172
H -3.160450 3.535293 2.300466
H -1.514457 3.081339 1.774622
H -2.112394 4.747112 1.519676

Energy parameters

HF=-3387.0630774

Zero-point vibrational energy 1915850.5 (Joules/Mol)

Zero-point correction= 0.729709 (Hartree/Particle)

Thermal correction to Energy= 0.778798

Thermal correction to Enthalpy= 0.779742

Thermal correction to Gibbs Free Energy= 0.651161

Sum of electronic and zero-point Energies= -3386.333368

Sum of electronic and thermal Energies= -3386.284280

Sum of electronic and thermal Enthalpies= -3386.283335

Sum of electronic and thermal Free Energies=-3386.411917

Compound 5m.

Cartesian Coordinates

Ru 1.812035 -0.021168 0.625200
Co -2.386210 0.001789 -0.280762
P 2.563514 -1.734917 -0.716727
P 2.748612 1.672877 -0.629414
P -0.113811 0.252391 -0.495660
P -1.310381 2.043045 -0.776470

P -2.367293 0.955376 -2.368391
P -1.133547 -0.848960 -2.065647
C 2.022773 -1.298685 2.496544
C 0.902944 -0.430069 2.664503
C 1.370781 0.934664 2.653109
C 2.794052 0.890032 2.485387
C 3.207408 -0.476175 2.379735
C 1.518067 -3.265879 -0.697934
C 2.824995 -1.498745 -2.536107
C 4.211913 -2.394265 -0.179542
C 2.310762 1.937152 -2.410966
C 4.600314 1.662271 -0.668851
C 2.336530 3.335655 0.079625
C -3.174100 -1.661358 0.686283
C -4.180198 -1.044643 -0.198122
C -4.341751 0.315637 0.264497
C -3.508508 0.568124 1.400049
C -2.800064 -0.645240 1.639520
C -2.658885 -3.092730 0.897357
C -5.091196 -1.615713 -1.300299
C -3.520257 1.785403 2.303252
H 1.987381 -2.383079 2.475025
H -0.124447 -0.747724 2.763122
H 0.761793 1.822533 2.776262
H 3.454681 1.749520 2.436816
H 4.225302 -0.825508 2.249893
H -4.982106 1.055428 -0.197409
H -2.103541 -0.786328 2.452545
H 4.537684 -3.193575 -0.862283
H 4.952544 -1.583586 -0.178673
H 4.129304 -2.798434 0.837762
H 3.079931 -2.465792 -2.994143
H 1.910629 -1.106394 -3.000965
H 3.651991 -0.797041 -2.707346
H 2.004031 -4.059783 -1.285267
H 1.378651 -3.604792 0.335802
H 0.532604 -3.046427 -1.130173
H 4.948185 0.770843 -1.208924
H 4.977508 2.563433 -1.175448
H 4.989631 1.626026 0.357351
H 2.691736 3.406216 1.115148
H 2.799933 4.131098 -0.523332
H 1.244282 3.458170 0.070927
H 2.635793 1.087609 -3.019711
H 1.223322 2.051554 -2.510277
H 2.807344 2.851515 -2.768178
C -3.621736 -3.771856 1.915762
H -3.252616 -4.784649 2.140319
H -3.655299 -3.196497 2.853344
H -4.642515 -3.851393 1.521185
C -2.547841 -3.969518 -0.365815
H -3.516757 -4.163145 -0.834788
H -1.882008 -3.503957 -1.104940
H -2.121211 -4.941781 -0.077473
C -1.246297 -3.057165 1.543861
H -0.565674 -2.415529 0.971017
H -1.281574 -2.696858 2.581214
H -0.836829 -4.076835 1.569592
C -5.949632 -2.760228 -0.692772
H -6.707848 -3.067847 -1.428941
H -5.354061 -3.641261 -0.434574
H -6.467380 -2.413067 0.214403
C -4.342529 -2.106623 -2.563800
H -3.513680 -2.781487 -2.345933
H -5.056951 -2.626440 -3.221073
H -3.942563 -1.243297 -3.114980
C -6.088436 -0.531074 -1.788774
H -6.724913 -0.968778 -2.571113

H -6.738020 -0.182083 -0.972314
H -5.557224 0.330457 -2.219344
C -4.076951 3.027667 1.578266
H -5.108760 2.856553 1.236674
H -4.084181 3.881923 2.271514
H -3.454868 3.283205 0.709257
C -2.114328 2.088644 2.866087
H -1.702820 1.221490 3.402476
H -1.424091 2.363188 2.056847
H -2.178215 2.927392 3.575337
C -4.465668 1.427128 3.487848
H -4.527354 2.284328 4.175912
H -5.477817 1.196588 3.122367
H -4.084217 0.556757 4.042953

Energy parameters

HF=-3387.0880595

Zero-point vibrational energy 1920563.4 (Joules/Mol)

Zero-point correction= 0.731504 (Hartree/Particle)

Thermal correction to Energy= 0.779841

Thermal correction to Enthalpy= 0.780785

Thermal correction to Gibbs Free Energy= 0.656059

Sum of electronic and zero-point Energies= -3386.356556

Sum of electronic and thermal Energies= -3386.308219

Sum of electronic and thermal Enthalpies= -3386.307275

Sum of electronic and thermal Free Energies= -3386.432000

Compound THF.

Cartesian Coordinates

O 0.276663 -1.173984 1.160152
C 1.708906 -0.958755 1.034170
C 0.026051 -2.123828 2.231524
C 2.383460 -2.057664 1.872373
H 1.971258 -0.999166 -0.034065
H 1.955167 0.044587 1.427022
C 1.350919 -2.263046 2.999705
H -0.800029 -1.737981 2.848167
H -0.276883 -3.090409 1.789026
H 3.374347 -1.754745 2.238970
H 2.491180 -2.980285 1.281166
H 1.444274 -1.464826 3.752402
H 1.442489 -3.235997 3.502688

Energy parameters

HF=-232.3068047

Zero-point vibrational energy 296767.5 (Joules/Mol)

Zero-point correction= 0.113033 (Hartree/Particle)

Thermal correction to Energy= 0.118119

Thermal correction to Enthalpy= 0.119063

Thermal correction to Gibbs Free Energy= 0.084446

Sum of electronic and zero-point Energies= -232.193772

Sum of electronic and thermal Energies= -232.188686

Sum of electronic and thermal Enthalpies= -232.187742

Sum of electronic and thermal Free Energies= -232.222359

References

[1] J. J. Schneider, D. Wolf, C. Janiak, O. Heinemann, J. Rust, C. Krüger, *Chem. Eur. J.* **1998**, *4*, 1982-1991.

[2] F. Spitzer, C. Graßl, G. Balázs, E. M. Zolnhofer, K. Meyer, M. Scheer, *Angew. Chem. Int. Ed.* **2016**, *55*, 4340-4344.

[3] F. Spitzer, C. Graßl, G. Balázs, E. Mädl, M. Keilwerth, E. M. Zolnhofer, K. Meyer, M. Scheer, *Chem. Eur. J.* **2017**, *23*, 2716-2721.

[4] M. Di Vaira, P. Frediani, S. Seniori Costantini, M. Peruzzini, P. Stoppioni, *Dalton Trans.* **2005**, 2234-2236.

[5] S. Heinl, E. V. Peresypkina, A. Y. Timoshkin, P. Mastrorilli, V. Gallo, M. Scheer, *Angew. Chem. Int. Ed.* **2013**, *52*, 10887-10891.

[6] D. F. Evans, *J. Chem. Soc. (Resumed)* **1959**, 2003-2005.

[7] G. J. P. Britovsek, V. C. Gibson, S. K. Spitzmesser, K. P. Tellmann, A. J. P. White, D. J. Williams, *J. Chem. Soc., Dalton Trans.* **2002**, 1159-1171.

[8] S. Stoll, A. Schweiger: EasySpin, a comprehensive software package for spectral simulation and analysis in EPR, *J. Magn. Reson.* ***2006****, 178(1)*, 42-55.

[9] CrysAlisPro Software System, Agilent Technologies UK Ltd, Yarnton, Oxford, UK (2014).

[10] A. Altomare, M. C. Burla, M. Camalli, G.L.Cascarano, C. Giacovazzo, A. Guagliardi, A. G. G. Moliterni, G. Polidori, R. Spagna, *J.Appl. Cryst.* **1999**, *32*, 115-119.

[11] Sheldrick, G.M., ShelXT, *Acta Cryst.*, **2014**, *A71*, 3-8.

[12] O.V. Dolomanov and L.J. Bourhis and R.J. Gildea and J.A.K. Howard and H. Puschmann, Olex2: A complete structure solution, refinement and analysis program, *J. Appl. Cryst.*, **2009**, *42*, 339-341.

[13] G. M. Sheldrick, *Acta Cryst.* **2008**, *A64*, 112-122.

[14] Sheldrick, G.M., A short history of ShelX, *Acta Cryst.*, **2008**, *A64*, 339-341.

[15] P. van der Sluis & A.L.Spek (1990).Acta Cryst., A46, 194-201.

[16] Gaussian 09, Revision E.01, M. J. Frisch, G. W. Trucks, H. B. Schlegel, G. E. Scuseria, M. A. Robb, J. R. Cheeseman, G. Scalmani, V. Barone, B. Mennucci, G. A. Petersson, H. Nakatsuji, M. Caricato, X. Li, H. P. Hratchian, A. F. Izmaylov, J. Bloino, G. Zheng, J. L. Sonnenberg, M. Hada, M. Ehara, K. Toyota, R. Fukuda, J. Hasegawa, M. Ishida, T. Nakajima, Y. Honda, O. Kitao, H. Nakai, T. Vreven, J. A. Montgomery, Jr., J. E. Peralta, F. Ogliaro, M. Bearpark, J. J. Heyd, E. Brothers, K. N. Kudin, V. N. Staroverov, R. Kobayashi, J. Normand, K. Raghavachari, A. Rendell, J. C. Burant, S. S. Iyengar, J. Tomasi, M. Cossi, N. Rega, J. M. Millam, M. Klene, J. E. Knox, J. B. Cross, V. Bakken, C. Adamo, J. Jaramillo, R. Gomperts, R. E. Stratmann, O. Yazyev, A. J. Austin, R. Cammi, C. Pomelli, J. W. Ochterski, R. L. Martin, K. Morokuma, V. G. Zakrzewski, G. A. Voth, P. Salvador, J. J. Dannenberg, S. Dapprich, A. D. Daniels, Ö. Farkas, J. B. Foresman, J. V. Ortiz, J. Cioslowski, and D. J. Fox, Gaussian, Inc., Wallingford CT, 2009.

[17] S. Grimme, *J. Comput. Chem.* **2006**, *27*, 1787-1799.

[18] a) V. Barone, M. Cossi, *J. Phys. Chem. A* **1998**, *102*, 1995-2001. b) M. Cossi, N. Rega, G. Scalmani, V. Barone, *J. Comput. Chem.* **2003**, *24*, 669-681.

[19] M. Dolg, H. Stoll, H. Preuss, R. M. Pitzer, *J. Phys. Chem.* **1993**, *97*, 5852-5859.

6 Thermal Activation of Mixed Group 15/16 Cage Compounds

Moritz Modl, Florian Buchecker, Manfred Scheer

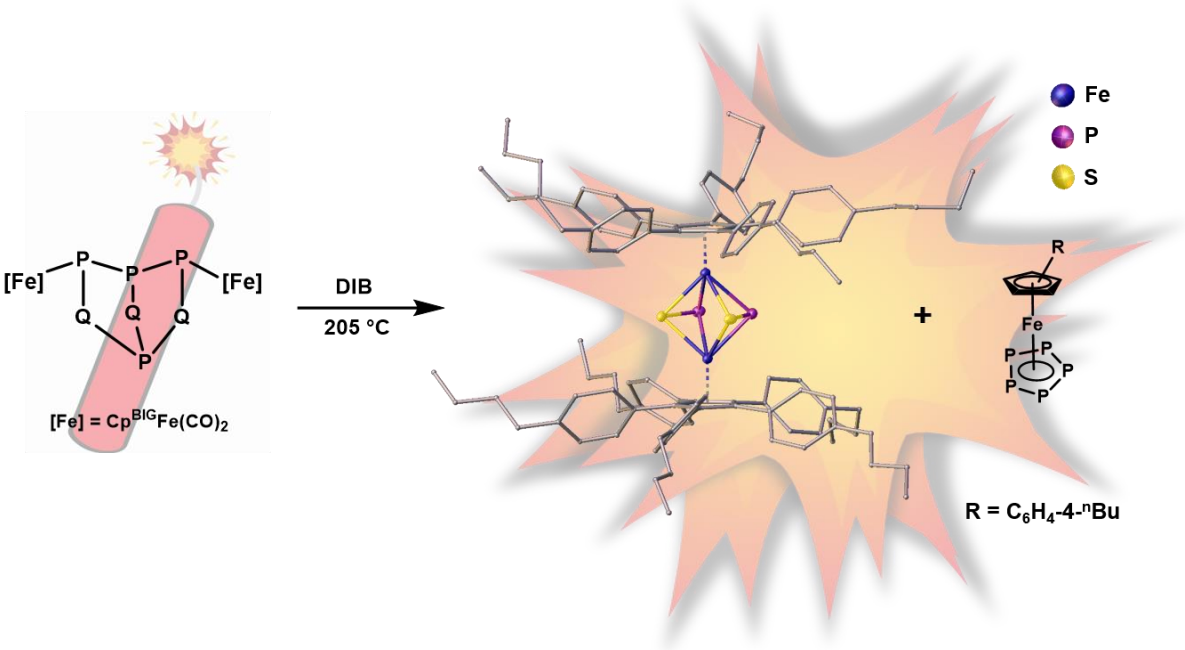

- **All syntheses and characterizations were performed by Moritz Modl with the aid of Florian Buchecker within the scope of his Bachelor Thesis (2015, Referee: Manfred Scheer) with supervision of Moritz Modl**
- **Manuscript was written by Moritz Modl**
- **Figures were made by Moritz Modl**
- **X-Ray structure analyses and refinement were performed by Moritz Modl**

6.1 Introduction

A large number of transition metal complexes bearing homoatomic pnictogenide (E = P, As)[1] or chalcogenide (Q = S, Se, Te)[2] ligands, respectively, are known these days, exhibiting a wide range of structural motifs. In the case of complexes with mixed ligands of Groups 15 and 16 elements (E_mQ_n), the number is considerably smaller.[3] According to Kanatzidis *et al.*,[4] the introduction of trivalent E^- building blocks into chalcogenide units, offers additional branching possibilities. Thereby, compared to homoatomic E_m or Q_n ligands, a larger variety of E_mQ_n moieties is accessible. According to Wachter *et al.* these mixed ligands can be divided into three groups: small, covalently bound ligands, heteroatomic Zintl anions and neutral cage molecules.[3] A possible source for mixed E/Q ligand synthesis are cage molecules of the nortricyclane-type structure E_4Q_3 (E = P, Q = S, Se; E = As, Q = S) (**A**), which can be reacted with unsaturated transition metal complexes.

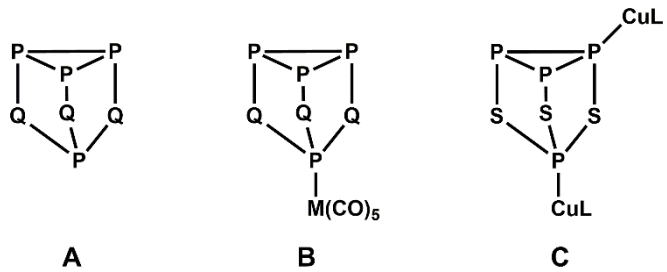

Scheme 1. Mixed cage compounds E_4Q_3 (E = P, Q = S, Se; E = As, Q = S) (**A**). Selected examples of intact **A** coordinated by transition metal fragments (**B**: M = Mo, W; **C**: L = $[\{N(C_6H_3{}^iPr_2\text{-}2,6)C(Me)\}_2CH]^-$).

The obtained products are strongly dependent on the reaction partners, as well as the conditions and vary from simple coordination, selective bond cleavage to substantial fragmentation of the cage compound. The stoichiometric reaction of Lewis acidic fragments like $[M(CO)_5]$ (M = Mo, W) towards P_4Q_3 leads to the formation of Lewis acid-Lewis base adducts $[(CO)_5M(P_4Q_3)]$ (**B**), in which the P_4Q_3 ligand coordinates through the apical phosphorus site.[5] Otherwise, the reaction of P_4S_3 towards copper(I) halides exhibits one, two and even three-dimensional frameworks upon coordination of two to four P atoms.[6] The coordination behavior of E_4S_3 (E = P, As) towards the Lewis acidic transition metal complex $[NacNacCu(CH_3CN)]$ (NacNac = $[\{N(C_6H_3{}^iPr_2\text{-}2,6)C(Me)\}_2CH]^-$) was investigated by Scheer *et al.*.[7] The obtained products $[(NacNacCu)_2P_4S_3]$ (**C**) contain an intact P_4S_3 cage ligand in two superposed conformations. Whereas the reaction of the heavier homologue As_4S_3 leads to the formation of stereoisomers $[(NacNacCu)_2As_4S_3]$ as a racemic mixture.

All the mentioned compounds contain an intact E_4Q_3 moiety. A selective bond cleavage, as reported by Scheer *et al.*, can be achieved by the reaction of P_4Q_3 with organometallic radicals under mild conditions.[8] That was done by using the dimeric compound $[Cp^{BIG}Fe(CO)_2]_2$ (Cp^{BIG} = $C_5(C_6H_5{}^nBu)_5$), which in solution readily dissociates into 17 VE radical fragments. These

fragments react with P_4Q_3 (X = S, Se) under selective cleavage of a P-P bond of the basal P_3 unit to give [{$Cp^{BIG}Fe(CO)_2$}$_2$(μ,$η^{1:1}$-P_4Q_3)] (type **I**) (Q = S (**1**), Se (**2**)).

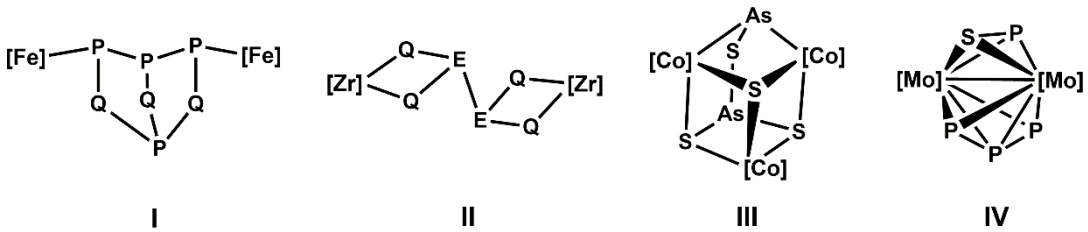

Scheme 2. Selected examples of different structural motifs of complexes (type **I** – **IV**) obtained by reaction of unsaturated transition metal complexes with **A**.

In contrast to the coordination or the selective bond cleavage, where the initial cage core is more or less maintained, co-thermolysis of transition metal complexes, especially carbonyl cyclopentadienyl complexes, with E_4Q_3 leads to fragmentation and potentially subsequent recombination reactions. Thus complexes with manifold mixed E_mQ_n and homoatomic E_n ligands are formed. For example, Scheer *et al.* reported on the thermolytic transformation of E_4Q_3 by a zirconium(II) complex in boiling toluene, resulting in the formation of compounds with a bridging E_2Q_4 ligand (type **II**) ([M] = ($η^5$-$C_5H_3{}^tBu_2$)Zr; E = P, Q = S, Se; E = As, Q = S).[9] In contrast, Wachter *et al.* described the synthesis of the trinuclear complex [($Cp^XCo)_3As_2S_4$] (type **III**) ([Co] = ($η^5$-C_5Me_4Et)Co)[10] or a unique mixed five-membered ring ligand in [($Cp^*Mo)_2P_4S$] (type **IV**) ([Mo] = ($η^5$-C_5Me_5)Mo)[11] by co-thermolysis reaction of [$Cp^RM(CO)_n]_2$ (Cp^R = Cp^X, M = Co, n = 1; Cp^R = Cp*, M = Mo, n = 2) and E_4S_3 in boiling toluene.

As mentioned above, E_mQ_n ligands show versatile reaction pathways under thermal conditions. In this regard, we got interested in the thermolytic behavior of the P_4Q_3 moiety in [{$Cp^{BIG}Fe(CO)_2$}$_2$(μ,$η^{1:1}$-P_4Q_3)] (Q = S (**1**), Se (**2**)), respectively, since there is already an activated P_4Q_3 unit present. The investigation of a conversion of a P_4Q_3 cage from an already first step activation stage could give further insight into the transformation pathway of such compounds. Herein we report on the investigations of the thermal activation of complexes **1** and **2**, respectively. The thermolysis of **1** leads to the formation of the homoatomic complex [$Cp^{BIG}Fe(η^5$-$P_5)$] (**3**)[12] and the unprecedented complex [($Cp^{BIG}Fe)_2$(μ,$η^{4:4}$-P_2S_2)] (**4**), whereas **2** undergoes complete decomposition under similar reaction conditions, according to NMR investigations.

6.2 Results and Discussion

The thermolysis of a pink solution of **1** in boiling 1,3-diisopropylbenzene (DIB) for 18 h results in a color change to dark green. The $^{31}P\{^1H\}$ NMR measurement of the crude reaction mixture suggests a full conversion of the educt. Chromatographic workup provides the green

complex [$Cp^{BIG}Fe(\eta^5\text{-}P_5)$] (**3**) and the dark green compound [$(Cp^{BIG}Fe)_2(\mu,\eta^{4:4}\text{-}P_2S_2)$] (**4**) in 35% and 62% yield, respectively.

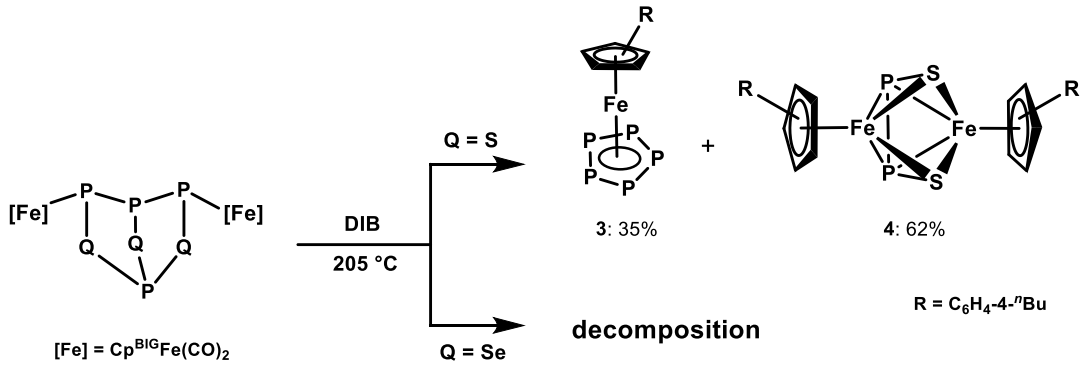

Scheme 3. Synthesis of **3** and **4**.

Compound **3** was characterized by ^1H and $^{31}P\{^1H\}$ NMR spectroscopy and was already obtained by the co-thermolysis of [$Cp^{BIG}Fe(CO)_2]_2$ with an excess of white phosphorus in decalin or 1,3-diisopropylbenzene, besides [$(Cp^{BIG}Fe)_2(\mu,\eta^{4:4}\text{-}P_4)$], in 40% or 66% yield, respectively, as a side product.[12] The all-phosphorus complex **3** exhibits a *cyclo*-P_5 moiety, containing no sulfur. This evidences the assumption of the fragmentation of compound **1** and subsequent recombination of the fragments, if **1** is exposed to elevated temperatures. Similar behavior is observed for the reaction of [$CpCr(CO)_3]_2$ at 60 °C and [$Cp^*Mo(CO)_2]_2$ at 115 °C, respectively, towards P_4S_3 to give products with the P/S components of the former cage in separated form.[13] The only exceptions are the mixed sandwich complexes of molybdenum [$(Cp^*Mo)_2(\mu,\eta^{5:5}\text{-}P_4S)$] and [$(Cp^*Mo)_2(\mu,\eta^{5:5}\text{-}P_2S_3)$], that could be isolated together with the homoatomic products.

It was possible to crystallize complex **4** by slow diffusion of CH_3CN into a toluene solution of the pure sample as dark green plates. X-ray diffraction measurements revealed an unprecedented mixed $Fe_2P_2S_2$ core, bearing a SPPS ligand. The Fe-Fe distance of 3.1557(7) Å can be considered as nonbonding. This is in agreement with the reported “bonding isomers” of [$(Cp'''Fe)_2As_4$] (Cp’’’ = $C_5H_2{}^tBu_3$), exhibiting a Fe-Fe bond with 2.6927(6) Å in a *cisoid*-As_4 arrangement and no Fe-Fe bond (3.5019(9) Å) with a *cyclo*-As_4 moiety.[14] The Cp^{BIG} ligands in **4** exhibit a staggered conformation, to minimize the steric repulsion. The short S-P bonds (S1-P1 2.0433(8) Å, P2-S2 2.0437(8) Å) are in the range of slightly elongated double bonds.[15] The observed distance between the P atoms is 2.3244(8) Å, which corresponds to a P-P single bond,[16] and is shorter as the related bond in the tetraphosphabutadiene complex [$(Cp^{BIG}Fe)_2(\mu,\eta^{4:4}\text{-}P_4)$] (2.368(2) Å).[12] This gives rise to the consideration of a *cisoid*-P_2S_2 moiety, the analogue to a tetraphosphabuta-1,3-diene ligand, with two shorter and one longer bond, instead of two separated S=P units. The trapezoidal arrangement is in line with the

arsenic derivative $[(Cp^{+}Fe)_2(\mu,\eta^{4:4}\text{-}As_2S_2)]$ ($Cp^{+} = C_5Me_4Et$), reported by Brunner *et al.*, which contains a butadiene analogue S=As-As=S unit.[17]

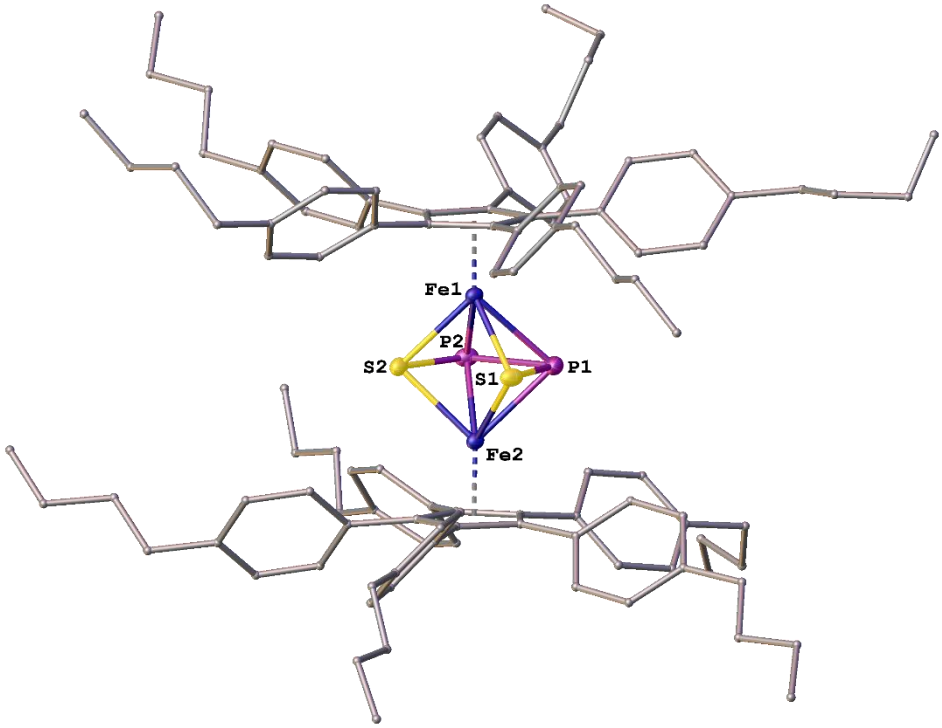

Figure 1. Solid-state molecular structure of **4**. Thermal ellipsoids are set at 50% probability. For clarity reasons H atoms are omitted and Cp^{BIG} ligands are drawn in 'wire-or-stick' model. Selected bond lengths [Å] and angles [°] in **4**: S1-P1 2.0433(8), P1-P2 2.3244(8), P2-S2 2.0437(8), S1-S2 2.9887(8), Fe1-Fe2 3.1557(7), Fe1-S1 2.2932(8), Fe1-S2 2.2933(8), Fe1-P1 2.3513(7), Fe1-P2 2.3473(7), Fe2-S1 2.2893(8), Fe2-S2 2.2916(8), Fe2-P1 2.3449(7), Fe2-P2 2.3549(7), S1-P1-P2 99.54(3), P1-P2-S2 99.16(3). A representation of the $Fe_2P_2S_2$ core of **4** with view along the Fe-Fe axis (Cp^{BIG} ligands are omitted for clarity) is shown in the inset.

The ^{1}H and $^{13}C\{^{1}H\}$ NMR spectra of **4** show that the Cp^{BIG} ligands are chemically equivalent. A triplet, two multiplets and a quartet, corresponding to the *n*-butyl groups, arise at 0.77 ppm, 1.13 ppm, 1.38 ppm and 2.32 ppm, while the aromatic protons appear as two doublets at 6.85 ppm and 7.55 ppm. Complex **4** was further studied by $^{31}P\{^{1}H\}$ NMR spectroscopy at 300 K in C_6D_6 and 373 K in toluene-d_8, respectively. At both temperatures a sharp singlet at -82.8 ppm (C_6D_6) and at -80.9 ppm (toluene-d_8), respectively, was observed, consistent with two chemically and magnetically equivalent P atoms in solution. The analogue all-phosphorus compound shows dynamic behavior in solution, exhibiting two very broad signals at r.t., which show a sharpening at low temperatures.[12] The absence of a dynamic behavior in **4**, can be caused by the presence of two different elements, phosphorus and sulfur in such butadiene-like arrangement.

In contrast to **1**, the selenium analogue **2** shows complete decomposition under thermolytic reaction conditions. After thermolysis for 18 h in boiling DIB, a black insoluble solid is formed

and only $Cp^{BIG}H$ and minor amounts of free P_4Se_3 are observed in the ^1H and $^{31}P\{^1H\}$ NMR spectra of the reaction mixture.

6.3 Conclusion

In summary, we have shown that complex **1** containing a mixed ligand of Groups 15 and 16 elements, is a suitable source for the synthesis of further mixed ligand complexes. It undergoes complete decarbonylation at elevated temperatures to yield the all-phosphorus compound $[Cp^{BIG}Fe(\eta^5\text{-}P_5)]$ (**3**) and the mixed ligand complex $[(Cp^{BIG}Fe)_2(\mu,\eta^{4:4}\text{-}P_2S_2)]$ (**4**), bearing an unprecedented butadiene like S=P-P=S moiety. To the best of our knowledge, **4** represents the first compound with such a mixed phosphorus/sulfur ligand. In comparison, the selenium analogue compound **2** is not a convenient source for mixed P/Se ligands under analogous conditions, since only decomposition products of **2** were observed.

6.4 References

[1] a) B. M. Cossairt, N. A. Piro, C. C. Cummins, *Chem. Rev. (Washington, DC, U. S.)* **2010**, *110*, 4164-4177; b) M. Caporali, L. Gonsalvi, A. Rossin, M. Peruzzini, *Chem. Rev. (Washington, DC, U. S.)* **2010**, *110*, 4178-4235; c) O. J. Scherer, *Angew. Chem.* **1990**, *102*, 1137-1155.

[2] a) W. Hieber, J. Gruber, *Z. Anorg. Allg. Chem.* **1958**, *296*, 91-103. b) C. H. Wei, L. F. Dahl, *Inorg. Chem.* **1965**, *4*, 1-11. c) C. Giannotti, A. M. Ducourant, H. Chanaud, A. Chiaroni, D. Riche, *J. Organomet. Chem.* **1977**, *140*, 289-295. d) H. Brunner, N. Janietz, W. Meier, G. Sergeson, J. Wachter, T. Zahn, M. L. Ziegler, *Angew. Chem., Int. Ed.* **1985**, *24*, 1060-1061; e) M. Draganjac, T. B. Rauchfuss, *Angew. Chem.* **1985**, *97*, 745; f) A. Müller, E. Diemann, *Adv. Inorg. Chem.* **1987**, *31*, 89; g) A. Müller, W. Jaegermann, J. H. Enemark, *Coord. Chem. Rev.* **1982**, *46*, 245; h) J. Wachter, *Angew. Chem.* **1989**, *101*, 1645; i) L. C. Roof, J. W. Kolis, *Chem. Rev.* **1993**, *93*, 1037.

[3] J. Wachter, *Angew. Chem., Int. Ed.* **1998**, *37*, 750-768.

[4] M. G. Kanatzidis, J.-H. Chou, *J. Solid State Chem.* **1996**, *127*, 186.

[5] a) R. Jefferson, H. F. Klein, J. F. Nixon, *Chem. Commun.* **1969**, 536; b) A. W. Cordes, R. D. Joyner, R. D. Shores, E. D. Dill, *Inorg. Chem.* **1974**, *13*, 132.

[6] J. Wachter, *Coord. Chem. Rev.* **2010**, *254*, 2078-2085.

[7] F. Spitzer, PhD thesis, *University of Regensburg*, **2017**.

[8] S. Heinl, M. Scheer, *Chemical Science* **2014**, *5*, 3221-3225.

[9] A. E. Seitz, V. Heinl, A. Y. Timoshkin, M. Scheer, *Chem. Commun.* **2017**, *53*, 1172-1175.

[10] H. Brunner, H. Kauermann, L. Poll, B. Nuber, J. Wachter, *Chem. Ber.* **1996**, *129*, 657-662.

[11] H. Brunner, U. Klement, W. Meier, J. Wachter, O. Serhadle, M. L. Ziegler, *J. Organomet. Chem.* **1987**, *335*, 339-352.

[12] S. Heinl, G. Balazs, M. Scheer, *Phosphorus, Sulfur Silicon Relat. Elem.* **2014**, *189*, 924-932.

[13] a) H. Brunner, U. Klement, W. Meier, J. Wachter, O. Serhadle, M. L. Ziegler, *J. Organomet. Chem*. **1987**, *335*, 339-352; b) L. Y. Goh, W. Chen, R. C. S. Wong, *Organometallics* **1995**, *14*, 3886-3896.

[14] M. Schmidt, A. E. Seitz, M. Eckhardt, G. Balázs, E. V. Peresypkina, A. V. Virovets, F. Riedlberger, M. Bodensteiner, E. M. Zolnhofer, K. Meyer, M. Scheer, *J. Am. Chem. Soc.* **2017**, *139*, 13981-13984.

[15] P. Pyykkö, M. Atsumi, *Chem. Eur. J.* **2009**, *15*, 12770-12779.

[16] P. Pyykkö, M. Atsumi, *Chem. Eur. J.* **2009**, *15*, 186-197.

[17] H. Brunner, L. Poll, J. Wachter, B. Nuber, *J. Organomet. Chem.* **1994**, *471*, 117-122.

6.5 Supporting Information

General Remarks

All experiments were performed with dry argon or nitrogen using glove box and Schlenk techniques. Solvents were dried using a MB SPS-800 device of company MBRAUN. ^{1}H, ^{13}C and ^{31}P NMR spectra were measured on a Bruker Avance 400 (^{1}H: 400.130 MHz, ^{13}C: 100.613 MHz, ^{31}P: 161.976 MHz). The chemical shifts are reported in ppm relative to external TMS (^{1}H, ^{13}C) and H_3PO_4 (^{31}P). Mass spectra were performed on a Finnigan MAT95 LIFDI-MS spectrometer. Elemental analysis (CHN) was determined using a Vario micro cube and Vario EL III instrument. Compounds [{$Cp^{BIG}Fe(CO)_2$}$_2$(μ,η$^{1:1}$-P_4Q_3)])] (Q = S (**1**), Se (**2**))[1] were synthesized according to literature procedures.

Synthesis of [{$Cp^{BIG}Fe$}$_2$(μ,η$^{4:4}$-P_2S_2)] (4)

Compound **1** (285 mg, 0.15 mmol) was dissolved in 50 mL 1,3-diisopropylbenzene and the pink solution was refluxed for 18 h. The solution turned dark green during the reaction. After removal of the solvent in vacuum, the crude product was purified by column chromatography (silica, hexane/toluene 5:1). Complex **3** was eluted first, as a light green band. Compound **4** was collected as a second dark green fraction. After removal of the solvent, **3** and **4** can be isolated as green solids. Complex **4** can be crystallized from a CH_2Cl_2 solution, layered with CH_3CN.

3: Yield: 50 mg (35 %).

4: Yield: 157 mg (62 %).

^{1}H NMR (C_6D_6): δ [ppm] = 0.77 (30H, t, $^{3}J_{HH}$ = 7.5 Hz, C*H*$_3$), 1.13 (20H, m, $^{3}J_{HH}$ = 7.5 Hz, C*H*$_2$), 1.38 (20H, m, $^{3}J_{HH}$ = 7.5 Hz, C*H*$_2$), 2.32 (20H, t, $^{3}J_{HH}$ = 7.5 Hz, C*H*$_2$), 6.85 (20H, d, $^{3}J_{HH}$ = 8.2 Hz, C*H*), 7.55 (20H, d, $^{3}J_{HH}$ = 8.2 Hz, C*H*).

^{13}C{^{1}H} NMR (C_6D_6): δ [ppm] = 14.1 (^{n}Bu), 22.7 (^{n}Bu), 33.2 (^{n}Bu), 35.6 (^{n}Bu), 90.3 (C_5), 127.9 (Ph), 131.2 (Ph), 133.6 (Ph), 141.6 (Ph).

^{31}P{^{1}H} NMR (C_6D_6): δ [ppm] = -82.8 (2P, s).

Elemental analysis ($C_{110}H_{130}Fe_2P_2S_2$): calculated: C 78.18, H 7.75; found: C 78.11, H 7.56.

Mass spectrometry (EI, toluene): m/z 1689.80 (38%) $[M]^+$, 1627.86 (5%) $[M-P_2]^+$, 844.90 (15%) $[M-Cp^{BIG}FePS]^+$, 726.52 (100%) $[Cp^{BIG}]^+$.

NMR Investigations

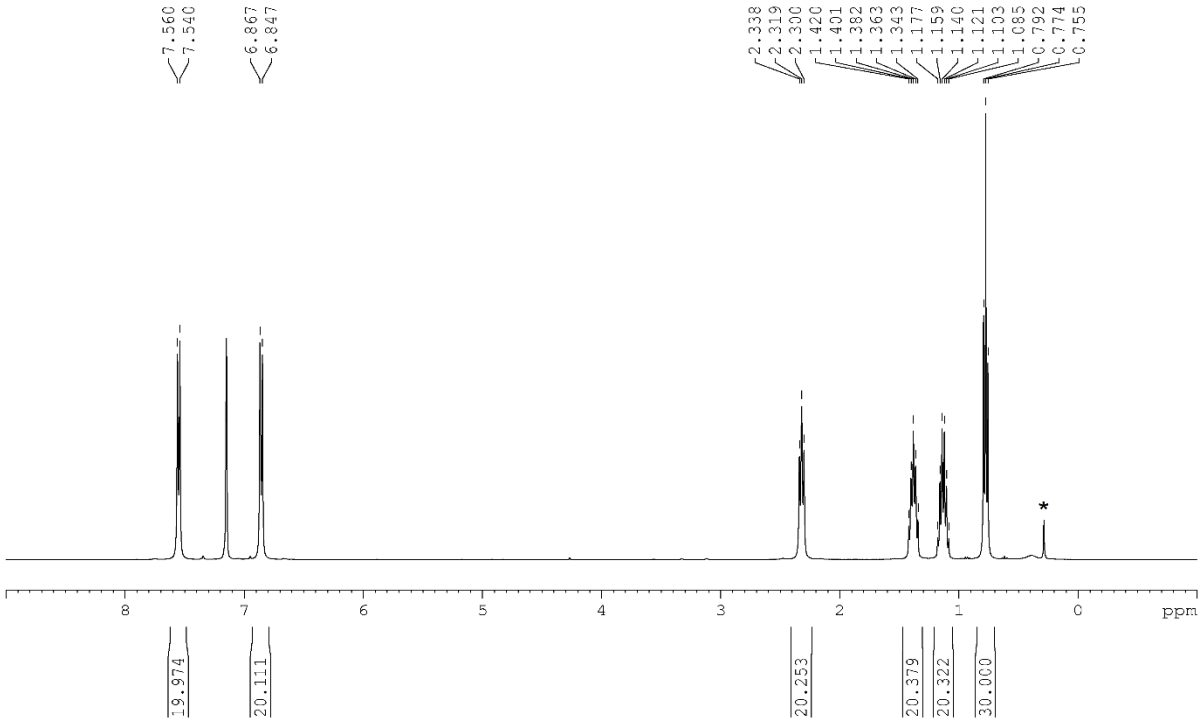

Figure S1. ^{1}H NMR spectrum of **4** in C_6D_6. * = impurities (silicon grease).

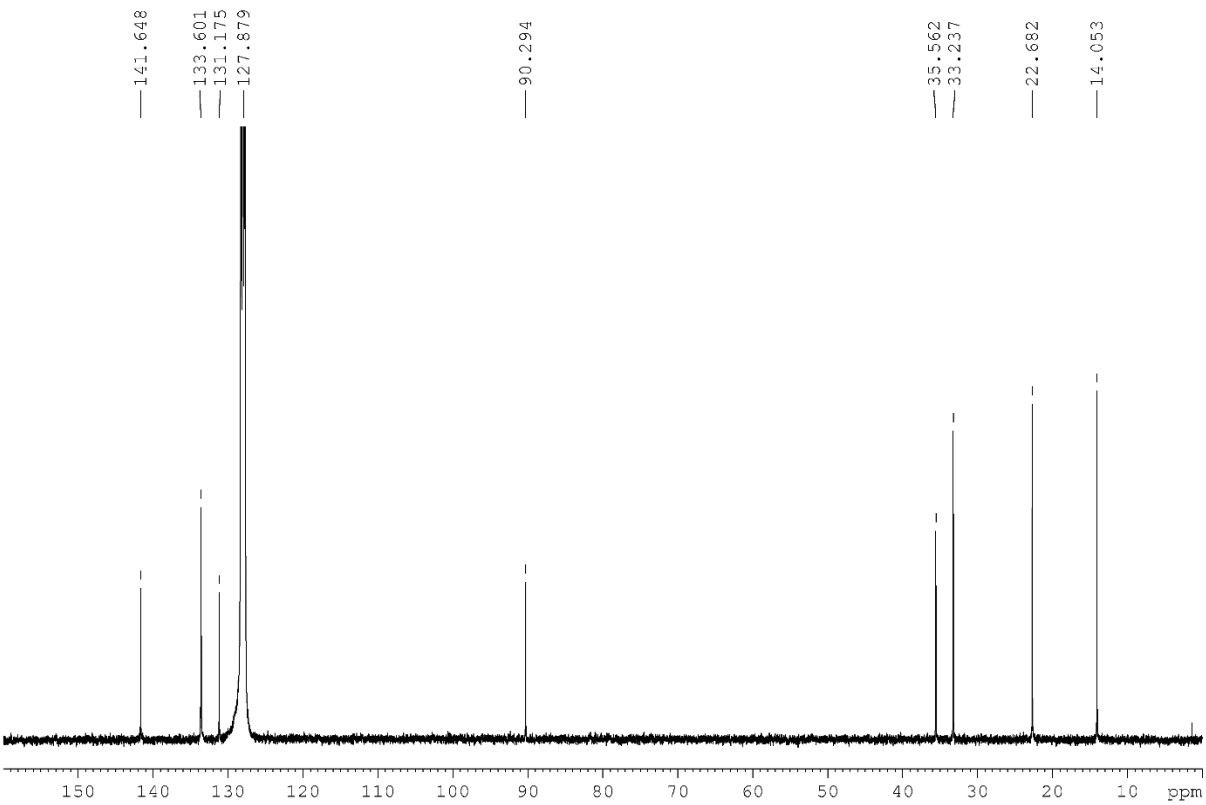

Figure S2. ^{13}C{^{1}H} NMR spectrum of **4** in C_6D_6.

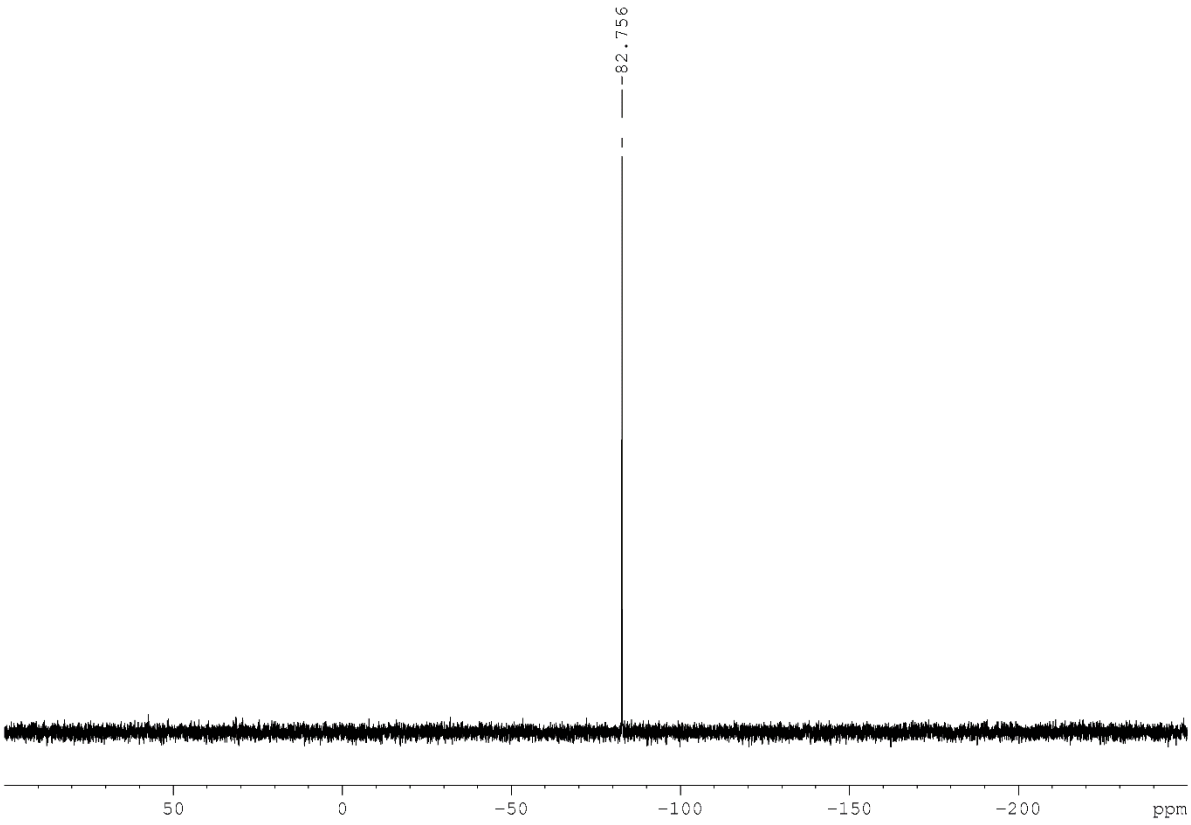

Figure S3. $^{31}P\{^{1}H\}$ NMR spectrum of **4** in C_6D_6 at 300 K.

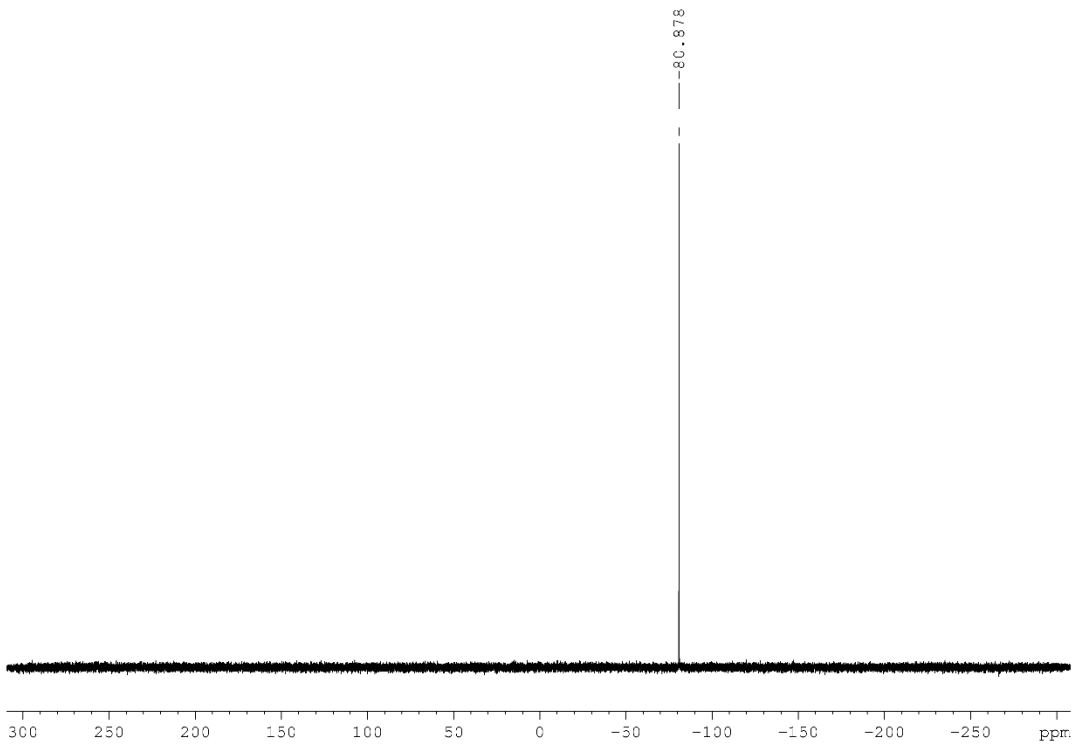

Figure S4. HT $^{31}P\{^{1}H\}$ NMR spectrum of **4** in Tol-d_8 at 373 K.

Crystallographic Details

Single crystal structure analyses were performed on a Rigaku Technologies diffractometer (GV50, Titan^{S2}). Data reduction was performed using the CrysAlisPro[2] software package. The structure solution was carried out using the program ShelXT[3] (Sheldrick, 2015) using the Olex2[4] software. Least squares refinements on F_0^2 were employed using SHELXL-2014.[5]

Table S1. Crystallographic data and details of diffraction experiments for **4**.

Compound	**4**
Formula	$C_{110}H_{130}Fe_2P_2S_2$
$\rho_{calc.}$/ g cm^{-3}	1.201
μ/mm^{-1}	3.582
Formula Weight	1689.89
Colour	dark green
Shape	plank
Size/mm^3	0.47×0.10×0.07
T/K	122.97(15)
Crystal System	orthorhombic
Space Group	*Pbca*
a/Å	26.8338(4)
b/Å	23.5143(4)
c/Å	29.6187(4)
α/°	90
β/°	90
γ/°	90
V/Å^3	18688.7(5)
Z	8
Z'	1
Wavelength/Å	1.54184
Radiation type	CuK$_\alpha$
θ_{min}/°	2.910
Θ_{max}/°	74.759
Measured Refl.	71921
Independent Refl.	18333
Reflections Used	15395
R_{int}	0.0489
Parameters	1055
Restraints	11
Largest Peak	0.881
Deepest Hole	-0.537
GooF	1.028
wR_2 (all data)	0.1518
wR_2	0.1422
R_1 (all data)	0.0598
R_1	0.0504

References

[1] S. Heinl, M. Scheer, *Chemical Science* **2014**, *5*, 3221-3225.

[2] CrysAlisPro Software System, Agilent Technologies UK Ltd, Yarnton, Oxford, UK (2014).

[3] Sheldrick, G.M., ShelXT, *Acta Cryst.*, **2014**, *A71*, 3-8.

[4] O.V. Dolomanov and L.J. Bourhis and R.J. Gildea and J.A.K. Howard and H. Puschmann, Olex2: A complete structure solution, refinement and analysis program, *J. Appl. Cryst.*, **2009**, *42*, 339-341.

[5] Sheldrick, G.M., A short history of ShelX, *Acta Cryst.*, **2008**, *A64*, 339-341.

Preface

The following chapter includes preliminary, unpublished results, which will be included in future publications or provide a basis for future research efforts.

The obtained compounds could not be fully characterized. However, all data and knowledge that was acquired about the described products and reactions are presented.

7 Thesis Treasury

7.1 Reactivity of $[Cp^{PEt}NiBr]_2$ with $[Na(dioxane)_x][AsCO]$

The reaction of $[Cp^{PEt}Ni(\mu\text{-}Br)]_2$ with two equivalents of $[Na(dioxane)_{3.3}][AsCO]$ was conducted in THF at ambient temperatures. The ^1H NMR spectroscopic investigations of the crude reaction mixture in C_6D_6 reveal a complete conversion of the educt $[Cp^{PEt}Ni(\mu\text{-}Br)]_2$ and the formation of several products. After purification, a dark violet solid, consisting of different complexes could be isolated (**T1**). Despite many intensive attempts have been made by column and thin-layer chromatography the separation of the mixture was unsuccessful due to the similar solubility of the products caused by the Cp^{PEt} ligands.

Single-crystals could be grown from CH_2Cl_2 solutions, layered with CH_3CN after complete diffusion. X-ray diffraction studies display several complexes with the general composition $[(Cp^{PEt}Ni)_2As_n]$ (**T1**), co-crystallizing on the same position due to their similar structure and the dominating effect of the sterically highly demanding Cp^{PEt} ligands, leading to a highly disordered As_n middle-deck. According to the X-ray diffraction measurement, complexes with an As_n ligand (n = 2, 4) and a cubic Ni_2As_6 structural core motif can be assumed, but a certain assignment was not possible.

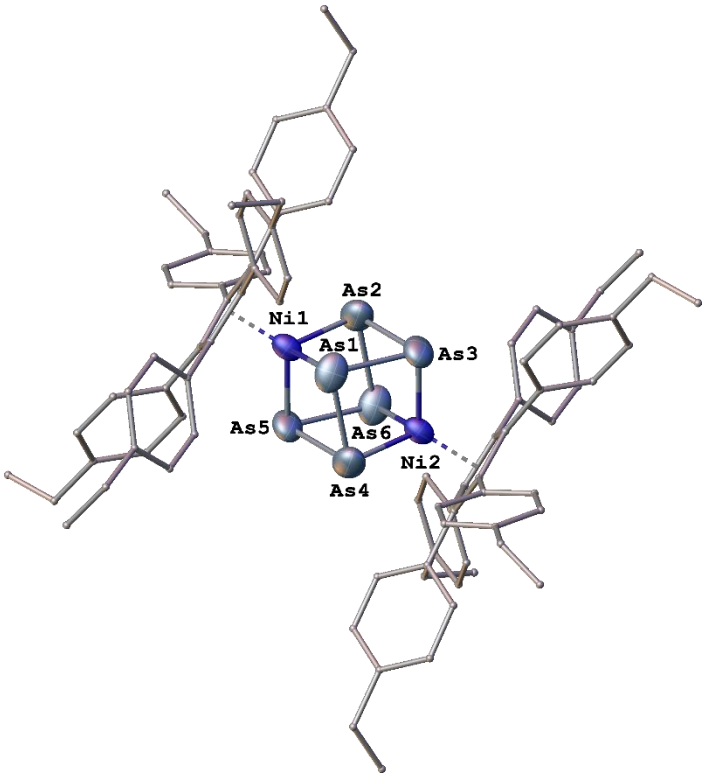

Figure 1. Preliminary molecular structure of the $[Ni_2As_6]$ part of **T1**. Hydrogen atoms and disorders are omitted for clarity.

A FD mass spectrum of crystals in toluene exhibits five assignable peaks at m/z = 585.4 (100%), m/z = 1228.6, m/z = 1344.6, m/z = 1513.4 and m/z = 1588.3 corresponding to $[Cp^{BIG}]^+$, $[Cp^{PEt}{}_2Ni]^+$, $[Cp^{PEt}{}_2Ni_2(CO)_2]^+$, $[Cp^{PEt}{}_2Ni_2As_3]^+$ and $[Cp^{PEt}{}_2Ni_2As_4]^+$, respectively.

7.2 Reactivity of $[Cp^{BIG}FeP_5]$ with $CuCl_2$

The reaction of $[Cp^{BIG}Fe(\eta^5\text{-}P_5)]$ with five equivalents of $CuCl_2$ was conducted in CH_2Cl_2 at ambient temperatures. The mixture was stirred for 18 h, resulting in a color change from green to red-brown and the formation of a light yellow precipitate. The filtered solution was layered with a small amount of toluene and another layer of *n*-hexane.

After complete diffusion, red single-crystals of **T2**, suitable for X-ray diffraction measurements were obtained. The X-ray structural analysis displays the molecular composition $[\{Cp^{BIG}Fe(\eta^5\text{-}P_5)\}_6Cu_{31}Cl_{31}]$ (**T2**), exhibiting a lens-shaped scaffold. The whole molecule can be dissected for clarity in an outer and an inner shell (see Figure 2). The outer shell consists of six $[Cp^{BIG}FeP_5]$ units, arranged as a trigonal antiprism (flattened octahedron) and a CuCl-framework with an ordered central part and a partly occupied peripheral part (Figure 3). The disorder of the latter is still under interpretation. Therefore, the P_5 ligands are 1,2,3,4-coordinated by Cu atoms.

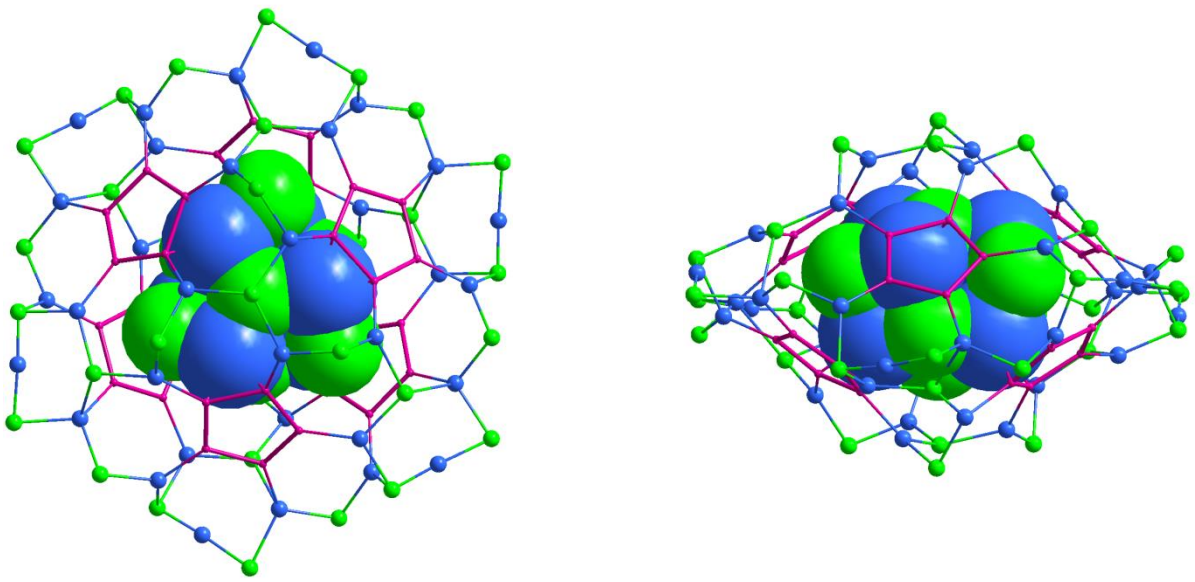

Figure 2. Molecular structure of **T2**: up (left) and side (right) view. The whole scaffold is constructed from an outer (ball-and-sticks) and an inner part (space filling). Atoms: Cu (blue), Cl (green), P (pink).

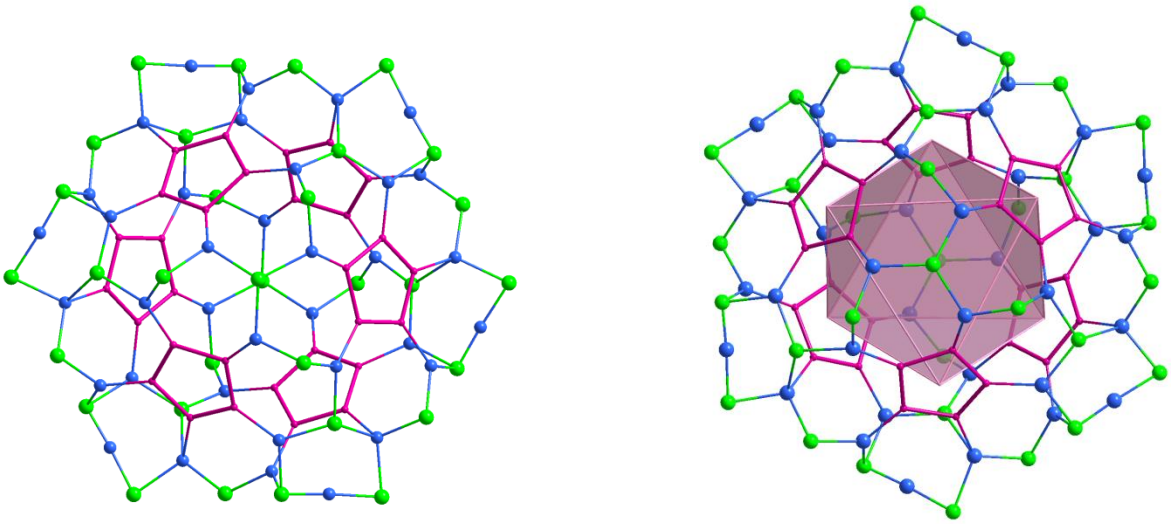

Figure 3. The outer shell of **T2** and the trigonal antiprismatic arrangement of six [$Cp^{BIG}FeP_5$] units. Some of the Cu and Cl positions are partly vacant.

The 'inner part' consists of a copper and chloride framework and occupies the whole cavity provided by the outer shell (Figure 4). The inner Cu atoms are side-on coordinated by P_5 ligands in η^2-mode (Figure 5).

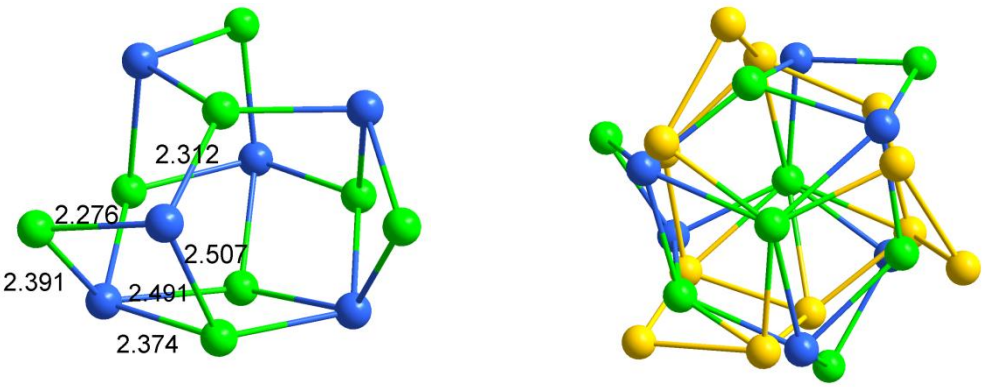

Figure 4. The distances (Å) in the ordered part of the inner shell $\{Cu_6Cl_8\}^{2-}$ (left); and its disorder over two positions by an inversion center (second position is shown in yellow) (right).

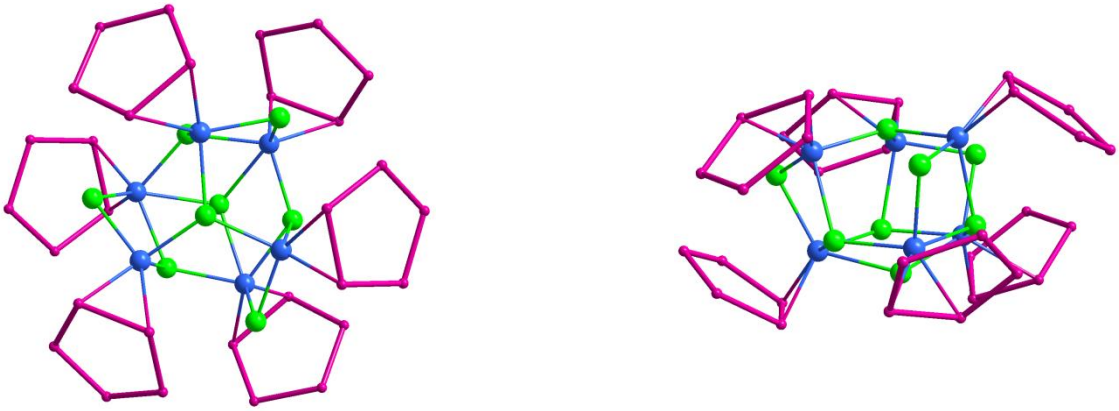

Figure 5. The ordered inner part of **T2** in-between of the trigonal antiprismatic arrangement of six [$Cp^{BIG}FeP_5$] units, up view (left) and side view (right). The disorder over the three-fold inversion axis is not shown.

The $^{31}P\{^1H\}$ NMR spectrum of **T2** in CD_2Cl_2 shows several signals in the range of 125 ppm to -50 ppm for non-equivalent P-Atoms. A further assignment of the signals to the related P atoms was not possible. The ^1H NMR spectrum of **T2** shows a large number of superimposed signals, consistent with a hindered rotation of the Cp^{BIG} ligands.

7.3 Supporting Information

General Remarks

All experiments were performed with dry argon or nitrogen using glove box and Schlenk techniques. Solvents were dried using a MB SPS-800 device of company MBRAUN. ^{1}H, ^{13}C and ^{31}P NMR spectra were measured on a Bruker Avance 400 (^{1}H: 400.130 MHz, ^{13}C: 100.613 MHz, ^{31}P: 161.976 MHz). The chemical shifts are reported in ppm relative to external TMS (^{1}H, ^{13}C) and H_3PO_4 (^{31}P). Mass spectra were performed on a Finnigan MAT95 LIFDI-MS spectrometer. Elemental analysis (CHN) was determined using a Vario micro cube and Vario EL III instrument. Compounds [Na(dioxane)$_x$][AsCO][1], [{Cp^{BIG}Fe(η^5-P$_5$)][2] were synthesized according to literature procedures.

Synthesis of [(Cp^{PEt}Ni)$_2$As$_n$] (T1)

A solution of [Na(dioxane)$_{3.3}$][AsCO] (58 mg, 0.14 mmol) in 3 mL THF was added to a solution of [Cp^{PEt}NiBr]$_2$ (100 mg, 0.07 mmol) in 5 mL THF and stirred at ambient temperature for 18 h. After removal of all volatiles in vacuum, the dark residue was extracted with 10 mL toluene. The filtrate was dried and subsequently washed with *n*-hexane and CH_3CN, which afforded a dark violet solid (70 mg, **T1**). Single crystals suitable for X-ray analysis were grown from CH_2Cl_2 (5 mL) solutions, layered with double the amount of CH_3CN.

Mass spectrometry (LIFDI, toluene): m/z 585.4 (100%) [CpPEt]$^+$, 1228.6 [Cp$^{PEt}_2$Ni]$^+$, 1344.6 [Cp$^{PEt}_2$Ni$_2$(CO)$_2$]$^+$, 1513.4 [Cp$^{PEt}_2$Ni$_2$As$_3$]$^+$, 1588.3 [Cp$^{PEt}_2$Ni$_2$As$_4$]$^+$.

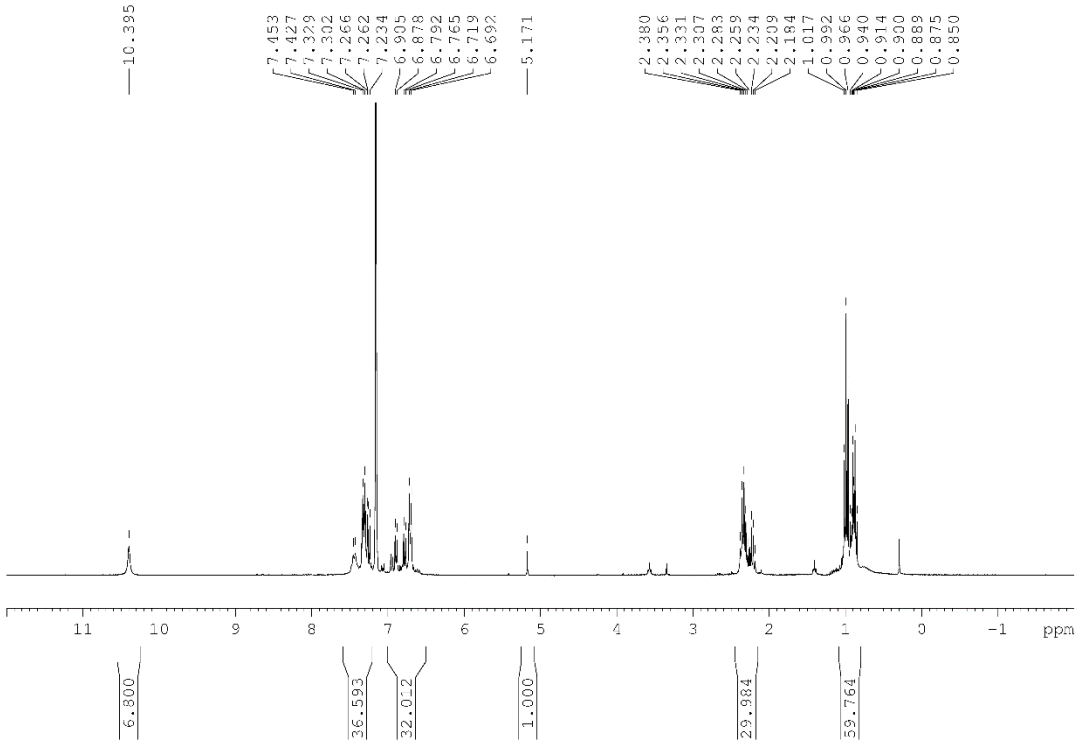

Figure S1. ^{1}H NMR spectrum of the crude reaction mixture of **T1** in C_6D_6.

Synthesis of [{$Cp^{BIG}Fe(\eta^5\text{-}P_5)$}$_6Cu_{31}Cl_{31}$] (T2)

A mixture of [$Cp^{BIG}FeP_5$] (25 mg, 0.03 mmol) and $CuCl_2$ (18 mg, 0.15 mmol) is dissolved in 3 mL CH_2Cl_2 and stirred for 18 h. The resulting red solution is filtered via a cannula into a thin Schlenk tube. The reaction mixture is layered with a small amount of toluene and 6 mL *n*-hexane. After complete diffusion red crystals of **T2** are obtained.

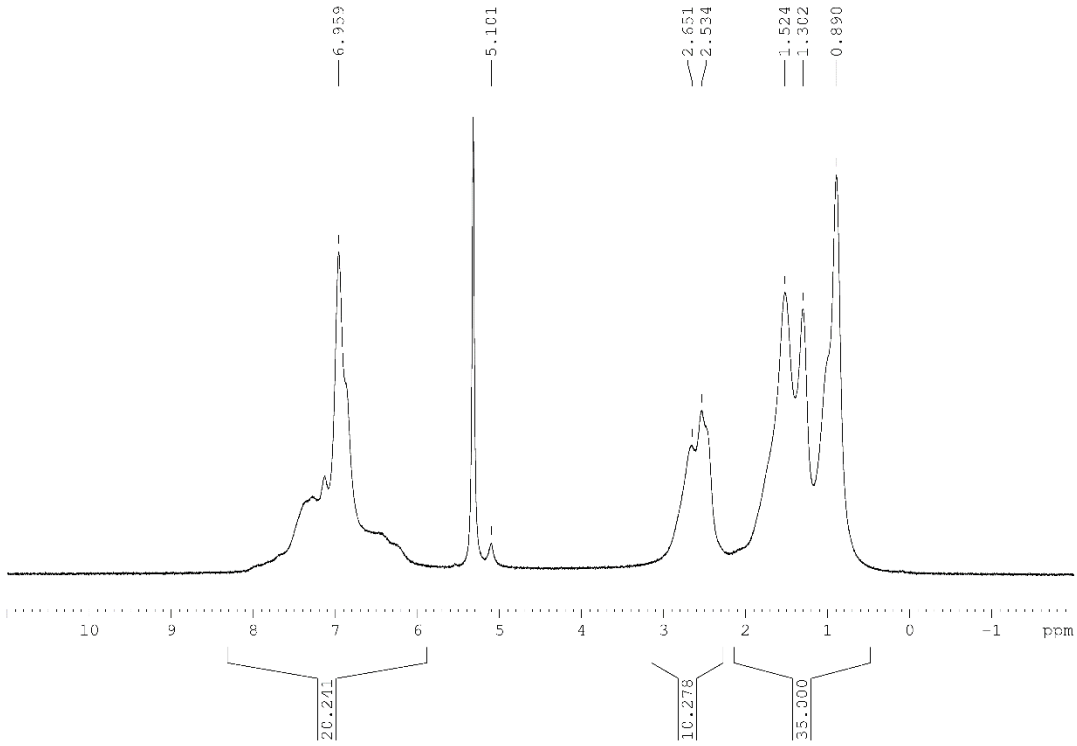

Figure S2. ^{1}H NMR spectrum of crystals of **T2** in CD_2Cl_2.

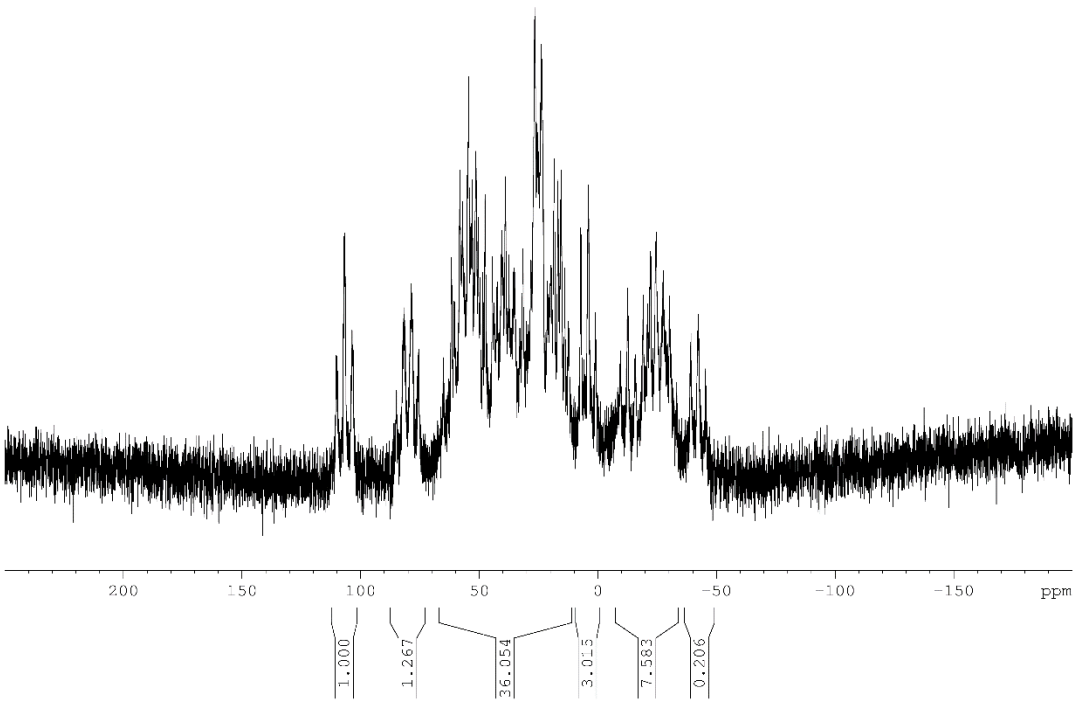

Figure S3. ^{31}P{^{1}H} NMR spectrum of crystals of **T2** in CD_2Cl_2.

Crystallographic Details

Single crystal structure analyses were performed on a Rigaku Technologies diffractometer (GV50, Titan[S2]). Data reduction was performed using the CrysAlisPro[3] software package. The structure solution was carried out using the program ShelXT[4] (Sheldrick, 2015) using the Olex2[5] software. Least squares refinements on F_0^2 were employed using SHELXL-2014.[6]

A final refinement for **T2** was not possible. Therefore, all given values in Table S1 are preliminary and not complete. No data is given in the case of **T1** (mixture), because no final statement can be given about the disordered As_n middle-deck.

Table S1. Preliminary crystallographic data and details of diffraction experiments for **T2**.

Compound	**T2 · x CH_2Cl_2**
Formula	$C_{330}H_{390}Fe_6P_{30}Cu_{31}Cl_{31}(CH_2Cl_2)_x$
$\rho_{calc.}$/ g cm^{-3}	-
μ/mm^{-1}	-
Formula Weight	-
Colour	red
Shape	cube
Size/mm^3	0.16×0.12×0.03
T/K	123.0(1)
Crystal System	trigonal
Space Group	*R*-3
a/Å	29.1659(9)
b/Å	29.1218(8)
c/Å	39.1594(7)
α/°	90.201(2)
β/°	89.950(2)
γ/°	120.082(3)
V/Å^3	28780(1)
Z	4
Z'	-
Wavelength/Å	1.54184
Radiation type	CuK_a
θ_{min}/°	3.3866
Θ_{max}/°	73.9970
Measured Refl.	21874

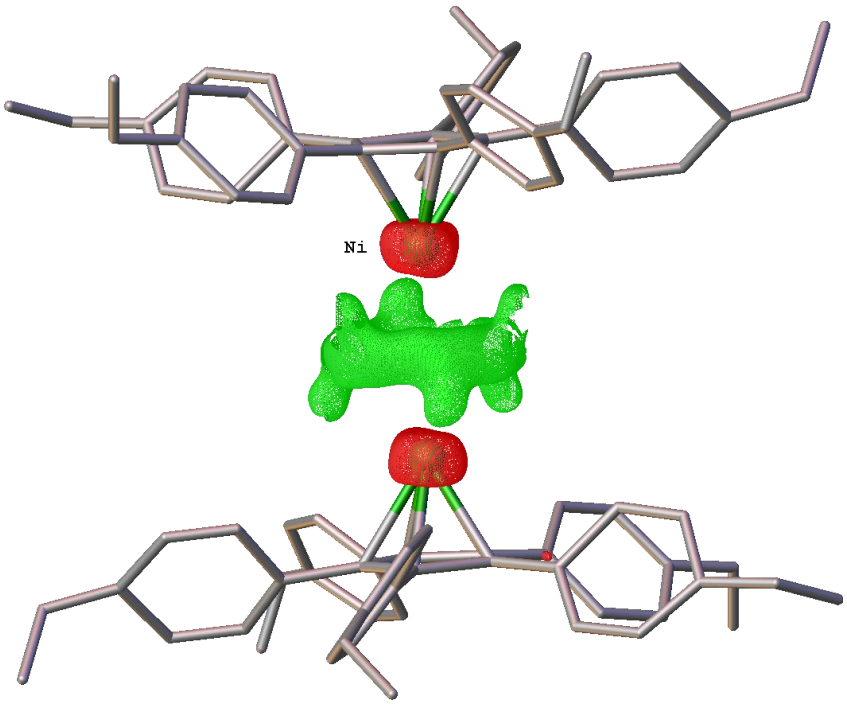

Figure S4. Electron density map in the crystal of the mixture **T1**. Hydrogen atoms are omitted and Cp^{BIG} ligands are drawn in 'wire-or-stick' model for clarity.

References

[1] A. Hinz, J. M. Goicoechea, *Angew. Chem., Int. Ed.* **2016**, *55*, 8536-8541.

[2] S. Heinl, M. Scheer, *Chemical Science* **2014**, *5*, 3221-3225.

[3] CrysAlisPro Software System, Agilent Technologies UK Ltd, Yarnton, Oxford, UK (2014).

[4] Sheldrick, G.M., ShelXT, *Acta Cryst.*, **2014**, *A71*, 3-8.

[5] O.V. Dolomanov and L.J. Bourhis and R.J. Gildea and J.A.K. Howard and H. Puschmann, Olex2: A complete structure solution, refinement and analysis program, *J. Appl. Cryst.*, **2009**, *42*, 339-341.

[6] Sheldrick, G.M., A short history of ShelX, *Acta Cryst.*, **2008**, *A64*, 339-341.

8 Conclusion

This work provides an insight into the preparation and reactivity of transition metal (Mn, Fe, Ni) complexes, bearing the sterically highly demanding perarylated ligands Cp^{PEt} or Cp^{BIG}, respectively.

Different E_n (E = P, As) ligand complexes of nickel were synthesized by E_4 activation or the reaction with the PCO^- anion. Moreover, the reactivity of the E_n (E = P, As) ligand complexes of manganese, iron and nickel has been investigated towards reactive metal(I) complexes (Co, Fe) at ambient temperatures and under thermolytic conditions.

Synthesis and Reactivity of E_n Ligand Complexes of Nickel

Numerous P_n ligand compounds containing early and late transition metals and or main group elements are known and have been well studied. The general approach involves the activation of white phosphorus by reactive metal species. Nevertheless, lately also the 2-phosphaethynolate anion, PCO^-, has emerged as a versatile reagent for the synthesis of P_n ligand complexes. Although it was first isolated in 1992 as $[Li(DME)_2][PCO]$ (DME = dimethoxyethane), it took over two decades before it got rising interest, because of the difficulties relating to its handling. With the publication of novel syntheses of the sodium salt in 2011 and 2012, followed by the report of a reliable and scalable synthesis in 2014, the 2-phosphaethynolate anion has been employed for the preparation of many different phosphorus-containing compounds. In this regard, P_n and As_n ligand compounds ($n \geq 2$) have been synthesized from $[Cp^{PEt}Ni(\mu\text{-}Br)]_2$ by E_4 (E = P, As) activation and reaction with $[Na(dioxane)_x][PCO]$, respectively.

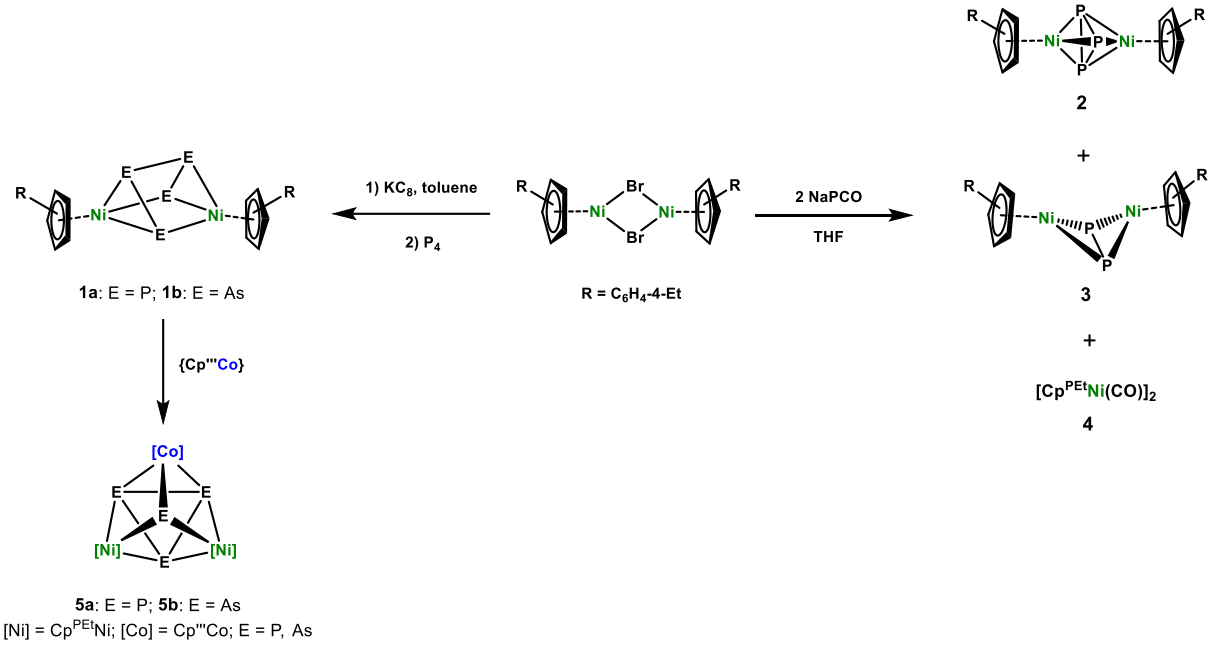

Scheme 1. Synthesis of E_n ligand complexes of nickel.

The reduction of $[Cp^{PEt}Ni(\mu\text{-}Br)]_2$ with two equivalents of potassium graphite in toluene and further reaction of the formed "$Cp^{PEt}Ni(I)$" species with P_4 and As_4, respectively, at -10 °C leads to the formation of $[(Cp^{PEt}Ni)_2(\mu,\eta^{3:3}\text{-}E_4)]$ (E = P (**1a**), As (**1b**)). Both products **1a** and **1b** display a prismatic Ni_2E_4 core in the solid state. For **1a** a dynamic behavior in solution was observed that was further investigated by variable-temperature $^{31}P\{^1H\}$ NMR spectroscopy. The observed broadened singlet at room temperature splits into two doublets at 193 K, being characteristic of a dynamic process involving the P_4 ligand.

The salt metathesis of $[Cp^{PEt}Ni(\mu\text{-}Br)]_2$ with two equivalents of $[Na(dioxane)_{2.4}][PCO]$ leads to the triple-decker complexes $[(Cp^{PEt}Ni)_2(\mu,\eta^{3:3}\text{-}P_3)]$ (**2**) and $[(Cp^{PEt}Ni)_2(\mu,\eta^{2:2}\text{-}P_2)]$ (**3**), together with $[Cp^{PEt}Ni(\mu\text{-}CO)]_2$ (**4**). The paramagnetic compound **2** is one of the rare examples of a cyclopentadienyl nickel sandwich complex with a *cyclo*-P_3 unit, showing an allylic distortion with one longer P-P bond distance. Complex **3** exhibits a butterfly-like structural motif with two cyclopentadienyl nickel fragments bridged by a P_2 moiety. Whereas this structural motif is well known for Group 10 compounds, complex **3** is the first example with cyclopentadienyl nickel fragments. This is contrast to reported Cp^4 and Cp''' derivatives as well as the predicted ground state geometry in the gas phase found by DFT calculations, which exhibit a diphospha-dinickela-tetrahedrane like structure with a Ni-Ni bond. A geometry for **3**, which is in good agreement with the experimentally found geometric parameters, with a longer Ni-Ni distance (3.453 Å), could also be obtained from DFT calculations as a local minimum (+16.3 kcal/mol). Considering these results, the sterically highly demanding Cp^{PEt} ligands play an essential role in the formation of the butterfly-like structure of **3**.

Furthermore, complexes **1a** and **1b**, respectively, were reacted with the triple-decker complex [(Cp'''Co)$_2$(μ-toluene)] in toluene at room temperature. The isolated products [(Cp^{PEt}Ni)$_2$(Cp'''Co)(μ$_3$,η$^{1:1:1}$-E)(μ$_3$,η$^{2:2:2}$-E$_3$)] (E = P (**5a**), As (**5b**)), are formed selectively and reveal an unprecedented Ni$_2$CoE$_4$ core with a tetrahedral E$_4$ unit with three metal-capped faces. The E$_4$ tetrahedron is separated into an E$_1$ and a *cyclo*-E$_3$ ligand, bridging the three metal fragments. The average E-E distance between the E$_1$ and the E$_3$ moieties is 2.649(1) Å in **1a** and 2.850(1) Å in **1b**, respectively. In addition, the threefold coordination leads to the elongation of the E-E bond distances within the *cyclo*-E$_3$ unit. Further ^{31}P{^{1}H} NMR investigations of **5a** confirm the presence of two independent ligands, exhibiting a singlet for the P$_1$ unit and a doublet and a triplet, corresponding to the *cyclo*-P$_3$ ligand, with small $^1J_{PP}$ coupling constants.

Reactivity of Coordinated P$_4$ Compared to White Phosphorus

Numerous transition metal compounds and their reactions towards P$_4$ have been conducted and the resulting P$_n$ ligand complexes were characterized. However, investigations of the reactivity of coordinated, but still intact P$_4$ tetrahedra as a ligand are rare. For this purpose the complex [{Cp^{BIG}Mn(CO)$_2$}$_2$(μ,η$^{1:1}$-P$_4$)], bearing an intact P$_4$ tetrahedron, was selected as a suitable starting material. The compounds [L^{0}M(toluene)] (L^0 = CH[CHN(2,6-Me$_2$C$_6$H$_3$)]$_2$; M = Fe, Co) represent a convenient system to emphasize any differences in the reactivity of free white phosphorus compared to the coordinated P$_4$ moiety in [{Cp^{BIG}Mn(CO)$_2$}$_2$(μ,η$^{1:1}$-P$_4$)], since a detailed insight into the reactivity towards white phosphorus was provided by Scheer *et al.*.[1]

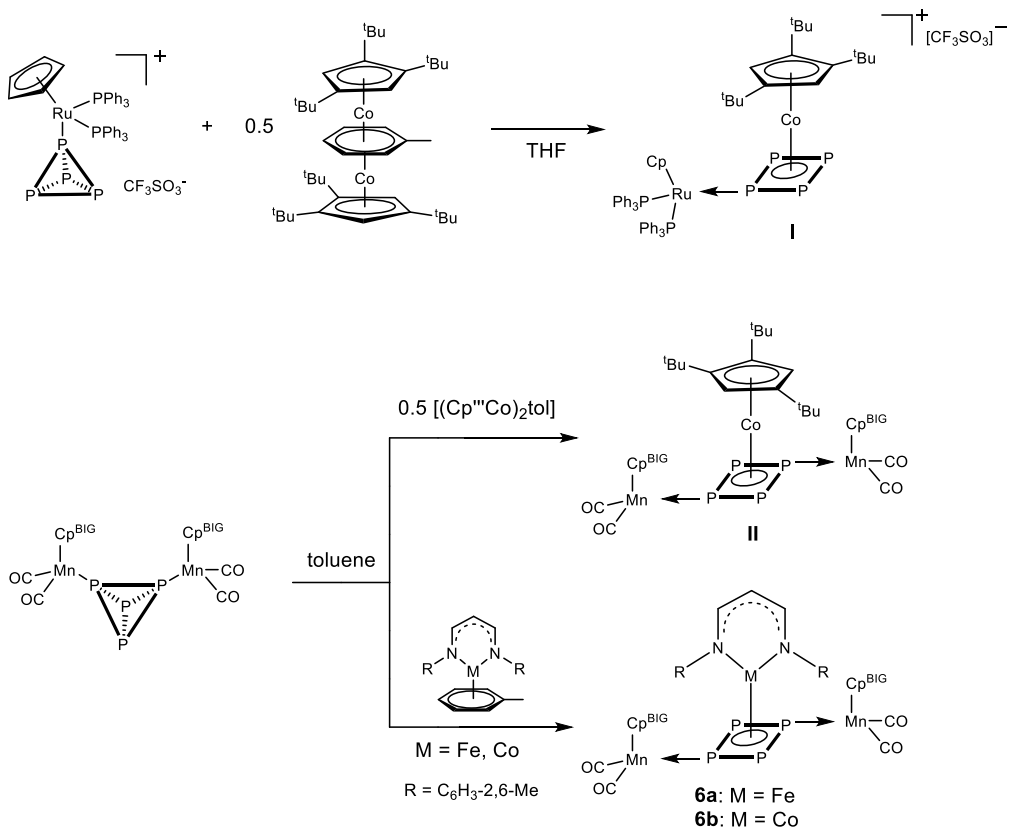

Scheme 2. Activation of coordinated P_4.

The complex $[\{Cp^{BIG}Mn(CO)_2\}_2(\mu,\eta^{1:1}\text{-}P_4)]$ was reacted with $[L^0M(toluene)]$ (M = Fe, Co) in toluene at ambient temperatures. The resulting products $[\{Cp^{BIG}Mn(CO)_2\}_2\{L^0M\}(\mu,\eta^{1:1:4}\text{-}P_4)]$ (M = Fe (**6a**), Co (**6b**)) show a *cyclo*-P_4 moiety, derived from the intact P_4 tetrahedron by two P-P bond cleavages. The very labile ligand benefits from the stabilizing effect of the three metal fragments in **6a** and **6b**, respectively. The average P–P bond length in the *cyclo*-P_4 ligand lies with 2.152(1) Å between a P–P single bond and a P=P double bond. This is an evidence for almost perfectly planar aromatic P_4 cycles. Therefore, the *cyclo*-P_4 ligand can be described as a $[P_4]^{2-}$ dianion.

In comparison to the studies of the reactivity of $[L^0M(toluene)]$ towards pure white phosphorus, a different reaction behavior is observed. The P_4 activation by $[L^0Fe(toluene)]$ leads to the selective formation of a realgar-type P_8 ligand coordinating to four metal fragments, derived from dimerization reactions. The isolated product, yielded by reaction of $[L^0Co(toluene)]$ towards P_4, exhibits a rectangularly shaped P_4 moiety, spanned by two shorter and two longer P-P atom distances with a Co_2P_4 core. The mentioned reactions indicate the differences in the reaction behavior of free white phosphorus compared to pre-coordinated tetrahedral P_4 ligands.

A similar reaction outcome was observed by Dr. Sebastian Heinl, reacting $[\{Cp^{BIG}Mn(CO)_2\}_2(\mu,\eta^{1:1}\text{-}P_4)]$ and the cationic mononuclear complex

$[CpRu(PPh_3)_2(\eta^1\text{-}P_4)][CF_3SO_3]$ with the triple-decker complex $[(Cp'''Co)_2(\mu\text{-toluene})]$. Both products **I** and **II** show a planar *cyclo*-P_4 moiety, stabilized by two and three metal fragments, respectively.

Synthesis of Mixed Group 15/16 Compounds

The activation of Group 15 based cage compounds such as white phosphorus P_4 and yellow arsenic As_4 with transition metal complexes or main group compounds is of special interest in research. Mostly carbonyl complexes are used for it under thermolytic or photolytic conditions. In contrast, little is known about the activation of the mixed Group 15/16 cage compounds of the type E_4Q_3 (E = P, Q = S, Se; E = As, Q = S) by organometallic complexes. Besides the coordination and partial bond cleavage of the more or less intact E_4Q_3 cages, the co-thermolysis of these cages, accompanied by complete fragmentation, leads to the formation of unique E_mQ_n ligands. Regarding this, we got interested in the reaction behavior of the complex $[\{Cp^{BIG}Fe(CO)_2\}_2(\mu,\eta^{1:1}\text{-}P_4Q_3)]$ (Q = S, Se), bearing an already activated P_4Q_3 moiety, under thermolytic conditions and the novel E_mQ_n ligands that might arise.

The reaction of $[\{Cp^{BIG}Fe(CO)_2\}_2(\mu,\eta^{1:1}\text{-}P_4S_3)]$ under thermal conditions in the high boiling solvent 1,3-diisopropylbenzene (DIB) leads to the formation of the all-phosphorus compound $[Cp^{BIG}Fe(\eta^5\text{-}P_5)]$ and the unprecedented complex $[(Cp^{BIG}Fe)_2(\mu,\eta^{4:4}\text{-}P_2S_2)]$ (**7**).

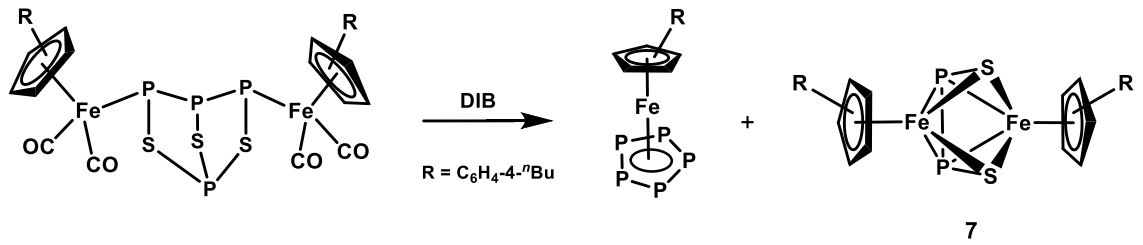

Scheme 3. Thermal activation of activated P_4S_3.

This evidences the assumption of the fragmentation of the P_4S_3 ligand and subsequent recombination of the fragments under elevated temperatures. The all-phosphorus complex $[Cp^{BIG}Fe(\eta^5\text{-}P_5)]$ has been reported by Scheer *et al.* and was obtained by co-thermolysis of $[Cp^{BIG}Fe(CO)_2]_2$ with an excess of white phosphorus in decalin or 1,3-diisopropylbenzene. The mixed group 15/16 ligand complex **7** exhibits a butadiene like S=P-P=S unit in the solid state structure, confirmed by X-ray diffraction studies. In contrast to the all-phosphorus derivative, compound **7** shows no dynamic behavior involving the P_2S_2 ligand in solution and a sharp singlet is observed in the $^{31}P\{^1H\}$ NMR spectrum at 300 K as well as 373 K.

Considering that, [{$Cp^{BIG}Fe(CO)_2$}$_2$(μ,η$^{1:1}$-P_4S_3)] represents a suitable source for mixed P/S ligands, while on the contrary, the selenium containing compound [{$Cp^{BIG}Fe(CO)_2$}$_2$(μ,η$^{1:1}$-P_4Se_3)] undergoes complete decomposition under the same thermal conditions, since only decomposition products were observed.

References

[1] a) F. Spitzer, C. Graßl, G. Balázs, E. M. Zolnhofer, K. Meyer, M. Scheer, *Angew. Chem., Int. Ed.* **2016**, *55*, 4340-4344; b) F. Spitzer, C. Graßl, G. Balázs, E. Mädl, M. Keilwerth, E. M. Zolnhofer, K. Meyer, M. Scheer, *Chem. Eur. J.* **2017**, *23*, 2716-2721.

9 Appendix

9.1 Thematic List of Abbreviations

NMR Spectroscopy

NMR	Nuclear Magnetic Resonance
δ	chemical shift
ppm	part per million
Hz	Hertz, s^{-1}
J	coupling constant, Hz
s	singlet
d	doublet
t	triplet
q	quartet
m	multiplet
br	broad
$\omega_{1/2}$	half width, Hz
VT	variable temperature
HT	high temperature
TMS	Tetramethylsilane, $Si(CH_3)_4$

Solvents

THF	tetrahydrofuran, C_4H_8O
Tol	toluene, C_7H_8
DIB	1,3-diisopropylbenzene, $C_{12}H_{18}$
DME	1,2-dimethoxyethane, $C_4H_{10}O_2$
CH_2Cl_2	dichloromethane
CH_3CN	acetonitrile

Mass Spectrometry

MS	mass spectrometry
$[M]^+$	molecular ion peak
m/z	mass to charge ratio
LIFDI	liquid injection field desorption ionization
FD	field desorption
ESI	electron spray ionization
EI	electron impact

Evans Method

μ_{eff}	effective magnetic moment
μ_B	Bohr magneton
χ_M	molar measured magnetic susceptibility
Δf	chemical shift difference, Hz
f	operating frequency of NMR spectrometer, Hz

Mössbauer Spectroscopy

δ	isomer shift, mm·s^{-1}
ΔE_Q	quadrupole splitting, mm·s^{-1}

IR Spectroscopy

IR	infrared spectroscopy
v	wavenumber, cm^{-1}
s	strong
w	weak

Other

Å	Angstroem, 1 Å = 1·10^{-10} m
T	temperature
K	Kelvin
°C	Degree Celsius
c	concentration, mol · L^{-1}
d	distance, Å
∢	Angle, °
r.t.	room temperature
M	metal
E	Group 15 element
Q	Group 16 element
1D	one dimensional
2D	two dimensional
3D	three dimensional
DFT	density functional theory
VE	valence electrons

Ligands and substituents

Ar	aromatic substituent
dmp	2,6-dimethylphenyl
R	organic substituent
Me	Methyl, CH_3
Et	Ethyl, -C_4H_9
*t*Bu	*tert*-Butyl, -C_4H_9
*n*Bu	*iso*-Butyl, -C_4H_9
NacNac	*β*-diketiminato
L^0	*β*-dialdiminato ligand, $CH[CHN(2,6\text{-}Me_2C_6H_3)]_2$
Ph	Phenyl, -C_6H_5
Cp	cyclopentadienyl, η^5-C_5H_5
Cp*	η^5-C_5Me_5
Cp^{4iPr}	η^5-C_5iPr_4H
Cp''	1,3-di-*tert*-butylcyclopentadienyl, η^5-$C_5H_3tBu_2$
Cp'''	1,2,4-tris-*tert*-butylcyclopentadienyl, η^5-$C_5H_2tBu_3$
Cp^{Ph}	pentakis-phenylcyclopentadienyl, η^5-$C_5(C_6H_5)_5$

Cp^{PEt}	pentakis-4-ethylphenylcyclopentadienyl, η^5-$C_5(4\text{-}EtC_6H_4)_5$
Cp^{BIG}	pentakis-4-*n*butylphenylcyclopentadienyl, η^5-$C_5(4\text{-}nBuC_6H_4)_5$

9.2 Acknowledgements

Finally, I would like to thank…

- Prof. Dr. Manfred Scheer for providing the interesting research topic and always ensuring excellent working conditions.
- Dr. Gábor Balázs for all his helpful advice, DFT calculations, proofreading and the infamous 'Toxic' plastic bottles.
- Dr. Eugenia Peresypkina, Prof. Dr. Alexander V. Virovets and Dr. Michael Bodensteiner for their great help with X-ray structure analyses.
- Prof. Dr. Karsten Meyer and Martin Keilwerth for the Mössbauer experiments.
- all staff of the Central Analytical Services of the University of Regensburg: X-Ray, NMR, MS and EA department. Especially, Wolfgang Söllner for the countless LIFDI-MS measurements as well as Anette Schramm and Georgine Stühler for all the measurements of the NMR spectra.
- the staff of the glass blowing, electronics and mechanics facilities of the University of Regensburg.
- my present and former lab colleagues Dr. Sebastian Heinl (his helpful advice and always providing a 'Koffer'), Dr. Fabian Spitzer (the encouraging discussions and for being the 'best' paper ball thrower of all time), Julian Müller (for always helping out and 'Keep filtrating!'), Maria Haimerl (for being a pleasant desk-neighbor and always unlocking the lab-door in the morning), Monika Schmidt (for her guided tour through Zoo Leipzig) and Bastian Hiltl (for passing the 'Administrator' job on to me).
- the 'Pumper' group Jens Braese (for all the 'breaks' and hanging out), Dr. Christian Marquardt (always good for a '#!?' talk), Oliver Hegen (for having a good laugh during lunch and carrying around heavy stuff together anywhere in the working group), Eric Mädl (for his 'Feuerzangenbowle' and always achieving 'personal records' when no one is present), Michael Weinhart (having the 'best' Magic decks and 'Naaa, heute nicht') and Matthias H. (for being one of the nicest persons and my 'breakfast/tea-buddy').
- all present and former members of the Scheer group for an unforgettable time: Andi (most intelligent trash TV expert and 'thank you'), Andrea (ice-skating to work), Barbara B., Barbara K., Barbara T., Bianca, Choleric, Claudi, Claudia (good luck with Cp^{PEt}), Dani, David, Eva (always a pleasure), Fabi, Felix, Gábor, Helena, Hias, Jana, Jens, Julian, Karin, Küken, Lena, Liese (a lot of funny moments), Luigi, Luis, Maria, Martin P., Martina, Matthias A. (the Boy), Matthias H., Matthias L., Mehdi, Mia, Michi, Moartl, Moni, Musch, Muschine, Nase, Olli, Petra, Rebecca, Reini, Robert (eating a whole loaf of bread with camembert for lunch), Rudi (have fun changing passwords), Schotti, Sebi, Stubi, Susanne, Sµ, Thomsi, Tobi, Vroni, Walter, Wast, Wurzl.
- especially my family for their enduring support und always being there.
- and Claudia for her endless encouragement and putting up with me. I'm so happy to be with you each and every day!